Synthesis, Characterization and Detection of Novel Protein Modifications *in vitro* and *in vivo*.

Dissertation

zur Erlangung des Doktorgrades der Naturwissenschaften
(Dr. rer. nat.)

der

Naturwissenschaftlichen Fakultät II
Chemie, Physik und Mathematik
der Martin-Luther-Universität
Halle-Wittenberg

vorgelegt von
Tim Baldensperger
geb. am 16.03.1992 in Magdeburg

1. Gutachter: Prof. Dr. Marcus A. Glomb
2. Gutachter: Prof. Dr. Monika Pischetsrieder

Halle (Saale), 21.07.2020

Vorwort

Die vorliegende Arbeit wurde vom Juli 2016 bis Juni 2019 an der Martin-Luther-Universität am Institut für Chemie, Fachbereich Lebensmittelchemie und Umweltchemie im Arbeitskreis von Prof. Dr. Marcus A. Glomb angefertigt.

Die Arbeit wurde über die gesamte Zeit durch das DFG Graduiertenkolleg 2155 Proteinmodifikationen: Schlüsselmechanismen des Alterns (ProMoAge) gefördert.

Die erhaltenen Forschungsergebnisse wurden in international anerkannten Fachzeitschriften publiziert.

Die Dissertation wurde in kumulativer Form angefertigt. Die Darstellung von experimentellen Daten, deren Einordnung, Bewertung und Diskussion erfolgte dabei in den beigefügten Publikationen.

Das Ziel der vorliegenden Arbeit war es, die wissenschaftlichen Einzelaspekte aus den Veröffentlichungen zusammenzufassen und in den Kontext des Titels „Synthesis, Characterization and Detection of Novel Protein Modifications *in vitro* and *in vivo*“ einzuordnen.

Danksagung

Zunächst möchte ich an dieser Stelle Prof. Dr. Marcus A. Glomb für die Möglichkeit der Bearbeitung dieses spannenden und facettenreichen Themas in seinem Arbeitskreis und die stets hervorragende Betreuung danken.

Ein besonderer Dank gilt dem gesamten ProMoAge Graduiertenkolleg, welches den finanziellen und fachlichen Rahmen für meine Promotion maßgeblich geprägt hat.

Ohne die Unterstützung durch Prof. Dr. med. Alexander Zipprich mittels Gewebeproben und Hilfestellung in biochemischen Fragestellungen durch Dr. habil. Thorsten Pfirrmann wäre die Anfertigung dieser Arbeit nicht möglich gewesen. Hierfür möchte ich mich von ganzem Herzen bedanken.

Für die Aufnahme der zahlreichen NMR-Spektren danke ich Dr. Dieter Ströhl. Ebenfalls bin ich Dr. Andrej Frolov für die Aufnahme der hochauflösenden Massenspektren zu Dank verpflichtet.

Meinen ehemaligen Diplomanden Michael Eggen und Jonas Kappen danke ich für die tatkräftige Unterstützung bei der Anfertigung dieser Arbeit.

Mein Dank gilt außerdem allen aktuellen und ehemaligen Doktoranden im Arbeitskreis für das hervorragende Arbeitsklima, sowie Dr. Thomas Heymann für das Korrekturlesen der vorliegenden Dissertation.

Zu guter Letzt möchte ich mich bei meiner Familie und Freunden bedanken, insbesondere meinen Eltern und Lara, die mich jederzeit unterstützt haben.

Publikationsliste

Publikationen

05/2020 **Baldensperger, T.**; Eggen, M.; Kappen, J.; Winterhalter, P. R.; Pfirrmann, T.; Glomb, M. A. Comprehensive analysis of posttranslational protein modifications in aging of subcellular compartments, *Sci. Rep.* **2020**, *10,* p. 7596. **(Publication 3)**

09/2019 **Baldensperger, T.**; Di Sanzo, S.; Ori, A.; Glomb, M. A. Quantitation of Reactive Acyl-CoA Species Mediated Protein Acylation by HPLC–MS/MS, *Anal. Chem.* **2019**, *91,* pp. 12336–12343. **(Publication 2)**

02/2018 **Baldensperger, T.**; Jost, T.; Zipprich, A.; Glomb, M. A. Novel α-Oxoamide Advanced-Glycation Endproducts within the N^6-Carboxymethyl Lysine and N^6-Carboxyethyl Lysine Reaction Cascades, *J. Agric. Food Chem.* **2018**, *66,* pp. 1898–1906. **(Publication 1)**

02/2018 Klaus, A.; **Baldensperger, T.**; Fiedler, R.; Girndt, M.; Glomb, M. A. Influence of Transketolase-Catalyzed Reactions on the Formation of Glycolaldehyde and Glyoxal Specific Posttranslational Modifications under Physiological Conditions, *J. Agric. Food Chem.* **2018**, *66,* pp. 1498–1508.

Präsentationen

09/2019 **Vortrag:** Quantitation of non-enzymatic protein acylation. *Epigenetics: Playing with the game of life*, Halle, 13.-15.09.2019.

05/2019 **Vortrag:** Quantitation of activated thioester mediated protein acylation. *Mechanisms of Ageing; From bench to translation*, Wittenberg, 13.-15.05.2019.

09/2018 **Poster:** Novel α-Oxoamide AGEs as Oxidative Stress Markers. *13th International Symposium on the Maillard Reaction*, Montreal, 10.-13.09.2018.

09/2017 **Poster:** Novel Amide AGEs as Oxidative Stress Markers. *Modulating Ageing/Antiageing: From molecular biology to clinical perspectives*, Halle, 01.-03.09.2017.

Contents

1 INTRODUCTION 1

2 THEORETICAL BACKGROUND 2

2.1 Acetylation 2

2.1.1 Lysine acetyltransferases 2
2.1.2 Lysine deacetylases 4
2.1.3 Recognition domains 5
2.1.4 Acetylation in metabolism 6

2.2 Acylation by reactive acyl-CoA species 7

2.2.1 Novel lysine acylation structures 7
2.2.2 Reactive acyl-CoA species 8
2.2.3 Acylation mechanisms 9
2.2.4 Sirtuins 11
2.2.5 Acylation in metabolism 13

2.3 Acylation by Maillard reaction 14

2.3.1 Initial phase and α-dicarbonyl formation 14
2.3.2 Fragmentation 15
2.3.3 Isomerization 16
2.3.4 Regulation of glycation 18
2.3.5 Glycation in aging and disease 21

3 OBJECTIVES 24

4 DISCUSSION 25

4.1 Acylation by isomerization of short-chain α-dicarbonyls 25

4.2 Quantitation of acylation by HPLC-MS/MS 33

4.3 Posttranslational protein modifications in aging 40

5 PUBLICATIONS 48

5.1 Publication 1 48

5.2 Publication 2 57

5.3 Publication 3 65

6 SUMMARY 76

7 ZUSAMMENFASSUNG 78

8 REFERENCES 80

9 LIST OF FIGURES 107

10 LIST OF TABLES 108

11 APPENDIX 109

LEBENSLAUF 124

EIGENSTÄNDIGKEITSERKLÄRUNG 125

1 Introduction

The demographic change is one of the most urgent problems in Germany and compared to 2005 the population is expected to decrease about 16 % until 2050. At the same time persons aged over 65 years will increase by 38 % and persons aged over 80 years will increase by 156 %. Currently, about half of health care costs account for elderly patients above 65 years of age. Assuming comparable disease prevalence these costs and age-related diseases like diabetes, atherosclerosis, cancer, and dementia will increase tremendously.[1]

Several of these diseases are caused or at least mediated by posttranslational protein modifications (PTMs).[2–5] In comparison to biosynthesis of new proteins, PTMs are formed at much faster rates and facilitate rapid adaption of metabolism to environmental changes.[6] Thus, the number of about 70000 human proteins is increased to several million protein species by PTMs.[7]

Acetylation of proteins was one of the first PTMs discovered in histones by Phillips in 1963.[8] It has to be differentiated between N-terminal acetylation of proteins during translation[9] and posttranslational N^6-acetylation of lysine residues. Due to the high complexity the present thesis focuses solely on PTMs. Acetylation is considered a major regulatory mechanism in epigenetics and metabolism. The modification is formed by acetyltransferases ("writers"), removed by deacetylases ("erasers") and detected by several "reader" domains.[2] In recent years metabolic intermediates like reactive acyl-CoA thioesters (RACS) and α-dicarbonyls were identified as precursors for structurally related non-enzymatic lysine acylation. Acetylation and acylation are competing for lysine residues and influence each other.[10] Based on their individual structure they share several functions in metabolism but can cause very distinct and unique reactions as well.[11] While acetylation is mainly an enzymatic process, acylation is generally considered a non-enzymatic reaction. Consequently, fundamental important enzymatic regulatory pathways are paralleled by non-enzymatic acylation by RACS[12] and Maillard-mediated acylation by α-dicarbonyl intermediates.[13] This fact is discussed in the present thesis as a potential molecular mechanism leading to impairment of tissues and metabolism observed in the aging process. Finally, our experimental data are compared to the currently available literature about acetylation, acylation by RACS and Maillard processes in the following chapters with an emphasis on mechanisms of modification, potential enzymatic and non-enzymatic regulation as well as metabolic consequences for aging and disease.

2 Theoretical background

2.1 Acetylation

2.1.1 Lysine acetyltransferases

Lysine acetyltransferases (KATs) are "writers" of acetylation and catalyze the transfer of acetyl groups from acetyl-CoA to N^6-amino functions of lysine residues. The human proteome contains 22 putative KATs (Table 1). Based on catalytic mechanism and homology to yeast proteins KATs are categorized into the three major groups GCN5-related N-acetyltransferase (GNAT), p300/CREB-binding protein (p300/CBP), and the **M**OZ, **Y**bf2, **S**as2, and **T**ip60 (MYST) family. In addition, several proteins outside of this categorization show acyltransferase activity, e.g., steroid receptor coactivators (SRCs) and α-tubulin acetyltransferase (αTAT1).[2]

Table 1: Putative lysine acetyltransferases.[2]

Name	Aliases	Subfamily	Cellular localization
KAT1	HAT1	GNAT	Nucleus, Cytoplasm
KAT2A	GCN5	GNAT	Nucleus
KAT2B	PCAF	GNAT	Nucleus
ATF2	CREB2	GNAT	Nucleus
KAT3A	CBP	p300/CBP	Nucleus, Cytoplasm
KAT3B	P300	p300/CBP	Nucleus, Cytoplasm
KAT4	TAF1, TAFII250	TAFII250	Nucleus
KAT5	TIP60	MYST	Nucleus, Cytoplasm
KAT6A	MYST3, MOZ	MYST	Nucleus
KAT6B	MYST4, MORF	MYST	Nucleus
KAT7	MYST2, HBO1	MYST	Nucleus
KAT8	MYST1, MOF	MYST	Nucleus, Mitochondria
KAT9	ELP3	ELP3	Nucleus, Cytoplasm
GCN5L1	BLOS1	-	Nucleus, Mitochondria
ACAT1	-	-	Mitochondria
αTAT1	MEC17	-	Cytoplasm
KAT12	GTF3C4	-	Nucleus, Cytoplasm
KAT13A	NCoA-1, SRC1	SRC	Nucleus, Cytoplasm
KAT13B	NCoA-3, TRAM1	SRC	Nucleus, Cytoplasm, Exosome
KAT13C	NCoA-2, TIF2, SRC3	SRC	Nucleus, Cytoplasm
KAT13D	CLOCK	SRC	Nucleus, Cytoplasm
KAT14	CSR2B	-	Nucleus, Cytoplasm

Most KATs contain a characteristic and highly conserved α/β fold (Motif A) as the acetyl-CoA binding site.[14] While primary structures of KATs are similar within members of the same family, KATs of distinct families show little to no structural similarity. This

sequence variability between subfamilies is considered to be responsible for different substrate recognition. For example GNATs prefer acetylation of histone H3 while members of MYST preferentially acetylate histone H4.[15]

KATs of the GNAT and MYST subfamilies share the same catalytic mechanism (Figure 1) and use an active site glutamate to deprotonate the N^6-amino functions of lysine residues.[2] This facilitates the nucleophilic attack of the amino function at the activated carbonyl function of acetyl-CoA. Collapse of the transient tetrahedral intermediate leads to lysine acetylation and coenzyme A.[16,17] A previously reported MYST mechanism by active site acetyl cysteine intermediate[18] was proven wrong by site-directed mutagenesis of the respective cysteine, which had no effect on enzyme activity while depletion of glutamate caused complete loss of acetyltransferase activity.[16]

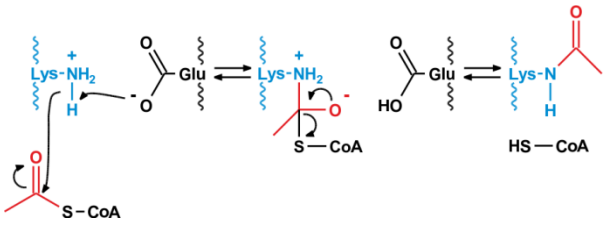

Figure 1: Proposed reaction mechanisms for GNAT and MYST acetyltransferases.[2,17]

In contrast to GNAT and MYST, a "hit and run" (Theorell-Chance) mechanism is utilized by p300/CBP (Figure 2).[2] Instead of glutamate this reaction is catalyzed by aromatic amino acids, which steer the nucleophilic attack of the lysine substrate at acetyl-CoA. Finally, tyrosine protonates the sulfhydryl group of coenzyme A. In this ordered and rapid mechanism, the ternary complex formed is kinetically irrelevant.[19] This alternative reaction mechanism may partially explain the relative substrate promiscuity observed for p300/CBP compared to GNAT and MYST KATs.[20]

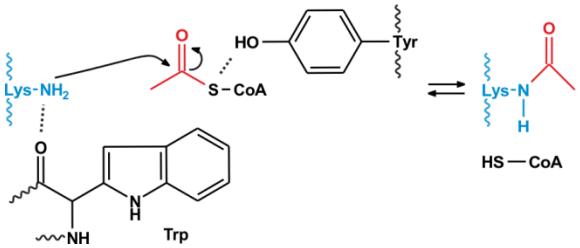

Figure 2: Proposed reaction mechanisms for p300/CBP acetyltransferases.[21]

2.1.2 Lysine deacetylases

Reversibility of lysine acetylation by "erasers" is mandatory for metabolic regulation. The existence of lysine deacetylases (KDACs) was postulated in 1978 after treatment of erythroleukemic cells with *n*-butyrate and Trapoxin resulted in histone hyperacetylation.[22] The inhibitor Trapoxin was used to generate an affinity phase for isolation of the first KDAC.[23] In total, 11 Zn^{2+} dependent KDACs were discovered using sequence homology analyses (Table 2).[2]

Table 2: Zn^{2+} dependent lysine deacetylases.[2]

Name	Subfamily	Cellular localization
KDAC1	I	Nucleus, Cytoplasm
KDAC2	I	Nucleus, Cytoplasm
KDAC3	I	Nucleus, Cytoplasm
KDAC8	I	Nucleus, Cytoplasm
KDAC4	IIA	Nucleus, Cytoplasm
KDAC5	IIA	Nucleus, Cytoplasm
KDAC7	IIA	Nucleus, Cytoplasm, Mitochondria
KDAC9	IIA	Nucleus, Cytoplasm
KDAC6	IIB	Nucleus, Cytoplasm
KDAC10	IIB	Nucleus, Cytoplasm
KDAC11	IV	Nucleus, Cytoplasm

In the deacetylation process Zn^{2+} forms a charge relay network with histidine, aspartic acid residues, and water. The substrate N^6-acetyl lysine interacts with this catalytic triad and Zn^{2+} polarizes the carbonyl bond. In the next step water is deprotonated by histidine and attacks the activated carbonyl carbon. The resulting tetrahedral intermediate is stabilized by tyrosine and finally the amide bond is cleaved by proton transfer from histidine yielding acetate and deacetylated lysine (Figure 3).[24]

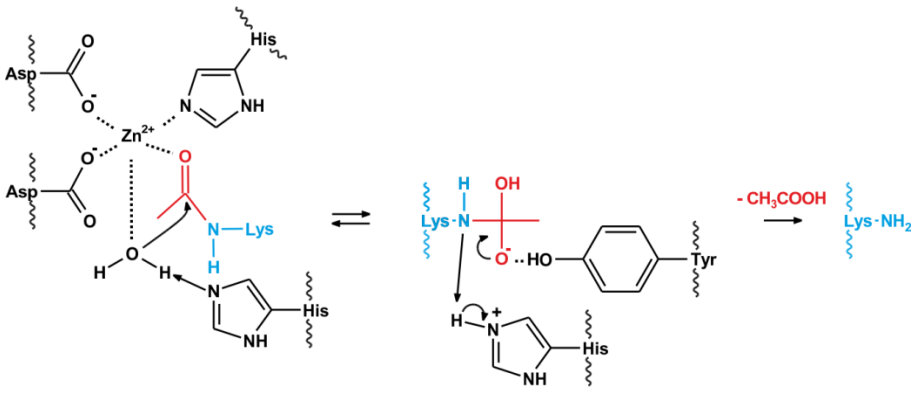

Figure 3: Proposed reaction mechanism for Zn^{2+} dependent lysine deacetylases.[25]

2.1.3 Recognition domains

Acetylation is recognized by several "reader" domains translating the acetylation code into various phenotypes. The bromodomain was discovered in 1992 and is by far the best characterized recognition module of N^6-acetyl lysine. In total, 61 bromodomains are encoded by 46 proteins (Table 3).[2]

Table 3: Bromodomain containing proteins.[2]

Localization	Proteins
Nucleus	KAT2A (GCN5), KAT2B (PCAF), CECR2, BRDT, BRD4, BRD3, BRD2, BAZ1A, BRD8B, BAZ1B, BRD9, BRD7, BRPF3, BRD1, ATAD2B, TRIM33, SP110, SP140, SP140L, BAZ2B, BAZ2A, KMT2A, TAF1L, TAF1, ZMYND8, PBRM1, BRG1, SMARCA2
Nucleus / Cytoplasm	IBPTF, KAT3A (CBP), KAT3B (p300), BRWD1, PHIP, BRPF1, TRIM24, SP100, KAP1, ZMYND11
Nucleus / Extracellular	BRWD3
Nucleus / Exosome	ATAD2
Nucleus/ Tight junctions	ASH1L

The bromodomain is approximately 110 amino acids in length and structurally conserved from yeast to humans. A hydrophobic cleft is formed by four left-handed α-helices (αZ, αA, αB, and αC) connected by two loops (ZA and BC loops). The carbonyl function of N^6-acetyl lysine is bond in the center of this cleft by asparagine via a hydrogen bond. Tyrosine residues play an important role in ligand positioning via π–π stacking and hydrogen bond formation with critical water molecules.[26]

Interestingly, many KATs contain bromodomain motifs and nearly all bromodomain containing proteins are nuclear factors binding to chromatin and changing its conformation. In most cases, this leads to activation of transcription, e.g., KAT3B (p300), but inhibitory "readers" are known as well, e.g., BAZ2A.

Beside bromodomain the YEATS domain (named after founding members **Y**af9, **E**NL, **A**F9, **T**af14, and **S**as5) and tandem plant homodomain (PHD) are important "readers" of acetylation and known for binding and remodeling chromatin structures. The N^6-acetyl lysine ligand is bond by aspartic acid in PHD[27] and several hydrogen bonds in YEATS.[28] In contrast to bromodomain, tandem PHD as well as YEATS, unmodified lysine residues are selectively recognized by SET proteins (**S**u(var)3-9 **E**nhancer-of-zeste and **T**rithorax). These proteins bind to non-acetylated lysine rich substrates like tumor suppressor p53 via their acidic domains.[29]

2.1.4 Acetylation in metabolism

Acetylation's pivotal role in gene regulation was proposed by Allfrey in 1964, who discovered that acetylated histones were less inhibitory for RNA polymerase.[30] Later, the same group identified weakened interaction between negatively charged DNA and histones due to neutralization of positively charged lysine moieties via acetylation as a molecular mechanism of gene activation.[31] Notably, gene regulation by acetylation is not limited to modification of histones. Acetylation of transcription factors and proteins of the basal transcription machinery are alternative regulatory pathways. Mechanistically, acetylation activates transcription factors by nuclear translocation, protein stabilization, enhanced chromatin binding, or modification of molecular complex composition.[2] As an example nuclear factor "kappa-light-chain-enhancer" of activated B-cells (NF-κB), which is a major regulator for immune response and apoptosis, is located inactive in the cytoplasm and is activated by acetylation mediated translocation to the nucleus.[32] On the other hand, stability of tumor suppressor p53 is increased by acetylation counteracting ubiquitination and subsequent proteasomal degradation.[33] In case of positive transcription factor b (P-TEFb) acetylation is needed to modify the complex structure and activate basal transcription machinery of RNA polymerase II complex.[2]

Beside the important role in nuclear transcription processes, acetylation regulates the aggregation and stability of proteins in the cytoplasm. As an example acetylation of non-histone proteins was discovered in cytoskeletal α-tubulin. It is unclear whether acetylation is a cause or consequence of high α-tubulin stability, but acetylation is generally considered as a marker of protein longevity.[34] While increased stability of cytoskeletal proteins may be beneficial, acetylation of microtubule-associated proteins like Tau possibly facilitates dementia and Alzheimer's disease pathogenesis.[2]

Proteomic studies revealed that every single protein involved in central mitochondrial metabolism like citric acid cycle, lipid β-oxidation and urea cycle is potentially acetylated. Because of the correlation with acetyl-CoA concentrations, acetylation and deacetylation of lysine residues may serve as a sensor and regulator of metabolic state in mitochondria.[35]

Despite acetylation's ubiquitous abundance in metabolic regulation its role in aging remains poorly understood. Several contrary trends are reported in literature depending on organism, tissue, subcellular location and site-specific position in proteins.[36–38] Consequently, (site-specific) quantitation of acetylation remains a compelling task to understand the aging process.

2.2 Acylation by reactive acyl-CoA species

2.2.1 Novel lysine acylation structures

Progress in analytical chemistry and improved instruments like highly sensitive mass spectrometers resulted in discovery of several novel N^6-acyl lysine modifications, which are structurally closely related to traditional acetylation (Table 4).

Table 4: Novel N^6-acyl lysine modifications.

Modification	Year	Discovered in
Myristoylation	1992	Monocyte tumor necrosis factor alpha precursor[39]
Formylation	2006	TK6 cell histones[40]
Propionylation	2007	HeLa cell histones[41]
Butyrylation	2007	HeLa cell histones[41]
Succinylation	2010	*E. Coli* isocitrate dehydrogenase[42]
Crotonylation	2011	HeLa cell histones[43]
Malonylation	2011	HeLa whole-cell lysate[44]
Glutarylation	2014	HeLa whole-cell lysate[45]
2-Hydroxyisobutyrylation	2014	Mouse testis histones[46]
3-Hydroxybutyrylation	2016	HEK293 cell histones[47]
3-Hydroxy-3-methylglutarylation	2017	Mouse liver lysate[48]
3-Methylglutarylation	2017	Mouse liver lysate[48]
3-Methylglutaconylation	2017	Mouse liver lysate[48]
Benzoylation	2018	HepG2 cell histones[49]

Fatty acylation of lysine residues was first described in 1992. At this time, the proteome was mainly analyzed by 2D-gel electrophoresis and myristoylation was detected by incorporation of radioactive [^{3}H] myristate.[39] Proteomic approaches using mass spectrometry were established in the 1990s.[50] This innovation was a big step towards discovery of short-chain lysine acylation, e.g., formylation, propionylation, and butyrylation of histone proteins in 2006 and 2007.[40,41] The first unsaturated acylation detected was crotonylation of histones in 2011. Acidic modifications succinylation, malonylation and glutarylation were detected in several metabolic pathways between 2010 and 2014.[42,44,45] The spectrum of lysine acylation was expanded by polar modifications 2-hydroxyisobutyrylation and 3-hydroxybutyrylation.[46,47] In analogy to the mechanism of glutarylation formation of several branched-chain derivatives was verified by mass spectrometry.[48] Aromatic lysine benzoylation is the most recently proven acylation in histones and links acylation to the food preservative sodium benzoate.[49]

2.2.2 Reactive acyl-CoA species

Reactive acyl-CoA species (RACS) are activated thioesters and precursors of lysine acylation.[12,51] They are essential intermediates in cellular metabolism (Table 5) reaching concentrations up to 100 µmol/g wet weight depending on tissue and metabolic status.[52]

Table 5: Reactive acyl-CoA species and their metabolic pathways.

Structure	Metabolic pathways
Formyl-CoA	α-Oxidation[53,54]
Acetyl-CoA	Citric acid cycle, metabolism of fatty acids, carbohydrates, and amino acids, synthesis of steroids and acetylcholine[55]
Propionyl-CoA	Odd-chain fatty acid oxidation,[56] amino acid catabolism,[57] bile acid synthesis[58]
Butyryl-CoA	Lipid metabolism[41]
2-Methylbutyryl-CoA	Isoleucine metabolism[59]
Isovaleryl-CoA	Leucine metabolism[60]
Crotonyl-CoA	Metabolism of lysine and tryptophan[61]
Tiglyl-CoA	Isoleucine metabolism[59]
Acetoacetyl-CoA	Ketogenesis,[62] cholesterol biosynthesis,[63] mevalonate pathway[64]
3-Hydroxybutyryl-CoA	Ketogenesis[65,47]
Malonyl-CoA	Lipogenesis[44]
Succinyl-CoA	Citric acid cycle,[66] amino acid metabolism[42]
Glutaryl-CoA	Metabolism of lysine and tryptophan[61]
3-Hydroxy-3-methyl-glutaryl-CoA	Ketogenesis,[62] mevalonate pathway[64]
Medium-chain acyl-CoA (C6-12 acyl-CoA)	Lipid metabolism[67]
Long-chain acyl-CoA (C14-22 acyl-CoA)	Lipid metabolism[68]

Acetyl-CoA as the most abundant thioester structure is a central molecule in energy metabolism of carbohydrates, lipids, and amino acids in mitochondria.[55] The mitochondrial membrane is impermeable for acetyl-CoA and mitochondrial concentrations are estimated to be 20 – 30-fold higher compared to concentrations found outside of mitochondria. Anyhow, transfer to cytoplasm and nucleus is possible in form of citrate and reformation of acetyl-CoA by ATP citrate lyase.[69]

Beside acetyl-CoA several linear and even-numbered C4-C22 RACS are generated by lipid metabolism, e.g., β-oxidation in mitochondria and lipogenesis in cytoplasm.[41,67,68] The latter pathway requires malonyl-CoA as the first building block.[44] Catabolism of odd-numbered fatty acids or α-oxidation of 3-methylated fatty acids results in propionyl-CoA[56] and formyl-CoA,[53,54] respectively.

In analogy to acetyl-CoA the citric acid cycle is a major source of succinyl-CoA. In addition, succinyl-CoA is generated by amino acid metabolism.[70] Further RACS are formed in

metabolism of leucine (isovaleryl-CoA),[60] isoleucine (2-methylbutyryl-CoA and tiglyl-CoA),[59] and lysine/tryptophan (crotonyl-CoA and glutaryl-CoA).[61]

Alternative pathways leading to RACS like 3-hydroxybutyryl-CoA, 3-hydroxy-3-methyl-glutaryl-CoA, and acetoacetyl-CoA are ketogenesis and mevalonate pathway.[62,64] Additionally, RACS can be formed *in vivo* by activation of their corresponding carboxylic acids via acyl-CoA synthetases.[11]

2.2.3 Acylation mechanisms

RACS are highly reactive due to polarization of the carbonyl carbon of the thioester moiety and the excellent leaving group coenzyme A. Especially under the conditions found in mitochondria with elevated pH of 8.0 and high acyl-CoA concentrations non-enzymatic acylation of lysine residues is facilitated. The reaction is initiated by nucleophilic attack of the N^6-amino function of lysine at acyl-CoA and proceeds via a transient tetrahedral intermediate to N^6-acetyl lysine and coenzyme A (Figure 4).[12]

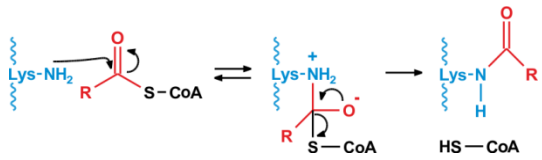

Figure 4: Mechanism of non-enzymatic acylation.[12]

Dicarboxylic acyl-CoA compounds with four- or five-carbon backbones, e.g., succinyl-CoA, glutaryl-CoA, and 3-hydroxy-3-methyl-glutaryl-CoA undergo intramolecular catalysis and anhydride formation (Figure 5). These anhydrides are the reactive species acylating lysine residues without tetrahedral intermediate formation. Compared to acetylation by acetyl-CoA reactivity is increased by a factor of up to 150.[51]

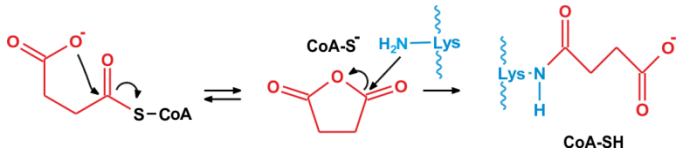

Figure 5: Mechanism of non-enzymatic acylation by succinyl-CoA.[48]

The concept of non-enzymatic lysine acylation is generally accepted and incubations of proteins as well as denatured mitochondrial lysates with various RACS under physiological conditions indeed proved the concept of non-enzymatic acylation.[12,48,51]

Nevertheless, recent publications suggested additional enzymatic pathways especially for nuclear acylation.[11] Specific acyltransferases are currently unknown, but several lysine acetyltransferases were shown to have an expanded repertoire of promiscuous acyltransferase activities (Table 6).

Table 6: Potential acyltransferases.

Name	Catalytic activity
KAT3B (p300)	Acetylation, propionylation, butyrylation, crotonylation[71]
KAT2A (GCN5)	Acetylation, propionylation, butyrylation [72]
KAT2B (PCAF)	Acetylation, propionylation, butyrylation[73]
KAT5 (TIP60)	Acetylation, propionylation[74]
KAT8 (MOF)	Acetylation, propionylation[75]

Kinetic analysis of the most promiscuous KAT3B (p300) confirmed catalysis of acylation but revealed progressively slower rates with increasing chain length, e.g., efficiency of butyrylation decreased by a factor of 45 compared to acetylation.[71]

Acetylation, propionylation, and butyrylation activities were reported for GNATs KAT2A and KAT2B.[73,72] In case of KAT2A propionylation and butyrylation efficiencies equaled 75 % and 1 % of acetylation rates, respectively.[72] Values for KAT2B catalyzed propionylation equaled 10 % and butyrylation equaled 0.2 % of acetylation. These KAT2B values and propionylation of histone H4 by KAT5 were determined by 5,5'-dithiobis-(2-nitrobenzoic acid) (DTNB) assay.[74] However, DTNB is only an indicator of free thiols, but these groups are formed by RACS via hydrolysis and non-enzymatic acylation as well. In order to exclude false-positive results acylation specific detection and a blank using inactivated KAT are mandatory. This essential information was unfortunately not reported in studies cited above.

A positive example is the propionylation activity of KAT8 (MOF) reported by Han et al.[75] In this study propionylation activity was validated *in vitro* and by MOF overexpression in cell culture. These results are especially interesting, because KAT8 (MOF) is one of only three reported acetyltransferases in mitochondria, in which acylation was previously postulated as an exclusively non-enzymatic mechanism. [2,12]

2.2.4 Sirtuins

NAD^+ dependent sirtuins were originally discovered as deacetylases, but several members of this enzyme class have an expanded repertoire of deacylase activities.[76] The 7 mammalian sirtuins have characteristic subcellular localization i.e. SIRT1/6/7 in the nucleus, SIRT2 in cytoplasm, and SIRT3-5 in mitochondria (Table 7).[77]

Table 7: NAD^+ dependent sirtuins. [77,78]

Name	Primary localization	Catalytic activities
SIRT1	Nucleus	Deacylase (acetylation and medium-chain acylation)[76]
SIRT2	Cytoplasm	Deacylase (acetylation and medium-chain acylation),[76] ADP ribosyltransferase[79]
SIRT3	Mitochondria	Deacylase (aliphatic acylation)[80]
SIRT4	Mitochondria	Deacylase (branched-chain acylation),[81] ADP ribosyltransferase,[82] Lipoamidase,[82] Biotinidase[82]
SIRT5	Mitochondria	Deacylase (acidic acylation)[80]
SIRT6	Nucleus	Deacylase (acetylation and long-chain acylation),[83] ADP ribosyltransferase[84]
SIRT7	Nucleus	Deacetylase[85]

SIRT1 is a nuclear deacetylase with high deacylase activity for C6-C12 medium-chain acylation and mediocre affinity for propionylation and butyrylation *in vitro*.[76] It is the best-studied sirtuin and mediates lifespan extension effects observed in caloric restriction. Important mechanisms of SIRT1 are reduction of inflammation by NF-κB deacetylation, regulation of lipid metabolism via peroxisome proliferator-activated receptor gamma coactivator 1-alpha (PGC1α), activation of key transcription factors, e.g., forkhead box (FOXO), and tumor suppression by preserving genomic integrity. Consequently, enhancing SIRT1 is a promising target to improve health during aging.[86,87]

The only sirtuin primarily located in cytoplasm is SIRT2.[77] This excellent deacetylase has only average affinity for C8-C10 acylation and very low depropionylation, debutyrylation, and decrotonylation activity *in vitro*.[76] In addition, SIRT2 has ADP ribosyltransferase activity and a broad spectrum of target proteins.[79] Due to especially high concentrations in brain an important role in neuronal development is postulated for SIRT2.[78]

SIRT3 is a deacetylase located in mitochondria with very low *in vitro* activities for depropionylation and desuccinylation.[76] As a classical regulator of mitochondrial energy metabolism SIRT3 knock-out in mice leads to impaired maintenance of energy balance during stress.[87]

In contrast to SIRT3 mitochondrial sirtuin SIRT4 has very low deacetylation activity. On the other hand SIRT4 is an excellent branched-chain deacylase for, e.g., 3-hydroxy-3-methyl-glutarylation. This modification occurs in branched-chain amino acid metabolism, which is regulated by SIRT4.[81] Moreover, SIRT4 has an expanded repertoire of ADP ribosyltransferase, lipoamidase, and biotinidase activities.[82]

In analogy to SIRT4 mitochondrial SIRT5 has low affinity for acetylation but is an outstanding deacylase for acidic modifications, e.g., malonylation, succinylation, and glutarylation.[76] These modifications are formed by important mitochondrial intermediates and knock-out of SIRT5 leads to mitochondrial dysregulation, e.g., defects in the urea cycle.[87]

Deacetylase activity of nuclear SIRT6 is below average, medium-chain deacylase activity is mediocre and ADP ribosyltransferase activity very weak.[81] Nevertheless, SIRT6 is a good deacylase for long-chain C14-C16 acylation and plays an important role in maintaining both lifespan and healthspan by promoting genomic stability and telomere integrity.[88]

To be correct SIRT7 is not just another nuclear sirtuin, but mainly found in the nucleolus.[77] Very little is known about SIRT7 specificity except average deacetylation activity.[76] Despite rare literature about SIRT7 the enzyme is vitally important. Mice lacking SIRT7 are prone to hypertrophic inflammatory cardiomyopathy, fatty liver disease, age related hearing loss, and reduced mean and maximal lifespan.[76] On the other hand, SIRT7 knock-down in cancer cell lines inhibits tumor growth.[89]

Sirtuins catalyze deacylation by nucleophilic addition of acyl oxygen to the anomeric (C1′) carbon of the nicotinamide ribose resulting in the formation of a C1′-O-alkylamidate intermediate and nicotinamide (Figure 6). In the next step a bicyclic intermediate is formed by histidine catalyzed abstraction of an electron from the 2′-hydroxyl group of the NAD^+ ribose, which then attacks the C1′-O-alkylamidate carbon. Base catalyzed deprotonation of water and subsequent hydrolysis of the bicyclic intermediate deacylates lysine and generates 2′-O-acyl-ADP-ribose.[90,91]

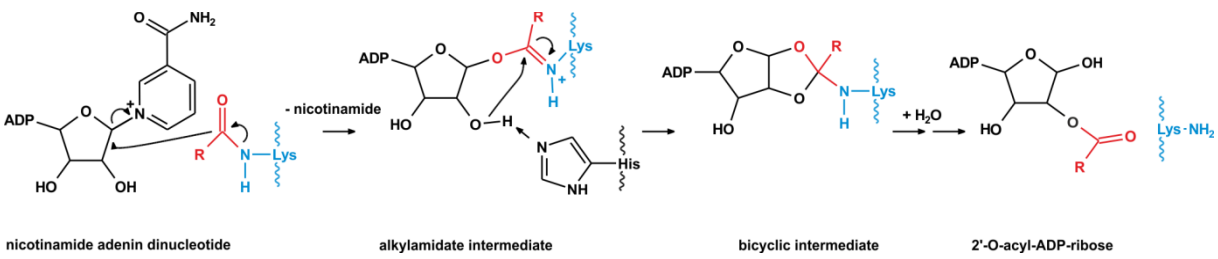

Figure 6: Proposed reaction mechanism for NAD^+ dependent sirtuins.[91]

2.2.5 Acylation in metabolism

Aliphatic acylations like propionylation, butyrylation, and crotonylation are very similar to acetylation regarding their structure. Consequently, these acylations have similar effects on chromatin structure and activation of transcription *in vitro* and *in vivo*.[92,93] In analogy to histone acetylation "reader" proteins can detect acylation and subsequently induce gene expression.[11] In an assay of 49 bromodomains for their binding of acylated peptides, all 49 bromodomains bound propionylated peptides, while only three bound butyrylated and one crotonylated peptides. To sum it up, bromodomains generally detect propionylation, but butyrylation and crotonylation are only detected by very few bromodomains and affinity decreases with chain length.[94] In contrast, YEATS domains have higher binding affinity towards propionylation and butyrylation compared to acetylation and highest affinity for crotonylation.[95] Tandem PHD has highest binding efficiency for crotonylation followed by acetylation, butyrylation, and propionylation.[96]

During fasting 3-hydroxybutyrate is formed via ketogenesis and transformed to 3-hydroxybutyryl-CoA by an acyl-CoA synthetase. Increased 3-hydroxybutyrylation of chromatin results in up-regulation of genes involved in starvation response pathways. Thus, acylation effectively couples metabolism to gene expression.[47] Recently discovered aromatic lysine benzoylation links the food preservative sodium benzoate to chromatin activation.[49]

Mitochondrial acylation, especially by acidic acylation, e.g., malonylation, succinylation, glutarylation, and 3-hydroxy-3-methylglutarylation, is another emerging regulatory mechanism in metabolism. Currently, available studies mainly focus on hyperacylation induced by knock-out of mitochondrial sirtuins.[66,80,97] Exemplary, hypersuccinylation activates succinate dehydrogenase leading to increased mitochondrial respiration[98] and hypermalonylation of glyceraldehyde 3-phosphate dehydrogenase is an efficient inhibitor of glycolytic flux.[99] Another example is inhibition of enzymes in leucine catabolism via 3-hydroxy-3-methylglutarylation after SIRT4 knock-out. As a result of this inhibition more insulin is secreted and age-dependent insulin resistance accelerates.[81]

Beside regulatory functions acylation is considered as a form of stress in aging and disease.[3] Mitochondrial acylation is significantly increasing with age in organisms lacking mitochondrial sirtuins, e.g., *C. elegans*. On the other hand acylation is not correlating with aging in rats, possibly explaining the gain of longevity in higher organisms.[100] In addition, sirtuins are important targets for treatment of age related diseases like cancer and neurodegeneration, hence, acylation may be involved in these pathologies.[4]

2.3 Acylation by Maillard reaction

2.3.1 Initial phase and α-dicarbonyl formation

The Maillard reaction or non-enzymatic browning was discovered in 1912 by Louis-Camille Maillard as the reaction between reducing sugars and amines such as proteins, peptides, or amino acids. The reaction cascade can be separated into three phases, namely initial phase, formation of α-dicarbonyls and finally formation of advanced glycation endproducts (AGEs) as well as browning structures (melanoidins).[101] First step of the initial phase is the nucleophilic attack of an amine at the carbonyl carbon atom of a reducing sugar, e.g., glucose and formation of an imine. This imine rearranges via an 1,2-enaminol intermediate to the Amadori product (Figure 7).[102] If fructose is the reducing sugar the equivalent Heyns product is formed.[103] In the second phase central α-dicarbonyl intermediates like 3-deoxyglucosone are formed via the 1,2-enaminol by β-elimination and glucosone from oxidation of Amadori product. Further keto-enol tautomerization of the Amadori product and β-elimination finally leads to 1-deoxyglucosone and Lederer glucosone (Figure 7).[13]

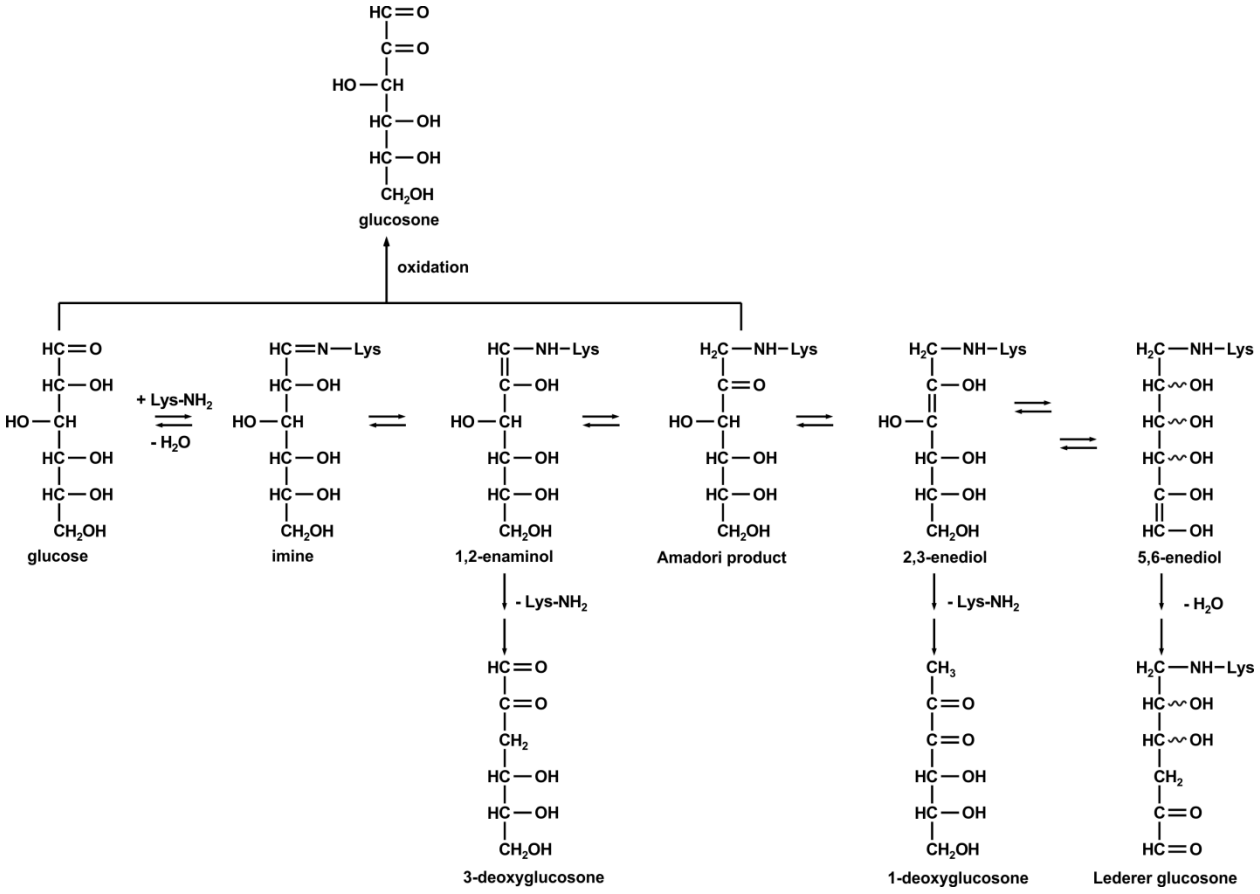

Figure 7: Initial phase of amine induced glucose degradation and α-dicarbonyl formation.[13]

2.3.2 Fragmentation

Keto-enol tautomerism of α-dicarbonyls, e.g., 1-deoxyglucosone results in formation of β-dicarbonyls 1-deoxy-2,4-hexodiulose, 1-deoxy-3,5-hexodiulose, and 1-deoxy-4,6-hexodiulose. These intermediates readily react with nucleophiles and, thus, carboxylic acids and highly reactive short-chain carbonyls are formed by hydrolytic β-dicarbonyl cleavage. As an example hydration of 2,4-deoxyglucosone induces scission to acetic acid and a C4-enediol intermediate, which further isomerizes to tetruloses and tetrosones.[104]

Alternatively, an amine induced β-dicarbonyl cleavage mechanism generates amide AGEs like N^6-acetyl, N^6-glycerinyl, N^6-lactoyl, and N^6-formyl lysine as well as their α-hydroxy carbonyl counterparts in incubations of 1-deoxyglucosone and lysine (Figure 8).[105]

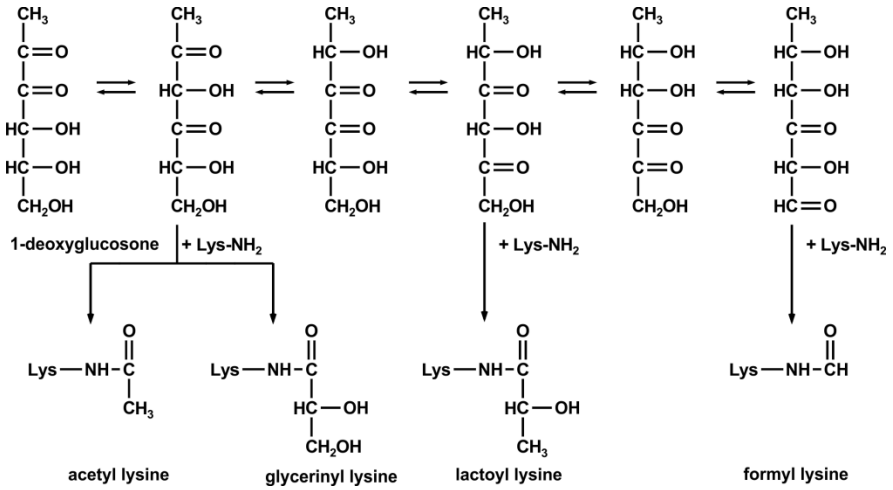

Figure 8: Amine induced β-dicarbonyl cleavage of 1-deoxyglucosone.[105]

Another mechanism leading to lysine acylation by amide AGEs is amine induced oxidative α-dicarbonyl cleavage. Exemplary, ascorbic acid is reversibly oxidized to dehydroascorbic acid and irreversibly hydrolyzed to 2,3-diketogulonic acid. This α-dicarbonyl is attacked by activated oxygen, which is incorporated into the carbon backbone forming an asymmetric carboxylic acid anhydride intermediate via a single-electron transfer reaction and subsequent Baeyer-Villiger type rearrangement.[106] The mechanism of oxygen incorporation was unequivocally verified by isotopic labeling experiments using ^{18}O-dioxygen.[107] Carboxylic acid anhydrides are highly reactive and the intermediate is cleaved into either N^6-oxalyl or N^6-threonyl lysine as well as their respective carboxylic acid counterparts (Figure 9).[106]

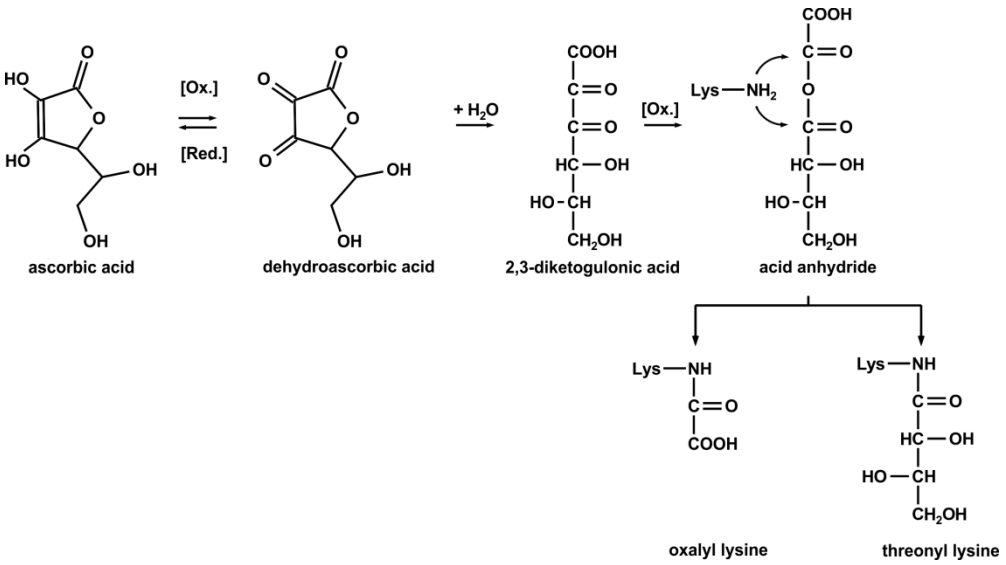

Figure 9: Amine induced oxidative α-dicarbonyl cleavage of 2,3-diketogulonic acid.[106]

2.3.3 Isomerization

Fragmentation processes during Maillard reaction and a plethora of different metabolic pathways result in highly reactive short-chain α-dicarbonyls like glyoxal (GO) and methylglyoxal (MGO) (Table 8).[108]

Table 8: Pathways of short-chain α-dicarbonyl formation.[108]

Dicarbonyl	Formation
Glyoxal	Lipid peroxidation[109]
	Degradation of glycated proteins[108]
	Oxidative degradation of serine via glycolaldehyde oxidation[110,111]
	Monosaccharide degradation[112]
	Disaccharide degradation[113]
	Degradation of nucleotides[114,115]
	Food and beverages[116]
Methylglyoxal	Degradation of glyceraldehyde-3-phosphate and dihydroxyacetonephosphate in anaerobic glycolysis, gluconeogenesis, glyceroneogenesis, and photosynthesis[117]
	Ketone body metabolism[118]
	Lipid peroxidation[109]
	Threonine metabolism[119]
	Degradation of glycated protein[108]
	Monosaccharide degradation[112]
	Disaccharide degradation[113]
	Food and beverages[116]

Isomerization of lysine adducts with short-chain dicarbonyls, e.g., GO and MGO were initially discovered as an important source of carboxyalkyl AGEs like N^6-carboxymethyl lysine (CML) and N^6-carboxyethyl lysine (CEL), respectively.[120] But CML and CEL are not the only endproducts in these isomerization cascades of GO and MGO. Alternatively, a plethora of acylated lysine species including α-hydroxyamide, α-oxoamide, and bivalent amide crosslink AGEs are formed (Figure 10). [13,121,122]

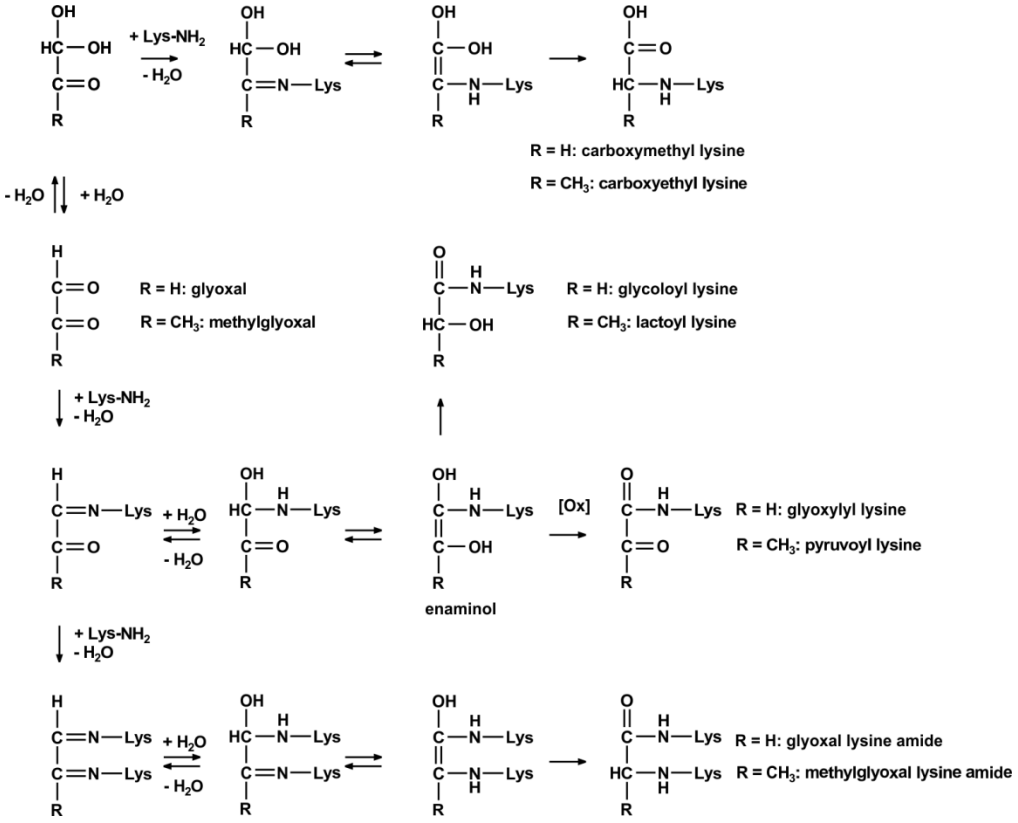

Figure 10: Isomerization cascades.[13,121,122]

In case of nucleophilic addition of water at the imine group under deaeration, isomerization leads to α-hydroxyamide AGEs N^6-glycoloyl lysine (GALA) by GO and N^6-lactoyloyl lysine by MGO. [122,123] Under aeration, oxidation of the electron rich enaminol intermediate yields α-oxoamides N^6-glyoxylyl lysine or N^6-pyruvoyl lysine, respectively.[122] Another option is nucleophilic attack of a second lysine at the imine resulting in crosslinking via bivalent GO lysine amide (GOLA) or MGO lysine amide (MOLA). [13,121]

2.3.4 Regulation of glycation

Early stage modifications like protein-bound Amadori products can be cleaved enzymatically.[102] One example is fructosamine-3-kinase (FN3K), which selectively phosphorylates the hydroxyl group at C-3 position under ATP consumption. The instable phosphate ester decomposes in a non-enzymatic way into recovered protein and 3-deoxyglucosone (Figure 11).[124] This mechanism is considered a major source of 3-deoxyglucosone *in vivo*.[108]

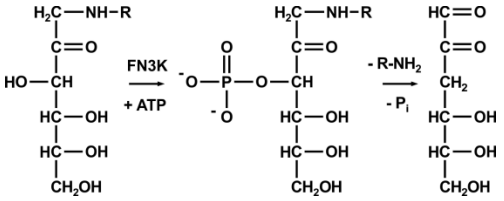

Figure 11: Mechanism of fructosamine-3-kinase.[102]

Several enzymes are involved in the limitation of glycation by detoxification of potential precursors like α-dicarbonyls. The cytosolic glyoxalase system is the major regulator of cellular GO and MGO concentrations. In the first step a hemithioacetal intermediate is formed by non-enzymatic reaction of a α-dicarbonyl, e.g., MGO and glutathione (GSH). Glyoxalase I catalyzes the intramolecular redox reaction (disproportionation) to the thioester, e.g., lactoylglutathione. Finally, glyoxalase II hydrolyzes the thioester resulting in the α-hydroxy carboxylic acid (e.g., lactic acid) and regeneration of GSH (Figure 12).[125]

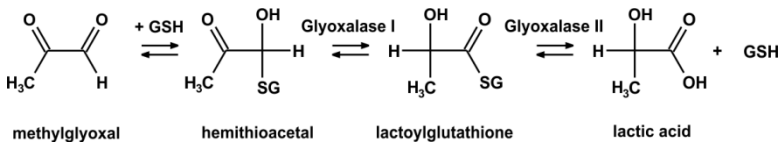

Figure 12: Detoxification of MGO by the glyoxalase system.[126]

An alternative minor pathway are enzymes of the aldo-keto reductase family, e.g., aldoreductase isoforms 1B1, 1B3, and 1B8 for GO and isoforms 1A4, 1B1, and 1B3 for MGO degradation.[127] Nevertheless, in tissues with low glyoxalase activity, e.g., renal medulla and for glucosones like 3-deoxyglucosone, which are not targeted by glyoxalase,[125] enzymes of aldo-keto reductase type are the primary detoxification mechanism.[128,129] The catalytic reduction of α-dicarbonyls by aldo-keto reductases is NADPH dependent. However, the product distribution is glutathione dependent, because the enzymes use either unhydrated

carbonyls or glutathione hemithioacetals. Acetol is the major product of enzymatic reduction of free MGO, while the hemithioacetal forms lactaldehyde. Both structures are possibly further reduced by aldo-keto reductases to propanediol (Figure 13). [130]

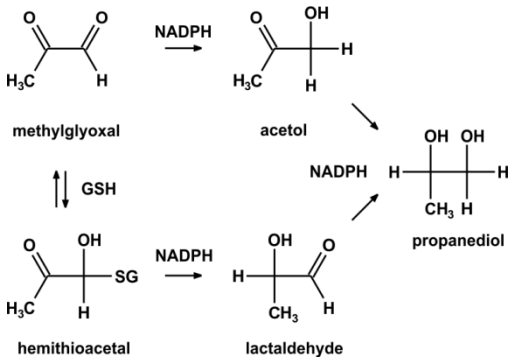

Figure 13: Detoxification of MGO by aldo-keto reductases.[130]

In addition, MGO dehydrogenases (aldehyde dehydrogenases E1, E2, and E3)[131] and 3-deoxyglucosone dehydrogenase (aldehyde dehydrogenase 1A1)[132] are described in literature as minor degradation mechanisms.[108] MGO and 3-deoxyglucosone dehydrogenases catalyze NAD or NADP dependent oxidation of unhydrated α-dicarbonyls (Figure 14).[130]

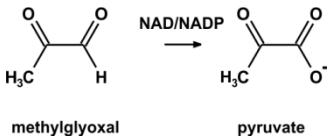

Figure 14: Detoxification of MGO by aldehyde dehydrogenases.[130]

Recently, DJ-1 was described as a novel regulator of glycation in human metabolism. DJ-1 was originally discovered as an oncogene and a factor in Parkinson's disease, but was later linked to protection against oxidative stress and cell death.[133] The exact biochemical mechanism of DJ-1 remains unclear, but several studies report low glyoxalase-like activity[133,134] and deglycase activity for GO/MGO derived AGEs.[135–138] In contrast, some studies start to question catalytic activity and relevance of DJ-1 for regulation of glycation *in vivo*.[139,140]

Chemicals like bardoxolone methyl, which is a nuclear factor erythroid 2-related factor 2 (NRF2) activator, are an effective way to stimulate expression of glyoxalase, aldo-keto reductases, and aldehyde dehydrogenases. This increases dicarbonyl detoxification, which is especially beneficial in diabetic patients with chronic renal disease.[141] Unfortunately,

bardoxolone methyl has serious heart-related adverse effects including heart failure and clinical trials were stopped.[142] Combination of NRF2 activators *trans*-resveratrol and hesperidin is an improved method currently under development.[143]

Another strategy to prevent carbonyl stress is activation of transketolase by thiamine or its monophosphate derivative benfotiamine. Thus, formation of triosephosphates and subsequently α-dicarbonyls is reduced.[144] An additional factor may be the recently reported enzymatic conversion of glycolaldehyde to less reactive erythrulose via transketolase, which decreased glycation up to 70 % *in vitro*.[145]

Beside activation of enzymatic regulatory pathways the scavenging of α-dicarbonyls is one of the oldest approaches to reduce dicarbonyl stress. The prototype compound is aminoguanidine, which reacts with dicarbonyls to form 3-amino-1,2,4-triazine derivatives (Figure 15).[146] Despite aminoguanidine is an excellent α-dicarbonyl scavenger *in vitro* it is not applicable *in vivo* due to toxicity problems at clinical relevant concentrations.[147] Alternatively, carbonyl scavenging by thiols is of central interest,[148] e.g., by cysteine derivatives like *N*-acetylcysteine[149] and penicillamine (3,3-dimethyl-cysteine).[150]

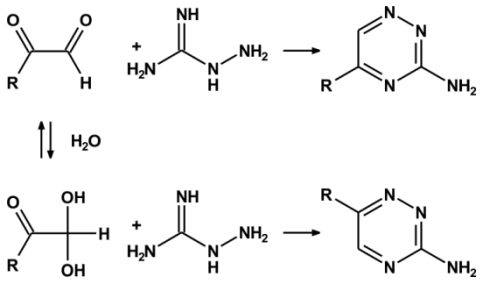

Figure 15: Scavenging of α-dicarbonyls by aminoguanidine.[146]

The chemical "breaking" of AGE crosslinks by *N*-phenacylthiazolium bromide (PTB) and its analogue alagebrium (ALT-711) was another idea to treat glycation. However, studies indicate ambiguous results and various alternative mechanisms. Consequently, the concept of crosslink breakers is controversial at best.[151]

In recent years, food-derived phenolic compounds gained interest as potential carbonyl scavengers.[152] Several flavonoids like luteolin, rutin, quercetin, and epigallocatechin-3-gallate (EGCG) inhibit MGO mediated AGE formation *in vitro* by 82.2 %, 77.7 %, 65.5 % and 69.1 %, respectively.[153] EGCG is the major flavonoid in green tea and traps about 90 % of MGO in 10 min under physiological conditions. Due to sterically reasons positions 6 and 8 of the A-ring show highest nucleophilicity and mixtures of 6-mono-MGOEGCG,

8-mono-MGOEGCG, and 6,8-di-MGOEGCG adducts are formed depending on reaction conditions (Figure 16).[154]

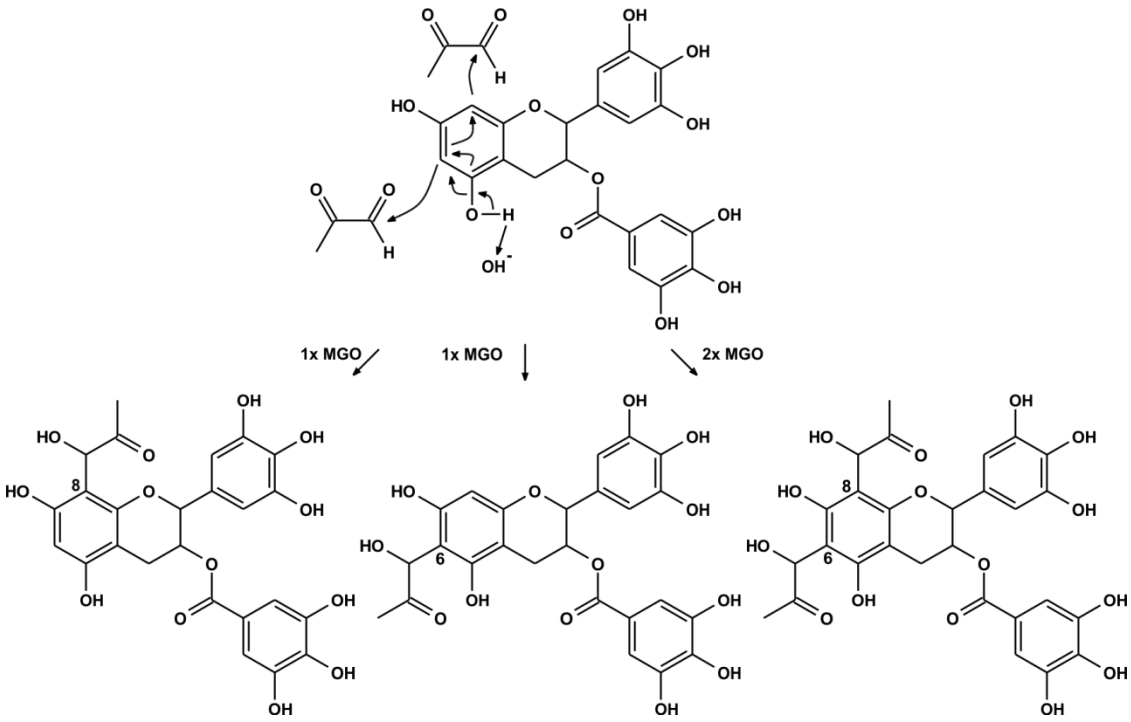

Figure 16: Scavenging of MGO by EGCG.[154]

Scavenging of dicarbonyls by flavonoids *in vivo* is more complex because of factors like bioavailability, metabolic processing, oxygen pressure, pH, and presence of competing compounds.[152] Nevertheless, dicarbonyl scavenging by soybean genistein, which shares the A-ring motif with EGCG and a MGO trapping efficiency of up to 97.7 %,[155] was extensively researched in mice. In contrast to *in vitro* experiments, only mono-MGO adducts as well as their metabolites were detected in mouse urine. Interestingly, except of 6-hydroxygenistein and 8-hydroxygenistein all genistein metabolites are comparable efficient scavengers, highlighting the importance of the A-ring motif.[156]

2.3.5 Glycation in aging and disease

Glycation is a potential biomarker of aging[157] and was made responsible as a potential cause of aging (glycation hypothesis of aging).[158] Especially in extracellular proteins with low turnover like collagen[121] and α-crystalline[159] levels of AGEs correlate with aging and several studies identified glycation as a molecular mechanism leading to age related tissue stiffening[121,160] and cataract formation.[161,162]

Glycation is not limited to extracellular proteins and modification of intracellular proteins is influencing several hallmarks of aging like loss of proteostasis, epigenetic alteration, mitochondrial dysfunction, and inflammation.[163] As an example AGEs cause reduced efficiency of the ubiquitin-proteasome system,[164] compete with ubiquitination sites[165] and prevent accessibility of substrates by aggregation and crosslinking.[166] Thus, regular protein homeostasis is readily impaired by glycation leading to serious complications, e.g., reduction of life span and contribution to pathologies like Alzheimer's disease.[166,167] Moreover, histones are highly modified by glycation with an increase in aging and diabetes.[168] Glycation changes the histone structure[169] and possibly competes with sites of acetylation, thus AGEs interfere with epigenetic regulation.[138] Aged mitochondria are characterized by a decrease of respiration and ATP production. Similar effects are inducible by glycation of, e.g., glutamate dehydrogenase and isolated mitochondria *in vitro* and *in vivo*.[170–172] But decrease of respiration is only one side of mitochondrial dysfunction induced by AGEs, as on the other side production of reactive oxygen species increases.[173] These reactive intermediates mediate acute inflammatory response.[174] In addition, proteins modified by CML and other AGEs are discussed as potential ligands binding to the receptor for AGE (RAGE).[175] RAGE was discovered in 1985[176] and characterized in 1992.[177] Binding to RAGE triggers intracellular signaling cascades leading to activation of NF-κB, which induces molecular mechanisms of inflammation reactions.[178] These RAGE mediated processes are involved in etiology of vascular diseases[179] and potentially explain late stage complications of diabetes and uremia.[179] Diabetes was first linked to glycation by detection of HbA1c, which is hemoglobin with an Amadori product at the N-terminal valine residue, as an important biomarker to assess long-term blood glucose concentrations.[180] Later, elevated concentrations of glucose and α-dicarbonyls[181] resulting in higher AGE concentrations were postulated as major causes for diabetic complications like atherosclerosis, neuropathy, and nephropathy.[182] Atherosclerosis is the most serious consequence of diabetes and the major cause of death in these patients. It is characterized by formation and deposition of atherosclerotic plaques in arterial walls, narrowing of blood vessels, and finally myocardial infarction.[5] Pathogenesis of atherosclerosis is facilitated by glycation because glycated low-density lipoprotein (LDL) is not recognized by LDL receptor but uptake by macrophages is enhanced.[183] In contrast, glycation of high-density lipoprotein (HDL) increases its turnover and reduces its efficiency during reverse cholesterol transport.[184] Thus, glycation of lipoproteins results in hyperlipidemia and accelerated foam cell formation.[5] As mentioned above, crosslinking of structure proteins, e.g., collagen[185] and activation of RAGE are additional triggers of diabetic

atherosclerosis.[186] Diabetic neuropathy is characterized by demyelination and axonal degeneration of peripheral neurons.[5] Glycated myelin stimulates macrophages to excrete proteases and is prone to phagocytosis.[187] Additionally, demyelination of neurons can be caused by AGEs binding to immunoglobulins.[188] Severity of diabetic nephropathy correlates with AGEs found in renal tissues.[189] In analogy to atherosclerosis, modification of collagen by AGEs thickens the basement membrane and impairs glomerular filtration. This effect is exaggerated by AGE mediated activation of transforming growth factor-β (TGF-β) which in turn stimulates synthesis of collagen.[190] Ultimately, loss of glomerular function causes renal failure and uremia.[5] Patients with chronic renal failure accumulate dicarbonyls and AGE free adducts, because these substances are not excreted via urine anymore.[191] The accumulation of dicarbonyl and oxidative stress damages DNA and interacts with RAGE, which possibly explains the higher incidence of cancer in chronic kidney disease.[192] RAGE is typically overexpressed in cancer and AGE induced proinflammatory RAGE-NF-κB signaling is considered as an important mechanism in development of cancer.[193] Moreover, AGE treatment of breast[194] and prostate[195] cancer cell lines promotes cell growth, migration, and invasion. Last but not least, glycation is a potential mechanism in Alzheimer's disease (AD). Hallmarks of this disease are formation of intracellular tau protein aggregates called neurofibrillary tangles (NFTs) and extracellular amyloid-β (Aβ) plaques.[196] In AD high sucrose diet increases Aβ concentrations,[197] while insulin improves performance in cognitive tasks.[198] AGEs upregulate production of the amyloid-β precursor protein[199] and levels of AGEs are 3 times higher in plaques extracted from AD brains compared to preparations from healthy and age-matched controls. Hence, glycation possibly stabilizes and promotes aggregation of Aβ and tau.[200] In addition, glycation increases neurotoxicity of Aβ plaques, which could be prevented by dicarbonyl scavenger aminoguanidine.[201]

3 Objectives

The central aim of this work was to elucidate mechanisms of non-enzymatic acylation *in vitro*, detect novel acylation structures and highlight the importance of acylation *in vivo* using models of aging and disease.

First of all, acylation by Maillard reaction in GO and MGO isomerization cascades was researched in N^2-Boc-lysine model incubations. Authentic reference standards of N^6-glyoxylyl and N^6-pyruvoyl lysine were synthesized and used to detect and quantitate these α-oxoamide AGEs for the first time using a novel HPLC-MS/MS method. The effects of aeration and pH on product spectrum of the complex GO/MGO isomerization cascades were extensively studied. Findings from incubations were transferred to rat liver models to establish α-oxoamide AGEs as markers of aging and oxidative stress.

To access acylation by RACS, a novel HPLC-MS/MS multimethod for simultaneous detection and quantitation of 14 acylation structures was developed including synthesis of authentic reference standards and structure elucidation. The method was validated and an optimized enzymatic hydrolysis protocol was developed. Levels of acylation were quantitated in a screening of mice liver, kidney, heart, and brain. Specific modification patterns were detected and liver was identified as a local "hotspot" of acylation. Enrichment of analytes by repetitive fractionation and pooling of samples resulted in the identification of 4 novel acylation structures *in vivo*.

Finally, 20 PTMs derived by glycation, acylation, oxidative stress, and citrullination were analyzed on a quantitative basis using HPLC-MS/MS analysis. A fractionation protocol was developed to extract and purify histone, mitochondrial, and cytosolic proteins from mouse liver. Changes of PTMs in subcellular compartments were correlated to aging and discussed comprehensively.

The results were published and discussed in international renowned peer-reviewed journals. Detailed experimental procedures were given in the attached publications. The following chapters aimed to further enhance the discussion by embedding the results in the context of currently available literature.

4 Discussion

4.1 Acylation by isomerization of short-chain α-dicarbonyls

Short-chain α-dicarbonyls like glyoxal (GO) and methylglyoxal (MGO) are reactive intermediates produced *in vivo* (chapter 2.3.3).[108] According to literature the relative reactivity of glucose compared to GO and MGO towards glycation is about 1:6000:20000.[127] This explains why short-chain α-dicarbonyls are the most relevant glycating structures *in vivo* despite blood plasma concentrations of GO (491 pmol/mL) and MGO (61 pmol/mL)[202] are magnitudes below glucose concentration (6100 pmol/mL).[203] Beside individual structure, the glycating potential of dicarbonyls *in vivo* depends on steady state concentration of reactive dicarbonyl form and reversible side reactions with cysteine residues.[127]

GO exists mainly in dihydrate form and only 0.002 % is in the highly reactive dicarbonyl form in aqueous solutions (Figure 17A). The half time for conversion of dihydrate form to dicarbonyl form is 35 s. Methylglyoxal is a mixture of 1 % dicarbonyl, 70 % monohydrate, and 29 % dihydrate form in aqueous solutions (Figure 17B). The half time for conversion is 20 s. Consequently, dicarbonyl forms of GO and MGO are rapidly regenerated after dicarbonyl consumption by glycation.[127]

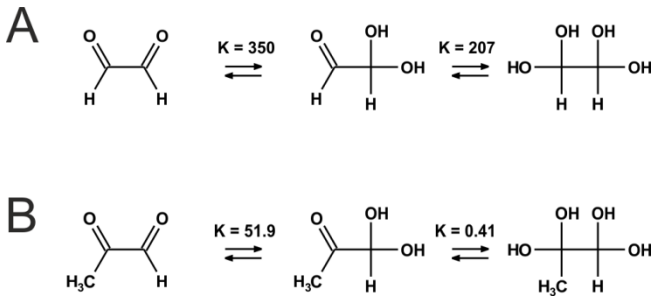

Figure 17: Equilibrium of GO (A) and MGO (B) hydration in aqueous solution.[127]

After the discovery of N^6-carboxymethyl lysine (CML) and N^6-carboxyethyl lysine (CEL) as two of the most abundant AGEs *in vivo*,[204] GO[120] and MGO[205] were identified as their potential precursors, respectively. In 2001, Glomb and Pfahler discovered the formation of amide AGEs, e.g., N^6-glycoloyl lysine (GALA) as alternative endproducts in the complex isomerization cascade of GO.[123] A similar isomerization mechanism of MGO leads to formation of N^6-lactoyl lysine.[206]

In the present thesis the modulation of the complex GO and MGO isomerization cascades was investigated. At first, formation of AGEs over time was quantitated *in vitro* using incubations

of 40 mM N^2-Boc-lysine and either 40 mM GO or 40 mM MGO under physiological conditions (100 mM phosphate buffer, pH 7.4, 37 °C) and aeration (Table 9).

Table 9: Formation of AGEs in N^2-Boc-lysine incubations under physiological conditions (pH 7.4, 37 °C) and aeration (mean ± standard deviation, n = 3).[122]

AGEs	[mmol/mol lysine]				
	24 h	**48 h**	**72 h**	**96 h**	**168 h**
GO incubation					
N^6-Carboxymethyl lysine	30 ± 9	54 ± 6	61 ± 7	73 ± 1	112 ± 14
N^6-Glycoloyl lysine	0.3 ± 0.1	2.0 ± 0.1	3.5 ± 0.4	4.3 ± 0.4	7.3 ± 0.5
N^6-Glyoxylyl lysine	0.4 ± 0.1	1.3 ± 0.2	2.1 ± 0.1	3.0 ± 0.2	4.8 ± 0.4
MGO incubation					
N^6-Carboxyethyl lysine	0.4 ± 0.1	0.6 ± 0.1	0.82 ± 0.02	0.9 ± 0.1	1.10 ± 0.02
N^6-Lactoyl lysine	0.23 ± 0.04	0.29 ± 0.01	0.32 ± 0.01	0.33 ± 0.02	0.39 ± 0.01
N^6-Pyruvoyl lysine	0.03 ± 0.01	0.03 ± 0.01	0.04 ± 0.01	0.04 ± 0.01	0.07 ± 0.02

After 168 h CML reached 112 mmol/mol lysine and GALA 7.3 mmol/mol lysine in GO incubations. CML levels were in the same magnitude as previously reported for incubations containing 40 mM ribose with 91 mmol/mol lysine and more than 4 times higher for GALA (1.7 mmol/mol lysine). In 40 mM GO incubations far more CML and GALA were formed than in incubations of 200 mM glucose with 0.85 and 0.13 mmol/mol lysine, respectively.[123] Thus, isomerization of GO has to be considered as a major pathway leading to CML and lysine acylation by GALA. The ratio between CML and GALA was 100:1 after 24 h and continuously dropped to 15:1 after 168 h.

In MGO incubations CEL reached 1.10 mmol/mol lysine and N^6-lactoyl lysine 0.39 mmol/mol lysine after 168 h. Similar concentrations of N^6-lactoyl lysine were previously published.[206] Compared to incubations containing 42 mM 1-deoxyglucosone about twice as much N^6-lactoyl lysine was formed by MGO after 72 h indicating the importance of MGO isomerization for lysine acylation.[105] In contrast to GO incubations, ratio between CEL and N^6-lactoyl lysine was constant between 2 and 3 in MGO incubations.

Comparing carboxyalkyl structures it was strikingly clear that about a factor of 100 more CML was formed than CEL, because N^2-Boc-lysine had to attack at the aldehyde function of GO and at the less reactive keto function of MGO, respectively (Figure 10). In case of α-hydroxyamide AGEs both structures required the attack of N^2-Boc-lysine at the respective aldehyde function of GO or MGO. This reduced the inductive effect (+I) of the additional methyl group of MGO and resulted in a factor of 15 between GALA and N^6-lactoyl lysine.

A novel HPLC-MS/MS method was developed using synthesized standards of N^6-glyoxylyl lysine and N^6-glyoxylyl lysine. Thus, formation of N^6-glyoxylyl lysine in aerated GO incubations and N^6-pyruvoyl lysine in aerated MGO incubations was detected for the first time. Putative direct oxidation of α-hydroxyamide AGEs to α-oxoamide AGEs was excluded by aerated incubations of GALA and N^6-lactoyl lysine. In addition, α-oxoamide AGEs were not detected in N^2-Boc-lysine incubations containing glyoxylic acid, pyruvic acid, ascorbic acid, maltose, or the Amadori product of glucose and N^2-Boc-lysine. Corresponding carboxylic acids are the main products of α- and β-dicarbonyl cleavages in aqueous systems.[106] Neither glyoxylic nor pyruvic acid were detected in GO and MGO incubations by GC-MS. Consequently, cleavage of a putative condensation product was ruled out and oxidation of an intermediate in the CML/CEL isomerization cascade was identified as the precursor of α-oxoamide AGEs.

This notion was further supported by incubations of either GO or MGO and N^2-Boc-lysine under aeration versus deaeration proving exclusive α-oxoamide AGE formation under aeration. In contrast to α-oxoamides no significant changes of carboxyalkyl and α-hydroxyamide AGEs were detected between aerated versus deaerated conditions confirming the non-oxidative pathways of their formation (Table 10).

Table 10: Effect of aeration and deaeration on formation of AGEs in N^2-Boc-lysine incubations under physiological conditions (pH 7.4, 37 °C) after 168 h (mean ± standard deviation, n = 3). [122]

AGEs	[mmol/mol lysine]			
	GO		MGO	
	Aeration	Deaeration	Aeration	Deaeration
N^6-Carboxymethyl lysine	112 ± 14	118 ± 5	-	-
N^6-Glycoloyl lysine	7.3 ± 0.5	6.2 ± 0.2	-	-
N^6-Glyoxylyl lysine	4.8 ± 0.4	< LOD	-	-
N^6-Carboxyethyl lysine	-	-	1.10 ± 0.02	1.17 ± 0.03
N^6-Lactoyl lysine	-	-	0.39 ± 0.01	0.31 ± 0.06
N^6-Pyruvoyl lysine	-	-	0.07 ± 0.02	< LOD

Last but not least, the effects of pH variation between 4.5, 7.4, and 9.6 on product spectrum of the CML/CEL isomerization cascades were examined *in vitro* (Table 11).

Table 11: Effect of pH on formation of AGEs in N^2-Boc-lysine incubations under aeration at 37 °C after 168 h (mean ± standard deviation, n = 3). [122]

AGEs	[mmol/mol lysine]					
	GO			MGO		
	pH 4.5	pH 7.4	pH 9.6	pH 4.5	pH 7.4	pH 9.6
N^6-Carboxymethyl lysine	0.6 ± 0.3	127 ± 6	150 ± 15	-	-	-
N^6-Glycoloyl lysine	< LOD	5.8 ± 0.1	24.4 ± 0.6	-	-	-
N^6-Glyoxylyl lysine	< LOD	3.1 ± 0.8	12.1 ± 0.9	-	-	-
N^6-Carboxyethyl lysine	-	-	-	0.12 ± 0.04	0.99 ± 0.04	0.98 ± 0.07
N^6-Lactoyl lysine	-	-	-	< LOD	0.38 ± 0.01	1.37 ± 0.06
N^6-Pyruvoyl lysine	-	-	-	< LOD	0.04 ± 0.01	0.14 ± 0.01

As expected, virtually no AGEs were detected at pH 4.5, because at this pH the N^6-amino function of N^2-Boc-lysine was protonated. Protonation decreased nucleophilicity of the amino function and the initial attack at the dicarbonyl was inhibited. At pH 7.4 the amino function was sufficiently deprotonated and after nucleophilic attack Schiff base adducts were formed and isomerized to yield AGEs. Interestingly, increase of pH from 7.4 to 9.6 had little to no effects on carboxyalkyl AGEs CML with 127 versus 150 mmol/mol lysine and CEL with 0.99 versus 0.98 mmol/mol lysine. On the other hand concentrations of α-hydroxyamide and α-oxoamide AGEs increased by a factor of 4 at pH 9.6 compared to pH 7.4, e.g., GALA increased from 5.8 to 24.4 mmol/mol lysine and N^6-glyoxylyl lysine from 3.1 to 12.1 mmol/mol lysine. Obviously, mechanism of isomerization and driving force were different for carboxyalkyl and amide AGEs. CML and CEL formation were pH independent, possibly because of the high thermodynamic stability of the carboxyalkyl AGEs. In contrast, pH-related changes in the kinetics of rearrangement prevailed in α-hydroxyamide and α-oxoamide formation. A possible explanation was stabilization of the central enaminol intermediate in amide AGE formation as described by Hofmann et al., who proved higher stability of acid labile enaminols at higher pH.[207]

Taking all data under consideration, a mechanism of α-oxoamide AGE formation was developed. As mentioned above, artifacts and cleavage mechanisms were excluded as possible sources. Hence, isomerization of GO and MGO lysine adducts remained as the only pathways. The pH variation indicated a similar pathway for α-oxoamides and α-hydroxyamides, but a mechanism distinct from carboxyalkyl isomerization. Compared to α-hydroxyamide AGEs an oxidation step was required by definition. Because direct oxidation of α-hydroxyamide AGEs GALA and N^6-lactoyl lysine was not observed, the central enaminol intermediate in the isomerization leading to amide AGEs remained as the most

promising candidate. Enaminols are electron rich intermediates and are readily oxidized as reported previously for the formation of acids in the Strecker degradation of amino acids. Isotopic labeling experiments ruled out direct oxidation of Strecker aldehydes to Strecker acids and supported our hypothesis. Under food related conditions at high temperatures ratio of Strecker aldehyde to acid shifted from 4:1 under deaeration to almost 1:2 under aeration.[207] A formation mechanism was postulated for α-oxoamides N^6-glyoxylyl lysine and N^6-pyruvoyl lysine (Figure 18A), which is very similar to the oxidative Strecker acid formation (Figure 18B).

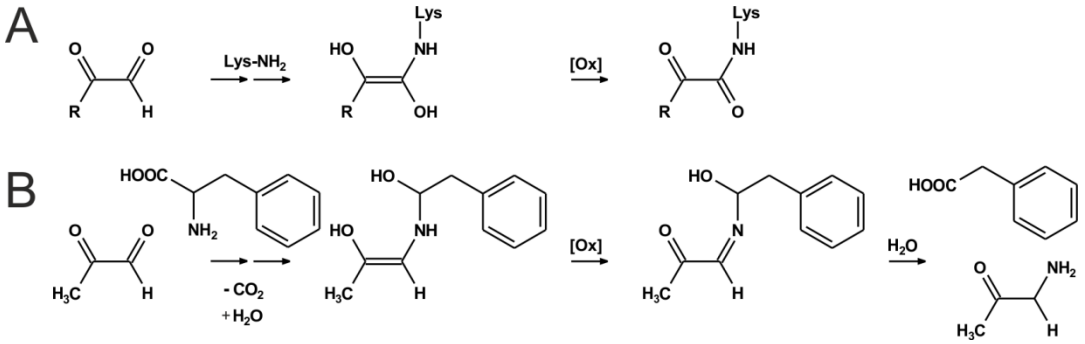

Figure 18: Mechanism of α-oxoamide AGE (A) and Strecker acid (B) formation.[122,207]

Prior to detection of N^6-glyoxylyl lysine and N^6-pyruvoyl lysine *in vivo*, the HPLC-MS/MS method had to be modified. Due to equilibrium between free α-oxoamide AGEs and their hydrated forms, chromatographic separation resulted in very broad peaks with up to 5 min peak width and very low signal to noise ratio. Limit of detection (LOD) and quantitation (LOQ) were significantly improved by derivatization using $NaBD_4$ prior to chromatographic separation. As indicated in Figure 19, N^6-glyoxylyl and N^6-pyruvoyl lysine were detected as their corresponding derivatives N^6-glycoloyl lysine-d1 and N^6-lactoyl lysine-d1, respectively. This required correction of α-oxoamide AGE concentrations by subtraction of interfering isotope peaks of GALA (10.16 %) and N^6-lactoyl lysine (11.17 %).

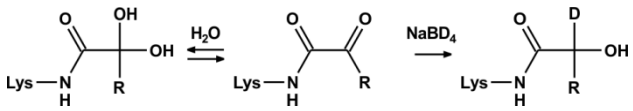

Figure 19: Stabilization of α-oxoamide AGEs by $NaBD_4$ reduction.

As mentioned above AGE precursors like α-dicarbonyls are mainly cleared by kidney via urinary excretion. The same mechanism is used to eliminate degradation products of AGE modified proteins, e.g., AGE free adducts.[208] However, the presumed size cut-off in the kidney filtration apparatus is approximately 45 kDa and glycated proteins exceeding this molecular mass are not directly excreted by urine.[209,210] In radioactive labeling studies with injection of glycated bovine serum albumin (BSA, 67 kDa) about 90 % of radioactivity accumulated in liver and only 2 – 3 % in kidney after 60 min. Uptake of AGE modified BSA in liver sinusoidal endothelial, Kupffer, and parenchymal cells was 60 %, 25 %, and 10 ± 15 %, respectively.[211] Hence, liver is potentially the primary organ for degradation of large AGE modified proteins in the blood circulation prior to urinary excretion of degradation products.[209]

On the basis of the extraordinary high importance of liver in AGE metabolism, cytosolic proteins were extracted from livers of 3 month old healthy, 3 month old cirrhotic, and 22 month old healthy rats. Extracted proteins were reduced by $NaBD_4$ and hydrolyzed. Finally, enzymatic hydrolysates were analyzed by HPLC-MS/MS and concentrations of CML, GALA, N^6-glyoxylyl lysine, CEL, N^6-lactoyl lysine, and N^6-pyruvoyl lysine were quantitated using standard addition calibration (Table 12).

Table 12: AGEs in cytosolic proteins from rat liver (mean ± standard deviation, n = 5). [122]

AGEs	[µmol/mol leucine-eq]		
	3 month old (healthy)	**3 month old (cirrhosis)**	**22 month old (healthy)**
N^6-Carboxymethyl lysine	5.22 ± 3.34	5.40 ± 3.83	10.07 ± 7.01**
N^6-Glycoloyl lysine	0.73 ± 0.07	0.70 ± 0.09	1.36 ± 0.32**
N^6-Glyoxylyl lysine	0.37 ± 0.03	0.57 ± 0.16*	0.58 ± 0.03*
N^6-Carboxyethyl lysine	11.73 ± 2.32	8.34 ± 2.52	17.27 ± 4.35**
N^6-Lactoyl lysine	0.28 ± 0.06	0.34 ± 0.09	0.55 ± 0.06**
N^6-Pyruvoyl lysine	0.11 ± 0.04	0.23 ± 0.05*	0.27 ± 0.07*

Significant differences (t-test) compared to AGE levels in 3 month old healthy rats: * $p < 0.05$, ** $p < 0.001$.

In general, the mean level of glycation approximately doubled comparing 3 and 22 month old rats, e.g., acylation by GALA increased from 0.73 to 1.36 µmol/mol leucine-eq and N^6-lactoyl lysine increased from 0.28 to 0.55 µmol/mol leucine-eq. The accumulation of AGEs in aging was significant with p-values below 5 % for α-oxoamide AGEs and p-values below 0.1 % for CML, CEL, GALA, and N^6-lactoyl lysine. Mechanisms like reduced glyoxalase activity,[125] decreased degradation of glycated proteins[166] and impaired excretion of AGE degradation products[209] potentially caused accumulation of AGEs observed in aged

liver. At first, ratio between CML and CEL *in vivo* was quite unexpected considering the much higher formation of CML *in vitro* and additional pathways leading to CML, e.g., oxidative fragmentation of Amadori product.[204] Unfortunately, AGE levels were never quantitated by HPLC-MS/MS in cytosolic proteins of liver before, but similar concentrations of CML (269 µmol/mol lysine) and CEL (329 µmol/mol lysine) were reported for rat kidney.[212] The accumulation of CML was previously reported for rat liver mitochondria[213] and human extracellular tissue of aged heart and kidney.[214]

Liver cirrhosis is the end-stage pathology of various chronic liver diseases. A pivotal mechanism in its pathogenesis is the activation of hepatic stellate cells and subsequent transforming growth factor β (TGF-β) mediated fibrosis, i.e., infiltration of hepatic tissue by collagen.[215] TGF-β is considered as the key regulator of fibrosis and can be activated by AGEs via RAGE signalling.[216,217] Consequently, involvement of AGEs in liver diseases was postulated.[218] This notion was supported by studies of Sebekova et al., who used a CML specific antibody to detect increased CML levels in plasma proteins of cirrhotic patients.[219] This study led to the development of a test for cirrhosis by analyzing CML concentrations in blood serum proteins via ELISA.[220]

In our model liver cirrhosis was induced in rats by inhalation of tetrachloromethane as described previously.[221] The pathogenesis of cirrhosis was verified by histological sirius red staining of collagen in liver (Table 13). Collagen increased from 0.5 % in healthy animals to 23 % in cirrhotic animals indicating severe fibrosis, which is characteristic for liver cirrhosis.[222] In addition, Western blotting of specific markers like TGF-β and α-smooth-muscle actin (α-SMA) were used to determine severity of cirrhosis.[223,224] Intensities of TGF-β and α-SMA were referenced as 100 % in Western blots from young and healthy rats and increased to 947 and 1995 % in cirrhotic liver, respectively. Collagen, TGF-β, and α-SMA increased in aging as well, but the increases in cirrhosis were up to 10-fold higher (Table 13).

Table 13: Markers of cirrhosis in rat liver (mean ± standard deviation, n = 5). [122]

Markers of cirrhosis	**[%]**		
	3 month old (healthy)	**3 month old (cirrhosis)**	**22 month old (healthy)**
Sirius red staining	0.5 ± 0.1	23 ± 3*	1.7 ± 0.4*
TGF-β	100 ± 26	947 ± 661*	478 ± 143*
Smooth muscle antigen	100 ± 31	1995 ± 1057*	453 ± 192*

Significant differences (Mann-Whitney) compared to markers of cirrhosis in 3 month old healthy rats: * $p < 0.05$.

Ahmed et al. used HPLC-MS/MS for AGE quantitation in hepatic blood of cirrhotic patients. They detected elevated levels of free and protein-bound CML in plasma but constant levels of CEL.[225] In our cirrhosis model levels of CML, CEL, and α-hydroxyamide AGEs remained constant in cytosolic liver proteins compared to healthy rats. The only exception were α-oxoamide AGEs (Table 12). N^6-glyoxylyl lysine significantly increased from 0.37 to 0.58 µmol/mol leucine-eq and N^6-pyruvoyl lysine from 0.11 to 0.27 µmol/mol leucine-eq. Apparently, accumulation of α-oxoamide AGEs was not exclusively caused by aging but additional factors as well. Considering the exclusive formation of α-oxoamide AGEs under aeration the elevated oxidative stress in liver cirrhosis was the most likely factor. Indeed, elevated production of superoxide in cirrhosis was reported in literature.[226] Whereas the average N^6-glyoxylyl lysine/GALA and N^6-pyruvoyl lysine/N^6-lactoyl lysine ratios were constant at 0.5 in healthy young and aged rat livers, the ratios in cirrhotic livers increased to 0.8 for N^6-glyoxylyl lysine/GALA and 0.7 for N^6-pyruvoyl lysine/N^6-lactoyl lysine. Thus, the ratio between oxidation of enaminol precursor to α-oxoamide AGEs and oxidation independent isomerization to α-hydroxyamide AGEs is possibly an excellent marker to measure long-term oxidative stress *in vivo*. While elevated CML concentration in serum proteins is a validated predictor of cirrhosis,[220] CML levels in cytosolic liver protein were not changed in cirrhosis. In contrast, α-oxoamide AGE levels increased in cytosolic liver proteins of cirrhotic animals. Consequently, α-oxoamide AGEs seem to be a more sensitive marker of cirrhosis and oxidative stress than CML. A possible explanation is that several oxidative and non-oxidative pathways generate CML,[111] but α-oxoamide AGEs are exclusively formed by oxidative pathways.

4.2 Quantitation of acylation by HPLC-MS/MS

Acetylation of histone proteins was discovered in 1963[8] and the modification's pivotal role in epigenetic regulation was postulated by Allfrey in 1964.[30] Prior to detection of the first histone acetyltransferase in 1995 lysine acetylation was considered as a non-enzymatic mechanism,[227] because Paik et al. measured incorporation of radioactivity in isolated histones incubated with ^{14}C-labeled acetyl-CoA.[228] Recently, the concept of non-enzymatic modification of lysine was established for several additional reactive acyl-CoA species (RACS) and a plethora of novel acylated lysine modifications was quantitated in the present thesis (Figure 20).[3,12,48,51]

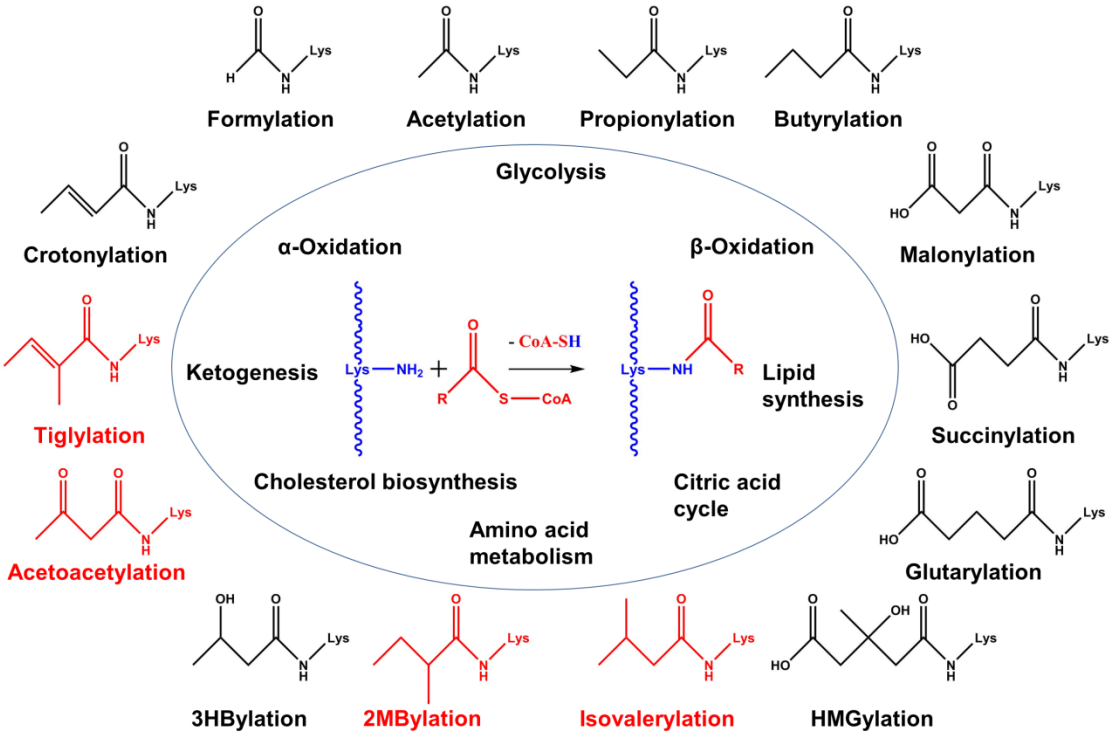

Figure 20: Lysine acylations by RACS quantitated in the present study (red = novel modification).

The traditional way to measure and detect novel acyl lysine modifications is the proteomic approach. Therefore, isolated proteins are incubated with trypsin and the resulting peptides are analyzed using HPLC-MS/MS. After detection of acylation specific mass shifts the identity must be verified by high resolution MS/MS spectra and coelution with synthetic (modified) peptides.[11,229] This approach is limited to high abundant modifications, e.g., formylation[230] and succinylation.[42] Modifications with lower abundance, e.g., butyrylation[41] and glutarylation[45] require additional enrichment by immunoprecipitation prior to mass

spectrometry. Depending on availability of specific antibodies immunological methods like Western blotting are useful tools to analyze acylation. Both methods detect site-specific and relative changes in the acylome. However, absolute quantitation and monitoring of more than one type of acylation at a time is not possible using this approach.[80,100]

A novel HPLC-MS/MS method in combination with quantitative enzymatic hydrolysis of proteins was developed to overcome these drawbacks and measure acylation in mice liver, brain, kidney, and heart (Table 14).

Table 14: Acylated lysine modifications in mouse organ lysates (mean ± standard deviation, n = 7). [231]

Modification	[µmol/mol leucine-eq]			
	Liver	**Kidney**	**Heart**	**Brain**
N^6-Formyl lysine	9.61 ± 1.68	10.60 ± 3.05	14.11 ± 1.20	6.15 ± 1.35
N^6-Malonyl lysine	2.11 ± 0.20	1.11 ± 0.20	0.69 ± 0.15	0.50 ± 0.12
N^6-Acetyl lysine	37.31 ± 3.60	15.01 ± 1.19	16.11 ± 3.16	34.62 ± 8.10
N^6-Succinyl lysine	6.12 ± 0.60	5.53 ± 0.70	4.73 ± 0.75	3.22 ± 0.53
N^6-Propionyl lysine	0.36 ± 0.05	0.29 ± 0.10	0.66 ± 0.12	0.13 ± 0.02
N^6-Glutaryl lysine	0.81 ± 0.19	0.42 ± 0.06	0.34 ± 0.10	0.40 ± 0.13
N^6-Butyryl lysine	0.13 ± 0.03	0.05 ± 0.04	0.38 ± 0.06	0.22 ± 0.04
N^6-Crotonyl lysine	0.02 ± 0.01	0.02 ± 0.01	0.02 ± 0.01	0.01 ± 0.01
Total	**56.47**	**33.03**	**37.04**	**45.25**

Liver was identified as the local hotspot of acylation with total acylation levels of 56.47 µmol/mol leucine-eq and lowest concentrations were measured in kidney with 33.03 µmol/mol leucine-eq. Acetylation is formed by several acetyl-CoA dependent enzymatic pathways[2] as well as non-enzymatic reactions like Maillard catalyzed degradation of 1-deoxyglucosone.[105] As expected, acetylation was the most abundant modification in all organs. Concentrations reached up to 37.31 µmol/mol leucine-eq in liver, which equaled roughly 65 % of total acylation measured in this organ. Second highest N^6-acetyl lysine concentrations were detected in brain with 34.62 µmol/mol leucine-eq, which equaled 75 % of total acylation. This highlighted the previously described pivotal role of acetylation in brain development and neuropathies.[235] In kidney and heart acetylation was responsible for about 50 % of total acylation. Conversely, this means that 25 % of total acylation in brain, 35 % in liver, as well as 50 % in kidney and heart were not caused by enzymatic acetylation, but RACS mediated acylation. Obviously, these acyl lysine modifications are quite high abundant, which justifies the question for their functions in metabolism.

Formylation was the second most abundant modification detected in our screening. Concentrations were especially high in heart with 14.11 µmol/mol leucine-eq, which was nearly equivalent to levels of acetylation in the same organ. *In vitro* formation of N^6-formyl lysine by formaldehyde was first described in 1985.[236] More than 20 years later formylation was discovered in histones.[40] Modification sites in core and linker histones as well as other nuclear proteins, e.g., high-mobility-group proteins, lamins, and calgizzarin were identified by mass spectrometry.[230] In contrast to all other acyl lysine modifications detected, corresponding formyl-CoA is probably not the major source of formylation. Formate was not activated as formyl-CoA by acyl-CoA synthetase and the only described minor pathway leading to formyl-CoA *in vivo* was α-oxidation of β-substituted fatty acids, e.g., phytanic acid.[53] The group around Dedon linked formylation to reactive formyl phosphate generated by oxidative DNA degradation. As a proof of concept neocarzinostatin was used to catalyze 5'-oxidation of deoxyribose in DNA and subsequently induced lysine formylation.[40] Later, the same group identified formaldehyde as an alternative source of formylation by experiments with isotopically labeled [^{13}C, ^{2}H]-formaldehyde in cell culture[237] and rats.[238] Formaldehyde was found at high concentrations in blood ranging between 10 – 87 µM[239] and is detoxified by mitochondrial aldehyde dehydrogenase 2 or glutathione dependent alcohol dehydrogenase 3. The latter one oxidizes S-hydroxymethyl glutathione, i.e., the non-enzymatic adduct of formaldehyde and glutathione, to S-formyl glutathione.[240] Attempts to establish N^6-formyl lysine as a biomarker of chronic low-dose formaldehyde exposure were only successful in nasal epithelium and to some extent in trachea, but not in distant tissues of lung, bone marrow, or white blood cells.[241] An alternative pathway of formylation is the Maillard reaction. Lysine induced degradation of glucosone under aeration and deaeration *in vitro* resulted in N^6-formyl lysine formation of 2.60 and 0.89 mmol/mol lysine, respectively.[206] The deacetylase class I and II inhibitor suberoylanilide hydroxamic acid had no effect on formylation *in vitro*[237] and deformylase activity of SIRT1 corresponded only to 10 % of deacetylase activity.[237,242] Despite the high abundance of formylation no literature about metabolic effects of the modification is available. Consequently, further research is mandatory to access the metabolic significance of this modification.

Aliphatic acylations propionylation and butyrylation were quantitative less important and concentrations were about a factor of 100 below acetylation levels. In analogy to formylation, highest concentrations of propionylation (0.66 µmol/mol leucine-eq) and butyrylation (0.38 µmol/mol leucine-eq) were measured in heart protein. Both modifications were discovered in 2007 after immunoprecipitation of histones using a N^6-acetyl lysine antibody.[41] Later,

modification sites in non-histone proteins, e.g., p53 were identified by proteomic approaches.[243] Propionylation and butyrylation were formed in a non-enzymatic way by their corresponding RACS *in vitro*. Compared to acetyl-CoA the acylation efficiency was 3 times lower for propionyl-CoA and 5 times lower for butyryl-CoA.[51] Acylation activity of KAT3B (p300) was confirmed *in vitro*, but revealed progressively slower rates with increasing chain length, e.g., efficiency of butyrylation decreased by a factor of 45 compared to acetylation.[71] In addition, acetylation, propionylation, and butyrylation activities were reported for GNATs KAT2A and KAT2B *in vitro*. [72,73] In case of KAT2A propionylation and butyrylation efficiencies equaled 75 % and 1 % of acetylation rates, respectively.[72] The only prove of acylation activity *in vivo* was the decrease of propionylation after MOF knock-out in cell culture.[75] Propionylation and butyrylation were described as potential targets of reader proteins. While compared to acetylation a reduced affinity was reported for bromodomains,[94] affinity increased for YEATS domains.[95] Both modifications were targeted by deacylases SIRT1, 2, and 3 *in vitro*.[244] Propionylation of *Salmonella enterica* propionyl-CoA synthetase resulted in 70 % loss of specific activity, which may serve as a metabolic sensor of propionyl-CoA levels.[245] Butyrylation was up to 10 times increased in the pathology of short-chain acyl-CoA dehydrogenase deficiency and increased in neuroblastoma after treatment with anti-cancer drug suberoylanilide hydroxamic acid.[246,247]

Crotonylation was another order of magnitude below propionylation and butyrylation modifications with maximum concentrations of 0.02 µmol/mol leucine-eq in liver, kidney, and heart. This unsaturated acylation was originally reported as an enhancer of transcription.[43] The catalysis of p300 mediated crotonylation was higher than acetylation *in vitro*.[93] SIRT1-3 as well as histone deacetylases 1, 2, 3, and 8 were identified as decrotonylases.[248] Crotonylation was downregulated in liver, stomach and kidney carcinomas[249] and several effects on important pathways like regulation of spermatogenesis[250] and telomere maintenance[251] were previously reported.

Acidic acylation by malonylation, succinylation, and glutarylation was quantitatively more important. The most abundant acidic acylation was N^6-succinyl lysine with concentrations between 6.12 µmol/mol leucine-eq in liver and 3.22 µmol/mol leucine-eq in brain. With brain as the only exception succinylation reached between 20 – 30 % of acetylation in all organs. Succinylation was first discovered in 2010[42] and was shown to modify the chromatin structure.[252] The precursor succinyl-CoA formed a cyclic anhydride intermediate *in vitro* explaining the much higher reactivity compared to acetyl-CoA.[48] The strong overlap between acetylation and succinylation sites was postulated as a metabolic switch.[253] As an example

ethanol induced hyposuccinylation and hyperacetylation in mice liver.[254] Succinylation was increased in breast[255] and gastric cancer.[256] First studies identified succinylation as an activator of chaperone activity in the eye lens[257] and a regulator of respiration by modification of pyruvate dehydrogenase and succinate dehydrogenase.[98] Mitochondrial SIRT5 was previously described as a weak deacetylase but an excellent desuccinylase.[80] Another target of SIRT5 is malonylation,[80] which reached up to 2.11 µmol/mol leucine-eq in liver. Lowest concentration was measured in brain with 0.50 µmol/mol leucine-eq. Elevated levels of protein malonylation were recently observed in human fibroblasts[247] and malonylation of glyceraldehyde-3-phosphate dehydrogenase was postulated as an inducer of inflammation.[258] The malonyl-CoA synthetase ACSF3 was identified as a mandatory enzyme in protein malonylation.[259] The least abundant target of SIRT5[80] was glutarylation. Concentrations of glutarylation were in the range of about 0.4 µmol/mol leucine-eq, except for liver in which levels were about twice as high. The role of glutarylation in metabolism is currently unknown, but mitochondrial glutarylation was significantly elevated in a mouse model of glutaric acidemia, an inborn error of metabolism caused by a deleterious mutation in glutaryl-CoA dehydrogenase.[45]

After enrichment by repetitive HPLC fractionation 6 additional acyl lysine modifications were quantitated including 4 novel structures N^6-acetoacetyl lysine, N^6-(2-methylbutyryl) lysine, N^6-tiglyl lysine, and N^6-isovaleryl lysine (Table 15).

Table 15: Additional acylated lysine modifications in pooled mouse organ lysates quantitated after enrichment. [231]

Modification	[µmol/mol leucine-eq]			
	Liver	Kidney	Heart	Brain
N^6-(3-Hydroxybutyryl) lysine	0.19	0.33	0.19	0.22
N^6-(3-Hydroxy-3-methylglutaryl) lysine	0.10	0.17	0.06	0.12
N^6-Acetoacetyl lysine	0.29	0.20	0.10	0.04
N^6-(2-Methylbutyryl) lysine	0.26	0.07	0.03	0.01
N^6-Tiglyl lysine	0.04	0.04	0.05	0.06
N^6-Isovaleryl lysine	0.03	0.03	0.05	0.05

One of the most abundant modifications quantitated after enrichment was 3-hydroxybutyrylation with concentrations up to 0.33 µmol/mol leucine-eq in kidney. Hydroxybutyrate was established as a precursor for hydroxybutyrylation. It is formed in ketogenesis, activated by acyl-CoA synthetase and finally promotes gene activation of starvation response, e.g., amino acid catabolism.[47] In addition, hydroxybutyrylation was

reported to attenuate p53 activity and as a potential target of SIRT3.[260,261] Another modification previously described in literature was N^6-(3-hydroxy-3-methylglutaryl) lysine with concentrations between 0.17 µmol/mol leucine-eq in kidney and 0.06 µmol/mol leucine-eq in heart. In analogy to succinylation the corresponding acyl-CoA thioester formed a cyclic anhydride, which acylated lysine residues with high efficiency.[48] While most acidic acylation structures were reported as targets of SIRT5, N^6-(3-hydroxy-3-methylglutaryl) lysine was targeted by SIRT4.[81] Both 3-hydroxybutyryl-CoA and 3-hydroxy-3-methylglutaryl-CoA are important intermediates in ketogenesis. The third reactive intermediate involved in ketogenesis is acetoacetyl-CoA.[262] Corresponding acetoacetylation was detected for the first time using our novel HPLC-MS/MS approach. Concentrations reached up to 0.29 µmol/mol leucine-eq, but very low concentrations were measured in brain and heart with 0.04 and 0.10 µmol/mol leucine-eq, respectively. Although 3-hydroxybutyrylation, 3-hydroxy-3-methylglutarylation, and acetoacetylation are rather low abundant, their corresponding RACS are highly specific for ketogenesis. Consequently, these modifications are potential markers of metabolic regulation and nutrient sensing by acylation. Similarly, 2-methylbutyryl-CoA, tiglyl-CoA, and isovaleryl-CoA are important intermediates in branched-chain amino acid metabolism.[263] The corresponding acyl lysine modifications were detected and quantitated for the first time in the present thesis. Extraordinary high concentrations of 0.26 µmol/mol leucine-eq were detected for 2-methylbutyrylation in liver. N^6-tiglyl lysine and N^6-isovaleryl lysine were generally rather low abundant in a range between 0.03 and 0.07 µmol/mol leucine-eq. The modifications are highly specific for branched-chain amino acid metabolism and may serve as potential regulators in this pathway.

One of the biggest problems to correlate acylation levels and RACS was inconsistent data reported in the literature (Table 16). As an extreme example concentrations of acetyl-CoA in mouse liver ranged between 4 nmol/g reported by Abranko et al.[264] and 100 nmol/g reported by King et al.[265] This huge variation by a factor of 25 was caused by differences in the methods used for quantitation, e.g., sample preparation, enrichment, separation, and detection. Abranko et al. added isotopically labeled malonyl-CoA as isotope dilution standard to the organ lysates, enriched by solid phase extraction and quantitated by UHPLC-ESI-MS/MS.[264] King on the other hand did no enrichment and analyzed the lysates directly after protein precipitation via HPLC-UV.[265] In addition, data about RACS were incomplete, e.g., formyl-, crotonyl-, tiglyl-, and glutaryl-CoA concentrations were never published. Consequently, the development of a robust analytical method for quantitation of RACS *in vivo* remains one of the most urgent tasks to access the mechanisms underlying lysine acylation processes.

Table 16: Concentrations of acylation precursors reported in literature.

Structure	Concentration in tissue
Acetyl-CoA	4 nmol/g liver (mouse)[264] 36 nmol/g liver (mouse)[266] 110 nmol/g liver (mouse)[267] 44 nmol/g liver (human)[52] 9 nmol/g liver (rat)[268] 100 nmol/g liver (rat)[265] 28 nmol/g liver (rat)[269] 30 nmol/g heart (mouse)[270] 5 nmol/g heart (rat)[268] 0.6 nmol/g heart (rat)[269] 5 nmol/g kidney (rat)[268] 6.9 nmol/g kidney (rat)[269] 7.6 nmol/g brain (rat)[271]
Propionyl-CoA	3.9 nmol/g liver (rat)[266] < 2 nmol/g liver (human)[52] 109 nmol/g liver (rat)[269] 52.9 nmol/g heart (rat)[269] 62.6 nmol/g kidney (rat)[269]
Butyryl-CoA	6 nmol/g liver (mouse)[264] 8 nmol/g liver (mouse)[270] < 2 nmol/g liver (human)[52] 1.5 nmol/g liver (rat)[272] 0.8 nmol/g heart (mouse)[270] 30.6 nmol/g brain (rat)[271]
2-Methylbutyryl-CoA	4 nmol/g liver (mouse)[264] < 2 nmol/g liver (human)[52]
Isovaleryl-CoA	4 nmol/g liver (mouse)[264] < 2 nmol/g liver (human)[52]
Acetoacetyl-CoA	0.5 nmol/g liver (mouse)[267] 1.0 nmol/g liver (rat)[266]
3-Hydroxybutyryl-CoA	0.8 nmol/g liver (mouse)[264] 3.5 nmol/g liver (mouse)[270] 1.1 nmol/g heart (mouse)[270]
Malonyl-CoA	0.1 nmol/g liver (mouse)[264] 0.8 nmol/g liver (mouse)[270] 1.9 nmol/g liver (rat)[266] 1.5 nmol/g liver (rat)[265] 32 nmol/g liver (rat)[269] 2.7 nmol/g heart (mouse)[270] 10.6 nmol/g heart (rat)[269] 4.5 nmol/g kidney (rat)[269]
Succinyl-CoA	22 nmol/g liver (mouse)[270] 45 nmol/g liver (mouse)[267] 42 nmol/g liver (human)[52] 13.5 nmol/g liver (rat)[265] 5.4 nmol/g liver (rat)[269] 1.2 nmol/g heart (rat)[269] 10 nmol/g heart (mouse)[270] 5.3 nmol/g kidney (rat)[269]
3-Hydroxy-3-methyl-glutaryl-CoA	1.7 nmol/g liver (rat)[266] 22 nmol/g liver (human)[52] 7 nmol/g liver (rat)[265] 2.7 nmol/g brain (rat)[271]

4.3 Posttranslational protein modifications in aging

After identification of liver as a local "hotspot" of acylation and detection of novel α-oxoamide AGEs the interactions between different posttranslational protein modifications and their characteristic changes in the aging process of subcellular compartments were of special interest. A fractionation protocol was developed for mouse liver, which combined protocols for isolation of histones,[273,274] mitochondria,[275] and cytosolic proteins.[122] The method was validated by (fluorescence) microscopy, proteomics, and Western blotting.[276]

The amount of protein isolated by the fractionation protocol was determined by Lowry assay, referenced to the wet weight of weighed-in liver, and compared to methods previously reported in the literature (Table 17).

Table 17: Yield of protein extraction from liver.

Fraction	**Protein Mean (minimum – maximum) [mg/g liver]**	**Literature Mean [mg/g liver]**
Histones	2.5 (0.7 – 6.6)	1.6[277]
Mitochondria	14.8 (8.7 – 23.7)	10 – 20[278,279]
Cytosol	42.5 (21.2 – 57.4)	30[280]

After successful extraction of histones, mitochondrial, and cytosolic protein from livers of 10 young (3 month old) and 10 old (24 month old) mice, proteins were digested by enzymatic and acid hydrolysis. Levels of protein acylation were determined by HPLC-MS/MS (Table 18).

Table 18: Protein acylation in subcellular compartments of mice liver (mean ± standard deviation, n = 10). Significant differences (t-test, $p < 0.05$) between young and old animals are indicated by an asterisk. [276]

Modifications	**[µmol/mol leucine-eq]**					
	Histones		**Mitochondria**		**Cytosol**	
	Young (3 month)	**Old (24 month)**	**Young (3 month)**	**Old (24 month)**	**Young (3 month)**	**Old (24 month)**
N^6-Formyl lysine	57.8 ± 44.5	126.1 ± 44.4*	35.3 ± 13.0	35.6 ± 9.2	17.1 ± 1.7	22.4 ± 4.9*
N^6-Acetyl lysine	350.5 ± 119.1	304.5 ± 142.2	43.9 ± 6.9	44.4 ± 13.0	40.1 ± 3.6	44.1 ± 6.3
N^6-Propionyl lysine	1.0 ± 0.5	1.7 ± 0.4*	0.7 ± 0.2	0.7 ± 0.3	0.4 ± 0.1	0.7 ± 0.1*
N^6-Butyryl lysine	0.3 ± 0.3	0.8 ± 0.3*	0.2 ± 0.1	0.3 ± 0.1*	0.1 ± 0.1	0.3 ± 0.1*
N^6-Malonyl lysine	< LOD	< LOD	2.6 ± 0.4	2.3 ± 0.4	2.9 ± 0.4	3.5 ± 0.6*
N^6-Succinyl lysine	2.1 ± 0.3	2.7 ± 0.4*	4.2 ± 0.7	4.2 ± 1.9	0.4 ± 0.1	0.6 ± 0.1*

The most abundant protein acylation was N^6-acetyl lysine with mean concentrations reaching up to 350.5 µmol/mol leucine-eq in histones, which was nearly ten times higher compared to 44.4 µmol/mol leucine-eq in mitochondria and 44.1 µmol/mol leucine-eq in cytosol. Previous studies reported below 1 % stoichiometry of acetylated lysine residues[10,281] in mice liver proteins with a median stoichiometry of 0.05 %,[282] which was supported by our results. Acetylation is a fundamental important regulatory mechanism and is controlled by a plethora of acetyltransferases and deacetylases.[2] The presence of this modification is highly dynamic with half-times between 1 – 2 h in histones.[283] Hence, no correlation with aging was detected. This was in line with previously published results in aging mitochondria extracted from rat liver.[100] Inconsistent trends were previously reported for histone acetylation.[36,37,284] The second most abundant acyl lysine modification was N^6-formyl lysine with up to 126 µmol/mol leucine-eq in histones. In mitochondrial and cytosolic proteins mean N^6-formyl lysine concentrations were between 17.1 and 35.6 µmol/mol leucine-eq. Similar results of about 1 – 4 formylated amino acids per 10^4 lysine residues were reported by Edrissi et al.[237] Formylation increased significantly by 120 % in histones ($p = 0.002$) and 31 % in cytosolic proteins ($p = 0.005$), but concentrations were not changed in aging mitochondria. Literature about a potential regulation of formylation by mitochondrial sirtuins like SIRT3 is currently unavailable. The only known enzyme potentially targeting formylation is nuclear SIRT1, which had a weak deformylase activity *in vitro.*[242] Several sources of formylation were postulated including oxidative DNA degradation,[40] Maillard reaction,[206] and formaldehyde metabolism.[237] The question which of these pathways is the major source *in vivo* needs to be addressed in future research. Aliphatic acylations N^6-propionyl lysine and N^6-butyryl lysine were quantitative less important and were generally concentrated below 2 % of N^6-acetyl lysine levels. This low abundance was in full agreement with literature, because propionylation and butyrylation were exclusively detectable by proteomic approaches after antibody enrichment.[41] However, propionylation and butyrylation significantly correlated with aging ($p < 0.005$) and increased between 40 and 150 %. Again, mitochondria were the single exception, because mitochondrial SIRT3 limited propionylation in aging.[80] Acidic acylations N^6-malonyl lysine and N^6-succinyl lysine were relatively high abundant in mitochondria with average concentrations up to 4.2 and 2.6 µmol/mol leucine-eq, respectively. Due to enzymatic regulation by mitochondrial SIRT5 no correlation with aging was detected, which is in line with literature.[100] In contrast, acidic acylation increased about 25 % in the aging process of histones and cytosolic proteins. The present thesis is the first

quantitative and comprehensive study of acyl lysine modifications in subcellular compartments and our results may provide a novel molecular mechanism of aging.

As mentioned above, Maillard induced fragmentations of glucosone and 1-deoxyglucosone were reported as alternative pathways leading to N^6-formyl lysine and N^6-acetyl lysine, respectively.[206] In addition, several Maillard derived AGEs were quantitated in subcellular compartments of mice liver (Table 19).

Table 19: Protein glycation in subcellular compartments of mice liver (mean ± standard deviation, n = 10). Significant differences (t-test, $p < 0.05$) between young and old animals are indicated by an asterisk.[276]

Modifications	[µmol/mol leucine-eq]					
	Histones		Mitochondria		Cytosol	
	Young (3 month)	Old (24 month)	Young (3 month)	Old (24 month)	Young (3 month)	Old (24 month)
CML	13.5 ± 3.9	22.1 ± 7.0*	4.5 ± 0.7	7.2 ± 2.1*	6.1 ± 1.1	7.5 ± 1.3*
GALA	1.2 ± 0.3	1.8 ± 0.4*	0.4 ± 0.1	0.5 ± 0.2*	0.3 ± 0.1	0.4 ± 0.1*
G-H	15.7 ± 4.8	22.6 ± 8.5*	14.9 ± 4.3	24.1 ± 11.6*	23.4 ± 10.6	40.9 ± 6.4*
CEL	2.7 ± 0.4	3.4 ± 0.6*	3.1 ± 0.6	4.1 ± 0.6*	13.0 ± 2.8	15.6 ± 3.3*
N^6-Lactoyl lysine	< LOD	< LOD	0.2 ± 0.1	0.3 ± 0.1*	0.1 ± 0.1	0.2 ± 0.1*
MG-H	6.7 ± 2.4	8.6 ± 2.1*	5.6 ± 0.7	7.0 ± 1.0*	15.0 ± 3.9	24.3 ± 13.2*
Furosine	2.5 ± 0.2	3.1 ± 1.1*	0.6 ± 0.5	0.9 ± 0.9	2.9 ± 0.7	2.7 ± 0.7

Glycation increased about 50 % in aging of subcellular compartments with furosine as the single exception. Furosine is no AGE in the classical way, but formed from the Amadori product after acid hydrolysis. Consequently, furosine is a marker of early stage Maillard reaction between glucose and lysine residues.[101] The Amadori product precursor is no stable endproduct and is additionally degraded by enzymes like fructosamine-3-kinase,[124] which potentially explains the observed steady-state levels in mitochondrial and cytosolic proteins while furosine accumulated in aging histones. Furosine was one of the first markers of glycation and increased in diabetes.[285] The GO specific lysine modifications CML and GALA were especially high abundant in histones and increased by approximately 60 % in aging to 22.1 and 1.8 µmol/mol leucine-eq, respectively. Obviously, the reported degradation of DNA was a major source of their precursor GO *in vivo*.[114] On the other hand, levels of MGO specific lysine modifications CEL and N^6-lactoyl lysine were highest in cytosolic proteins, because their precursor MGO was mainly generated by cytosolic triosephosphate metabolism.[108] Similar trends were detected for GO specific arginine modification G-H and

MGO specific arginine modification MG-H. Concentrations of up to 40.9 µmol/mol leucine-eq G-H and 24.3 µmol/mol leucine-eq MG-H were higher compared to corresponding lysine modifications, because the guanidine function of arginine has a higher reactivity towards α-dicarbonyls under physiological conditions compared to the amino function of lysine.[111] Reported values for CML (0.5 - 1 mmol/mol lysine) and CEL (0.2 - 0.5 mmol/mol lysine) concentrations in rat liver mitochondria were in the same magnitude as measured by our analysis.[286] In cytosolic proteins extracted from mice liver concentrations of carboxyalkyl AGEs CML and CEL were in the same range and slightly lower for amide AGEs GALA and N^6-lactoyl lysine compared to our previously published data in rat liver.[122] Our results are the first quantitative data about glycation in histones, thus no comparable values are available in the literature. Total levels of all detected AGEs were highest in cytosolic proteins (88.9 µmol/mol leucine-eq) followed by histones (61.6 µmol/mol leucine-eq) and mitochondria (43.2 µmol/mol leucine-eq). In full agreement with literature about CML in aging mitochondria, AGE levels increased about 50 % in all compartments.[213]

Novel α-oxoamide AGEs N^6-glyoxylyl and N^6-pyruvoyl lysine are formed by glycation and additional oxidative stress.[122] They were quantitated along with other oxidative stress markers and citrullination (Table 20).

Table 20: Protein oxidation and citrullination in subcellular compartments of mice liver (mean ± standard deviation, n = 10). Significant differences (t-test, p < 0.05) between young and old animals are indicated by an asterisk. [276]

Modifications	[µmol/mol leucine-eq]					
	Histones		Mitochondria		Cytosol	
	Young (3 month)	Old (24 month)	Young (3 month)	Old (24 month)	Young (3 month)	Old (24 month)
N^6-Glyoxylyl lysine	0.4 ± 0.2	0.8 ± 0.2*	< LOQ	< LOQ	< LOQ	< LOQ
N^6-Pyruvoyl lysine	0.8 ± 0.3	1.5 ± 0.3*	< LOQ	< LOQ	< LOQ	< LOQ
o-Tyrosine	0.7 ± 0.2	1.1 ± 0.3*	4.4 ± 0.8	5.8 ± 0.9*	3.6 ± 1.0	6.1 ± 1.4*
o,o-Dityrosine	2.1 ± 0.4	4.7 ± 2.4*	< LOQ	< LOQ	< LOQ	< LOQ
Methionine sulfoxide	704.9±323.2	595.8±251.0	2454.9±1084.2	1449.3±767.0	1200.4±777.7	1845.1±770.3*
Methionine sulfone	64.8 ± 42.6	104.9 ± 27.7*	41.3 ± 22.1	40.9 ± 21.1	20.9 ± 16.6	39.0 ± 21.5*
Citrulline	37.6 ± 13.9	55.2 ± 16.2*	27.9 ± 16.4	30.0 ± 12.4	5.3 ± 1.8	5.7 ± 1.3

Although α-oxoamide AGEs were rather low abundant, they were excellent markers of aging in histone proteins and increased about 85 %. Another important oxidative stress marker in histones was *o,o*-dityrosine, which is generated by oxidative cross-linking of tyrosine via

hydroxyl or tyrosyl radicals and approximately doubled in aging.[287] In contrast, the monomer *o*-tyrosine is formed by reaction of phenylalanine residues with hydroxyl radicals.[287] The modification was an excellent marker of aging with p-values below 0.008 and was rather high abundant in mitochondrial and cytosolic proteins with 5.8 and 6.1 µmol/mol leucine-eq, respectively. The methionine oxidation product methionine sulfoxide was the most abundant modification and concentrations reached up to 2500 µmol/mol leucine-eq in mitochondria, which was 50-times higher compared to lysine modification by acetylation. Similar concentrations were reported in kidney cells.[288] Methionine sulfoxide was described as a regulator of the cellular redox status by operating as an oxidative sink. While the oxidation requires no enzymes, the reduction is catalyzed by methionine sulfoxide reductases.[289] Methionine sulfoxide reductases A, B, and several isoforms are ubiquitous located in the nucleus, mitochondria, and cytosol.[290] Low methionine oxidation is reversed by the enzymatic regulatory system and oxidative stress exceeding the repair capacity results in further non-enzymatic oxidation of methionine sulfoxide to methionine sulfone.[288] The sulfone is not targeted by methionine sulfoxide reductases and has to be considered as a stable modification. Consequently, increased levels of methionine sulfone in aging histones and cytosol were detected for the first time in the present thesis, while contradicting trends were measured in different compartments for instable methionine sulfoxide. The most abundant arginine modification in histones and mitochondria was citrullination with concentrations of 55.2 µmol/mol leucine-eq and 30.0 µmol/mol leucine-eq, respectively. This is the first time protein-bound citrulline was quantitated in liver. Citrullination is formed enzymatically by peptidyl arginine deiminases.[291] No changes in aging were detected in mitochondrial and cytosolic proteins, but citrullination of histone proteins correlated with aging ($p = 0.01$). This is especially dramatic, because citrullination is closely associated with inflammatory processes and DNA damaging pathways leading to carcinogenesis.[292] The increase of several oxidative stress marker structures indicated elevated levels of oxidative stress in aging of liver, which was supported by previously published studies.[293]

In general, accumulation of non-enzymatic PTMs was observed in aging liver (Table 21). This trend was especially strong in histones in which levels of protein acylation, glycation, and oxidation elevated about 115 %, 45 %, and 65 %, respectively. Increase of enzymatic citrullination by up to 50 % was exclusively detected in histones. Protein acylation increased only by 30 % in cytosol, while glycation increased by 50 % and oxidation increased 85 % in the aging process. Most PTMs were not accumulating in aged mitochondria, but AGEs accumulated by 50 %.

Table 21: PTMs in aging of subcellular mouse liver compartments. [276]

Modifications	[µmol/mol leucine-eq]					
	Histones		Mitochondria		Cytosol	
	Young (3 month)	Old (24 month)	Young (3 month)	Old (24 month)	Young (3 month)	Old (24 month)
Acetylation	350.5	304.5	43.9	44.4	40.1	44.1
Acylation	61.2	131.3	43.0	43.1	20.9	27.5
Glycation	42.3	61.6	29.3	44.1	60.8	91.6
Oxidation[a]	69.0	113.0	45.7	46.7	24.5	45.1
Citrullination	37.6	55.2	27.9	30.0	5.3	5.7

[a]Methionine sulfoxide excluded

Levels of modifications depend on protein turnover, enzymatic regulation and precursor concentration. As an example subcellular location has a huge impact on protein half-life. Histones are extraordinary long-lived with a half-time of 127 days.[294] In contrast, half-life between 12 min and 6 days is magnitudes lower for most cytosolic proteins.[295] Mitochondrial proteins are in the same range with a turnover between 20 min and 5 days.[296] Next to canonical proteasomal degradation, about 20 – 25 % of whole mitochondria are degraded by an additional pathway via lysosomal autophagy in rat liver.[297] The huge variation between protein half-times in different subcellular organelles potentially caused the extraordinary high accumulation of modifications in histones compared to cytosolic and mitochondrial proteins. Another important factor is enzymatic regulation of PTMs, e.g., acidic acylation increased in histones and cytosolic proteins during aging, but SIRT5 limited accumulation of N^6-malonyl lysine and N^6-succinyl lysine in mitochondria.[80] A particular interesting observation was aliphatic acylation in histones. These modifications were targeted by nuclear SIRT1, which has very high affinity for acetylation and significantly lower affinity towards propionylation and butyrylation.[76] Decreased SIRT1 expression[298] and enzyme activity were reported in aging liver.[299] This explained increased N^6-propionyl lysine and N^6-butyryl lysine levels in histones extracted from old animals. On the other hand, acetylation levels remained constant, possibly due to the high affinity of SIRT1 and the 11 additional Zn^{2+} dependent KDACs. Similar processes may be involved by SIRT2 mediated regulation of aliphatic acylation in the cytosol. Last but not least, the concentrations of precursors facilitate formation of PTMs. As an example concentrations of RACS are estimated approximately 3 – 50 times higher in mitochondria compared to other cellular compartments,[12] which explains high abundance of acylation in mitochondria despite deacylase activities of mitochondrial sirtuins. Moreover,

reactive oxygen species (ROS) are generated primarily by the respiratory chain complex in the mitochondria.[300] Resulting ROS like the superoxide anion ($O_2^{\bullet-}$), hydrogen peroxide (H_2O_2), and the hydroxyl radical ($^{\bullet}OH$)[301] were responsible for the high methionine oxidation detected in mitochondria. The glycolytic metabolism is located in the cytosol and generates triosephosphates, which are the major source of MGO *in vivo*.[108] Consequently, MGO specific modifications CEL and MG-H were especially high abundant in cytosolic proteins. The cytosolic glyoxalase system detoxifies α-dicarbonyls like MGO and links enzymatic regulation to availability of precursors.[302] The reported decrease of glyoxalase I and II activity in aging liver[303] results in an increase of α-dicarbonyls,[108] which explains accumulation of glycation in aging.

In summary, most previous studies focused on a single stressor like protein oxidation by ROS (oxidative stress),[304] glycation by α-dicarbonyls (dicarbonyl stress),[108] or acylation by RACS (RACS stress) as potential molecular mechanisms underlying aging and disease. The present study combined the concepts of oxidative, dicarbonyl, and RACS stress for the first time by comprehensive and quantitative analysis of their corresponding PTMs. This step was necessary, because potential interactions between the different stressors were reported (Figure 21).

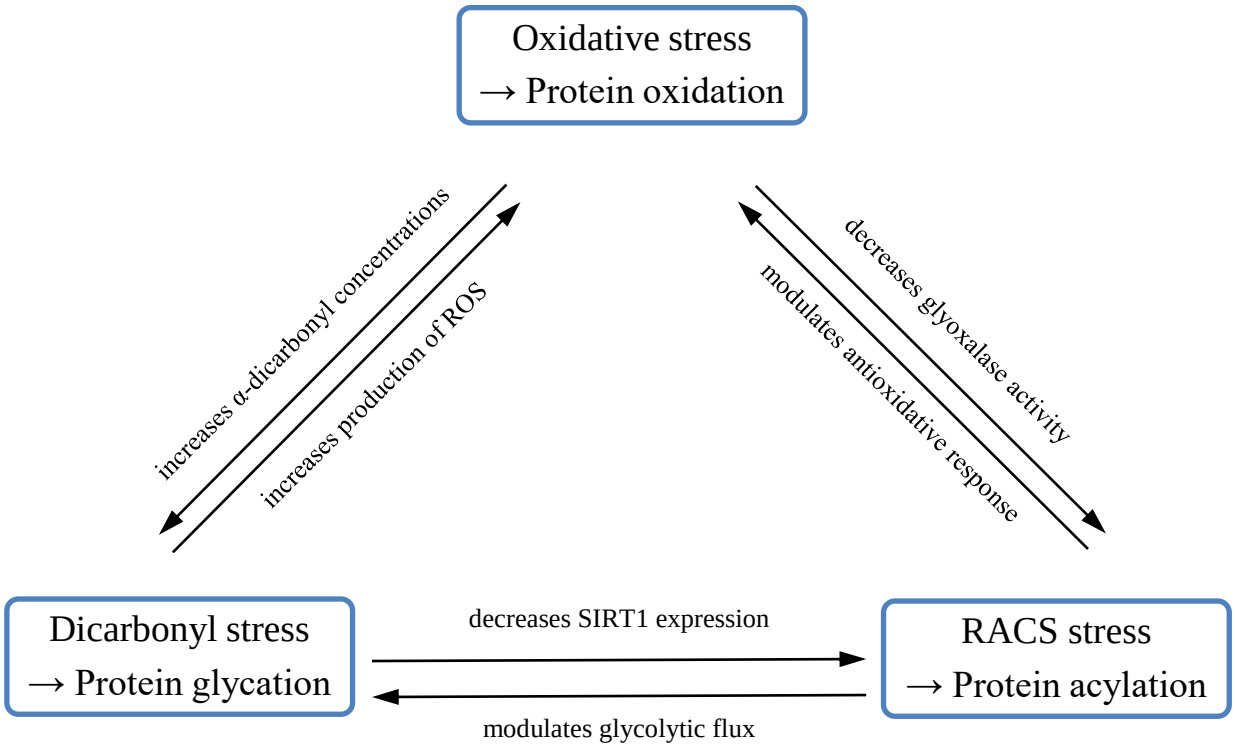

Figure 21: Connection between protein oxidation by oxidative stress, protein glycation by dicarbonyl stress, and protein acylation by RACS stress.

The most important source of oxidative stress *in vivo* is ROS production by the mitochondrial respiratory chain.[300] The majority of electrons precedes through mitochondrial respiratory complexes I – IV and finally reduce molecular oxygen to water. However, a small percentage of electrons prematurely leak out of the transport chain and generate the superoxide anion ($O_2^{\bullet-}$). This anionic radical is detoxified by superoxide dismutase (SOD) and hydrogen peroxide (H_2O_2) is formed. Enzymes like catalase, glutathione peroxidase, and the peroxiredoxins reduce H_2O_2 to H_2O and O_2. Unfortunately, transition metal-catalyzed cleavage of H_2O_2 can produce highly reactive hydroxyl radicals ($^{\bullet}OH$). The hydroxyl radicals react with several small molecules and damage proteins, which is the end-stage of oxidative stress.[301] Hydroxyl radicals facilitate lipid peroxidation and subsequently α-dicarbonyl formation.[109] Additionally, experiments in cell culture proved ROS mediated reduction in GSH concentration decreased glyoxalase activity and impaired dicarbonyl detoxification.[305] Thus, oxidative stress enhanced dicarbonyl stress. Vice versa, dicarbonyl stress potentially induced oxidative stress. As an example production of ROS was increased via glycation of respiratory chain proteins by α-dicarbonyls[173] and detoxification of ROS by SOD and catalase was impaired by glycation.[306] Protein acylation is quite a novel research field and interactions between dicarbonyl stress and RACS stress are less understood, but some studies connected glycation and acylation. First of all α-dicarbonyls GO and MGO are potential precursors of non-enzymatic acylation by formation of amide AGEs, hence, dicarbonyls are an alternative pathway to non-enzymatic acylation by RACS.[206] Moreover, diet enriched with AGEs by MGO treatment caused lower expression of SIRT1 and increased acylation.[307] On the other hand, acidic acylation by enhanced RACS stress was identified as a modulator of glycolytic flux.[99] Glycolysis is a major source of dicarbonyl stress[108] and the effect of acylation on dicarbonyl production is a particular interesting topic for further research. Acylation is controlling cellular antioxidative stress response,[301] e.g., only deacetylated SOD detoxifies ROS.[308] In return, glyoxalase and GSH, which are closely linked to oxidative stress and dicarbonyl stress, play an important role in controlling non-enzymatic lysine acylation.[309] The described interactions between oxidative stress, dicarbonyl stress, and RACS stress influenced the formation of oxidized, glycated, and acylated proteins. This highlighted the importance of comprehensive analysis of PTMs *in vivo* to elucidate the molecular mechanisms of aging.

5 Publications

5.1 Publication 1

JOURNAL OF AGRICULTURAL AND FOOD CHEMISTRY

Article

Cite This: J. Agric. Food Chem. 2018, 66, 1898−1906

pubs.acs.org/JAFC

Novel α-Oxoamide Advanced-Glycation Endproducts within the N^6-Carboxymethyl Lysine and N^6-Carboxyethyl Lysine Reaction Cascades

Tim Baldensperger,[†] Tobias Jost,[†] Alexander Zipprich,[‡] and Marcus A. Glomb*[,†]

[†]Institute of Chemistry, Food Chemistry, Martin-Luther-University Halle-Wittenberg, Kurt-Mothes-Strasse 2, 06120 Halle/Saale, Germany

[‡]Department of Internal Medicine I, Martin-Luther-University Halle-Wittenberg, Ernst-Grube-Strasse 40, 06120 Halle/Saale, Germany

ABSTRACT: The highly reactive α-dicarbonyl compounds glyoxal and methylglyoxal are major precursors of posttranslational protein modifications in vivo. Model incubations of N^2-*t*-Boc-lysine and either glyoxal or methylglyoxal were used to further elucidate the underlying mechanisms of the N^6-carboxymethyl lysine and N^6-carboxyethyl lysine reaction cascades. After independent synthesis of the authentic reference standards, we were able to detect N^6-glyoxylyl lysine and N^6-pyruvoyl lysine for the first time by HPLC-MS^2 analyses. These two novel amide advanced-glycation endproducts were exclusively formed under aerated conditions, suggesting that they were potent markers for oxidative stress. Analogous to the well-known Strecker degradation pathway, leading from amino acids to Strecker acids, the oxidation of an enaminol intermediate is suggested to be the key mechanistic step. A highly sensitive workup for the determination of AGEs in tissues was developed. In support of our hypothesis, the levels of N^6-glyoxylyl lysine and N^6-pyruvoyl lysine in rat livers indeed correlated with liver cirrhosis and aging.

KEYWORDS: *Maillard reaction, amide advanced-glycation endproducts, methylglyoxal, glyoxal, oxidative stress, aging*

■ INTRODUCTION

Louis-Camille Maillard described the nonenzymatic browning reaction of reducing sugars and amines upon heating in 1912. Already at this early stage, he postulated the reaction's great importance in the physiology and pathology of humans on the basis of the wide availability of carbohydrates and amines.[1] Starting in the 1940s, Maillard-reaction research focused not only on the formation of colors, aromas, and tastes in food[2] but also on the negative side-effects, like the formation of foodborne toxins, such as acrylamide.[3] In addition, Maillard reactions are widely accepted as an important source of reactive intermediates that lead to advanced-glycation endproducts (AGEs) in vivo. AGEs are stable posttranslational protein modifications and were correlated with the development and progression of various chronic and age-related pathologies. As an example, the levels of the most abundant AGE, N^6-carboxymethyl lysine (CML), increased with the severity of diabetes[4] and rose in an almost linear fashion with age in human lens proteins.[5]

Because of the progress in analytical methods, the understanding of Maillard-reaction mechanisms has strongly improved in recent years. Highly reactive α-dicarbonyl compounds, like glyoxal (GO), methylglyoxal (MGO), and deoxyglucosones, have been identified as key intermediates and quantitated in order to understand the chemistry of AGE formation in vitro and in vivo.[6−10] These precursors are transformed to the stable endproducts mainly by three different mechanisms under physiological conditions:[9] oxidative α-dicarbonyl cleavage,[11] amine-induced β-dicarbonyl cleavage,[12] and isomerization.[13] Rather-long-chained dicarbonyl structures, for example, 1-deoxyglucosone and 2,3-diketogulonic acid, tend to fragment by oxidative α-dicarbonyl cleavage and amine-induced β-dicarbonyl cleavage, resulting in mixtures of short-chained carbonyls, carboxylic acids, and their corresponding amide AGEs.[14,15] On the other hand, two of the quantitatively most relevant AGEs, CML and N^6-carboxyethyl lysine (CEL), are formed nonoxidatively by isomerization after a reaction between protein-bound lysines and the short-chained dicarbonyl structures GO and MGO, respectively. Alternative products formed in the complex reaction cascades include monovalent AGEs with an amide structure, like N^6-glycoloyl lysine (GALA) and N^6-lactoyl lysine, and cross-linking compounds, like the glyoxal lysine amide (GOLA) and the glyoxal lysine dimer (GOLD).[9]

It is important to understand that in contrast to all the other structures identified so far within this mechanistic scheme, only CML can be formed by additional oxidative pathways. A main route was shown to proceed via the direct oxidative fragmentation of the Amadori product of lysine and glucose, although the exact mechanism is still lacking. In addition, multiple minor reaction pathways have been published, mainly related to the formation of glyoxal or glycolaldehyde from higher sugars via, for example, the metal-catalyzed autoxidation of glucose or the amine-catalyzed single-electron transfers of pyrazinium-radical cations within the Namiki pathway.[16] Consequently, CML has been used as a marker of oxidative stress in diabetes, for example, which is generally characterized

Received: December 11, 2017
Revised: January 29, 2018
Accepted: February 6, 2018
Published: February 13, 2018

ACS Publications © 2018 American Chemical Society

DOI: 10.1021/acs.jafc.7b05813
J. Agric. Food Chem. 2018, 66, 1898−1906

by increases in both carbonyls and oxidative stress, accelerating the formation of late-stage complications.[17] However, because of the multiple routes leading to CML formation, the value of CML as a suitable chemical parameter for oxidative stress has to be challenged. The present work therefore successfully aimed to identify two novel AGEs specific for oxidation within the isomerization-reaction cascade and test their applicability in vivo.

MATERIALS AND METHODS

Chemicals. All chemicals of the highest quality available were provided by Sigma-Aldrich (Munich/Steinheim, Germany), Fluka (Taufkirchen, Germany), Merck (Darmstadt, Germany), Roth (Karlsruhe, Germany) and Sigma (Taufkirchen, Germany), unless otherwise indicated. The NMR solvents were purchased from ARMAR Chemicals (Leipzig/Doettingen, Germany).

The standard reference substances CML,[7] GALA,[13] CEL,[18] and N^6-lactoyl lysine[12] as well as the Amadori product of glucose and N^2-*t*-Boc-lysine,[7] N^2-*t*-Boc-lysine *t*-butyl ester (**1**),[19] glyoxylic acid diethyl acetal (**2**),[20] and pyruvic acid *N*,*N*-dimethyl hydrazone (**4**)[21] were synthesized according to the literature.

*N^2-t-Boc-N^6-(2,2-diethoxy acetyl) Lysine t-Butyl Ester (**3**).* Compound **2** (647 mg, 4.37 mmol) and hydroxybenzotriazole (HOBt, 590 mg, 4.37 mmol) were dissolved in 10 mL of dry THF under an argon atmosphere at 0 °C. After 10 min, 745 mg (4.8 mmol) of 1-ethyl-3-(3-(dimethylamino)propyl)carbodiimide (EDC) was added. A solution of 1.319 g (4.37 mmol) of **1** in 5 mL of dry THF was added dropwise after 20 min. The reaction mixture was warmed to room temperature and stirred for 16 h. The solvent was evaporated under a vacuum, and the residue was dissolved in 10 mL of EtOAc and washed with a saturated $NaHCO_3$ solution and brine (10 mL each). The organic layer was dried over Na_2SO_4, and the solvents were evaporated. The crude product was purified by column chromatography on a silica gel 60 using hexane−acetone (3:1). Fractions containing **3** (TLC: R_f 0.35 in hexane−acetone (3:1), ninhydrin detection) were collected, concentrated in vacuo and dried under a high vacuum to afford compound **3** as a yellow viscous oil (633 mg, 34%). ^{1}H NMR (400 MHz, MeOH-d_4): δ (ppm) = 1.23 (t, ^3J = 7.1 Hz, 6H), 1.44 (s, 9H), 1.46 (s, 9H), 1.38 (m, 2H), 1.56 (m, 2H), 1.75 (m, 2H), 3.22 (t, ^3J = 7.0 Hz, 2H), 3.61 (m, 4H), 3.93 (t, ^3J = 5.0 Hz, 1H), 4.79 (s, 1H). ^{13}C NMR (100 MHz, MeOH-d_4): δ (ppm) = 15.4, 24.3, 28.3, 28.8, 30.0, 32.7, 39.8, 55.8, 63.4, 99.7, 158.2, 170.4, 173.8. HR-MS: *m*/*z* 433.2900 (found); *m*/*z* 433.2908 (calcd for $C_{21}H_{41}O_7N_2$ $[M + H]^+$).

N^6-Glyoxylyl Lysine. Compound **3** (178 mg, 0.41 mmol) was dissolved in acetone and 6 M HCl (10 mL each). After being stirred for 30 min, the mixture was diluted with 100 mL of water and concentrated to a volume of approximately 20 mL under a vacuum. After being washed with 20 mL of EtOAc, the aqueous phase was separated and evaporated to dryness. The crude product was purified by column chromatography on a Lichroprep RP C18 using water−methanol (9:1). Fractions with positive ninhydrin detections (TLC: R_f 0.14 in water−butanol−acetic acid (8:1:1)) were collected, evaporated, and lyophilized to afford N^6-glyoxylyl lysine as an amorphic material (75 mg, 90%). ^{1}H NMR (400 MHz, D_2O): δ (ppm) = 1.34 (m, 2H), 1.48 (m, 2H), 1.85 (m, 2H), 3.13 (t, ^3J = 7.0 Hz, 2H), 3.96 (t, ^3J = 6.5 Hz, 1H), 5.15 (s, 1H). ^{13}C NMR (100 MHz, D_2O): δ (ppm) = 21.4, 27.7, 29.3, 38.5, 52.7, 86.7, 172.0, 172.1. HR-MS: *m*/*z* 203.1028 (found); *m*/*z* 203.1026 (calcd for $C_8H_{15}O_4N_2$ $[M + H]^+$).

*N^2-t-Boc-N^6-pyruvoyl Lysine t-Butyl Ester (**5**).* Compound **4** (590 mg, 4.54 mmol) and HOBt (613 mg, 4.54 mmol) were dissolved in 10 mL of dry THF under an argon atmosphere at 0 °C. After 10 min, 775 mg (5.0 mmol) of EDC was added. A solution of 1.369 g (4.54 mmol) of **1** in 5 mL of dry THF was added dropwise after 20 min. The reaction mixture was warmed to room temperature and stirred for 16 h. The solvent was evaporated under a vacuum, and the residue was dissolved in 10 mL of EtOAc and washed with saturated $NaHCO_3$ solution and brine (10 mL each). The organic layer was dried over Na_2SO_4, and solvents were evaporated. The crude product was purified by column chromatography on a silica gel 60 using hexane−acetone (3:1). Fractions containing **5** (TLC: R_f 0.22 in hexane−acetone (3:1), ninhydrin detection) were collected, concentrated in vacuo, and dried under a high vacuum to afford compound **5** as a yellow viscous oil (841 mg, 50%). As described by Katayama, the *N*,*N*-dimethyl hydrazone protective group was removed by silica-gel purification.[22] ^{1}H NMR (400 MHz, MeOH-d_4): δ (ppm) = 1.44 (s, 9H), 1.46 (s, 9H), 1.56 (m, 2H), 1.63 (m, 2H), 1.74 (m, 2H), 2.38 (s, 3H), 3.24 (t, ^3J = 7.0 Hz, 2H), 3.93 (t, ^3J = 5.4 Hz, 1H). ^{13}C NMR (100 MHz, MeOH-d_4): δ (ppm) = 24.2, 24.8, 28.3, 28.7, 29.7, 32.3, 39.9, 55.7, 157.8, 162.9, 172.3, 197.6. HR-MS: *m*/*z* 373.2333 (found); *m*/*z* 373.2338 (calcd for $C_{18}H_{33}O_6N_2$ $[M + H]^+$).

N^6-Pyruvoyl Lysine. Compound **5** (590 mg, 1.59 mmol) was dissolved in acetone and 6 M HCl (10 mL each). After being stirred for 30 min, the mixture was diluted with 100 mL of water and concentrated to a volume of approximately 20 mL under a vacuum. After being washed with 20 mL of EtOAc, the aqueous phase was separated and evaporated to dryness. The crude product was purified by column chromatography on a Lichroprep RP C18 using water−methanol (9:1). Fractions with positive ninhydrin detections (TLC: R_f 0.19 in water−butanol−acetic acid (8:1:1)) were collected, evaporated to dryness, and lyophilized to afford N^6-pyruvoyl lysine as an orange amorphic material (302 mg, 88%). ^{1}H NMR (400 MHz, D_2O): δ (ppm) = 1.42 (m, 2H), 1.61 (m, 2H), 1.90 (m, 2H), 2.43 (s, 3H), 3.26 (t, ^3J = 7.0 Hz, 2H), 3.82 (m, 1H). ^{13}C NMR (100 MHz, D_2O): δ (ppm) = 22.7, 25.3, 28.7, 30.8, 39.7, 55.1, 163.1, 174.7, 199.1. HR-MS: *m*/*z* 217.1186 (found); *m*/*z* 217.1188 (calcd for $C_9H_{17}O_4N_2$ $[M + H]^+$).

Aerated Incubations. Mixtures containing N^2-*t*-Boc-lysine (40 mM), phosphate buffer (0.1 M, pH 7.4), and either GO, MGO, ascorbic acid, the Amadori product, maltose, pyruvic acid, or glyoxylic acid (40 mM) were incubated in screw-cap vials. Incubations were done at 37 °C in a shaker for 7 days. Aliquots of 100 μL were collected each day and instantly stored at −20 °C until the analyses.

AGEs were analyzed by HPLC-MS^2 after the deprotection of the N^2-*t*-Boc group. Pyruvic and glyoxylic acid formation were analyzed by GC-MS after silylation. Each sample was prepared at least three times.

Deaerated Incubations. The incubations were modified by using a phosphate buffer with 1 mM diethylenetriaminepentaacetic acid. The buffer was degassed with helium before the samples were placed in 0.7 mL screw-cap vials without air and incubated under an argon atmosphere.

pH Incubations. Aerated incubations were performed as described above, but the pH of the phosphate buffer was adjusted to 4.5 or 9.6 using 1 M HCl or NaOH.

Housing of Animals and Induction of Cirrhosis by Carbon Tetrachloride (CCl_4). Male Wistar rats were used for all the experiments. The control and cirrhotic rats were bred in the Center of Medical Basic Research (ZMG), Medical Faculty, University of Halle, and the old rats were purchased from Janvier Laboratories (Le Genest-Saint-Isle, France). The rats were housed in standard cages in a climate room with 12 h light and dark phases and free access to food. The cirrhotic rats underwent inhalation exposure to CCl_4 three times a week. Phenobarbital (0.35 g/L) was added to the drinking water as described previously.[23] The treatment was given for 12 weeks. The livers were isolated 7−10 days after the last dose of CCl_4. The principles for the care and use of animals from the American Physiological Society guide were followed. All animal experiments were approved by the local animal committee (42502-2-1123 MLU, Landesverwaltungsamt Sachsen-Anhalt, Germany).

Tissue Collection. The rats were anaesthetized with 150 mg/kg bodyweight narcoren (Merial, Lyon, France). In deep narcosis, the animals were killed by exsanguination, the livers were dissected after perfusion with Krebs-Ringer, and the samples were immediately snap-frozen. For the sirius-red staining, the livers were fixed in formaline (Histofix Roth, Karlsruhe, Germany) and processed routinely. For the Western blots, the livers were treated with a protein lysis buffer (RIPA) for the protein isolation. The primary antibodies were for vinculin (SC-5573, Santa Cruz Biotechnology, Dallas, Texas), α-SMA (ab5694), and TGF-β (ab66043, both abcam, Cambridge, UK). The

DOI: 10.1021/acs.jafc.7b05813
J. Agric. Food Chem. 2018, 66, 1898−1906

Table 1. Mass-Spectrometric Parameters for AGE Quantitation

AGE	retention time (min)	precursor		product ion 1[a]			product ion 2[b]			product ion 3[b]		
		m/z (amu)	DP (V)	*m/z* (amu)	CE (eV)	CXP (V)	*m/z* (amu)	CE (eV)	CXP (V)	*m/z* (amu)	CE (eV)	CXP (V)
N^6-carboxymethyl lysine	12.3	205.1	42	130.2	17	9	84.1	30	14	56.1	59	9
N^6-glycoloyl lysine	12.2	205.2	40	142.1	20	11	84.1	36	14	56.2	64	8
N^6-glyoxylyl lysine hydrate	11.7	221.1	40	203.3	15	13	140.1	25	12	157.3	19	12
N^6-carboxyethyl lysine	17.8	219.1	54	130.1	18	11	84.1	33	7	56.1	59	8
N^6-lactoyl lysine	16.2	219.2	40	156.2	20	8	84.1	35	9	173.1	17	8
N^6-pyruvoyl lysine	19.5	217.0	55	154.0	19	12	84.1	32	6	171.0	15	12
N^6-glycoloyl lysine-d1	12.2	206.2	40	143.1	20	11	84.1	36	14	160.1	64	8
N^6-lactoyl lysine-d1	16.2	220.2	40	157.2	20	8	84.1	35	9	174.1	17	8

[a]MRM transition used for quantitation. [b]MRM transition used for confirmation.

Western-blot signals were quantified using a Fusion-Fx-7 imager with BD-Software (Peqlab, Erlangen, Germany).

Protein Workup. The protein was worked up by a modified procedure from Pogo et al.[24] Minced rat liver (250 mg) was weighed in a 14 mL round-bottom cell-culture tube (Greiner Bio-One, Kremsmuenster, Austria). Cooled (4 °C) lysis buffer (2 mL, 0.32 M sucrose, 3 mM $MgC1_2$) was added, and the sample was lysed at 6500 rpm by an Ultra-Turrax (IKA, Staufen, Germany) for 2 min on ice. The lysate was cleared by 20 μm CellTrics filtration (Sysmex, Norderstedt, Germany) and centrifugation at 10 000 RCF for 15 min. The supernatant was separated, and 50% trichloroacetic acid (TCA) was added to a final concentration of 10%. The precipitate was washed twice with 5% TCA and isopropanol. After the precipitate was dried under a high vacuum, 3 mg of protein were dissolved in 1 mL of phosphate-buffered saline (PBS, pH 7.4, 150 mM NaCl, 10 mM phosphate) and homogenized by a MM 400 mixer mill (Retsch, Haan, Germany). After the addition of 200 μL of a $NaBD_4$ solution (15 mg/mL in 0.01 M NaOH), reduction was allowed to occur for 1 h at room temperature; then, the excess $NaBD_4$ was destroyed by 100 μL of 1 M HCl, and the solution was neutralized by 100 μL of 1 M NaOH. The samples were evaporated in a vacuum concentrator (Savant-Speed-Vac Plus SC 110 A combined with a Vapor Trap RVT 400, Thermo Fisher Scientific, Bremen, Germany), dissolved in water, and lyophilized. The lyophilizate was dissolved in 1 mL of PBS, and aliquots were used for the acid and enzymatic hydrolyses.

Acid Hydrolysis. The acid hydrolysis was performed as described by Glomb and Pfahler.[13] Aliquots of the protein solution (400 μL) were dried, and 800 μL of 6 M HCl was added. The solution was heated for 20 h at 110 °C under an argon atmosphere. The volatiles were removed in a vacuum concentrator, and the residue was dissolved in 492 μL of 0.05 M HCl. Prior to their injection into the HPLC-MS^2 system, the samples were filtered through 0.45 μm cellulose acetate Costar SpinX filters (Corning Inc., Corning, NY).

Enzymatic Hydrolysis. The enzymatic hydrolysis followed a slightly modified protocol by Smuda et al.[5] Pronase E (0.3 U, two additions), leucine aminopeptidase (1 U), and carboxypeptidase Y (0.95 U) were added to 500 μL aliquots of the protein solution. The enzymes were applied stepwise, and the incubations with each were for 24 h at 37 °C in a shaker incubator. A small crystal of thymol was added with the first digestion step. Once the total digestion procedure was completed, the reaction mixtures were filtered through 3000 Da molecular weight cutoff filters (VWR International, Radnor, PA).

For each sample, the efficiency of the acid hydrolysis was assigned to 100%, and the efficiency of the enzymatic hydrolysis was calculated by HPLC-MS^2 analysis of acid-stable CEL.

Analytical HPLC-MS^2. A Jasco PU-2080 Plus quaternary gradient pump with a degasser and a Jasco AS-2057 Plus autosampler (Jasco, Gross-Umstadt, Germany) were used. The mass analyses were performed using an Applied Biosystems API 4000 quadrupole instrument (Applied Biosystems, Foster City, CA) equipped with an API source that used an electrospray-ionization (ESI) interface. The HPLC system was connected directly to the probe of the mass spectrometer. Nitrogen was used as the sheath and auxiliary gas. To measure the analytes, the scheduled-multiple-reaction-monitoring (sMRM) mode of HPLC-MS^2 was used. The optimized parameters for the mass spectrometry are given in Table 1. The quantitation was based on the standard-addition method with known amounts of the pure authentic reference compounds. The values for the limits of detection (LOD) and limits of quantitation (LOQ) for the respective matrices are shown in Table 2.

Table 2. LODs and LOQs of AGEs in Incubations and Protein Hydrolysates

analyte	incubation		protein hydrolysate	
	LOD (mmol/mol lysine)	LOQ (mmol/mol lysine)	LOD (μmol/mol leucine)	LOQ (μmol/mol leucine)
N^6-carboxymethyl lysine	0.040	0.121	0.777	2.590
N^6-glycoloyl lysine	0.003	0.008	0.250	0.834
N^6-glyoxylyl lysine hydrate	0.130	0.391	nd[a]	nd
N^6-carboxyethyl lysine	0.019	0.058	0.413	1.375
N^6-lactoyl lysine	0.003	0.011	0.071	0.238
N^6-pyruvoyl lysine	0.009	0.028	nd	nd
N^6-glycoloyl lysine-d1	nd	nd	0.144	0.481
N^6-lactoyl lysine-d1	nd	nd	0.043	0.144

[a]nd = not determined.

Model Incubations. Prior to the injection into the HPLC-MS^2 system, 100 μL of 6 M HCl was added to 100 μL aliquots of the incubation solutions; the samples were kept at room temperature for 30 min and diluted on a scale of 1:10 with water.

Chromatographic separations were performed on a stainless-steel column (VYDAC 218TP54, 250 × 4.6 mm, RP18, 5 μm, Hesperia, CA) using a flow rate of 1 mL/min and a column temperature of 25 °C. The samples (10 μL) were injected at 2% B and run isocratically for 5 min. The gradient was changed to 100% B within 15 min (held for 10 min), and then the gradient was changed to 2% B within 5 min, at which it was held for 15 min. The eluents were ultrapure water (A) and a mixture of methanol and demineralized water (7:3, v/v; B), both of which were with 1.2 mL/L HFBA. sMRM mode was used for the mass-spectrometric detection.

Protein Hydrolysates. Chromatographic separations were performed on a stainless steel column (XSelect HSS T3, 250 × 3.0 mm, RP18, 5 μm, Waters, Milford, MA) using a flow rate of 0.7 mL/min and a column temperature of 25 °C. The samples (10 μL) were

DOI: 10.1021/acs.jafc.7b05813
J. Agric. Food Chem. 2018, 66, 1898−1906

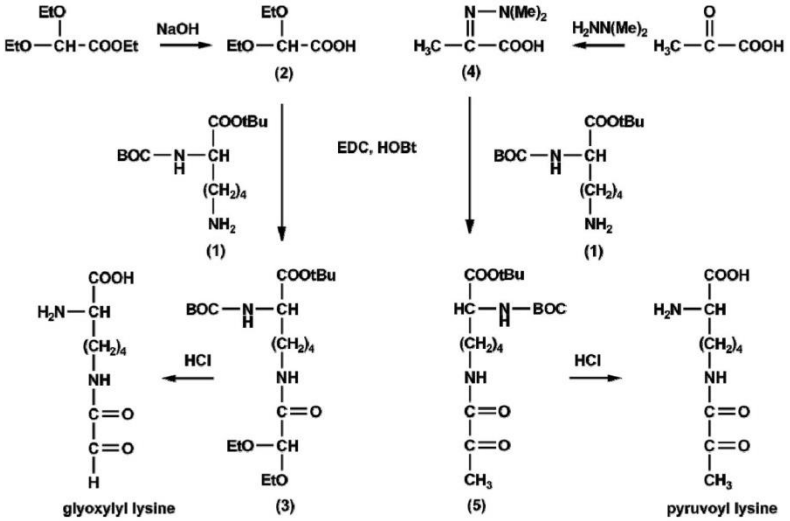

Figure 1. Synthesis of N^6-glyoxylyl lysine and N^6-pyruvoyl lysine.

injected at 2% B and run isocratically for 2 min. The gradient was changed to 14% B within 10 min (held for 0 min); 87% B within 22 min (held for 0 min); and 100% B within 0.5 min, at which it was held for 7 min. Then, the gradient was changed to 2% B within 2.5 min, at which it was held for 8 min. The eluents and mode were the same as described above.

Ninhydrin Assay. The ninhydrin assay was performed as described by Smuda et al.[5] After the complete workup, the contents of the amino acid modifications were standardized to that of L-leucine. A calibration of L-leucine, concentrated between 5 and 100 μM, was performed and referenced to the diluted samples. Each sample was prepared four times.

Analytical GC-MS. The GC-MS method was established by Smuda et al.[12] The samples were analyzed on a Thermo Finnigan Trace GC Ultra coupled to a Thermo Finnigan Trace DSQ (both Thermo Fisher Scientific GmbH, Bremen, Germany). The GC column was a HP-5 (30 m × 0.32 mm, 0.25 μm film thickness; Agilent Technologies, Palo Alto, CA), with an injector at 220 °C, a split ratio of 1:30, and a transfer line at 250 °C. The oven-temperature program was as follows: 100 °C (0 min), 7.5 °C/min to 200 °C (0 min), and 50 °C/min to 320 °C (10 min). Helium 5.0 was used as the carrier gas in constant-flow mode (linear velocity of 28 cm/s, flow of 1 mL/min). Mass spectra were obtained with EI at 70 eV (source: 210 °C) in selected-ion-monitoring mode: glyoxylic acid (m/z 221.0/193.0/73.0) and pyruvic acid (m/z 217.0/189.0/73.0). The retention times were as follows: glyoxylic acid was t_R= 5.85 min, and pyruvic acid was t_R= 4.00 min. Aliquots of the incubations (100 μL) were dried in vacuo, the residues were dissolved in 100 μL of pyridine, and 100 μL of *N,O*-bis(trimethylsilyl)-acetamide with 5% trimethylchlorosilane was added. The samples were kept 4 h at 70 °C prior to injection into the GC-MS system.

High-Resolution Mass Determination (HR-MS). Positive-ion high-resolution ESI mass spectra were obtained from an Orbitrap Elite mass spectrometer (Thermo Fisher Scientific, Bremen, Germany) equipped with an HESI electrospray ion source (spray voltage of 4 kV, capillary temperature of 275 °C, source heater temperature of 40 °C, FTMS resolution >30.000). Nitrogen was used as the sheath and auxiliary gas. The sample solutions were introduced continuously via a 500 μL Hamilton syringe pump with a flow rate of 5 μL/min. The data were evaluated by the Xcalibur software 2.7 SP1.

Nuclear-Magnetic-Resonance Spectroscopy (NMR). NMR spectra were recorded either on a Varian VXR 400 spectrometer operating at 400 MHz for ^{1}H and 100 MHz for ^{13}C or on a Varian Unity Inova 500 instrument operating at 500 MHz for ^{1}H and 125 MHz for ^{13}C. $SiMe_4$ was used as the reference for calibrating the chemical shift.

Statistical Analysis. Analyses were performed in triplicate for each model incubation and resulted in coefficients of variation less than 5% for the AGE concentrations. All significance tests for the AGEs were performed by two-sample *t*-tests. Nonparametric tests (Kurskal–Wallis or Mann–Whitney) were used to detect differences between the groups for the markers of fibrosis.

RESULTS AND DISCUSSION

Syntheses of Authentic Reference Standards. N^6-glyoxylyl lysine and N^6-pyruvoyl lysine were synthesized in an amide-coupling reaction catalyzed by EDC and HOBt (Figure 1). First, derivatives of glyoxylic acid and pyruvic acid with protected carbonyl functions were synthesized in order to increase their solubilities and prevent side reactions. Ethyl diethoxyacetate was treated with NaOH to yield glyoxylic acid diethoxy acetal, **2**, which was coupled with **1** to give the fully protected amide **3**. Pyruvic acid was protected as a *N,N*-dimethyl hydrazone, **4**, and coupled with **1** to give the protected amide **5**. The *N,N*-dimethyl hydrazone group had already been cleaved off during the silica gel chromatography, as described in literature.[22] Finally, amides **3** and **5** were deprotected by treatments with 3 M HCl to give N^6-glyoxylyl lysine and N^6-pyruvoyl lysine.

Both of the target compounds as well as the intermediates **2**, **3**, **4**, and **5** were unequivocally verified by nuclear-magnetic-resonance (NMR) experiments and accurate mass determinations via HR-MS. Furthermore, the chemical shifts at 5.15 ppm in the ^{1}H NMR experiments and 86.7 ppm in the ^{13}C NMR experiments for the terminal aldehyde function showed that N^6-glyoxylyl lysine existed mainly as a hydrate. In contrast, the keto function of N^6-pyruvoyl lysine had a chemical shift of 199.1 ppm in the ^{13}C NMR experiments, indicating its free carbonyl moiety.

Formation of N^6-Glyoxylyl Lysine and N^6-Pyruvoyl Lysine. The HPLC-MS^2 screenings of the aerated incubations of N^2-*t*-Boc-lysine, phosphate buffer and either glyoxal (GO), methylglyoxal (MGO), ascorbic acid, maltose, or the Amadori product of glucose and N^2-*t*-Boc-lysine under physiological conditions indicated the exclusive formation of N^6-glyoxylyl

DOI: 10.1021/acs.jafc.7b05813
J. Agric. Food Chem. 2018, 66, 1898–1906

lysine by GO and the formation of N^6-pyruvoyl lysine by MGO after 7 days at 37 °C. The time course of AGE formation was recorded by collecting aliquots every 24 h (Figure 2). After a 7

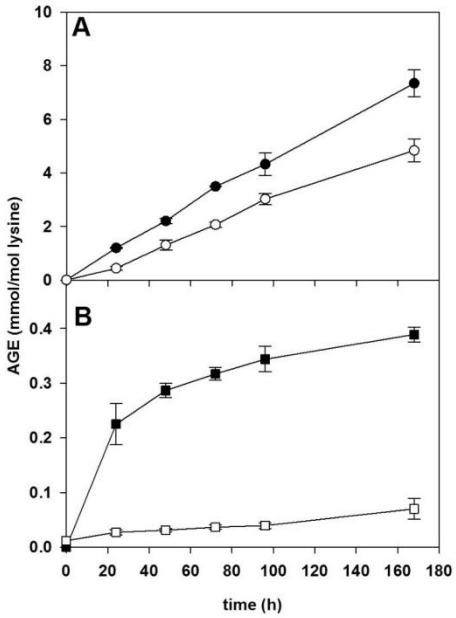

Figure 2. Formation of AGEs in incubations of N^2-*t*-Boc-lysine with glyoxal (A) or methylglyoxal (B) at 37 °C and pH 7.4 under aeration. N^6-Glycoloyl lysine (●), N^6-glyoxylyl lysine (○), N^6-lactoyl lysine (■), and N^6-pyruvoyl lysine (□).

day incubation, the molecular yield was 0.48 mol % N^6-glyoxylyl lysine and 0.01 mol % N^6-pyruvoyl lysine. Taking the short carbon chain of the precursors into account, a formation mechanism based on direct fragmentation of the educts was highly unlikely. Nevertheless, aliquots of the incubations were analyzed by GC-MS in order to determine the corresponding glyoxylic and pyruvic acids, which would be the main byproducts of any dicarbonyl-cleavage reaction.[14] No acid formation was monitored. This unequivocally excluded the formation of N^6-glyoxylyl lysine and N^6-pyruvoyl lysine by the oxidative α-dicarbonyl cleavage or amine-induced β-dicarbonyl cleavage of any putative reaction side-products resulting from, for example, aldol condensation. In addition, incubations of N^2-*t*-Boc-lysine with glyoxylic acid or pyruvic acid showed no formation of the corresponding amide AGEs, ruling out any mechanism of direct amide formation between the carboxylic acid function and the amine under the present conditions. The results therefore strongly pointed toward an isomerization-based reaction as the only possible source of N^6-glyoxylyl lysine and N^6-pyruvoyl lysine, which must include an oxidative step by definition. Consequently, the two novel amide AGEs should be alternative products of the established N^6-carboxymethyl lysine (CML)- and N^6-carboxyethyl lysine (CEL)-reaction cascades, which are based on isomerization (Figure 3).[9] The reaction starts with formation of the imine at one of the carbonyl functions (the keto function in the case of MGO, **I**). Hydration of the other carbonyl group allows the formation of an enamine, which rearranges to give the respective carboxyalkyl endproduct. If alternatively the isomerization starts from the hemiaminal intermediate (in the case of MGO at the aldehyde function, **II**) the respective α-hydroxyamide endproducts result via an enaminol intermediate. Typically, the formation of the carboxyalkyl structure is favored by a factor of 5−30. Indeed, in the above model incubation, both structural classes were detected, reaching 0.73 mol % N^6-glycoloyl lysine (glycolic acid lysine amide, GALA) and 11.24 mol % CML in the case of GO, and 0.03 mol % N^6-lactoyl lysine and 0.12 mol % CEL in the case of MGO (Figure 2, data not shown for CML and CEL). This opened up the hypothesis that the novel α-oxoamide AGEs, N^6-glyoxylyl lysine and N^6-pyruvoyl lysine, might stem from the direct oxidation of GALA and N^6-lactoyl lysine, respectively. However, this notion was undermined by an aerated incubation of the authentic α-hydroxyamide references, where no oxidation products were detected after 7 days.

Influence of Oxygen and pH. Comparative incubations under aerated and deaerated conditions confirmed the nonoxidative pathway of CML, CEL, GALA, and N^6-lactoyl lysine formation, as there were almost no changes in their concentrations (Figure 4, aerated and deaerated 113 and 118 mmol/mol lysine, respectively, for CML; aerated and deaerated both 1.2 mmol/mol lysine for CEL). On the other hand, N^6-glyoxylyl lysine and N^6-pyruvoyl lysine were formed exclusively under aeration. This again stressed the need for an oxidation

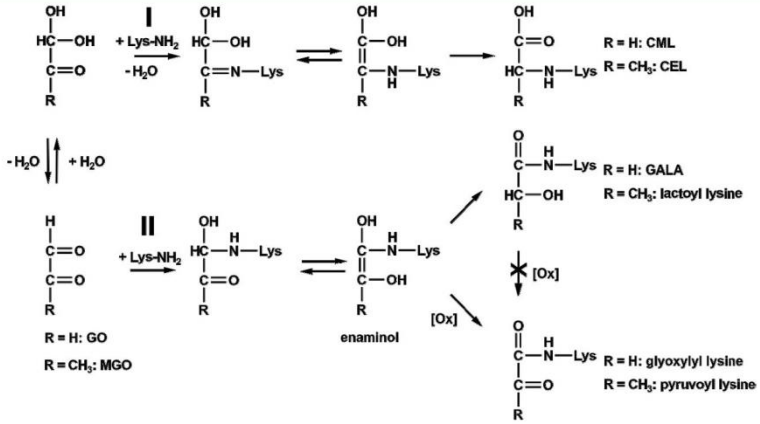

Figure 3. N^6-carboxymethyl lysine and N^6-carboxyethyl lysine isomerization reaction cascades.

DOI: 10.1021/acs.jafc.7b05813
J. Agric. Food Chem. 2018, 66, 1898−1906

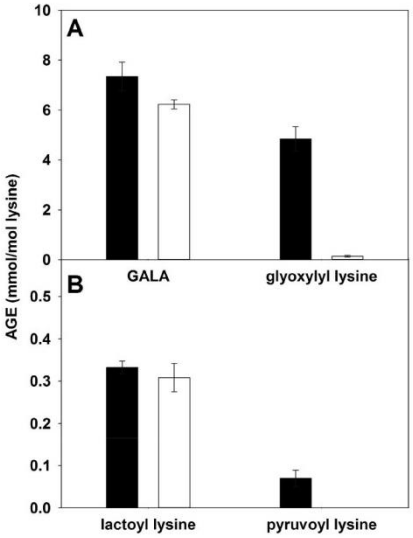

Figure 4. Effects of oxygen on the formation of AGEs in aerated (closed bars) and deaerated (open bars) incubations of N^2-*t*-Boc-lysine with glyoxal (A) or methylglyoxal (B) for 7 days at 37 °C and pH 7.4.

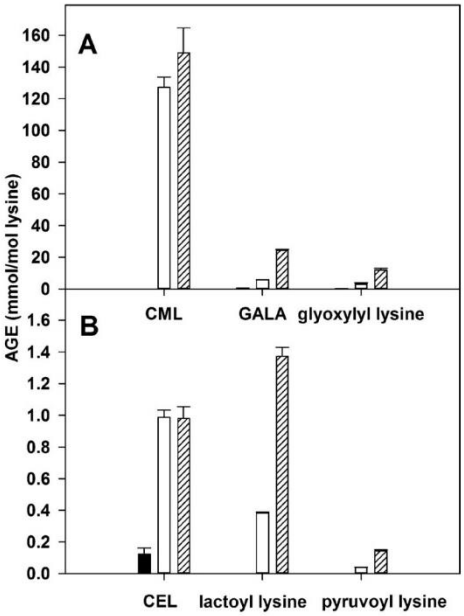

Figure 5. Effects of pH 4.5 (closed bars), 7.4 (open bars), and 9.6 (hatched bars) on the formation of AGEs in incubations of N^2-*t*-Boc-lysine with glyoxal (A) or methylglyoxal (B) for 7 days at 37 °C.

step within the isomerization-reaction scheme. The most likely electron-rich candidate is the enaminol (Figure 3), which should be readily oxidized to give the novel α-oxoamide AGEs. In fact, Hofmann et al. described a similar enaminol intermediate in their explanation of the alternative formation of acids in the general Strecker degradation of amino acids. The nonoxidative degradation of the enaminol led to Strecker aldehydes, whereas in the presence of oxygen, the ratio significantly shifted from 4:1 to almost 1:2 toward the Strecker acids. However, because their setup was more related to food processing at high temperatures, they measured 0.83 mol % phenylacetaldehyde and 1.22 mol % phenylacetic acid in aerated incubations of glyoxal and phenylalanine after 60 min. In full support of our results, a direct oxidation of Strecker aldehydes to Strecker acids was ruled out by isotope-labeling experiments that pointed strongly toward the enaminol as the Strecker acid precursor.[25]

The CML- and CEL-reaction cascades were strongly dependent on pH values (Figure 5). In general, hardly any AGEs are formed under acidic conditions, because the N^6-amino function of lysine is protonated. This leads to a loss of nucleophilicity and prevents the necessary formation of Schiff base adducts. In contrast, the N^6-amino function is sufficiently deprotonated at pH 7.4 to allow an attack at the carbonyl carbon and initiate the formation of AGEs. A factor of about 100 was found between the yields of CML and CEL regardless of whether the reaction proceeded at pH 7.4 or 9.6. This must be attributed to the different character of the carbonyl function initiating the reaction. Whereas for CML, the N^6-amino group of the lysine attacks an aldehyde function of GO, CEL formation requires an attack at the much-less-reactive ketone moiety of MGO. On the other hand, the reason for the pronounced difference in the concentrations of GALA and N^6-lactoyl lysine and of N^6-glyoxylyl lysine and N^6-pyruvoyl lysine at pH 7.4 versus 9.6 by a factor of approximately 4 is less obvious. In diluted aqueous solutions, dicarbonyl structures exist predominantly in their hydrated forms; that is, GO almost exclusively exists as the dihydrate,[26] and 56 and 44% of MGO exist in the mono- and dihydrated forms, respectively.[27] Although this does not change as a result of changes in the pH, the rate of enolization required for the rearrangement step does. This implies that the general course of the reaction is triggered mainly by two aspects, the stability of the endproducts and the rate of isomerization. Obviously in the case of CML and CEL, the high thermodynamic stabilities of the resulting carboxyalkyls are the main driving forces, resulting in almost no differences, whereas in the case of the α-hydroxyamides and α-oxoamides, pH-related changes in the kinetics of rearrangement prevail.

Oxidative-Stress and Aging Markers. Analyses of the AGEs in the model incubations were done after the acid hydrolysis of the BOC protection groups. As is apparent from the NMR data, there is an equilibrium between the carbonyl and hydrate forms. Consequently, HPLC separation led to very broad peaks with poor signal-to-noise ratios for the novel α-oxoamide AGEs. This was especially pronounced for N^6-glyoxylyl lysine (LOD, 0.130 mmol/mol lysine; LOQ, 0.391 mmol/mol lysine) but still satisfactory for quantitation. However, the signals for the native α-oxoamide AGEs were completely lost in the analyses of the liver-tissue samples because of the inevitable load of the matrix. In the first attempt to access the power of the novel AGEs as parameters of oxidative stress and aging, the soluble proteins of the rat livers were extracted by a lysis protocol. Because of their chemical natures, amide AGEs have to be released by enzymatic hydrolysis. The efficiency of this step was referenced to that of acid-stable CEL by a parallel acid-hydrolysis workup for each sample and was typically around 70−80%. Acid hydrolysis must include a reduction step with sodium borohydride to prevent any artifact formation, especially for CML. In the present study, the use of sodium borodeuteride allowed the differentiation of

DOI: 10.1021/acs.jafc.7b05813
J. Agric. Food Chem. 2018, 66, 1898−1906

N^6-glyoxylyl lysine, in the form of N^6-glycoloyl lysine-d1, from any parallel-formed GALA and of N^6-pyruvoyl lysine, in the form of N^6-lactoyl lysine-d1, from N^6-lactoyl lysine. This also eliminated the chromatographic issues with the native α-oxoamides and led to very sharp peaks and significantly reduced background noise. As a result, the sensitivity was improved by a factor of about 200 for N^6-glyoxylyl lysine (LOD, 0.144 μmol/mol leucine; LOQ, 0.481 μmol/mol leucine) and a factor of about 50 for N^6-pyruvoyl lysine (LOD, 0.043 μmol/mol leucine; LOQ, 0.144 μmol/mol leucine). The calculated concentrations of N^6-glyoxylyl lysine and N^6-pyruvoyl lysine were corrected by the subtraction of the natural-isotope peaks (10.16% of GALA and 11.17% of N^6-lactoyl lysine).

To test for the biological significance of the novel α-oxoamides in aging, a rat model was chosen, and the AGEs were analyzed in the soluble-protein fraction of the liver. Inflammatory processes and oxidative stress in this organ were triggered by the induction of cirrhosis with tetrachloromethane. As shown in Table 3, the mean levels of all the AGEs

Table 3. AGEs in Soluble Proteins from Rat-Liver Lysates[a]

AGE (μmol/mol leucine)	3 month old (healthy)	3 month old (cirrhosis)	22 month old (healthy)
N^6-carboxymethyl lysine	5.22 ± 3.34	5.40 ± 3.83	10.07 ± 7.01**
N^6-glycoloyl lysine	0.73 ± 0.07	0.70 ± 0.09	1.36 ± 0.32**
N^6-glyoxylyl lysine	0.37 ± 0.03	0.57 ± 0.16*	0.58 ± 0.03*
N^6-carboxyethyl lysine	11.73 ± 2.32	8.34 ± 2.52	17.27 ± 4.35**
N^6-lactoyl lysine	0.28 ± 0.06	0.34 ± 0.09	0.55 ± 0.06**
N^6-pyruvoyl lysine	0.11 ± 0.04	0.23 ± 0.05*	0.27 ± 0.07*
markers of fibrosis (%)			
sirius-red staining	0.49 ± 0.14	23.16 ± 2.67*	1.70 ± 0.40*
TGF-β	100 ± 26	947 ± 661*	478 ± 143*
smooth muscle antigen	100 ± 31	1995 ± 1057*	453 ± 192*

[a]Means ± standard deviations, n = 5. Significant differences were determined via the t-test or Mann–Whitney test by comparison with the AGE levels and markers of fibrosis in 3 month old healthy rats. *p < 0.05, **p < 0.001.

approximately doubled when 3 month and 22 month old rats were compared, showing p values <5% for N^6-glyoxyly lysine and N^6-pyruvoyl lysine and <0.1% for all the other modifications. It is important to understand that GALA and N^6-glyoxyly lysine are selective parameters for GO, whereas N^6-lactoyl lysine and N^6-pyruvoyl lysine are formed exclusively from MGO. On the other hand, CML can result not only from GO but also from many other precursors as glycolaldehyde or Amadori products. Taking the higher reactivity of GO and the various pathways leading to CML into account, it is quite surprising that the average CML levels in the aged rat livers (10.07 μmol/mol leucine) were lower than the CEL levels (17.27 μmol/mol leucine). A similar observation was found in the renal glomeruli of rats, in which CML was quantitated at 269 μmol/mol lysine, and CEL was quantitated at 329 μmol/mol lysine.[28]

When cirrhosis was induced, it was obvious that N^6-glyoxyly lysine and N^6-pyruvoyl lysine were influenced not only by age but also by oxidative stress. Whereas all the other AGE parameters showed virtually no changes compared with the age-matched healthy control group, the two α-oxoamides increased significantly (p < 5%). The prerequisite oxidation step in their formation mechanism was already highlighted by the above N^2-t-Boc-lysine model incubations. This implies that both of the parameters are indeed specific chemical markers for oxidative stress in vivo (Figure 6).

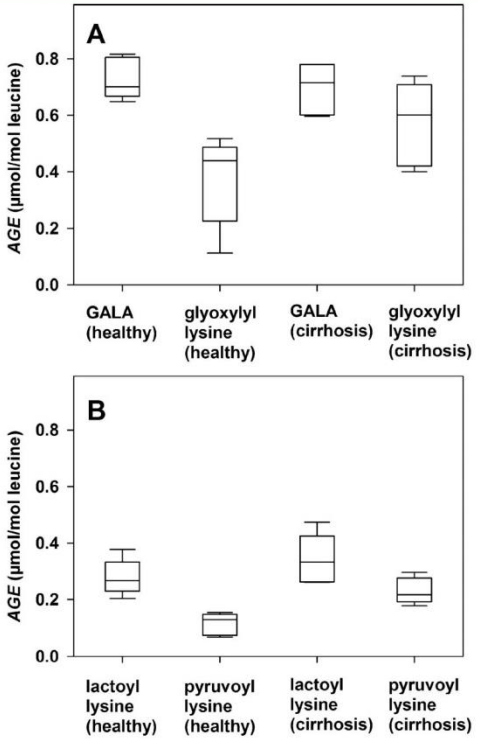

Figure 6. Correlation of GO-specific AGEs (A) and MGO-specific AGEs (B) in rat livers with cirrhosis. Black lines are median values.

The hypothesis of oxidative stress leading to α-oxoamide formation was supported by sirius-red staining and Western blotting of transforming growth factor β (TGF-β) and α smooth-muscle actin (α-SMA, Table 3). Histological sirius-red staining of collagen is an established test for fibrosis, which is associated with increased oxidative stress.[29] Whereas collagen was nearly absent in the healthy, young rat livers (0.49%), fibrosis increased slightly with age (1.70%) and by a factor of about 50 in the cirrhotic animals (23.16%). Western blotting of TGF-β and α-SMA was another method used to access fibrosis-induced tissue changes. Additionally, TGF-β signaling and expression as well as its activation from the latent complex are increased by reactive oxygen species, and TGF-β itself in turn induces the production of reactive oxygen species.[30] The intensity of both markers was referenced as 100% for the young- and healthy-rat-liver proteins. In the 22 month old rats, the levels of TGF-β (478%) and α-SMA (453%) were nearly 5-times higher than they were in the young rats. The induction of fibrosis under oxidative stress was strongly accelerated in the cirrhotic rats, in which the TGF-β levels elevated to 947%, and the α-SMA levels elevated to 1995%. These results were thus in line with the significantly higher amounts of α-oxoamides found in the old and cirrhotic rat livers.

To decouple the influences of aging and oxidative stress on the formation of α-oxoamides, the ratios between GALA and

DOI: 10.1021/acs.jafc.7b05813
J. Agric. Food Chem. 2018, 66, 1898–1906

N^6-glyoxylyl lysine and between N^6-lactoyl lysine and N^6-pyruvoyl lysine were calculated. Whereas the N^6-glyoxylyl/GALA and N^6-pyruvoyl/N^6-lactoyl lysine ratios remained on average constant at around 0.5 in the young and aged rat livers, the ratios in the cirrhotic livers increased to 0.8 for N^6-glyoxylyl/GALA and 0.7 for N^6-pyruvoyl/N^6-lactoyl lysine. These changes in the ratios may thus be valuable markers of liver cirrhosis in future research. Further investigations have to validate the present preliminary results and open up the applicability of these novel markers to other pathologies with inflammatory oxidative stress.

AUTHOR INFORMATION

Corresponding Author

*E-mail: marcus.glomb@chemie.uni-halle.de, Fax: ++049-345-5527341.

ORCID

Tim Baldensperger: 0000-0002-9653-3156

Marcus A. Glomb: 0000-0001-8826-0808

Funding

Funding was supported by the Deutsche Forschungsgemeinschaft (DFG, Germany) Research Training Group 2155, ProMoAge.

Notes

The authors declare no competing financial interest.

ACKNOWLEDGMENTS

We thank Dr. D. Ströhl from the Institute of Organic Chemistry, Halle, Germany, for recording the NMR spectra and Dr. A. Frolov from the Leibniz Institute of Plant Biochemistry, Halle, Germany, for performing the accurate mass determination.

ABBREVIATIONS USED

AGEs, advanced-glycation endproducts; GO, glyoxal; MGO, methylglyoxal; CML, N^6-carboxymethyl lysine; CEL, N^6-carboxyethyl lysine; GALA, N^6-glycoloyl lysine; EDC, 1-ethyl-3-(3-(dimethylamino)propyl)carbodiimide; HOBt, hydroxybenzotriazole; TCA, trichloroacetic acid; PBS, phosphate-buffered saline; HFBA, heptafluorobutyric acid; sMRM, scheduled multiple-reaction monitoring; TGF-β, transforming growth factor β; α-SMA, α smooth-muscle actin

REFERENCES

(1) Maillard, L. C. Action des acidesamines sur les sucres: formation des melanoidines par voie methodique. *CR Acad. Sci. Paris* **1912**, *66*–68.

(2) Hellwig, M.; Henle, T. Baking, ageing, diabetes. A short history of the Maillard reaction. *Angew. Chem., Int. Ed.* **2014**, *53*, 10316–10329.

(3) Mottram, D. S.; Wedzicha, B. L.; Dodson, A. T. Acrylamide is formed in the Maillard reaction. *Nature* **2002**, *419*, 448–449.

(4) Delgado-Andrade, C. Carboxymethyl-lysine. Thirty years of investigation in the field of AGE formation. *Food Funct.* **2016**, *7*, 46–57.

(5) Smuda, M.; Henning, C.; Raghavan, C. T.; Johar, K.; Vasavada, A. R.; Nagaraj, R. H.; Glomb, M. A. Comprehensive analysis of maillard protein modifications in human lenses. Effect of age and cataract. *Biochemistry* **2015**, *54*, 2500–2507.

(6) Henning, C.; Liehr, K.; Girndt, M.; Ulrich, C.; Glomb, M. A. Extending the spectrum of α-dicarbonyl compounds in vivo. *J. Biol. Chem.* **2014**, *289*, 28676–28688.

(7) Glomb, M. A.; Monnier, V. M. Mechanism of protein modification by glyoxal and glycolaldehyde, reactive intermediates of the Maillard reaction. *J. Biol. Chem.* **1995**, *270*, 10017–10026.

(8) Glomb, M. A.; Tschirnich, R. Detection of α-Dicarbonyl Compounds in Maillard Reaction Systems and in Vivo. *J. Agric. Food Chem.* **2001**, *49*, 5543–5550.

(9) Henning, C.; Glomb, M. A. Pathways of the Maillard reaction under physiological conditions. *Glycoconjugate J.* **2016**, *33*, 499–512.

(10) Uchida, K.; Khor, O. T.; Oya, T.; Osawa, T.; Yasuda, Y.; Miyata, T. Protein modification by a Maillard reaction intermediate methylglyoxal. *FEBS Lett.* **1997**, *410*, 313–318.

(11) Davídek, T.; Robert, F.; Devaud, S.; Vera, F. A.; Blank, I. Sugar fragmentation in the Maillard reaction cascade. Formation of short-chain carboxylic acids by a new oxidative α-dicarbonyl cleavage pathway. *J. Agric. Food Chem.* **2006**, *54*, 6677–6684.

(12) Smuda, M.; Voigt, M.; Glomb, M. A. Degradation of 1-deoxy-D-erythro-hexo-2,3-diulose in the presence of lysine leads to formation of carboxylic acid amides. *J. Agric. Food Chem.* **2010**, *58*, 6458–6464.

(13) Glomb, M. A.; Pfahler, C. Amides are novel protein modifications formed by physiological sugars. *J. Biol. Chem.* **2001**, *276*, 41638–41647.

(14) Smuda, M.; Glomb, M. A. Fragmentation pathways during Maillard-induced carbohydrate degradation. *J. Agric. Food Chem.* **2013**, *61*, 10198–10208.

(15) Smuda, M.; Glomb, M. A. Maillard degradation pathways of vitamin C. *Angew. Chem., Int. Ed.* **2013**, *52*, 4887–4891.

(16) Thorpe, S. R.; Baynes, J. W. CML. A brief history. *Int. Congr. Ser.* **2002**, *1245*, 91–99.

(17) Nowotny, K.; Jung, T.; Höhn, A.; Weber, D.; Grune, T. Advanced glycation end products and oxidative stress in type 2 diabetes mellitus. *Biomolecules* **2015**, *5*, 194–222.

(18) Fujioka, M.; Tanaka, M. Enzymic and Chemical Synthesis of e-N-(L-Propionyl-2)-L-Lysine. *Eur. J. Biochem.* **1978**, *90*, 297–300.

(19) Gellett, A. M.; Huber, P. W.; Higgins, P. J. Synthesis of the unnatural amino acid Nα-Nε-(ferrocene-1-acetyl)-l-lysine. A novel organometallic nuclease. *J. Organomet. Chem.* **2008**, *693*, 2959–2962.

(20) Pinto, A.; Conti, P.; Grazioso, G.; Tamborini, L.; Madsen, U.; Nielsen, B.; De Micheli, C. Synthesis of new isoxazoline-based acidic amino acids and investigation of their affinity and selectivity profile at ionotropic glutamate receptors. *Eur. J. Med. Chem.* **2011**, *46*, 787–793.

(21) Tapia, I.; Alcazar, V.; Moran, R. Synthesis of chromanes using pyruvic acid dimethylhydrazone dianion. *Can. J. Chem.* **1990**, *68*, 2190–2191.

(22) Katayama, H.; Utsumi, T.; Ozawa, C.; Nakahara, Y.; Hojo, H.; Nakahara, Y. Pyruvoyl, a novel amino protecting group on the solid phase peptide synthesis and the peptide condensation reaction. *Tetrahedron Lett.* **2009**, *50*, 818–821.

(23) Zipprich, A.; Loureiro-Silva, M. R.; Jain, D.; D'Silva, I.; Groszmann, R. J. Nitric oxide and vascular remodeling modulate hepatic arterial vascular resistance in the isolated perfused cirrhotic rat liver. *J. Hepatol.* **2008**, *49*, 739–745.

(24) Pogo, A. O.; Allfrey, V. G.; Mirsky, A. E. Evidence for increased DNA template activity in regenerating liver nuclei. *Proc. Natl. Acad. Sci. U. S. A.* **1966**, *56*, 550–557.

(25) Hofmann, T.; Münch, P.; Schieberle, P. Quantitative Model Studies on the Formation of Aroma-Active Aldehydes and Acids by Strecker-Type Reactions. *J. Agric. Food Chem.* **2000**, *48*, 434–440.

(26) Avzianova, E.; Brooks, S. D. Raman spectroscopy of glyoxal oligomers in aqueous solutions. *Spectrochim. Acta, Part A* **2013**, *101*, 40–48.

(27) McLellan, A. C.; Thornalley, P. J. Synthesis and chromatography of 1,2-diamino-4,5-dimethoxybenzene, 6,7-dimethoxy-2-methylquinoxaline and 6,7-dimethoxy-2,3-dimethylquinoxaline for use in a liquid chromatographic fluorimetric assay of methylglyoxal. *Anal. Chim. Acta* **1992**, *263*, 137–142.

(28) Thornalley, P. J.; Battah, S.; Ahmed, N.; Karachalias, N.; Agalou, S.; Babaei-Jadidi, R.; Dawnay, A. Quantitative screening of advanced glycation endproducts in cellular and extracellular proteins by tandem mass spectrometry. *Biochem. J.* **2003**, *375*, 581–592.

DOI: 10.1021/acs.jafc.7b05813
J. Agric. Food Chem. 2018, 66, 1898–1906

(29) Moeller, M.; Thonig, A.; Pohl, S.; Ripoll, C.; Zipprich, A. Hepatic arterial vasodilation is independent of portal hypertension in early stages of cirrhosis. *PLoS One* **2015**, *10*, e0121229.
(30) Liu, R.-M.; Gaston Pravia, K. A. Oxidative stress and glutathione in TGF-β-mediated fibrogenesis. *Free Radical Biol. Med.* **2010**, *48*, 1–15.

DOI: 10.1021/acs.jafc.7b05813
J. Agric. Food Chem. 2018, 66, 1898–1906

Reprinted with permission from Baldensperger, T.; Jost, T.; Zipprich, A.; Glomb, M. A. Novel α-Oxoamide Advanced-Glycation Endproducts within the N^6-Carboxymethyl Lysine and N^6-Carboxyethyl Lysine Reaction Cascades, *J. Agric. Food Chem.* **2018**, *66*, pp. 1898-1906. Copyright 2018 American Chemical Society.

5.2 Publication 2

analytical chemistry

Article

Cite This: Anal. Chem. 2019, 91, 12336−12343

pubs.acs.org/ac

Quantitation of Reactive Acyl-CoA Species Mediated Protein Acylation by HPLC−MS/MS

Tim Baldensperger,[†] Simone Di Sanzo,[‡] Alessandro Ori,[‡] and Marcus A. Glomb*[,†]

[†]Institute of Chemistry, Food Chemistry, Martin-Luther-University Halle-Wittenberg, Kurt-Mothes-Straße 2, 06120 Halle (Saale), Germany

[‡]Leibniz Institute on Aging—Fritz Lipmann Institute (FLI), Beutenbergstraße 11, 07745 Jena, Germany

Supporting Information

ABSTRACT: Recently discovered acylation by reactive acyl-CoA species is considered a novel regulatory mechanism in epigenetics and metabolism. Established analytical methods like Western blotting and proteomics fail to detect the plethora of acylation structures in a single analysis and lack the ability of absolute quantitation. In this paper, we developed an HPLC−MS/MS method for the simultaneous detection and quantitation of 14 acylated lysine species in biological samples. Extensive effort was invested into method validation resulting in recovery rates between 75 and 93% and levels of detection in the nanomolar range. Thus, we were able to quantitate 8 acylation structures in mouse liver, kidney, heart, and brain. Further enrichment by repetitive HPLC fractionation resulted in the quantitation of 6 additional acylation structures including 4 novel modifications: N^6-acetoacetyl lysine, N^6-isovaleryl lysine, N^6-(2-methylbutyryl) lysine, and N^6-tiglyl lysine.

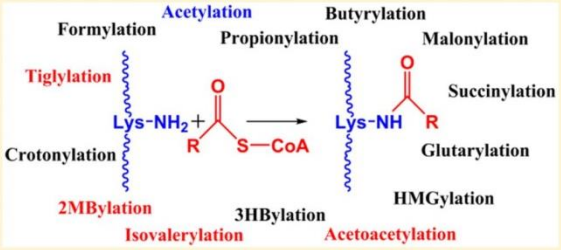

The structure and function of proteins is highly regulated by post-translational modifications (PTMs). Acetylation of lysine side chains is one of the most abundant PTMs and was discovered in histone proteins by Phillips in 1963.[1] The modification's pivotal role in gene regulation was proposed by Allfrey in 1964, who linked the neutralization of positively charged lysine in chromatin via acetylation to weakened interaction with negatively charged DNA and hence increased gene expression.[2] Apart from its role in epigenetics, acetylation emerged as a major regulatory mechanism in metabolism, cell signaling and disease.[3] Recent advances in mass spectrometry led to the discovery of several structurally related PTMs called short-chain lysine acylations. Depending on their hydrophobicity and charge lysine acylations are categorized into hydrophobic (formylation,[4,5] propionylation,[6] butyrylation,[6] crotonylation[7]), polar (β-hydroxybutyrylation[8]), and acidic (malonylation,[9] succinylation,[10] glutarylation,[11] 3-hydroxy-3-methylglutarylation[12]) modifications.[13] In analogy to acetylation these novel PTMs are expected to be important regulators of metabolism, aging, and disease.[14−16]

While N^6-formyl lysine is formed during Maillard reactions[5] and potentially during oxidative DNA damage,[4] all other short-chained acylations known so far originate from their corresponding acyl-CoA thioesters.[17] These highly reactive acyl-CoA species (RACS) are central intermediates in carbohydrate, lipid, and amino acid metabolism. RACS are concentrated between 1 and 100 nmol/g wet weight in mice and humans depending on organ and individual thioester structure.[18,19] Mitochondria are local hotspots of RACS and estimated concentrations of acetyl-CoA are 3−50 times higher compared to cytosol and nucleus.[20] One of the most controversial questions is whether lysine is acylated by RACS enzymatically or nonenzymatically. The human proteome contains 21 putative lysine acetyltransferases mainly located at the nucleus and cytosol. Consequently, nuclear acetylation is considered an enzymatic pathway.[21] Specific acyltransferases are currently unknown, but in recent publications several lysine acetyltransferases were shown to have an expanded repertoire of promiscuous acyltransferase activities. However, it has to be considered that these acyltransferase activities are significantly lower than corresponding acetyltransferase activities.[13] Alternative nonenzymatic acetylation and acylation by RACS are postulated especially for mitochondrial proteins. Besides the low number of acetyltransferases in mitochondria[21] the unique chemical conditions with high RACS concentrations on the one hand and slightly basic pH of 8 on the other hand provide rising evidence for an enzyme independent acylation.[17] In vitro incubations of proteins as well as denatured mitochondrial lysates with various RACS under physiological conditions indeed proved the concept of nonenzymatic acylation.[12,20,22]

First analytical techniques to identify and characterize the acylome were based on mass spectrometry of peptides after trypsin digestion of proteins.[6] The big advantage of this approach is the site-specific identification of PTMs. Unfortu-

Received: June 11, 2019
Accepted: August 28, 2019
Published: September 10, 2019

ACS Publications © 2019 American Chemical Society

DOI: 10.1021/acs.analchem.9b02656
Anal. Chem. 2019, 91, 12336−12343

nately, acylation occurs at relatively low stoichiometry leading to problems identifying low abundant modification sites. This problem was partially solved by enrichment of acylated proteins using immunoprecipitation prior to trypsin digestion. As a result the number of identified modification sites increased significantly, but costs and time for sample preparation increased as well. A further drawback is the complicated quantitation of acylated peptides.[15] An easy way to monitor relative changes in the acylome is separation of proteins by SDS-PAGE and visualization via Western blotting using specific antibodies. Absolute quantitation and monitoring of more than one type of acylation at a time is not possible using this approach.[16] In order to face the main disadvantages of acylomics and Western blotting, we herein present a fast, sensitive and reliable HPLC−MS/MS multimethod for simultaneous identification and quantitation of 14 different acylated lysine species in enzymatic protein hydrolysates.

■ EXPERIMENTAL SECTION

Chemicals and Enzymes. All chemicals of the highest quality available were provided by Sigma-Aldrich (Munich/Steinheim, Germany), unless otherwise indicated. Tiglic acid, 4-hydroxy-4-methyl-dihydro-pyran-2,6-dione, and 3-hydroxybutyric acid were purchased from Abcr GmbH (Karlsruhe, Germany). NMR solvents were purchased from ARMAR Chemicals (Leipzig/Doettingen, Germany). Authentic reference standards of N^6-formyl lysine and N^6-acetyl lysine were purchased from Sigma-Aldrich. N^2-*t*-Boc-lysine *t*-butyl ester was synthesized as published previously.[23] Syntheses and structure elucidation of authentic reference standards is described in the Supporting Information (SI). Pronase E (ProE) was purchased from Sigma-Aldrich. Carboxypeptidase Y (CPY) was prepared as described by Johansen et al.[24] Leucine aminopeptidase (LAP) was prepared as described by Wachsmuth et al.[25]

High Resolution Mass Determination (HR-MS). Positive ion high resolution electrospray ionization (ESI) mass spectra were obtained from an Orbitrap Elite mass spectrometer (Thermofisher Scientific, Bremen, Germany) equipped with an HESI electrospray ion source (spray voltage 4 kV, capillary temperature 275 °C, source heater temperature 40 °C, FTMS resolution >30.000). Nitrogen was used as sheath and auxiliary gas. The sample solutions were introduced continuously via a 500 μL Hamilton syringe pump (Reno, U.S.A.) with a flow rate of 5 μL/min. The data were evaluated by the Xcalibur software 2.7 SP1.

Nuclear Magnetic Resonance Spectroscopy (NMR). NMR spectra were recorded on a VXR 400 spectrometer (Varian, Palo Alto, U.S.A.) operating at 400 MHz for ^{1}H and 100 MHz for ^{13}C. $SiMe_4$ was used as a reference for calibrating the chemical shift.

Analytical HPLC−MS/MS. A PU-2080 Plus quaternary gradient pump with degasser and a AS-2057 Plus autosampler (Jasco, Gross-Umstadt, Germany) were used. The mass analyses were performed using an API 4000 quadrupole instrument (Applied Biosystems, Foster City, U.S.A.) equipped with an API source using ESI. The HPLC system was connected directly to the probe of the mass spectrometer. Nitrogen was used as sheath and auxiliary gas. To measure the analytes the scheduled multiple-reaction monitoring (sMRM) mode of HPLC−MS/MS was used. The optimized parameters for mass spectrometry are given in Table 1. Values for limit of detection (LOD) and limit of quantitation (LOQ) for respective matrices are shown in Table 2.

Chromatographic separations were performed on a stainless steel column (XSelect HSS T3, 250 × 3.0 mm, RP18, 5 μm, Waters, U.S.A.) using a flow rate of 0.7 mL/min and a column temperature of 25 °C. Eluents were ultrapure water (A) and a mixture of methanol and ultrapure water (7:3, v/v; B), both supplemented with 1.2 mL/L heptafluorobutyric acid. Samples were injected (10 μL) at 2% B and run isocratic for 2 min, gradient was changed to 14% B within 10 min (held for 0 min), 87% B within 22 min (held for 0 min), 100% B within 0.5 min (held for 7 min) and 2% B within 2.5 min (held 8 min).

Quantitation. Quantitation was based on the standard addition method using known amounts of the pure authentic reference compounds. More precisely, increasing concentrations of authentic reference compounds at factors of approximately 0.5, 1, and 2 times the concentration of the compounds in the sample were added to separate aliquots of the hydrolyzed sample. The aliquots were analyzed, and a regression of response (peak area) versus concentration was used to determine the concentration of the analyte in the sample. Calibration with this method resolves potential matrix interferences. Peak areas were determined using the Analyst software version 1.6.2 (Applied Biosystems, Foster City, U.S.A.).

Enrichment of Analytes. The HPLC setup was as described for the analytical HPLC−MS/MS except chromatographic separations were performed on a stainless steel column (VYDAC 218TP54, 250 × 4.6 mm, RP18, 5 μm, Hesperia, U.S.A.) using a flow rate of 1 mL/min and a column temperature of 25 °C. Samples were injected (25 μL) at 2% B and run isocratic for 5 min, gradient was changed to 100% B within 15 min (held for 10 min). Then gradient was changed to 2% B within 5 min (held 15 min). Fractions containing respective analytes were collected using a CHF122SB fraction collector (Advantec MFS, Dublin, U.S.A.), pooled and concentrated by a factor of 5. The concentrated sample was applied to analytical HPLC−MS/MS.

Enzymatic Hydrolysis. To 250 μL aliquots containing 3 mg of protein per mL in 0.1 M Tris buffer (pH 7.4) a small crystal of thymol was added. Enzymes were added stepwise starting with 30 μL ProE (0.3 units), 40 μL CPY (0.1 units) after 48 h and 10 μL LAP (0.5 units) after 72 h. Samples were incubated at 37 °C in a shaker incubator for 96 h. Once the total digestion procedure was completed, reaction mixtures were filtered through 3 kDa molecular weight cutoff filters (VWR International, Radnor, U.S.A.).

Acid Hydrolysis. Aliquots of protein solution (250 μL) were dried in a vacuum concentrator (Savant-Speed-Vac Plus SC 110 A combined with a Vapor Trap RVT 400, Thermofisher Scientific, Bremen, Germany). 800 μL of 6 M HCl was added, and the solution was heated 20 h at 110 °C under an argon atmosphere. Volatiles were removed in a vacuum concentrator and the residue was dissolved in 330 μL of ultrapure water. Samples were filtered through 0.45 μm cellulose acetate Costar SpinX filters (Corning Inc., Corning, U.S.A.).

Ninhydrin Assay. After complete workup and 250-fold dilution in ultrapure water, the amount of amino acids in hydrolysates was determined by ninhydrin assay and referenced to a calibration of L-leucine concentrated between 5 and 100 μM. The absorbance was determined at 546 nm

DOI: 10.1021/acs.analchem.9b02656
Anal. Chem. 2019, 91, 12336−12343

Table 1. Mass Spectrometric Parameters for Quantitation

modification	retention time (min)	precursor		product ion 1[a]			product ion 2[b]			product ion 3[b]		
		m/z (amu)	DP (V)	m/z (amu)	CE (eV)	CXP (V)	m/z (amu)	CE (eV)	CXP (V)	m/z (amu)	CE (eV)	CXP (V)
N^6-formyl lysine	11.5	175.1	40	112.1	20	13	84.1	35	7	129.1	15	13
N^6-malonyl lysine	13.4	233.2	45	126.2	20	10	84.2	38	10	170.3	22	12
N^6-acetyl lysine	14.7	189.2	40	126.1	18	10	84.2	31	5	143.1	14	10
N^6-(3-hydroxybutyryl) lysine	16.5	233.3	50	84.2	34	5	147.3	16	10	130.2	21	6
N^6-acetoacetyl lysine	16.7	230.8	50	84.3	38	7	168.2	20	12	147.4	19	11
N^6-succinyl lysine	16.8	247.1	50	84.3	40	10	184.4	21	12	130.1	26	12
N^6-propionyl lysine	19.1	203.0	45	84.3	35	12	140.4	19	13	157.4	15	10
N^6-(3-hydroxy-3-methylglutaryl) lysine	19.5	291.0	55	84.2	45	6	130.3	29	10	229.3	20	15
N^6-glutaryl lysine	19.7	261.1	55	84.3	40	10	198.3	20	15	225.2	19	15
N^6-crotonyl lysine	23.2	215.2	50	152.4	18	11	84.3	32	5	169.1	16	10
N^6-butyryl lysine	23.3	217.0	50	84.3	32	5	154.3	18	10	171.4	17	10
N^6-(2-methylbutyryl) lysine	26.3	231.0	50	84.2	28	7	168.4	18	10	185.1	15	11
N^6-tiglyl lysine	26.4	229.4	40	166.2	18	11	84.3	25	6	183.3	15	12
N^6-isovaleryl lysine	27.1	231.2	50	84.2	33	7	168.3	19	12	185.0	16	12

[a]MRM transition used for quantitation. [b]MRM transition used for confirmation.

with an Infinite M200 microplate reader (Tecan, Männedorf, Switzerland) using 96-well plates. Each sample was prepared three times.

Efficiency of Hydrolysis. The efficiency of acid hydrolysis was assigned 100%. Consequently, the efficiency of enzymatic hydrolysis is the quotient of leucine equivalents in enzymatic hydrolysates and acid hydrolysates.

Recovery of Analytes. 250 μL bovine serum albumin (BSA) solution (3 mg/mL) in 0.1 M Tris buffer (pH 7.4) was enzymatically digested as a blank. To the same setup authentic acylation standards (final concentration of 0.1 μM) were added prior to addition of enzymes. Concentrations of acylation standards were determined after digestion using standard addition calibration and corrected by the blank value. Recovery was defined as the quotient of measured concentration in samples and theoretically added concentration.

Housing of Animals. All mice were C57BL/6J obtained from Janvier (Le Genest-Saint-Isle, France) or from internal breeding. Animals were maintained at the Leibniz Institute on Aging—Fritz Lipmann Institute (FLI) in a specific pathogen-free animal facility with a 12 h light/dark cycle. Mice were euthanized with CO_2. The protocols of animal maintenance and euthanasia were approved by the local authority in the State of Thuringia, Germany.

Tissue Collection and Protein Workup. Organs from 3 to 4 months old mice were collected and snap frozen in liquid nitrogen. Organs were transferred into 2 mL Precellys lysing kit tubes (Ceramic-kit 1.4/2.8 mm, Bertin Technologies, France) and 1 mL of PBS with EDTA-free protease inhibitor (Roche, Basel, Switzerland) was added. Samples were homogenized using a Precellys 24 homogenizer (Bertin Technologies, France) applying 2 cycles at 6000 rpm for 30 s. After centrifugation at 18 000g for 5 min homogenates were transferred to 2 mL Eppendorf tubes. 75 μL lysis buffer (4% SDS, 100 mM HEPES, pH 8.0, 20 mM DTT) was added to 300 μL homogenate. Samples were sonicated using a Bioruptor Plus (Diagenode, Belgium) for 10 cycles (30 s ON/60 s OFF) at high setting. The samples were quickly centrifuged and a second sonication cycle was performed as described above. The samples were centrifuged at 18 000g for 1 min, and the supernatant transferred to 15 mL Falcon tubes. Proteins were precipitated overnight at −20 °C by addition of 4 volumes ice-cold acetone. Samples were centrifuged at 3220g for 30 min at 4 °C, and pellets were washed twice with 1 mL ice-cold 80% acetone in water (v/v). Pellets were allowed to air-dry and were dissolved in 2 mL PBS with sonication. Samples were stored at −20 °C until further use.

Statistical Analysis. All significance tests were performed by two-sample t-Test.

RESULTS AND DISCUSSION

Syntheses of Authentic Reference Standards. Aliphatic lysine acylation structures were synthesized in an amide coupling reaction between the corresponding carboxylic acid and N^2-*t*-Boc-lysine *t*-butyl ester catalyzed by EDC and HOBt. The protected amides were purified by silica gel chromatography. Authentic reference standards were obtained after deprotection using 3 M HCl and purification by reverse phase chromatography.

Acidic acylation standards were synthesized in a similar way, except for the use of mono-t-butyl esters of corresponding dicarboxylic acids. In case of N^6-(3-hydroxy-3-methyl) glutaryl lysine the carboxylic acid anhydride (4-hydroxy-4-methyl-

DOI: 10.1021/acs.analchem.9b02656
Anal. Chem. 2019, 91, 12336−12343

Table 2. LODs and LOQs of Acylated Lysine Modifications

modification	liver		kidney		heart		brain	
	LOD	LOQ	LOD	LOQ	LOD	LOQ	LOD	LOQ
	(μmol/mol leucine)							
N^6-formyl lysine	0.122	0.406	0.230	0.767	0.217	0.724	0.100	0.335
N^6-malonyl lysine	0.249	0.829	0.097	0.324	0.156	0.525	0.177	0.389
N^6-acetyl lysine	0.078	0.260	0.058	0.192	0.026	0.087	0.064	0.212
N^6-acetoacetyl lysine	0.111	0.371	0.079	0.264	0.114	0.381	0.058	0.193
N^6-(3-hydroxybutyryl) lysine	0.280	0.933	0.173	0.578	0.241	0.804	0.175	0.582
N^6-succinyl lysine	0.067	0.223	0.084	0.280	0.041	0.138	0.041	0.136
N^6-propionyl lysine	0.065	0.216	0.018	0.060	0.020	0.066	0.022	0.072
N^6-(3-hydroxy-3-methylglutaryl) lysine	0.055	0.184	0.074	0.246	0.065	0.216	0.068	0.227
N^6-glutaryl lysine	0.081	0.270	0.083	0.275	0.053	0.178	0.055	0.185
N^6-butyryl lysine	0.031	0.104	0.028	0.095	0.015	0.049	0.028	0.095
N^6-crotonyl lysine	0.003	0.011	0.004	0.013	0.002	0.006	0.003	0.011
N^6-(2-methylbutyryl) lysine	0.081	0.271	0.032	0.105	0.037	0.125	0.022	0.074
N^6-tiglyl lysine	0.013	0.043	0.015	0.050	0.016	0.055	0.022	0.073
N^6-isovaleryl lysine	0.044	0.148	0.041	0.137	0.066	0.219	0.030	0.100

dihydro-pyran-2,6-dione) was directly coupled with N^2-*t*-Boc-lysine *t*-butyl ester.

The synthesis of N^6-(3-hydroxybutyryl) lysine required the protection of the hydroxyl functionality prior to amide coupling. Therefore, alcoholysis of acetic anhydride in $HClO_4$ was used to protect 3-hydroxybutyric acid as 3-acetoxybutyric acid, which was further processed as described for aliphatic modifications.

Synthesis of N^6-acetoacetyl lysine started with the synthesis of the protected acetoacetylic acid ketal ((2-methyl-1,3-dioxolan-2-yl) acetic acid) from base catalyzed hydrolysis of fructone (ethyl (2-methyl-1,3-dioxolan-2-yl) acetate). Instead of the free corresponding acid the protected ketal was coupled with N^2-*t*-Boc-lysine *t*-butyl ester to prevent undesired side reactions by the carbonyl function.

All target compounds as well as their intermediates were unequivocally verified by nuclear magnetic resonance experiments and accurate mass determination via high resolution mass spectrometry. Detailed synthesis routes and spectra of authentic reference standards can be found in the SI.

Development of HPLC–MS/MS Method. The diluted authentic reference standards of lysine acylations were introduced continuously into the mass spectrometer via a syringe pump for compound optimization and determination of MRM transitions (Table 1). Ramping of the declustering potential (DP) in Q1 mode was used to obtain the maximum signal for the precursor ion M + H^+ in positive electrospray ionization. In general, structures with higher molecular masses and higher content of electronegative oxygen required higher potentials for optimal declustering. In the next step specific product ions were determined for every structure via collision energy (CE) ramping. Characteristic fragmentations were the neutral loss of formic acid (m/z −46), ammonia (m/z −17) and formation of pyrrolinium ion (m/z 84). As an example the fragmentation of N^6-acetyl lysine (m/z 189.2) by loss of formic acid resulted in product ion 3 (m/z 143.1). Additional loss of ammonia resulted in product ion 1 (m/z 126.1) and product ion 2 was the lysine specific pyrrolinium ion (m/z 84.2). The specific product ions were used to optimize the signal intensity of MRM transitions by ramping CE and collision cell exit potential (CXP). The most abundant MRM transition was chosen for analyte quantitation and two additional transitions were selected for analyte confirmation.

Analytes were separated by reverse-phase HPLC using a water–methanol gradient and heptafluorobutyric acid (HFBA) as ion pair reagent (Figure 1). HFBA was added to improve

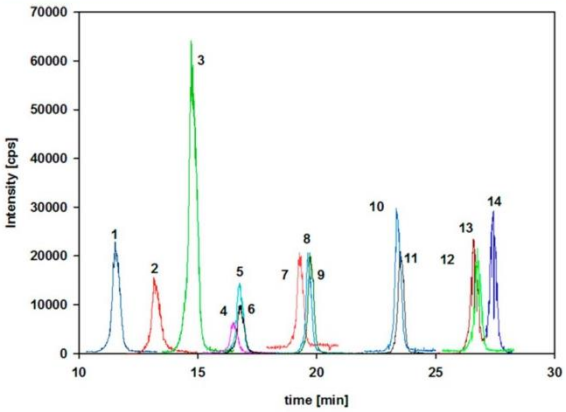

Figure 1. Chromatographic separation of analytes by HPLC–MS/MS (**1** N^6-formyl lysine, **2** N^6-malonyl lysine, **3** N^6-acetyl lysine, **4** N^6-(3-hydroxybutyryl) lysine, **5** N^6-acetoacetyl lysine, **6** N^6-succinyl lysine, **7** N^6-propionyl lysine, **8** N^6-(3-hydroxy-3-methylglutaryl) lysine, **9** N^6-glutaryl lysine, **10** N^6-crotonyl lysine, **11** N^6-butyryl lysine, **12** N^6-(2-methylbutyryl) lysine, **13** N^6-tiglyl lysine, and **14** N^6-isovaleryl lysine).

the separation of acylated lysine species by ion-pair formation and increased the signal in positive electrospray ionization. A special challenge in the HPLC method development was the separation of isomers and structures with same mass to charge ratio. N^6-malonyl lysine and N^6-(3-hydroxybutyryl) lysine share the same parent m/z of 233, but were separated by their retention times of 13.4 and 16.5 min, respectively. For isomers N^6-(2-methylbutyryl) lysine (retention time 26.3 min) and N^6-isovaleryl lysine (retention time 27.1 min) baseline separation was achieved. However, separation of saturated N^6-butyryl lysine and unsaturated N^6-crotonylyl lysine as well as saturated N^6-(2-methylbutyryl) lysine and unsaturated N^6-tiglyl lysine was not possible. Nevertheless, the differences in mass to charge ratio of respective structures allowed unequivocally differentiation.

DOI: 10.1021/acs.analchem.9b02656
Anal. Chem. 2019, 91, 12336–12343

Development of Enzymatic Hydrolysis. Appropriate sample preparation is crucial for the validity and reliability of the analytical procedure and, thus, an important step in method development. Optimized hydrolysis is a prerequisite of successful analysis prior to HPLC−MS/MS separation, identification, and quantitation of acylated lysine residues in proteins. An established protein hydrolysis protocol is acid hydrolysis using 6 M HCl for 20 h at 110 °C.[26] Acid hydrolysis is considered a total hydrolysis cleaving every peptide bond and converting the complete amount of protein into amino acids. By definition, the amide structure of acylated lysine is not stable leading to total loss under these conditions. A possible solution for this problem is total enzymatic hydrolysis as it is reported in literature for amide advanced glycation endproducts.[27]

Here, a sequentially added protease cocktail was optimized to accomplish almost complete hydrolysis of proteins extracted from mouse liver, kidney, heart, and brain. Prior to enzymatic hydrolysis a thymol crystal was added to prevent microbial spoilage. Hydrolysis was initiated by 0.3 units Pronase E (ProE) for 48 h. ProE is a mixture of several proteases from *Streptomyces griseus* including endopeptidases and exopeptidases.[28] The endopeptidase activity cleaves proteins into peptides leading to better dissolution and more potential targets for exopeptidases. The exopeptidase activity of ProE cleaves the peptides into free amino acids. However, maximum efficiency of hydrolysis reached was about 70% compared to acid hydrolysis as determined by ninhydrin assay, which could be improved neither by additional ProE nor prolonged reaction times. As reported in literature several peptides remain uncleaved by ProE.[29] Further hydrolysis was induced by 0.1 units carboxypeptidase Y (CPY) for 24 h and 0.5 units leucine aminopeptidase (LAP) for an additional 24 h. Addition of CPY and LAP increased efficiency of hydrolysis to average rates of 86% in liver, 85% in kidney, 88% in heart and 88% in brain.

Validation. One of the most important aspects concerning method validation is the recovery of analytes. As mentioned above, amide structures are acid labile. Thus, the recovery of our 14 acylation structures was tested by enzymatic hydrolysis of bovine serum albumin (BSA) solution. Acylation standards were added at the start of enzymatic hydrolysis and compared to BSA solution without added standards digested as a blank. After MWCO filtration of samples, concentrations were determined by standard addition calibration. Recovery rates were expressed as quotient of actual and calculated value. Average recovery was 81% with a maximum of 93% for N^6-formyl lysine and minimum recovery of N^6-malonyl lysine with about 75% (Figure 2). Overall, taking the complex protein preparation from tissue and biological variation into account, achieved recovery rates were suitable to measure acylated lysine protein modifications in vivo.

In this work, a signal-to-noise ratio above 3 was calculated as LOD and a signal-to-noise ratio above 10 as LOQ.[30] The LODs and LOQs of liver, kidney, heart, and brain are presented in Table 2. As a rule of thumb, the LODs/LOQs were decreasing with increasing chain length of acylation. As an example the LOD/LOQ of N^6-formyl lysine in liver was around 2 times higher compared to N^6-propionyl lysine and 4 times higher compared to N^6-butyryl lysine. A similar trend was observable for charged acylations N^6-malonyl lysine and N^6-succinyl lysine. Especially low LODs/LOQs were calculated for unsaturated acylations. The sensitivity for saturated

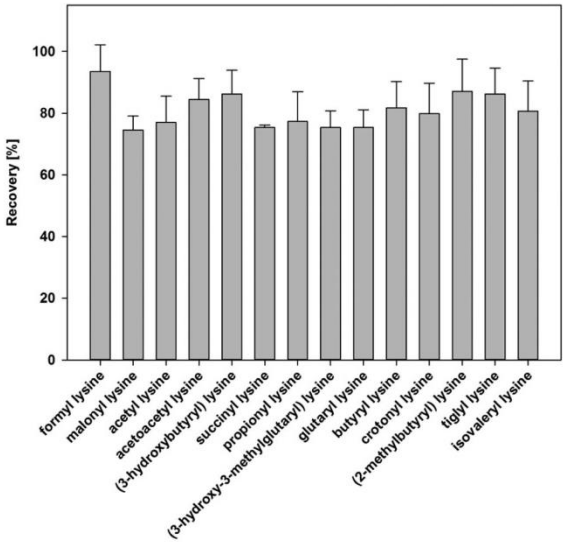

Figure 2. Recovery of analytes in enzymatic hydrolysates (n = 3).

N^6-butyryl lysine and N^6-(2-methylbutyryl) lysine was up to 10 times worse than their unsaturated analogues N^6-crotonyl lysine and N^6-tiglyl lysine, respectively. Beside structure and ionization the individual matrices and their background noise had significant effects on LODs/LOQs. However, most analytes showed comparable LODs/LOQs in different matrices.

Acylation In Vivo. Using our standard workup protocol and novel HPLC−MS/MS method we were able to quantitate 8 acylation structures in mouse liver, kidney, heart, and brain in a single run (Table 3). A detailed work-flow can be found in the SI (Figure S1). Liver was a local "hotspot" of protein acylation with a total of 56.47 μmol/mol leucine followed by brain, heart, and kidney with 45.25, 37.04, and 33.03 μmol/mol leucine, respectively. Liver is the central organ of acyl-CoA metabolism and RACS are concentrated between 1.5 and 2.0 fold higher in mouse liver compared to heart.[18] As a consequence, levels of total acylation were about the same magnitude higher in liver than in kidney and heart. The extraordinary high total acylation levels in brain were quite unexpected and mainly due to the strikingly high values of N^6-acetyl lysine (34.62 μmol/mol leucine). While this was in the same range as that in liver (37.31 μmol/mol leucine), levels were significantly lower in kidney (15.01 μmol/mol leucine) and heart (16.11 μmol/mol leucine). Interestingly, the ratios between levels of acetylation and reported levels for the precursor acetyl-CoA in kidney (0.013 nmol/mg protein) and brain (0.028 nmol/mg protein) are in line with each other.[31] Alternatively, acetyl-CoA is concentrated about 10 times higher in liver (0.194 nmol/mg protein) but acetylation is obviously strictly downregulated by enzymatic processes. A different picture emerged for the second most abundant acylation N^6-formyl lysine, which was lowest in brain (6.15 μmol/mol leucine) and highest in heart (14.11 μmol/mol leucine). Liver and kidney showed similar levels with 9.61 and 10.60 μmol/mol leucine, respectively. Formylation reached between 20% (brain) and 90% (heart) of N^6-acetyl lysine levels. However, in contradiction to the relatively high concentrations of N^6-formyl lysine in tissue and its putative

DOI: 10.1021/acs.analchem.9b02656
Anal. Chem. 2019, 91, 12336−12343

Table 3. Acylated Lysine Modifications in Mouse Organ Lysates[a]

modification	liver	kidney	heart	brain
	(μmol/mol leucine)			
N^6-formyl lysine	9.61 ± 1.68	10.60 ± 3.05	14.11 ± 1.20	6.15 ± 1.35
N^6-malonyl lysine	2.11 ± 0.20	1.11 ± 0.20	0.69 ± 0.15	0.50 ± 0.12
N^6-acetyl lysine	37.31 ± 3.60	15.01 ± 1.19	16.11 ± 3.16	34.62 ± 8.10
N^6-acetoacetyl lysine	<LOQ	<LOQ	<LOD	<LOD
N^6-(3-hydroxybutyryl) lysine	<LOD	<LOQ	<LOD	<LOQ
N^6-succinyl lysine	6.12 ± 0.60	5.53 ± 0.70	4.73 ± 0.75	3.22 ± 0.53
N^6-propionyl lysine	0.36 ± 0.05	0.29 ± 0.10	0.66 ± 0.12	0.13 ± 0.02
N^6-(3-hydroxy-3-methylglutaryl) lysine	<LOQ	<LOQ	<LOD	<LOQ
N^6-glutaryl lysine	0.81 ± 0.19	0.42 ± 0.06	0.34 ± 0.10	0.40 ± 0.13
N^6-butyryl lysine	0.13 ± 0.03	0.05 ± 0.04	0.38 ± 0.06	0.22 ± 0.04
N^6-crotonyl lysine	0.02 ± 0.01	0.02 ± 0.01	0.02 ± 0.01	0.01 ± 0.01
N^6-(2-methylbutyryl) lysine	<LOQ	<LOQ	<LOD	<LOD
N^6-tiglyl lysine	<LOQ	<LOQ	<LOQ	<LOQ
N^6-isovaleryl lysine	<LOD	<LOD	<LOD	<LOQ
total	56.47	33.03	37.04	45.25

[a]Mean ± standard deviation, n = 7.

important role in vivo only very little is known about mechanisms leading to formylation. The nonenzymatic formation was first described to be initiated by oxidative DNA degradation in cell culture experiments via a hypothetical formylphosphate intermediate.[4] Later studies on deoxyosone cleavage mechanisms verified the formation via Maillard reactions and led to the identification and quantitation in various human tissues.[5,32,33] N^6-Formyl lysine is a poor substrate for sirtuins in vitro[34] and increases with aging in eye lens proteins.[32] Nevertheless, the physiological relevance of formylation remains poorly understood and further research in this field is mandatory. Herein, the aliphatic saturated acylations N^6-propionyl lysine and N^6-butyryl lysine were measured at about a magnitude of 100 and the unsaturated N^6-crotonyl lysine by a factor of 1000 below acetylation. A particularly interesting aspect was the relatively high propionylation (0.66 μmol/mol leucine) and butyrylation (0.38 μmol/mol leucine) in heart. To our knowledge concentrations of corresponding acyl-CoA thioesters were never determined by a single working group leading to inconclusive reports in literature, e.g., Corkey analyzed (iso)butyryl-CoA below 2 nmol/g in liver,[19] while Gao found (iso)butyryl-CoA concentrations of 8 nmol/g in liver.[18] In general, in the present paper propionylation, butyrylation, and crotonylation were rather low abundant but possibly they are valuable marker structures. Quantitative more important was the group of acidic lysine acylations. N^6-succinyl lysine was the most abundant structure of this class with concentrations between 6.12 μmol/mol leucine in liver and 3.22 μmol/mol leucine in brain, which equals 10−35% of N^6-acetyl lysine concentrations. The high abundance of succinylation might be a consequence of high succinyl-CoA concentrations, e.g., 21.81 nmol/g in liver[18] and its extraordinary high reactivity due to intramolecular formation of a 5-membered cyclic anhydride intermediate.[12] A comparable mechanism using a 6-membered cyclic anhydride was described for glutarylation. The N^6-glutaryl lysine concentrations ranged between 0.34 μmol/mol in heart and 0.81 μmol/mol leucine in liver. Nevertheless, this mechanism is not possible for malonyl-CoA, still, malonylation was about 2 times higher compared to glutarylation (e.g., 2.11 μmol/mol leucine in liver and 0.69 μmol/mol leucine in heart). Contrary to N^6-malonyl lysine reported concentrations of malonyl-CoA are higher in heart (2.67 nmol/g) than in liver (0.78 nmol/g).[18] This is an excellent example that acylation is not exclusively dependent on RACS concentration and reactivity, but on protein half-life and degradation by sirtuins as well.

Enrichment. In order to further expand the repertoire of acylation structures we used an enrichment strategy for the enzymatic hydrolysates based on repetitive quantitative fractionation by HPLC. Interfering matrix was thus removed by reverse phase chromatography and fractions containing the analytes were concentrated by a factor of 5. This approach resulted in the quantitation of 6 additional structures in the pooled organ lysates (Table 4). The polar acylation N^6-(3-hydroxybutyryl) lysine was already described in literature as a regulator of gene expression in histone proteins.[8] Concentrations found were between 0.19 μmol/mol leucine in liver and 0.33 μmol/mol leucine in kidney. Despite concentrations were comparable to N^6-propionyl lysine, matrix induced poor ionization resulted in 5−10 times higher LODs/LOQs of N^6-(3-hydroxybutyryl) lysine which was resolved by the enrichment step. Acidic N^6-(3-hydroxy-3-methylglutaryl) lysine was another recently discovered structure. The corresponding 3-hydroxy-3-methylglutaryl-CoA is an important intermediate in leucine metabolism and forms highly reactive 6-membered cyclic anhydrides in analogy to glutaryl-CoA.[12] Nevertheless, N^6-(3-hydroxy-3-methylglutaryl) lysine concentrations were significantly lower compared to glutarylation. The physiological role of N^6-(3-hydroxy-3-methylglutaryl) lysine is unknown, but it is one of the few reported targets of

Table 4. Additional Acylated Lysine Modifications in Pooled Mouse Organ Lysates Quantitated after Enrichment

modification	liver	kidney	heart	brain
	(μmol/mol leucine)			
N^6-acetoacetyl lysine	0.29	0.20	0.10	0.04
N^6-(3-hydroxy-butyryl) lysine	0.19	0.33	0.19	0.22
N^6-(3-hydroxy-3-methylglutaryl) lysine	0.10	0.17	0.06	0.12
N^6-(2-methylbutyryl) lysine	0.26	0.07	0.03	0.01
N^6-tiglyl lysine	0.04	0.04	0.05	0.06
N^6-isovaleryl lysine	0.03	0.03	0.05	0.05

DOI: 10.1021/acs.analchem.9b02656
Anal. Chem. 2019, 91, 12336−12343

mitochondrial sirtuin 4, which controls the leucine metabolism.[35] Further important RACS in branched chain amino acid metabolism are 2-methylbutyryl-CoA and isovaleryl-CoA. The existence of corresponding lysine 2-methylbutyrylation and isovalerylation has been postulated;[36] however, this is the first time that both structures were unequivocally analyzed by HPLC−MS/MS. Figure 3 exemplarily shows the results of a

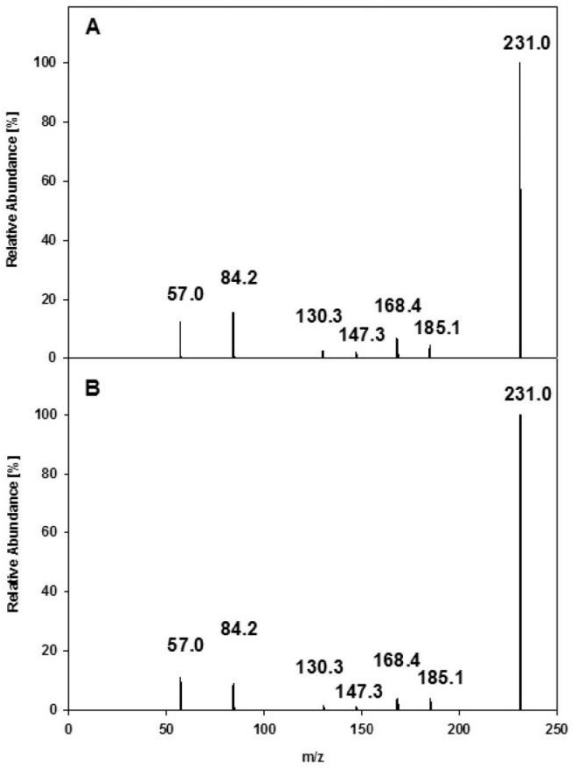

Figure 3. Verification of N^6-(2-methylbutyryl) lysine by collision-induced dissociation (CID) of m/z 231.0 $[M + H]^+$: standard (A) and enriched liver protein hydrolysate (B).

collision-induced dissociation experiment for N^6-(2-methylbutyryl) lysine. Mass spectra obtained for the authentic reference standard were virtually identical to the data obtained from organ hydrolysates after enrichment. While levels of 2-methylbutyrylation and isovalerylation were below 0.1 μmol/mol leucine in general, N^6-(2-methylbutyryl) lysine was exceptionally highly concentrated in liver (0.26 μmol/mol leucine). In addition, N^6-tiglyl lysine as the unsaturated equivalent of N^6-(2-methylbutyryl) lysine, was detected as a novel lysine acylation derivative. Nevertheless, although 2-methylbutyrylation, isovalerylation, and tiglylation were quantitatively low abundant, they might have a significant impact on the regulation of essential branched-chain amino acid metabolism. N^6-acetoacetyl lysine was another novel acylation structure discovered in the present study. Rather high concentrations were measured in liver (0.29 μmol/mol leucine) and kidney (0.20 μmol/mol leucine) while only traces were detected in brain (0.04 μmol/mol leucine). Corresponding acetoacetyl-CoA is an important intermediate in ketogenesis[37] and cholesterol biosynthesis.[38] Consequently, acetoacetylation of proteins might be a regulative motive of these two pathways.

CONCLUSIONS

Recently discovered activated thioester mediated lysine acylation has emerged as an alternative pathway to traditional regulation of gene expression and metabolism by acetylation. In this work, we developed and validated an HPLC−MS/MS method for the analysis of acylation in biological samples. This novel approach increased sensitivity superior to the time-consuming and expensive antibody enrichment used in traditional proteomics. In total, 14 acylation structures were quantitated simultaneously in liver, kidney, heart, and brain. A major task for future work is the development of a robust analytical method for determination of RACS and correlation to protein acylation. This approach will help to enhance our understanding of lysine acylation in vitro, e.g., by mechanistic studies with corresponding RACS and in vivo, e.g., by subcellular location of acylation and influence on metabolism from gene knockout experiments. Additionally, 4 novel acylation structures N^6-acetoacetyl lysine, N^6-isovaleryl lysine, N^6-(2-methylbutyryl) lysine, and N^6-tiglyl lysine were detected. Their regulation by sirtuins and their role in aging and disease are exciting topics for further research.

ASSOCIATED CONTENT

Supporting Information

The Supporting Information is available free of charge on the ACS Publications website at DOI: 10.1021/acs.analchem.9b02656.

Work-flow of analytical process, structures, and detailed synthesis routes of authentic reference standards (PDF)

AUTHOR INFORMATION

Corresponding Author

*Fax: ++049-345-5527341. E-mail: marcus.glomb@chemie.uni-halle.de.

ORCID

Tim Baldensperger: 0000-0002-9653-3156

Marcus A. Glomb: 0000-0001-8826-0808

Notes

The authors declare no competing financial interest.

ACKNOWLEDGMENTS

We thank Dr. D. Ströhl from the Institute of Organic Chemistry, Halle, Germany, for recording NMR spectra and Dr. A. Frolov from the Leibniz Institute of Plant Biochemistry, Halle, Germany, for performing accurate mass determination. Funding was supported by the Deutsche Forschungsgemeinschaft (DFG, Germany) Research Training Group 2155, ProMoAge. The FLI is a member of the Leibniz Association and is financially supported by the Federal Government of Germany and the State of Thuringia.

REFERENCES

(1) Phillips, D. M. *Biochem. J.* **1963**, *87* (2), 258.
(2) Allfrey, V. G.; Faulkner, R.; Mirsky, A. E. *Proc. Natl. Acad. Sci. U. S. A.* **1964**, *51* (5), 786.
(3) Ali, I.; Conrad, R. J.; Verdin, E.; Ott, M. *Chem. Rev.* **2018**, *118* (3), 1216.
(4) Jiang, T.; Zhou, X.; Taghizadeh, K.; Dong, M.; Dedon, P. C. *Proc. Natl. Acad. Sci. U. S. A.* **2007**, *104* (1), 60.

DOI: 10.1021/acs.analchem.9b02656
Anal. Chem. 2019, 91, 12336−12343

(5) Smuda, M.; Voigt, M.; Glomb, M. A. *J. Agric. Food Chem.* **2010**, *58* (10), 6458.
(6) Chen, Y.; Sprung, R.; Tang, Y.; Ball, H.; Sangras, B.; Kim, S. C.; Falck, J. R.; Peng, J.; Gu, W.; Zhao, Y. *Mol. Cell. Proteomics* **2007**, *6* (5), 812.
(7) Tan, M.; Luo, H.; Lee, S.; Jin, F.; Yang, J. S.; Montellier, E.; Buchou, T.; Cheng, Z.; Rousseaux, S.; Rajagopal, N.; Lu, Z.; Ye, Z.; Zhu, Q.; Wysocka, J.; Ye, Y.; Khochbin, S.; Ren, B.; Zhao, Y. *Cell* **2011**, *146* (6), 1016.
(8) Xie, Z.; Zhang, D.; Chung, D.; Tang, Z.; Huang, H.; Dai, L.; Qi, S.; Li, J.; Colak, G.; Chen, Y.et al. *Mol. Cell* **2016**, *62* (2), 194.
(9) Peng, C.; Lu, Z.; Xie, Z.; Cheng, Z.; Chen, Y.; Tan, M.; Luo, H.; Zhang, Y.; He, W.; Yang, K.et al. *Mol. Cell. Proteomics* **2011**, *10* (12), 012658.
(10) Zhang, Z.; Tan, M.; Xie, Z.; Dai, L.; Chen, Y.; Zhao, Y. *Nat. Chem. Biol.* **2011**, *7* (1), 58.
(11) Tan, M.; Peng, C.; Anderson, K. A.; Chhoy, P.; Xie, Z.; Dai, L.; Park, J.; Chen, Y.; Huang, H.; Zhang, Y.; Ro, J.; Wagner, G. R.; Green, M. F.; Madsen, A. S.; Schmiesing, J.; Peterson, B. S.; Xu, G.; Ilkayeva, O. R.; Muehlbauer, M. J.; Braulke, T.; Mühlhausen, C.; Backos, D. S.; Olsen, C. A.; McGuire, P. J.; Pletcher, S. D.; Lombard, D. B.; Hirschey, M. D.; Zhao, Y. *Cell Metab.* **2014**, *19* (4), 605.
(12) Wagner, G. R.; Bhatt, D. P.; O'Connell, T. M.; Thompson, J. W.; Dubois, L. G.; Backos, D. S.; Yang, H.; Mitchell, G. A.; Ilkayeva, O. R.; Stevens, R. D.; Grimsrud, P. A.; Hirschey, M. D. *Cell Metab.*. **2017**, *25* (4), 823.
(13) Sabari, B. R.; Zhang, D.; Allis, C. D.; Zhao, Y. *Nat. Rev. Mol. Cell Biol.* **2017**, *18* (2), 90.
(14) James, A. M.; Smith, C. L.; Smith, A. C.; Robinson, A. J.; Hoogewijs, K.; Murphy, M. P. *Trends Biochem. Sci.* **2018**, *43* (11), 921.
(15) Carrico, C.; Meyer, J. G.; He, W.; Gibson, B. W.; Verdin, E. *Cell Metab.*. **2018**, *27* (3), 497.
(16) Hong, S. Y.; Ng, L. T.; Ng, L. F.; Inoue, T.; Tolwinski, N. S.; Hagen, T.; Gruber, J. *PLoS One* **2016**, *11* (12), e0168752.
(17) Trub, A. G.; Hirschey, M. D. *Trends Biochem. Sci.* **2018**, *43* (5), 369.
(18) Gao, L.; Chiou, W.; Tang, H.; Cheng, X.; Camp, H. S.; Burns, D. J. *J. Chromatogr. B: Anal. Technol. Biomed. Life Sci.* **2007**, *853* (1−2), 303.
(19) Corkey, B. E.; Hale, D. E.; Glennon, M. C.; Kelley, R. I.; Coates, P. M.; Kilpatrick, L.; Stanley, C. A. *J. Clin. Invest.* **1988**, *82* (3), 782.
(20) Wagner, G. R.; Payne, R. M. *J. Biol. Chem.* **2013**, *288* (40), 29036.
(21) Ali, I.; Conrad, R. J.; Verdin, E.; Ott, M. *Chem. Rev.* **2018**, *118* (3), 1216.
(22) Simic, Z.; Weiwad, M.; Schierhorn, A.; Steegborn, C.; Schutkowski, M. *ChemBioChem* **2015**, *16* (16), 2337.
(23) Gellett, A. M.; Huber, P. W.; Higgins, P. J. *J. Organomet. Chem.* **2008**, *693* (18), 2959.
(24) Johansen, J. T.; Breddam, K.; Ottesen, M. *Carlsberg Res. Commun.* **1976**, *41* (1), 1.
(25) Wachsmuth, E. D.; Fritze, I.; Pfleiderer, G. *Biochemistry* **1966**, *5* (1), 169.
(26) Fountoulakis, M.; Lahm, H.-W. *J. Chromatogr. A* **1998**, *826* (2), 109.
(27) Glomb, M. A.; Pfahler, C. *J. Biol. Chem.* **2001**, *276* (45), 41638.
(28) Narahashi, Y., Pronase. In *Proteolytic Enzymes*; Academic Press, 1970.
(29) Delatour, T.; Fenaille, F.; Parisod, V.; Richoz, J.; Vuichoud, J.; Mottier, P.; Buetler, T. *J. Chromatogr. B: Anal. Technol. Biomed. Life Sci.* **2007**, *851* (1−2), 268.
(30) Vial, J.; Jardy, A. *Anal. Chem.* **1999**, *71* (14), 2672.
(31) Shurubor, Y.; D'Aurelio, M.; Clark-Matott, J.; Isakova, E.; Deryabina, Y.; Beal, M.; Cooper, A.; Krasnikov, B. *Molecules* **2017**, *22* (9), 1388.
(32) Smuda, M.; Henning, C.; Raghavan, C. T.; Johar, K.; Vasavada, A. R.; Nagaraj, R. H.; Glomb, M. A. *Biochemistry* **2015**, *54* (15), 2500.
(33) Henning, C.; Smuda, M.; Girndt, M.; Ulrich, C.; Glomb, M. A. *J. Biol. Chem.* **2011**, *286* (52), 44350.
(34) Madsen, A. S.; Andersen, C.; Daoud, M.; Anderson, K. A.; Laursen, J. S.; Chakladar, S.; Huynh, F. K.; Colaço, A. R.; Backos, D. S.; Fristrup, P.; Hirschey, M. D.; Olsen, C. A. *J. Biol. Chem.* **2016**, *291* (13), 7128.
(35) Anderson, K. A.; Huynh, F. K.; Fisher-Wellman, K.; Stuart, J. D.; Peterson, B. S.; Douros, J. D.; Wagner, G. R.; Thompson, J. W.; Madsen, A. S.; Green, M. F.; Sivley, R. M.; Ilkayeva, O. R.; Stevens, R. D.; Backos, D. S.; Capra, J. A.; Olsen, C. A.; Campbell, J. E.; Muoio, D. M.; Grimsrud, P. A.; Hirschey, M. D. *Cell Metab.*. **2017**, *25* (4), 838.
(36) Baeza, J.; Smallegan, M. J.; Denu, J. M. *Trends Biochem. Sci.* **2016**, *41* (3), 231.
(37) Grabacka, M.; Pierzchalska, M.; Dean, M.; Reiss, K. *Int. J. Mol. Sci.* **2016**, *17* (12), 2093.
(38) Thompson, S. L.; Krisans, S. K.; Thompson, S. L. *J. Biol. Chem.* **1990**, *265* (10).

DOI: 10.1021/acs.analchem.9b02656
Anal. Chem. 2019, 91, 12336−12343

Reprinted with permission from Baldensperger, T.; Di Sanzo, S.; Ori, A.; Glomb, M. A. Quantitation of Reactive Acyl-CoA Species Mediated Protein Acylation by HPLC–MS/MS, *Anal. Chem.* **2019**, *91*, pp. 12336–12343. Copyright 2019 American Chemical Society.

5.3 Publication 3

www.nature.com/scientificreports

SCIENTIFIC REPORTS
nature research

Check for updates

OPEN

Comprehensive analysis of posttranslational protein modifications in aging of subcellular compartments

Tim Baldensperger[1], Michael Eggen[1], Jonas Kappen[1], Patrick R. Winterhalter[2], Thorsten Pfirrmann[3] & Marcus A. Glomb[1]✉

Enzymatic and non-enzymatic posttranslational protein modifications by oxidation, glycation and acylation are key regulatory mechanisms in hallmarks of aging like inflammation, altered epigenetics and decline in proteostasis. In this study a mouse cohort was used to monitor changes of posttranslational modifications in the aging process. A protocol for the extraction of histones, cytosolic and mitochondrial proteins from mouse liver was developed and validated. In total, 6 lysine acylation structures, 7 advanced glycation endproducts, 6 oxidative stress markers, and citrullination were quantitated in proteins of subcellular compartments using HPLC-MS/MS. Methionine sulfoxide, acetylation, formylation, and citrullination were the most abundant modifications. Histone proteins were extraordinary high modified and non-enzymatic modifications accumulated in all subcellular compartments during the aging process. Compared to acetylation of histone proteins which gave between 350 and 305 µmol/mol leucine equivalents in young and old animals, modifications like acylation, glycation, and citrullination raised to 43%, 20%, and 18% of acetylation, respectively. On the other hand there was an age related increase of selected oxidative stress markers by up to 150%. The data and patterns measured in this study are mandatory for further studies and will strongly facilitate understanding of the molecular mechanisms in aging.

The human genome consists of approximately 20000 genes, which express about 70000 different proteins via alternative splicing. This number is tremendously increased to several million protein species by posttranslational modifications (PTMs)[1]. In comparison to biosynthesis of new proteins, PTMs are formed at much faster rates. Hence, they facilitate rapid adaption of metabolism to environmental changes[2]. One of the most dramatic changes in life is the aging process. Unsurprisingly, hallmarks of aging like mitochondrial dysfunction, inflammation, alteration of epigenetics, and loss of proteostasis are strongly influenced by PTMs[3].

A key mechanism in gene regulation is the acetylation of lysine residues in histone proteins[4]. Beside regulation of transcription, reversible modification by lysine acetyltransferases and deacetylases is a critical control mechanism in metabolism[5]. Enzymatic citrullination of arginine residues was initially discovered in autoimmune diseases such as rheumatoid arthritis, in which citrullination was increased in inflammatory tissues. This relatively novel modification is formed by peptidyl arginine deiminases. Currently, research focuses on the DNA damage caused by citrullination, which eventually might lead to carcinogenesis[6].

In contrast to the PTMs described above, a plethora of modifications is formed non-enzymatically. Oxidative stress is a well-known mechanism leading to PTMs which are closely linked to inflammation and impaired proteostasis[7,8]. A long-term research field is the formation of advanced glycation endproducts (AGEs), which are established markers of aging in many extra- and intracellular tissues, e.g., in eye-lens proteins[9]. AGEs predominantly modify lysine and arginine residues of proteins. Previous work identified dysregulation of mitochondrial processes, increased inflammation, and the reduced degradation of proteins by the ubiquitin-proteasome system as results of glycation[10–12]. A special subtype are the amide AGEs, which are lysine acylation structures formed

[1]Institute of Chemistry, Food Chemistry, Martin-Luther-University Halle-Wittenberg, Kurt-Mothes-Str. 2, 06120, Halle/Saale, Germany. [2]Clinic for Heart Surgery, Martin-Luther-University Halle-Wittenberg, Ernst-Grube Str. 40, 06120, Halle/Saale, Germany. [3]Institute of Physiological Chemistry, Martin-Luther-University Halle-Wittenberg, Hollystr. 1, 06114, Halle/Saale, Germany. ✉e-mail: marcus.glomb@chemie.uni-halle.de

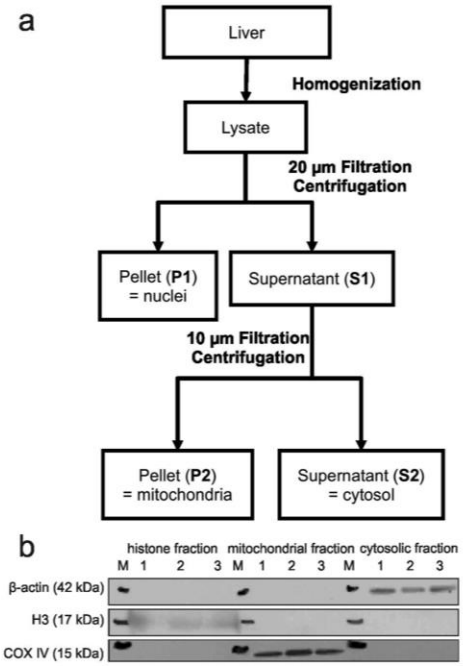

Figure 1. Subcellular fractionation protocol for mice liver (**a**). Western blotting was used to confirm purity of subcellular fractions by detection of cytosolic β-actin, mitochondrial COX IV, and histone H3 (**b**). M = molecular weight marker. Full-length blots are presented in the supporting information (Figure S1).

independently from enzymes by glycation[13]. Recently, reactive acyl-CoA species were identified as sources of non-enzymatic lysine acylation, while acylphosphates were hypothesized as a third pathway of non-enzymatic acylation[14]. Due to the structural similarity these lysine acylations are expected to be major alternative pathways to enzymatic acetylation in transcription and metabolic regulation[15].

Obviously, fundamental important enzymatic regulation of metabolism by PTMs is paralleled by non-enzymatic pathways in aging and disease as reviewed recently[16–18]. To our surprise, no comprehensive data of the various PTMs exists. We previously identified AGEs as excellent markers of aging and disease in cytosolic liver proteins[19] and identified liver as a local hotspot of protein acylation[20]. Hence, we quantitated 20 different PTMs including 6 lysine acylation modifications, 7 AGEs, 6 oxidative stress markers, and citrulline in histone, mitochondrial, and cytosolic proteins extracted from mice liver using a novel HPLC-MS/MS approach. The relevance of these PTMs in the aging process is discussed on a quantitative basis for the first time. We expect that the described changes of PTMs are key mechanisms in the aging process and will greatly contribute to identify targets for future studies.

Results

Fractionation and sample preparation. A fractionation protocol for mouse liver (Fig. 1a) was developed by combination and optimization of several methods for the isolation of histones[21,22], mitochondria[23], and cytosolic proteins[19]. After cell lysis using a tissue grinder in hypotonic sucrose buffer nuclei and mitochondria were separated from cytosol by centrifugation at 800 RCF and 7000 RCF, respectively. The crude fractions were purified by additional clean-up steps like centrifugation for cytosolic fraction, filtration for mitochondria and washing with detergents for nuclei. Finally, mitochondrial proteins were isolated by radioimmunoprecipitation assay buffer (RIPA buffer) and histones were extracted by 0.2 M sulfuric acid. After trichloroacetic acid (TCA) precipitation purity of protein fractions was controlled by Western blotting (Fig. 1b). Antibodies against proteins specific for each subcellular compartment were used, i.e. cytosolic β-actin, mitochondrial COX IV, and histone H3. Markers were exclusively detected in their respective fraction verifying the successful separation using our protocol.

In order to prevent artefact formation proteins were reduced by $NaBD_4$ prior to acid and enzymatic hydrolysis as described previously[8]. The average efficiency of enzymatic hydrolysis was about 90%. This was calculated in reference to acid hydrolysis using acid stable N^6-carboxymethyl lysine (CML). Protein hydrolysates were analyzed by HPLC-MS/MS as described under "Methods". In total, 6 lysine acylation modifications, 7 advanced glycation endproducts (AGEs), 6 oxidative stress markers, and citrulline were quantitated by standard addition calibration using authentic reference standards to cope for matrix influences on, e.g., ionization (Table 1).

Modifications	[µmol/mol leucine equivalent]					
	Histones		Mitochondria		Cytosol	
	Young (3 month)	Old (24 month)	Young (3 month)	Old (24 month)	Young (3 month)	Old (24 month)
N^6-formyl lysine	57.8 ± 44.5	126.1 ± 44.4*	35.3 ± 13.0	35.6 ± 9.2	17.1 ± 1.7	22.4 ± 4.9*
N^6-acetyl lysine	350.5 ± 119.1	304.5 ± 142.2	43.9 ± 6.9	44.4 ± 13.0	40.1 ± 3.6	44.1 ± 6.3
N^6-propionyl lysine	1.0 ± 0.5	1.7 ± 0.4*	0.7 ± 0.2	0.7 ± 0.3	0.4 ± 0.1	0.7 ± 0.1*
N^6-butyryl lysine	0.3 ± 0.3	0.8 ± 0.3*	0.2 ± 0.1	0.3 ± 0.1*	0.1 ± 0.1	0.3 ± 0.1*
N^6-malonyl lysine	<LOD	<LOD	2.6 ± 0.4	2.3 ± 0.4	2.9 ± 0.4	3.5 ± 0.6*
N^6-succinyl lysine	2.1 ± 0.3	2.7 ± 0.4*	4.2 ± 0.7	4.2 ± 1.9	0.4 ± 0.1	0.6 ± 0.1*
CML	13.5 ± 3.9	22.1 ± 7.0*	4.5 ± 0.7	7.2 ± 2.1*	6.1 ± 1.1	7.5 ± 1.3*
GALA	1.2 ± 0.3	1.8 ± 0.4*	0.4 ± 0.1	0.5 ± 0.2*	0.3 ± 0.1	0.4 ± 0.1*
G-H3	15.7 ± 4.8	22.6 ± 8.5*	14.9 ± 4.3	24.1 ± 11.6*	23.4 ± 10.6	40.9 ± 6.4*
CEL	2.7 ± 0.4	3.4 ± 0.6*	3.1 ± 0.6	4.1 ± 0.6*	13.0 ± 2.8	15.6 ± 3.3*
N^6-lactoyl lysine	<LOD	<LOD	0.2 ± 0.1	0.3 ± 0.1*	0.1 ± 0.1	0.2 ± 0.1*
MG-H	6.7 ± 2.4	8.6 ± 2.1*	5.6 ± 0.7	7.0 ± 1.0*	15.0 ± 3.9	24.3 ± 13.2*
furosine	2.5 ± 0.2	3.1 ± 1.1*	0.6 ± 0.5	0.9 ± 0.9	2.9 ± 0.7	2.7 ± 0.7
N^6-glyoxylyl lysine	0.4 ± 0.2	0.8 ± 0.2*	<LOQ	<LOQ	<LOQ	<LOQ
N^6-pyruvoyl lysine	0.8 ± 0.3	1.5 ± 0.3*	<LOQ	<LOQ	<LOQ	<LOQ
o-tyrosine	0.7 ± 0.2	1.1 ± 0.3*	4.4 ± 0.8	5.8 ± 0.9*	3.6 ± 1.0	6.1 ± 1.4*
o,o-dityrosine	2.1 ± 0.4	4.7 ± 2.4*	<LOQ	<LOQ	<LOQ	<LOQ
methionine sulfoxide	704.9 ± 323.2	595.8 ± 251.0	2454.9 ± 1084.2	1449.3 ± 767.0	1200.4 ± 777.7	1845.1 ± 770.3*
methionine sulfone	64.8 ± 42.6	104.9 ± 27.7*	41.3 ± 22.1	40.9 ± 21.1	20.9 ± 16.6	39.0 ± 21.5*
citrulline	37.6 ± 13.9	55.2 ± 16.2*	27.9 ± 16.4	30.0 ± 12.4	5.3 ± 1.8	5.7 ± 1.3

Table 1. Protein modifications in subcellular compartments of mice liver (mean ± standard deviation, n = 10). Significant differences (unpaired t-test, $p < 0.05$) between young and old animals (n = 10) are indicated by an asterisk. CML = *N6*-carboxymethyl lysine; GALA = *N6*-glycoloyl lysine, G-H3 = glyoxal hydroimidazolone 3; CEL = *N6*-carboxyethyl lysine; MG-H = methylglyoxal hydroimidazolone.

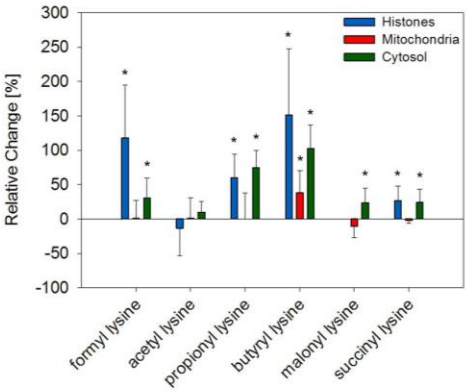

Figure 2. Changes of acylation in aging mice liver. Relative changes of mean modification levels in old mice were compared to mean levels in young mice. Error bars represent relative standard deviation of old animals. Significant differences (unpaired t-test, $p < 0.05$) between young and old animals (n = 10) are indicated by an asterisk.

Acylation. Enzymatically formed acetylation and non-enzymatic lysine acylation were quantitated in subcellular fractions of liver (Table 1) in the aging process (Fig. 2).

Here, 3 month old C57BL/6 N mice (n = 10) were compared to 24 month old animals (n = 10). Acetylation was the most abundant lysine modification in mice liver with average concentrations between 40.1 and 44.4 µmol/mol leucine equivalents (leucine-eq) in cytosolic as well as in mitochondrial proteins. Especially high concentrations were measured in histone proteins, in which N^6-acetyl lysine concentrations were approximately 10 times higher (350.5 µmol/mol leucine-eq) compared to cytosol and mitochondria. Despite the modification's pivotal role in epigenetics and metabolic regulation no correlation with aging was observed.

Formylation was the second most abundant lysine modification. Again, levels of N^6-formyl lysine were highest in histones (126.1 µmol/mol leucine-eq) and by a factor of 6 lower in cytosolic proteins (22.4 µmol/mol

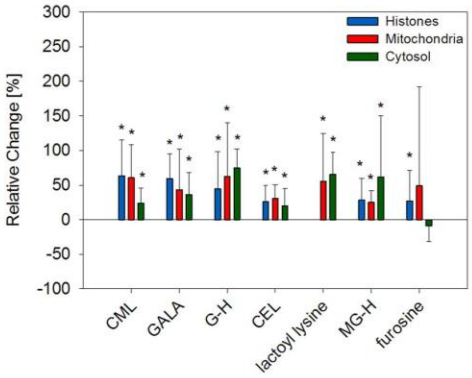

Figure 3. Changes of advanced glycation endproducts in aging mice liver. Relative changes of mean modification levels in old mice were compared to mean levels in young mice. Error bars represent relative standard deviation of old animals. Significant differences (unpaired t-test, $p < 0.05$) between young and old animals ($n = 10$) are indicated by an asterisk.

leucine-eq). This trend is in line with the lower abundant aliphatic acylation structures N^6-propionyl lysine with 1.7 µmol/mol leucine-eq in histones vs. 0.7 µmol/mol leucine-eq in cytosol and N^6-butyryl lysine with 0.8 µmol/mol leucine-eq in histones vs. 0.3 µmol/mol leucine-eq in cytosol. In contrast to acetylation aliphatic acylations increased about 50% in aged histones and cytosolic proteins with p-values ranging between 0.005 and 0.001. Another picture emerged for mitochondrial formylation and propionylation. While concentrations of 35.6 µmol/mol leucine-eq for N^6-formyl lysine and 0.7 µmol/mol leucine-eq for N^6-propionyl lysine were in between histone and cytosolic fraction, no age dependent increase was detected in mitochondria. On the other hand, butyrylation significantly increased ($p = 0.020$) with aging in mitochondria.

The acidic lysine acylations N^6-malonyl and N^6-succinyl lysine were especially high abundant in mitochondria with 2.3 and 4.2 µmol/mol leucine-eq, respectively. Succinylation was lowest in cytosolic proteins and malonylation was below limit of quantitation (LOD) in histones. Again, no correlation with aging was observed in mitochondria but concentrations of both structures increased significantly about 50% ($p < 0.006$) in aged histones and cytosolic proteins.

Glycation. Advanced glycation endproducts (AGEs) accumulated on average 50% during aging (Fig. 3, Table 1).

Furosine as a marker of early stage lysine glycation by Maillard reactions was low abundant (0.9 µmol/mol leucine-eq) in mitochondria. Concentrations were a factor of 3–5 higher in histones (3.1 µmol/mol leucine-eq) and cytosolic (2.7 µmol/mol leucine-eq) proteins. Contrary to all end-stage Maillard glycation AGEs measured herein, no age dependent increase was observed for furosine in mitochondria and cytosol but the structure significantly ($p = 0.044$) correlated with aging of histones.

Quantitative more important were the AGEs formed by short-chained α-dicarbonyls glyoxal and methylglyoxal. CML was extraordinary high abundant in histones (22.1 µmol/mol leucine-eq) and, thus, more than twice as high concentrated as in mitochondrial and cytosolic proteins. In contrast, N^6-carboxyethyl lysine (CEL) as the corresponding lysine modification by methylglyoxal was concentrated 5 times higher in cytosol compared to histones with 15.6 vs. 3.4 µmol/mol leucine-eq, respectively. The glyoxal specific amide AGE N^6-glycoloyl lysine (GALA) indicated the same trend. GALA concentrations were about 3 times higher in histones compared to mitochondria and cytosol. Levels of methylglyoxal specific N^6-lactoyl lysine were below LOD in histones and around 0.2 µmol/mol leucine-eq in mitochondria and cytosol. Glyoxal hydroimidazolone (G-H) as a measure for glyoxal-arginine AGEs and methylglyoxal hydroimidazolone (MG-H) were quantitative important modifications in all three compartments. Compared to lysine AGEs the differences between fractions were smaller, but average glycation levels of arginine were higher. Overall, modifications by short-chained α-dicarbonyls and aging correlated in all compartments with p-values between 0.001 and 0.043.

Oxidative stress. Markers of oxidative stress were quantitated in liver fractions (Table 1) of the aging mice cohort (Fig. 4).

The α-oxoamide AGEs N^6-glyoxylyl and N^6-pyruvoyl lysine are formed by glycation under oxidative conditions from glyoxal and methylglyoxal, respectively. Thus, they are markers of carbonyl stress as well as oxidative stress[19]. Concentrations of N^6-glyoxylyl lysine equalled 30% of corresponding α-hydroxyamide AGE GALA in histones of young mice (0.4 µmol/mol leucine-eq) and increased to 100% in old mice (0.8 µmol/mol leucine-eq). N^6-pyruvoyl lysine levels rose up in a similar way from 0.8 to 1.5 µmol/mol leucine-eq ($p < 0.001$). Unfortunately, N^6-glyoxylyl and N^6-pyruvoyl lysine were below LOQ in other fractions.

Oxidatively dimerized *o,o*-dityrosine is another confirmed oxidative stress marker, which was below LOQ in mitochondria and cytosol, but rather high abundant in histones. Moreover, significant effects ($p = 0.003$) were observed during aging with concentrations approximately twice as high at 4.7 µmol/mol leucine-eq in old

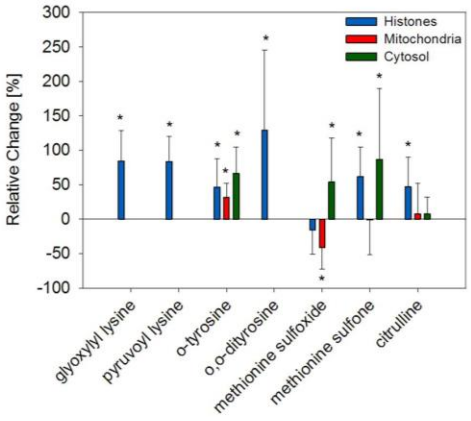

Figure 4. Changes of oxidative stress markers and citrullination in aging mice liver. Relative changes of mean modification levels in old mice were compared to mean levels in young mice. Error bars represent relative standard deviation of old animals. Significant differences (unpaired t-test, $p < 0.05$) between young and old animals ($n = 10$) are indicated by an asterisk.

animals. Oxidation of phenylalanine by hydroxyl radicals leads to *o*-tyrosine. This oxidative stress marker was detected in all analyzed compartments and was especially high concentrated in mitochondria and cytosol with up to 5.8 and 6.1 µmol/mol leucine-eq, respectively. On the other hand, in histones about 25% of the amount determined in the other fractions was found. Nevertheless, *o*-tyrosine was an excellent marker of aging with p-values below 0.008.

Methionine sulfoxide was the most abundant modification measured in the present study. Concentrations ranged between 2455 µmol/mol leucine-eq in mitochondria and 596 µmol/mol leucine-eq in histones. The development of methionine sulfoxide levels in aging was very different between analyzed subcellular fractions. While no significant trend was determined in histones, methionine sulfoxide significantly decreased in mitochondria ($p = 0.015$) and increased in cytosol ($p = 0.039$). In general, irreversible further oxidation from methionine sulfoxide to methionine sulfone occurred on a relatively low stoichiometry of about 2%. Nevertheless, about 10–20% oxidation to methionine sulfone was detected in histone proteins, which significantly increased in the aging process ($p = 0.013$).

Citrullination. The most abundant arginine modification in histones was enzymatic citrullination (Table 1). Concentrations reached up to 55.2 µmol/mol leucine-eq and were by a factor of 10 lower in cytosol. In mitochondria average values of about 30 µmol/mol leucine-eq were detected. While no correlation with aging was observed in mitochondrial and cytosolic proteins, a significant increase ($p = 0.010$) was measured in histone proteins (Fig. 4).

Discussion

Acetylation as the most abundant lysine modification is a key mechanism in regulation of transcription and metabolism[5]. Consequently, especially high concentrations of N^6-acetyl lysine were found in histone protein, in which acetylation modifies chromatin structures and, thus, accessibility of the DNA for, e.g., transcription. Due to the strict enzymatic regulation by acetyltransferases and deacetylases no changes were detected in the aging process in histones, but also for proteins in the other subcellular fractions. This latter observation was in line with previously published studies in rat liver mitochondria and human eye lens proteins[9,24]. However, for a total assessment of the concept of acetylation it has to be kept in mind that central intermediates of Maillard triggered glucose degradation also result in lysine acetylation. Specifically, *in vitro* incubations of 1-deoxyglucosone resulted in up to 65% acetic acid and related acetylation products via hydrolytic β-dicarbonyl cleavage[25,26]. This might also explain, why in case of histone acetylation, interrelationships are complex and contradictory trends were reported depending on organism, tissue, site-specific position etc[27,28]. Although no change of total N^6-acetyl lysine levels in mouse liver was detected in the present study, non-proliferating organs like brain and site specific analysis of acetylation remain important topics in the field of aging research.

Acetylation is paralleled by further structurally related non-enzymatic acylations via Maillard reactions, reactive acylphosphates, and acyl-CoA species[14,26,29]. For the latter, enzymatic acylation by promiscuous acyltransferase activities of several lysine acetyltransferases was discussed in recent publications. However, it has to be considered that these enzymatic activities are magnitudes lower than corresponding acetyltransferase activities[15]. Independent from origin, our data suggests that acylation is a major alternative pathway to lysine acetylation. While total acylation reached approximately 50% of N^6-acetyl lysine levels in histones and cytosol almost equivalent amounts of acylation and acetylation were found in mitochondria. Acylation was an extraordinary good marker of aging in histones and cytosolic proteins with p-values below 0.005. Research on the biological impact of these lysine modifications is very likely mandatory for a better understanding of epigenetic and metabolic dysregulation in aging and related fields. In contrast, mitochondrial acylation indicated no effects in aging despite

high abundance. A possible explanation is the presence of mitochondrial deacylases. Specifically, sirtuins 3–5 act on sites of propionylation, malonylation, and succinylation[30,31]. Obviously, this enzymatic control system maintains constant acylation levels during aging of mitochondria. The single exception from this observation was the increase of low abundant butyrylation, which is not targeted by any mitochondrial sirtuin[31]. Acidic acylations N^6-malonyl and N^6-succinyl lysine are closely linked to energy metabolism (citric acid cycle and fatty acid synthesis). Hence, they are considered as regulatory motives[32,33]. Previous work supports our findings, because it was shown that succinylation is not increasing with age in mammalian mitochondria but in *C. elegans* and *D. melanogaster* which are lacking any sirtuin 5 homologues[24].

An impact of sirtuins on formylation has not been reported so far, although only mitochondrial proteins showed no age correlation in the present study. Formylation was next to acetylation by far the most abundant acylation structure detected. First, formylation was described to be initiated by oxidative DNA degradation via a hypothetical formyl phosphate intermediate leading to changes in chromatin structure[29,34]. Later, formaldehyde metabolism emerged as a possible source of formylation[35]. In addition, Maillard glycation was verified as a source of lysine formylation. In parallel to the above fragmentation of 1-deoxyglucosone leading to acetylation, here fragmentation of glucosone was verified as the origin[36]. Despite the high abundance and strikingly clear correlation with aging, the physiological relevance of formylation remains poorly understood and further research in this field is mandatory.

It has to be stated that non-enzymatic glycation beside formylation and acetylation leads to many more acylation products collectively termed as amide AGEs, e.g., amides of glycolic acid (GALA), lactic acid, glyceric acid, oxalic acid, glyoxylic acid and pyruvic acid[37]. An established marker of early stage Maillard reaction is the Amadori product which can be accessed after acid hydrolysis as furosine[38]. Furosine was the only modification formed by glycation which was not increasing with age of mitochondrial and cytosolic proteins. In contrast, furosine accumulated in aged histones. Possible explanations for this apparent contradiction are the continuous formation and fragmentation of the Amadori product as an important reactive Maillard intermediate as well as the prolonged protein half-time of 117 days of histones from mice liver[39]. Quantitative more important was the glycation by short-chained α-dicarbonyl compounds glyoxal and methylglyoxal, which are reactive intermediates generated *in vivo* not only by Maillard degradation of sugars as glucose, but additionally stem to a major extend from lipoxidation and glycolysis[40]. Through complex isomerization cascades glyoxal leads to lysine modifications CML and GALA while corresponding structures CEL and N^6-lactoyl lysine are formed by methylglyoxal[19]. A particularly interesting observation herein was the relative accumulation of methylglyoxal specific CEL and N^6-lactoyl lysine especially in cytosol and mitochondria. This highlights the importance of triose phosphates from cytosolic glycolysis as important methylglyoxal precursors *in vivo*[40]. This notion is further supported by the highest concentrations found in cytosol for MG-H, which is a methylglyoxal specific arginine modification. Here, the values for MG-H are given as a sum for the two isomeric forms MG-H1 and MG-H3. The higher values of MG-H compared to CEL measured in all subcellular fractions is in line with the higher reactivity of the guanidine function of arginine versus the N^6-amino function of lysine towards α-dicarbonyl compounds[8]. In contrast, the glyoxal specific hydroimidazolinone G-H3 is an artefact of acid protein hydrolysis but has been shown to be a useful quantitative tool for glyoxal-dihydroxyimidazolidine and the AGE N^7-carboxymethyl arginine[41]. Obviously, glyoxal induced glycation increased in all cell fractions with age. The same was true for CML and GALA with exceptionally high values of 22.1 µmol/mol leucine-eq for CML in histones. In contrast to GALA and glyoxal arginine modifications it has to be considered, that there are major alternative pathways for CML formation. Notably, the oxidative fragmentation of the Amadori product which makes CML also a parameter of oxidative stress[8]. In total, AGEs were excellent markers of aging in all subcellular compartments. Beside correlation with aging several studies express causal relationships between AGEs and changed chromatin structure[42], mitochondrial dysfunction[10], loss of proteostasis[43], as well as inflammation[44].

The formation of α-oxoamide AGEs N^6-glyoxylyl and N^6-pyruvoyl lysine in the CML/CEL reaction cascades by oxidation of an enaminol intermediate represents a combination of carbonyl and oxidative stress[19]. Unfortunately, concentrations of α-oxoamide AGEs were below LOQ in mitochondrial and cytosolic proteins. In histones both α-oxoamide AGEs increased in aging as measured for all other AGEs. In addition, the ratio between oxidatively formed N^6-glyoxylyl lysine and corresponding non-oxidatively formed GALA changed from about 0.3 in young to 0.5 in old animals. Both AGEs share a common enaminol precursor and a shift from α-hydroxyamide to α-oxoamide AGE thus clearly indicated increased oxidative stress in aged animals. The established oxidative stress markers *o*-tyrosine and *o,o*-dityrosine confirmed the increase of oxidative stress with aging. While *o*-tyrosine is formed by oxidation of phenylalanine residues via hydroxyl radicals *o,o*-dityrosine is generated by cross-linking of tyrosine residues either by hydroxyl radicals or tyrosyl radicals[45]. Methionine sulfoxide was by far the most abundant modification detected in the present paper reaching up to 2500 µmol/mol leucine-eq. According to literature methionine oxidation to the sulfoxide has a pivotal role in maintaining the cellular redox state by operating as an oxidative sink[46]. One could assume that the herein proven increase of age associated oxidative stress should result in an increase of methionine sulfoxide concentration. It is important to understand that the oxidation of methionine is an equilibrium, which is regulated by methionine sulfoxide reductases. Consequently, methionine sulfoxide is no stable accumulative modification, but rather a snapshot of current cellular redox state and working antioxidative defence mechanisms. In contrary, further oxidation of methionine sulfoxide to methionine sulfone is an irreversible step resulting in an age dependent increase in histones and cytosol. To our knowledge we were the first group quantitating methionine sulfone *in vivo* via our highly sensitive HPLC-MS/MS approach.

Enzymatic citrullination is closely linked to inflammatory processes and was the most abundant arginine modification in histones and mitochondria, while in cytosolic proteins glyoxal and methylglyoxal arginine AGEs prevailed by a factor of 10. In addition, concentration of citrullination was exclusively increasing with aging in

histones. This is especially fatal, because citrullination is believed to activate DNA damaging pathways leading to carcinogenesis[6].

In summary, non-enzymatic posttranslational modifications were accumulating in all subcellular compartments in aging. On the other hand, the relative proportion of enzymatic acetylation among all detected modifications (excluding methionine sulfoxide) decreased from 60 to 45% in histones with age and from about 30% to 20% in mitochondria and cytosol. This decrease was mainly caused by non-enzymatic acylation rising to 43% of N^6-acetyl lysine concentration in histone proteins. In addition, glycation, oxidative stress markers and citrullination increased to 20%, 37% and 18% of acetylation levels during aging, respectively. Glycation was the single most important factor for the relative decrease of acetylation in aging mitochondria and increased to equal amounts compared to acetylation. Acylation, oxidative stress markers and citrullination were measured approximately in the same concentration, but no correlations with aging were detected in mitochondria. In cytosolic proteins of old mice glycation tremendously increased to 200% of N^6-acetyl lysine. While levels of citrullination were constant in cytosolic proteins, acylation and oxidative stress markers increased to 62% and 100% of acetylation, respectively. Finally, we postulate that comprehensive analysis of changes in protein modification patterns presented in this study will be mandatory to understand the molecular mechanisms of aging.

Methods

Chemicals and Enzymes. All chemicals of the highest quality available were provided by Sigma-Aldrich (Munich/Steinheim, Germany), unless otherwise indicated. Pronase E was purchased from Sigma-Aldrich. Carboxypeptidase Y and leucine aminopeptidase were prepared as described previously[47,48]. N^6-formyl lysine, N^6-acetyl lysine, furosine, methionine sulfoxide, methionine sulfone, *o*-tyrosine, *o,o*-dityrosine, and citrulline were purchased from Sigma-Aldrich. Synthesis and structure elucidation of commercially unavailable authentic reference standards was described previously[9,13,19,20]. Structural formulas of analytes are included in the supporting information (Figure S2).

Housing of animals. Male C57BL/6 N mice were purchased at the age of 6 weeks from Janvier Laboratories (Le Genest-Saint-Isle, France) and housed in individually ventilated cage systems in a climate room (20.3 °C, 62% humidity) with 12 hours circadian rhythm and fed ad libitum under barrier conditions in the Center of Medical Basic Research at the Medical Faculty (University of Halle, Germany). The tissues were collected at the age of 3 month (young) or 24 month (old). All work on the mice was performed at a sterile workbench in the same room. The principles for the care and use of animals from the American Physiological Society guide were followed. The announcement to kill vertebrates for scientific purposes for this tissue collection was approved by the local authority (K2BM3, MLU Landesverwaltungsamt, Sachsen-Anhalt, Germany).

Tissue collection. The mice were anaesthetized with 100 mg/kg bodyweight ketamine (Zoetis, Berlin, Germany) and 10 mg/kg bodyweight Xylazine (Bayer, Leverkusen, Germany). The animals were killed in deep narcosis by subluxation of cervical spine. The livers were dissected and immediately snap-frozen on dry ice.

Fractionation. The developed fractionation protocol (Fig. 1a) is a modified combination of several methods for the isolation of histones[21,22], mitochondria23 and cytosolic proteins[19].

All steps were performed at 4 °C using pre-cooled lab ware and solutions. About 300 mg mice liver was rinsed free of blood by repetitive washing in phosphate buffered saline. The liver was homogenized in 600 µL homogenization buffer (0.32 M sucrose, 3 mM $MgCl_2$, 10 mM nicotine amide, 500 nM trichostatin A) supplemented with EDTA-free protease inhibitor mixture (Roche, Pleasanton, USA) using a disposable tissue grinder (VWR International, Radnor, USA). Cell debris was removed by 20 µm Celltrics filtration (Sysmex, Norderstedt, Germany). Nuclei were pelleted (**P1**) by centrifugation at 800 RCF for 15 min. The supernatant (**S1**) was decanted and purified by 10 µm Celltrics filtration. After centrifugation at 7000 RCF for 15 min the resulting supernatant (**S2**) containing cytosolic proteins was separated from the pellet (**P2**) containing mitochondria.

Extraction histone proteins. Nuclear Pellet (**P1**) was washed using 1 mL nuclear washing buffer (0.35 M sucrose, 0.5% Triton-X100, 10 mM KCl and 1.5 mM $MgCl_2$ in 10 mM HEPES buffer pH 7.4) and a second time using 1 mL nuclear washing buffer without Triton-X100. Centrifugation at 800 RCF for 15 min pelleted purified nuclei. Histones were extracted from this pellet in 400 µL 0.2 M H_2SO_4 by a MM 400 mixer mill (Retsch, Haan, Germany) for 15 min and 1 h incubation on ice. Debris was removed by centrifugation at 16100 RCF for 15 min. The resulting supernatant contained purified histone proteins.

Extraction mitochondrial proteins. Mitochondrial pellet (**P2**) was washed twice using 1 mL mitochondrial washing buffer (0.2 M sucrose and 1 mM EDTA in 10 mM Tris buffer pH 7.4) and centrifuged at 7000 RCF for 15 min. Purified mitochondria were lysed in 400 µL RIPA buffer (150 mM NaCl, 1 mM EDTA, 0.25% deoxycholate, 1% Nonidet P-40, and 1% sodium dodecylsulfate in 50 mM Tris-HCl buffer pH 7.4) by a MM 400 mixer mill for 15 min and 2 h incubation on ice. Debris was removed by centrifugation at 16100 RCF for 15 min. The resulting supernatant contained purified mitochondrial proteins.

Extraction cytosolic proteins. Remaining mitochondria were removed from supernatant (**S2**) by additional centrifugation at 7000 and 16100 RCF for 15 min until no pellet formation was observed. The resulting supernatant contained purified cytosolic proteins.

Protein work-up. Proteins were precipitated at 10% trichloroacetic acid concentration by addition of 50% stock solution and centrifugation at 1000 RCF for 15 min. Pellets were washed 3 times using 80% ice-cold acetone and allowed to air-dry. Proteins were dissolved in 500 µL 0.1 M Tris buffer (pH 7.4) and homogenized by a MM

Modification	Retention time (min)	Precursor		Product ion 1[a]			Product ion 2[b]			Product ion 3[b]		
		m/z (amu)	DP (V)	m/z (amu)	CE (eV)	CXP (V)	m/z (amu)	CE (eV)	CXP (V)	m/z (amu)	CE (eV)	CXP (V)
Acylation												
N^6-formyl lysine	11.5	175.1	40	112.1	20	13	84.1	35	7	129.1	15	13
N^6-malonyl lysine	13.4	233.2	45	126.2	20	10	84.2	38	10	170.3	22	12
N^6-acetyl lysine	14.7	189.2	40	126.1	18	10	84.2	31	5	143.1	14	10
N^6-succinyl lysine	16.8	247.1	50	84.3	40	10	184.4	21	12	130.1	26	12
N^6-propionyl lysine	19.1	203.0	45	84.3	35	12	140.4	19	13	157.4	15	10
N^6-butyryl lysine	23.3	217.0	50	84.3	32	5	154.3	18	10	171.4	17	10
Glycation												
N^6-glycoloyl lysine	10.4	205.2	40	142.1	20	11	84.1	36	14	56.2	64	8
N^6-carboxymethyl lysine	9.6	205.1	42	130.2	17	9	84.1	30	14	56.1	59	9
N^6-lactoyl lysine	14.3	219.2	40	156.2	20	8	84.1	35	9	173.1	17	8
N^6-carboxyethyl lysine	14.4	219.1	54	84.1	33	7	130.1	18	11	56.1	59	8
glyoxal hydroimidazolone	17.3	215.1	48	100.1	20	8	70.1	38	11	116.2	20	10
methylglyoxal hydroimidazolone	23.0	229.2	45	114.2	21	9	70.2	45	11	116.1	21	9
furosine	24.4	255.2	50	84.1	33	7	130.3	21	10	192.0	23	12
Oxidative Stress												
methionine sulfone	4.4	182.2	45	136.0	16	9	56.2	35	8	—	—	—
methionine sulfoxide	4.5	165.9	33	74.2	20	12	56.1	30	10	102.1	19	18
N^6-glyoxylyl lysine	10.4	206.2	40	143.1	20	11	84.1	36	14	160.1	15	13
N^6-pyruvoyl lysine	14.3	220.2	40	157.2	20	8	84.1	35	9	174.1	30	15
o-tyrosine	25.3	182.1	45	136.2	18	11	91.1	42	15	119.1	27	10
o,o-dityrosine	27.9	361.2	25	315.3	23	7	254.2	33	15	237.2	34	21
Citrullination												
citrulline	5.5	176.2	40	159.2	14	11	70.3	35	11	113.1	22	7

Table 2. Mass spectrometric parameters for quantitation. [a]MRM transition used for quantitation. [b]MRM transition used for confirmation.

400 mixer mill. Protein concentrations were adjusted to a maximum of 3 mg/mL. Addition of 100 µL $NaBD_4$ solution (15 mg/mL in 0.01 M NaOH) and reduction for 1 h at room temperature was used to prevent artefact formation. Excess of $NaBD_4$ was destroyed by addition of 100 µL 1 M HCl and neutralization by 100 µL 1 M NaOH.

Western blotting. Proteins were extracted as described above. Total protein amount was determined by Lowry assay and 10 µg were loaded per lane. Novex Wedge Well 8–16% gradient gels (Invitrogen, Carlsbad, USA) and 0.45 µm Amersham Hybond PVDF membranes (GE Healthcare, Amersham, United Kingdom) were used. Primary antibodies (mouse anti β-actin, 1:5000, Sigma #A5441; mouse anti COX IV, 1:5000, Abcam #ab33985; rabbit anti H3, 1:1000, Abcam #ab1791) were applied, followed by HRP-conjugated secondary antibodies and Super Signal West Pico Plus chemiluminescence kit (Thermo Fisher Scientific, Waltham, MA), according to manufacturer instructions. Signals were detected by X-ray films and scanned in the transparency mode.

Enzymatic hydrolysis. Enzymatic hydrolysis was performed as described previously[20]. A small crystal of thymol was added to aliquots (250 µL) of protein solutions. Enzymes were added stepwise starting with 30 µL pronase E (0.3 units), 10 µL carboxypeptidase Y (0.1 units) after 48 h, and 10 µL leucine aminopeptidase (0.5 units) after 72 h. Samples were incubated at 37 °C in a shaker incubator for 96 h. Once the total digestion procedure was completed, reaction mixtures were filtered through 3 kDa molecular weight cut-off filters (VWR International, Radnor, USA).

Acid hydrolysis. Acid hydrolysis was performed as described previously[13]. Aliquots of protein solutions (250 µL) were dried in a vacuum concentrator (Savant-Speed-Vac Plus SC 110 A combined with a Vapor Trap RVT 400, Thermofisher Scientific, Bremen, Germany). 800 µL of 6 M HCl was added and the solution was heated 20 h at 110 °C under an argon atmosphere. Volatiles were removed in a vacuum concentrator and the residue was dissolved in 300 µL of ultra-pure water. Samples were filtered through 0.45 µm cellulose acetate Costar SpinX filters (Corning Inc., Corning, USA). Acid stable structures furosine, CML, CEL, G-H, methionine sulfoxide, methionine sulfone, *o*-tyrosine, and *o,o*-dityrosine were quantitated from acid hydrolysates, all other analytes from enzymatic hydrolysates.

Ninhydrin assay. After complete workup the amount of amino acids in hydrolysates was determined by ninhydrin assay and referenced to a calibration of L-leucine concentrated between 5 and 100 µM as described previously[9]. The absorbance was determined at 546 nm with an Infinite M200 microplate reader (Tecan, Männedorf, Switzerland) using 96-well plates. Each sample was prepared three times.

	[µmol/mol leucine equivalent]					
	Histones		Mitochondria		Cytosol	
Modifications	LOD	LOQ	LOD	LOQ	LOD	LOQ
N^6-formyl lysine	1.1	3.8	1.8	6.0	2.5	8.3
N^6-acetyl lysine	0.1	0.4	0.5	1.8	0.7	2.3
N^6-propionyl lysine	0.1	0.4	0.2	0.6	0.1	0.4
N^6-butyryl lysine	0.04	0.1	0.02	0.07	0.02	0.07
N^6-malonyl lysine	0.9	2.9	0.3	0.9	0.4	1.3
N^6-succinyl lysine	0.4	1.4	0.03	0.1	0.04	0.1
CML	0.4	1.2	0.5	1.7	0.7	2.4
GALA	0.3	0.9	0.1	0.3	0.1	0.2
G-H3	0.6	2.0	1.0	3.4	1.1	3.6
CEL	0.4	1.3	0.5	1.8	0.5	1.8
N^6-lactoyl lysine	0.3	1.0	0.1	0.2	0.03	0.1
MG-H	0.7	2.4	0.3	1.1	0.6	1.9
furosine	0.1	0.4	0.04	0.1	0.05	0.2
N^6-glyoxylyl lysine	0.1	0.4	0.3	0.8	0.4	1.5
N^6-pyruvoyl lysine	0.1	0.3	0.3	0.9	0.4	1.4
o-tyrosine	0.1	0.2	0.2	0.6	0.1	0.4
o,o-dityrosine	0.4	1.4	0.4	1.3	0.5	1.7
methionine sulfoxide	0.1	0.2	0.2	0.7	0.2	0.8
methionine sulfone	0.6	2.0	0.6	2.2	2.8	9.3
citrulline	0.4	1.3	0.4	1.2	0.3	0.9

Table 3. Limits of detection (LOD) and limits of quantitation (LOQ). CML = N^6-carboxymethyl lysine; GALA = N^6-glycoloyl lysine, G-H3 = glyoxal hydroimidazolone 3; CEL = N^6-carboxyethyl lysine; MG-H = methylglyoxal hydroimidazolone.

Analytical HPLC-MS/MS. A PU-2080 Plus quaternary gradient pump with degasser and a AS-2057 Plus autosampler (Jasco, Gross-Umstadt, Germany) were used as described previously[9]. The mass analyses were performed using an API 4000 quadrupole instrument (Applied Biosystems, Foster City, USA) equipped with an API source using electrospray ionization. The HPLC system was connected directly to the probe of the mass spectrometer. Nitrogen was used as sheath and auxiliary gas. To measure the analytes the scheduled multiple-reaction monitoring (sMRM) mode of HPLC-MS/MS was used. The optimized parameters for mass spectrometry are given in Table 2.

Quantitation was based on the standard addition method using known amounts of the pure authentic reference compounds to compensate for matrix effects. Authentic reference compounds were added at 0.5, 1, 2, and 4 times the concentration of the analyte in the sample and correlation coefficients were 0.9 or higher. Limits of detection and quantitation are given in Table 3.

Chromatographic separations were performed on a stainless steel column (XSelect HSS T3, 250 × 3.0 mm, RP18, 5 µm, Waters, Milford, USA) using a flow rate of 0.7 mL/min and a column temperature of 25 °C. Eluents were ultra-pure water (A) and a mixture of methanol and ultra-pure water (7:3, v/v; B), both supplemented with 1.2 mL/L heptafluorobutyric acid. Samples were injected (10 µL) at 2% B and run isocratic for 2 min, gradient was changed to 14% B within 10 min (held for 0 min), 87% B within 22 min (held for 0 min), 100% B within 0.5 min (held for 7 min) and 2% B within 2.5 min (held 8 min). Exemplary chromatographic separations are included in the supporting information (Figure S3).

Statistical analysis. Significant differences between 10 young and 10 old animals were determined by one-tailed and unpaired t-Test using n = 10 and alpha of 0.05. One-tailed test was used, because it is known from literature, that several non-enzymatic PTMs increase in aging. The unpaired t-Test was used, because of unequal variances of young and old subgroups as indicated by F-Test. The normal distribution was checked by Shapiro-Wilk Normality Test. A single analytical replicate from every biological replicate was used, because biological variability was much higher than the analytical error.

Data availability

We declare that all the data supporting the findings of this study are available within the paper and the supplementary information files.

Received: 2 December 2019; Accepted: 27 March 2020;
Published online: 05 May 2020

References

1. Aebersold, R. *et al.* How many human proteoforms are there? *Nat. Chem. Biol.* **14**, 206–214 (2018).
2. Lin, H. & Caroll, K. S. Introduction: Posttranslational Protein Modification. *Chem. Rev.* **118**, 887–888 (2018).
3. López-Otín, C., Blasco, M. A., Partridge, L., Serrano, M. & Kroemer, G. The Hallmarks of Aging. *Cell* **153**, 1194–1217 (2013).

4. Allfrey, V. G., Faulkner, R. & Mirsky, A. E. Acetylation and Methylation of Histones and Their Possible Role in the Regulation of RNA Synthesis. *Proc. Natl. Acad. Sci.* **51**, 786–794 (1964).
5. Ali, I., Conrad, R. J., Verdin, E. & Ott, M. Lysine Acetylation Goes Global: From Epigenetics to Metabolism and Therapeutics. *Chem. Rev.* **118**, 1216–1252 (2018).
6. Song, S. & Yu, Y. Progression on Citrullination of Proteins in Gastrointestinal Cancers. *Front. Oncol.* **9**, 113 (2019).
7. Höhn, A., König, J. & Grune, T. Protein oxidation in aging and the removal of oxidized proteins. *J. Proteom.* **92**, 132–159 (2013).
8. Henning, C., Liehr, K., Girndt, M., Ulrich, C. & Glomb, M. A. Analysis and Chemistry of Novel Protein Oxidation Markers *in Vivo*. *J. Agric. Food Chem.* **66**, 4692–4701 (2018).
9. Smuda, M. *et al*. Comprehensive Analysis of Maillard Protein Modifications in Human Lenses: Effect of Age and Cataract. *Biochemistry* **54**, 2500–2507 (2015).
10. Rosca, M. G. *et al*. Glycation of mitochondrial proteins from diabetic rat kidney is associated with excess superoxide formation. *Am. J. Physiol.* **289**, F420–F430 (2005).
11. Bierhaus, A. *et al*. Understanding RAGE, the receptor for advanced glycation end products. *J. Mol. Med.* **83**, 876–886 (2005).
12. Uchiki, T. *et al*. Glycation-altered proteolysis as a pathobiologic mechanism that links dietary glycemic index, aging, and age-related disease (in nondiabetics). *Aging Cell* **11**, 1–13 (2012).
13. Glomb, M. A. & Pfahler, C. Amides Are Novel Protein Modifications Formed by Physiological Sugars. *J. Biol. Chem.* **276**, 41638–41647 (2001).
14. Wagner, G. R. & Hirschey, M. D. Nonenzymatic Protein Acylation as a Carbon Stress Regulated by Sirtuin Deacylases. *Mol. Cell* **54**, 5–16 (2014).
15. Sabari, B. R. D. Z., Allis, C. D. & Zhao, Y. Metabolic regulation of gene expression through histone acylations. *Nat. Rev. Mol. Cell Biol.* **18**, 90–101 (2017).
16. Moldogazieva, N. T. Mokhosoev, I. M. Mel'nikova, T. I. Porozov, Y. B. & Terentiev, A. A. Oxidative Stress and Advanced Lipoxidation and Glycation End Products (ALEs and AGEs) in Aging and Age-Related Diseases, Oxid. Med. Cell. Longev. 2019, 1–14 (2019).
17. Chaudhuri, J. *et al*. The Role of Advanced Glycation End Products in Aging and Metabolic Diseases: Bridging Association and Causality. *Cell Metab.* **28**, 337–352 (2018).
18. Korovila, I. *et al*. Proteostasis, oxidative stress and aging. *Redox Biol.* **13**, 550–567 (2017).
19. Baldensperger, T., Jost, T., Zipprich, A. & Glomb, M. A. Novel α-Oxoamide Advanced-Glycation Endproducts within the N6 -Carboxymethyl Lysine and N6 -Carboxyethyl Lysine Reaction Cascades. *J. Agric. Food Chem.* **66**, 1898–1906 (2018).
20. Baldensperger, T., Di Sanzo, S., Ori, A. & Glomb, M. A. Quantitation of Reactive Acyl-CoA Species Mediated Protein Acylation by HPLC–MS/MS. *Anal. Chem.* **91**, 12336–12343 (2019).
21. Nie, L. *et al*. The Landscape of Histone Modifications in a High-Fat Diet-Induced Obese (DIO) Mouse Model. *Mol. Cell. Proteom.* **16**, 1324–1334 (2017).
22. Pogo, A. O., Allfrey, V. G. & Mirsky, A. E. Evidence for increased DNA template activity in regenerating liver nuclei. *Proc. Natl. Acad. Sci.* **56**, 550–557 (1966).
23. Frezza, C., Cipolat, S. & Scorrano, L. Organelle isolation: functional mitochondria from mouse liver, muscle and cultured filroblasts. *Nat. Protoc.* **2**, 287–295 (2007).
24. Hong, S. Y. *et al*. The Role of Mitochondrial Non-Enzymatic Protein Acylation in Ageing. *PLoS ONE* **11**, e0168752 (2016).
25. Voigt, M. & Glomb, M. A. Reactivity of 1-Deoxy- d - erythro -hexo-2,3-diulose: A Key Intermediate in the Maillard Chemistry of Hexoses. *J. Agric. Food Chem.* **57**, 4765–4770 (2009).
26. Smuda, M., Voigt, M. & Glomb, M. A. Degradation of 1-Deoxy- d - erythro -hexo-2,3-diulose in the Presence of Lysine Leads to Formation of Carboxylic Acid Amides. *J. Agric. Food Chem.* **58**, 6458–6464 (2010).
27. Feser, J. & Tyler, J. Chromatin structure as a mediator of aging. *FEBS Lett.* **585**, 2041–2048 (2011).
28. Wang, Y. Yuan, Q. & Xie, L. Histone Modifications in Aging: The Underlying Mechanisms and Implications, CSCR 13 (2018).
29. Jiang, T., Zhou, X., Taghizadeh, K., Dong, M. & Dedon, P. C. N-formylation of lysine in histone proteins as a secondary modification arising from oxidative DNA damage. *Proc. Natl. Acad. Sci.* **104**, 60–65 (2007).
30. Carrico, C., Meyer, J. G., He, W., Gibson, B. W. & Verdin, E. The Mitochondrial Acylome Emerges: Proteomics, Regulation by Sirtuins, and Metabolic and Disease Implications. *Cell Metab.* **27**, 497–512 (2018).
31. Anderson, K. A., Green, M. F., Huynh, F. K., Wagner, G. R. & Hirschey, M. D. SnapShot: Mammalian Sirtuins. *Cell* **159**, 956–956.e1 (2014).
32. Nishida, Y. *et al*. SIRT5 Regulates both Cytosolic and Mitochondrial Protein Malonylation with Glycolysis as a Major Target. *Mol. Cell* **59**, 321–332 (2015).
33. Rardin, M. J. *et al*. SIRT5 Regulates the Mitochondrial Lysine Succinylome and Metabolic Networks. *Cell Metab.* **18**, 920–933 (2013).
34. Wiśniewski, J. R., Zougman, A. & Mann, M. N ε -Formylation of lysine is a widespread post-translational modification of nuclear proteins occurring at residues involved in regulation of chromatin function. *Nucleic Acids Res.* **36**, 570–577 (2008).
35. Edrissi, B. *et al*. Dosimetry of N6 -Formyllysine Adducts Following [13 C 2 H 2]-Formaldehyde Exposures in Rats. *Chem. Res. Toxicol.* **26**, 1421–1423 (2013).
36. Henning, C., Smuda, M., Girndt, M., Ulrich, C. & Glomb, M. A. Molecular Basis of Maillard Amide-Advanced Glycation End Product (AGE) Formation *in Vivo*. *J. Biol. Chem.* **286**, 44350–44356 (2011).
37. Smuda, M. & Glomb, M. A. Maillard Degradation Pathways of Vitamin C, Angew. *Chem. Int. Ed.* **52**, 4887–4891 (2013).
38. Ledl, F. & Schleicher, E. New Aspects of the Maillard Reaction in Foods and in the Human Body. *Angew. Chem. Int. Ed. Engl.* **29**, 565–594 (1990).
39. Commerford, S. L., Carsten, A. L. & Cronkite, E. P. Histone turnover within nonproliferating cells. *Proc. Natl. Acad. Sci.* **79**, 1163–1165 (1982).
40. Rabbani, N. & Thornalley, P. J. Dicarbonyl stress in cell and tissue dysfunction contributing to ageing and disease. *Biochem. Biophys. Res. Commun.* **458**, 221–226 (2015).
41. Glomb, M. A. & Lang, G. Isolation and Characterization of Glyoxal−Arginine Modifications. *J. Agric. Food Chem.* **49**, 1493–1501 (2001).
42. Zheng, Q. *et al*. Reversible histone glycation is associated with disease-related changes in chromatin architecture. *Nat. Commun.* **10**, 1289 (2019).
43. Tsakiri, E. N. *et al*. Diet-derived advanced glycation end products or lipofuscin disrupts proteostasis and reduces life span in Drosophila melanogaster. *Free Radic. Biol. Med.* **65**, 1155–1163 (2013).
44. Kislinger, T. *et al*. Nε -(Carboxymethyl)Lysine Adducts of Proteins Are Ligands for Receptor for Advanced Glycation End Products That Activate Cell Signaling Pathways and Modulate Gene Expression. *J. Biol. Chem.* **274**, 31740–31749 (1999).
45. Leeuwenburgh, C., Hansen, P. A., Holloszy, J. O. & Heinecke, J. W. Oxidized amino acids in the urine of aging rats: potential markers for assessing oxidative stress *in vivo*. *Am. J. Physiol. Regul. Integr. Comp. Physiol.* **276**, R128–R135 (1999).
46. Vogt, W. Oxidation of methionyl residues in proteins: Tools, targets, and reversal. *Free Radic. Biol. Med.* **18**, 93–105 (1995).
47. Johansen, J. T., Breddam, K. & Ottesen, M. Isolation of carboxypeptidase Y by affinity chromatography. *Carlsberg Res. Commun.* **41**, 1–14 (1976).
48. Wachsmuth, E. D., Fritze, I. & Pfleiderer, G. An aminopeptidase occurring in pig kidney. I. An improved method of preparation. Physical and enzymic properties. *Biochemistry* **5**, 169–174 (1966).

Acknowledgements
Funding was supported by the Deutsche Forschungsgemeinschaft (DFG, Germany) Research Training Group 2155, ProMoAge.

Author contributions
T.B. developed the concept, prepared samples, performed HPLC-MS/MS analyses and wrote the manuscript. M.E. developed the fractionation protocol. J.K. and P.R.W. prepared samples. T.P. and J.K. validated the fractionation protocol by Western blotting. M.A.G. supervised the work and reviewed the manuscript.

Competing interests
The authors declare no competing interests.

Additional information
Supplementary information is available for this paper at https://doi.org/10.1038/s41598-020-64265-0.

Correspondence and requests for materials should be addressed to M.A.G.

Reprints and permissions information is available at www.nature.com/reprints.

Publisher's note Springer Nature remains neutral with regard to jurisdictional claims in published maps and institutional affiliations.

Open Access This article is licensed under a Creative Commons Attribution 4.0 International License, which permits use, sharing, adaptation, distribution and reproduction in any medium or format, as long as you give appropriate credit to the original author(s) and the source, provide a link to the Creative Commons license, and indicate if changes were made. The images or other third party material in this article are included in the article's Creative Commons license, unless indicated otherwise in a credit line to the material. If material is not included in the article's Creative Commons license and your intended use is not permitted by statutory regulation or exceeds the permitted use, you will need to obtain permission directly from the copyright holder. To view a copy of this license, visit http://creativecommons.org/licenses/by/4.0/.

© The Author(s) 2020

Reprinted with permission from Baldensperger, T.; Eggen, M.; Kappen, J.; Winterhalter, P. R.; Pfirrmann, T.; Glomb, M. A. Comprehensive analysis of posttranslational protein modifications in aging of subcellular compartments, *Sci. Rep.* **2020**, *10*, p. 7596. Copyright 2020 The Authors.

6 Summary

The enzymatic acylation of lysine is a major regulatory mechanism in epigenetics and metabolism. Recent studies discovered structural related non-enzymatic acylation of lysine by highly reactive α-dicarbonyls and acyl-CoA thioesters. The aim of the present thesis was the development and validation of a robust analytical method to elucidate the causes and consequences of these novel acyl lysine modifications in aging and disease.

Model incubations of N^2-Boc-lysine with α-dicarbonyls glyoxal and methylglyoxal were used to enhance understanding of non-enzymatic acylation by formation of amide advanced glycation endproducts via complex isomerization cascades. Authentic reference standards of N^6-glyoxylyl lysine and N^6-pyruvoyl lysine were synthesized and structures verified by NMR and HR-MS. A sensitive HPLC-MS/MS method was developed to prove the formation of N^6-glyoxylyl lysine by glyoxal and N^6-pyruvoyl lysine by methylglyoxal *in vitro* for the first time. The formation of these novel acyl lysine modifications was highly dependent on pH and α-oxoamide advanced glycation endproducts were exclusively formed under aeration. Consequently, the oxidation of the central enaminol intermediate was postulated as the key mechanistic step and α-oxoamides were suggested as potential oxidative stress markers. In support of this hypothesis, N^6-glyoxylyl lysine and N^6-pyruvoyl lysine were detected in rat liver and indeed increased by approximately 100 % in cirrhosis and aging.

Western blotting and proteomics are established analytical methods to measure acylation of lysine residues by reactive acyl-CoA species. However, they lack the ability to measure different acylation structures simultaneously in a quantitative manner. Authentic reference standards of 14 acylated lysine species were synthesized and used to develop a HPLC-MS/MS method for the quantitation of all 14 modifications in a single run. An enzymatic hydrolysis protocol with about 85 % efficiency of hydrolysis compared to acid hydrolysis was established for proteins to measure acylation in biological samples. The method was validated and had recovery rates between 75 – 93 % with LODs in the nanomolar range. Without further enrichment 8 acylation structures were quantitated in mouse liver, kidney, heart, and brain. Liver was identified as a hotspot for lysine acylation with acetylation (37.31 µmol/mol leucine-eq), formylation (9.61 µmol/mol leucine-eq), and succinylation (6.12 µmol/mol leucine-eq) as the quantitative most abundant modifications. Enrichment of analytes by repetitive HPLC fractionation enabled quantitation of 6 additional modifications including 4 novel acylation structures N^6-acetoacetyl lysine, N^6-isovaleryl lysine, N^6-(2-methylbutyryl) lysine, and N^6-tiglyl lysine. The existence of these novel modifications was verified by collision induced dissociation spectra and co-elution with synthesized standards.

Finally, the concepts of oxidative, dicarbonyl, and RACS stress were combined using a mouse cohort. A protocol for the extraction of histone, cytosolic, and mitochondrial proteins from mouse liver was developed and validated. Posttranslational modifications in subcellular compartments were quantitated by a novel HPLC-MS/MS method and changes in the aging process were monitored. Characteristic patterns were observed for 7 advanced glycation endproducts, 6 oxidative stress markers, 6 lysine acylation structures, and citrullination. Accumulation of non-enzymatic modifications was observed in all subcellular compartments during the aging process. This correlation was especially strong in histones in which protein acylation, glycation, and oxidation increased about 115 %, 45 %, and 65 %, respectively. Hence, non-enzymatic modification of proteins was suggested as a potential mechanism in hallmarks of aging.

7 Zusammenfassung

Die enzymatische Acetylierung von Lysinseitenketten ist ein etablierter Mechanismus in der Regulation der Epigenetik und des Metabolismus. Neueste Studien konnten strukturell verwandte nicht-enzymatische Acylierung von Lysin durch reaktive α-Dicarbonyle und Acyl-CoA Thioester identifizieren. Das Ziel der vorliegenden Dissertation war die Entwicklung und Validierung einer robusten Analytik, um die Mechanismen und Funktionen dieser neuartigen Lysinacylierungen in Alterungs- und Krankheitsprozessen aufzuklären.

Modellinkubationen von N^2-Boc-Lysin mit den α-Dicarbonylen Glyoxal und Methylglyoxal wurden benutzt um die zugrundeliegenden Mechanismen der nicht-enzymatischen Acylierung durch die Bildung von Amid *Advanced Glycation Endproducts* in komplexen Isomerisierungskaskaden aufzuklären. Synthesen der authentische Referenzstandards N^6-Glyoxylyllysin und N^6-Pyruvoyllysin wurden entwickelt und die Strukturen mittels NMR und HR-MS verifiziert. Eine sensitive HPLC-MS/MS Methode wurde entwickelt, um die Bildung von N^6-Glyoxylyllysin durch Glyoxal und N^6-Pyruvoyllysin durch Methylglyoxal *in vitro* erstmals nachzuweisen. Die Bildung dieser neuartigen Lysinacylierungen war stark vom pH abhängig und die α-Oxoamid *Advanced Glycation Endproducts* wurden ausschließlich unter aeroben Bedingungen gebildet. Daraufhin wurde die Oxidation des Enaminolintermediats als zentraler mechanistischer Schritt sowie α-Oxoamide als potentielle oxidative Stressmarker postuliert. Diese Hypothese wurde durch den Nachweis von N^6-Glyoxylyllysin und N^6-Pyruvoyllysin in Leber sowie den Anstieg um ca. 100 % in zirrhotischen sowie alten Tieren bestätigt.

Western blotting und *Proteomics* sind bewährte analytische Methoden um Lysinacylierung durch Acyl-CoA Thioester zu messen. Allerdings können sie nicht die ganze Bandbreite der Modifikationen in einer einzigen Analyse detektieren und eine absolute Quantifizierung ist kaum möglich. Authentische Referenzstandards von 14 acylierten Lysinderivaten wurden synthetisiert und genutzt, um eine HPLC-MS/MS Methode zur simultanen Detektion und Quantifizierung aller 14 Modifikationen zu entwickeln. Ein enzymatisches Hydrolyseprotokoll mit ca. 85 % Hydrolyseeffizienz im Vergleich zur sauren Hydrolyse wurde für Proteine etabliert, um die Acylierung in biologischen Proben messen zu können. Die Wiederfindungsraten lagen bei 75 – 93 % und die Nachweisgrenzen lagen im nanomolaren Bereich. Somit konnten 8 Acylierungsstrukturen in Leber, Niere, Herz und Gehirn von Mäusen quantifiziert werden. Die höchsten Konzentrationen wurden in Leber gemessen. Acylierung (37.31 µmol/mol Leucin-Eq), Formylierung (9.61 µmol/mol Leucin-Eq) und Succinylierung (6.12 µmol/mol Leucin-Eq) waren die quantitativ bedeutendsten

Modifikationen. Aufkonzentrierung durch mehrmalige HPLC-Fraktionierung führte zu der Quantifizierung von 6 weiteren Acylierungsstrukturen, darunter die 4 neuartigen Strukturen N^6-Acetoacetyllysin, N^6-Isovaleryllysin, N^6-(2-Methylbutyryl)-lysin und N^6-Tiglyllysin. Die Strukturen der neuen Modifikationen wurden durch kollisionsinduzierte Dissoziationsspektren verifiziert.

Abschließend wurden die Konzepte von oxidativem Stress, Dicarbonylstress und RACS Stress durch Untersuchung einer Mauskohorte kombiniert. Änderungen der posttranslationalen Modifikationen im Alterungsprozess wurden verfolgt und Muster identifiziert. Ein Protokoll zur Extraktion von Histonen, cytosolischen und mitochondrialen Proteinen aus Mausleber wurde entwickelt und validiert. Zusammenfassend wurden 6 Acylierungen, 7 Glykierungen, 6 oxidative Stressmarker und Citrullinierung in den subzellulären Kompartimenten mittels HPLC-MS/MS quantifiziert. Histonproteine waren besonders stark modifiziert. Methioninsulfoxid (595.8 µmol/mol Leucin-Eq), N^6-Acetyllysin (304.5 µmol/mol Leucin-Eq), N^6-Formyllysin (126.1 µmol/mol Leucin-Eq) und Citrullinierung (55.2 µmol/mol Leucin-Eq) waren die quantitative bedeutendsten Strukturen. Nicht-enzymatische Modifikationen akkumulierten im Alterungsprozess in allen subzellulären Kompartimenten. Besonders stark ausgeprägt war diese Korrelation in Histonen, in welchen Proteinacylierung um 115 %, Proteinglykierung um 45 % und Proteinoxidation um 65 % anstiegen. Daher wurde die nicht-enzymatische Modifikation von Proteinen als möglicher Mechanismus im Alterungsprozess postuliert.

8 References

(1) Peters, E.; Pritzkuleit, R.; Beske, F.; Katalinic, A. Demografischer Wandel und Krankheitshäufigkeiten, *Bundesgesundheitsbl.* **2010**, *53*, pp. 417–426.

(2) Ali, I.; Conrad, R. J.; Verdin, E.; Ott, M. Lysine Acetylation Goes Global: From Epigenetics to Metabolism and Therapeutics, *Chem. Rev.* **2017**, *118*, pp. 1216–1252.

(3) Wagner, G. R.; Hirschey, M. D. Nonenzymatic Protein Acylation as a Carbon Stress Regulated by Sirtuin Deacylases, *Mol. Cell.* **2014**, *54*, pp. 5–16.

(4) Osborne, B.; Bentley, N. L.; Montgomery, M. K.; Turner, N. The role of mitochondrial sirtuins in health and disease, *Free Radic. Biol. Med.* **2016**, *100*, pp. 164–174.

(5) Ahmed, N. Advanced glycation endproducts - role in pathology of diabetic complications, *Diabetes Res. Clin. Pract.* **2005**, *67*, pp. 3–21.

(6) Lin, H.; Caroll, K. S. Introduction: Posttranslational Protein Modification, *Chem. Rev.* **2017**, *118*, pp. 887–888.

(7) Aebersold, R.; Agar, J. N.; Amster, I. J.; Baker, M. S., et al. How many human proteoforms are there?, *Nat. Chem. Biol.* **2018**, *14*, pp. 206–214.

(8) Phillips, D. M. P. The presence of acetyl groups in histones, *Biochem. J.* **1963**, *87*, pp. 258–263.

(9) Aksnes, H.; Drazic, A.; Marie, M.; Arnesen, T. First Things First: Vital Protein Marks by N-Terminal Acetyltransferases, *Trends Biochem. Sci.* **2016**, *41*, pp. 746–760.

(10) Meyer, J. G.; Softic, S.; Basisty, N.; Rardin, M. J., et al. Temporal dynamics of liver mitochondrial protein acetylation and succinylation and metabolites due to high fat diet and/or excess glucose or fructose, *PLoS ONE.* **2018**, *13*, pp. e0208973.

(11) Sabari, B. R.; Di Zhang; Allis, C. D.; Zhao, Y. Metabolic regulation of gene expression through histone acylations, *Nat. Rev. Mol. Cell Biol.* **2017**, *18*, pp. 90–101.

(12) Wagner, G. R.; Payne, R. M. Widespread and Enzyme-independent Nϵ-Acetylation and Nϵ-Succinylation of Proteins in the Chemical Conditions of the Mitochondrial Matrix, *J. Biol. Chem.* **2013**, *288*, pp. 29036–29045.

(13) Henning, C.; Glomb, M. A. Pathways of the Maillard reaction under physiological conditions, *Glycoconj. J.* **2016**, *33*, pp. 499–512.

(14) Berndsen, C. E.; Denu, J. M. Catalysis and substrate selection by histone/protein lysine acetyltransferases, *Curr. Opin. Struct. Biol.* **2008**, *18*, pp. 682–689.

(15) Marmorstein, R.; Roth, S. Y. Histone acetyltransferases: function, structure, and catalysis, *Curr. Opin. Genet. Dev.* **2001**, *11*, pp. 155–161.

(16) Berndsen, C. E.; Albaugh, B. N.; Tan, S.; Denu, J. M. Catalytic Mechanism of a MYST Family Histone Acetyltransferase, *Biochemistry*. **2007**, *46*, pp. 623–629.

(17) Jiang, J.; Lu, J.; Lu, D.; Liang, Z., et al. Investigation of the Acetylation Mechanism by GCN5 Histone Acetyltransferase, *PLoS ONE*. **2012**, *7*, pp. e36660.

(18) Yan, Y.; Harper, S.; Speicher, D. W.; Marmorstein, R. The catalytic mechanism of the ESA1 histone acetyltransferase involves a self-acetylated intermediate, *Nat. Struct. Mol. Biol.* **2002**, *9*, pp. 862–869.

(19) Zhang, X.; Ouyang, S.; Kong, X.; Liang, Z., et al. Catalytic Mechanism of Histone Acetyltransferase p300: From the Proton Transfer to Acetylation Reaction, *J. Phys. Chem. B.* **2014**, *118*, pp. 2009–2019.

(20) Dancy, B. M.; Cole, P. A. Protein lysine acetylation by p300/CBP, *Chem. Rev.* **2015**, *115*, pp. 2419–2452.

(21) Liu, X.; Wang, L.; Zhao, K.; Thompson, P. R., et al. The structural basis of protein acetylation by the p300/CBP transcriptional coactivator, *Nature.* **2008**, *451*, pp. 846–850.

(22) Riggs, M. G., Whittacker, R. G.; Neumann, J. R., Ingram, V. M. n-Butyrate causes histone modification in HeLa and Friend erythroleukaemia cells, *Nature.* **1977**, *268*, p. 462.

(23) Taunton, J.; Hassig, C. A.; Schreiber, S. L. A Mammalian Histone Deacetylase Related to the Yeast Transcriptional Regulator Rpd3p, *Science.* **1996**, *272*, pp. 408–411.

(24) Finnin, M. S.; Donigian, J. R.; Cohen, A.; Richon, V. M., et al. Structures of a histone deacetylase homologue bound to the TSA and SAHA inhibitors, *Nature.* **1999**, *401*, pp. 188–193.

(25) Newkirk, T. L.; Bowers, A. A.; Williams, R. M. Discovery, biological activity, synthesis and potential therapeutic utility of naturally occurring histone deacetylase inhibitors, *Nat. Prod. Rep.* **2009**, *26*, pp. 1293–1320.

(26) Dhalluin, C.; Carlson, J. E.; Zeng, L.; He, C., et al. Structure and ligand of a histone acetyltransferase bromodomain, *Nature.* **1999**, *399*, pp. 491–496.

(27) Zeng, L.; Zhang, Q.; Li, S.; Plotnikov, A. N., et al. Mechanism and regulation of acetylated histone binding by the tandem PHD finger of DPF3b, *Nature.* **2010**, *466*, pp. 258–262.

(28) Li, Y.; Wen, H.; Xi, Y.; Tanaka, K., et al. AF9 YEATS Domain Links Histone Acetylation to DOT1L-Mediated H3K79 Methylation, *Cell.* **2014**, *159*, pp. 558–571.

(29) Wang, D.; Kon, N.; Lasso, G.; Jiang, L., et al. Acetylation-regulated interaction between p53 and SET reveals a widespread regulatory mode, *Nature.* **2016**, *538*, pp. 118–122.

(30) Allfrey, V. G.; Faulkner, R.; Mirsky, A. E. Acetylation and methylation of histones and their possible role in the regulation of RNA synthesis, *Proc. Natl. Acad. Sci.* **1964**, *51*, pp. 786–794.

(31) Vidali, G.; Gershey, E. L.; Allfrey, V. G. Chemical studies of histone acetylation the distribution of ε-N-acetyllysine in calf thymus histones, *J. Biol. Chem.* **1968**, *243*, pp. 6361–6366.

(32) Chen, L.-F.; Greene, W. C. Assessing acetylation of NF-κB, *Methods.* **2005**, *36*, pp. 368–375.

(33) Caron, C.; Boyault, C.; Khochbin, S. Regulatory cross-talk between lysine acetylation and ubiquitination: role in the control of protein stability, *BioEssays.* **2005**, *27*, pp. 408–415.

(34) L'Hernault, S. W.; Rosenbaum, J. L. Chlamydomonas alpha-tubulin is posttranslationally modified by acetylation on the epsilon-amino group of a lysine, *Biochemistry.* **1985**, *24*, pp. 473–478.

(35) Zhao, S.; Xu, W.; Jiang, W.; Yu, W., et al. Regulation of Cellular Metabolism by Protein Lysine Acetylation, *Science.* **2010**, *327*, pp. 1000–1004.

(36) Wang, Y.; Yuan, Q.; Xie, L. Histone Modifications in Aging: The Underlying Mechanisms and Implications, *Curr. Stem. Cell Res. Ther.* **2018**, *13*, pp. 125–135.

(37) Feser, J.; Tyler, J. Chromatin structure as a mediator of aging, *FEBS Lett.* **2011**, *585*, pp. 2041–2048.

(38) Kim-Ha, J.; Kim, Y.-J. Age-related epigenetic regulation in the brain and its role in neuronal diseases, *BMB Rep.* **2016**, *49*, pp. 671–680.

(39) Stevenson, F. T.; Bursten, S. L.; Locksley, R. M.; Lovett, D. H. Myristyl acylation of the tumor necrosis factor alpha precursor on specific lysine residues, *J. Exp. Med.* **1992**, *176*, pp. 1053–1062.

(40) Jiang, T.; Zhou, X.; Taghizadeh, K.; Dong, M.; Dedon, P. C. N-formylation of lysine in histone proteins as a secondary modification arising from oxidative DNA damage, *Proc. Natl. Acad. Sci.* **2007**, *104*, pp. 60–65.

(41) Chen, Y.; Sprung, R.; Tang, Y.; Ball, H., et al. Lysine Propionylation and Butyrylation Are Novel Post-translational Modifications in Histones, *Mol. Cell. Proteom.* **2007**, *6*, pp. 812–819.

(42) Zhang, Z.; Tan, M.; Xie, Z.; Dai, L., et al. Identification of lysine succinylation as a new post-translational modification, *Nat. Chem. Biol.* **2011**, *7*, pp. 58–63.

(43) Tan, M.; Luo, H.; Lee, S.; Jin, F., et al. Identification of 67 Histone Marks and Histone Lysine Crotonylation as a New Type of Histone Modification, *Cell.* **2011**, *146*, pp. 1016–1028.

(44) Peng, C.; Lu, Z.; Xie, Z.; Cheng, Z., et al. The First Identification of Lysine Malonylation Substrates and Its Regulatory Enzyme, *Mol. Cell. Proteom.* **2011**, *10*, pp. M111.012658.

(45) Tan, M.; Peng, C.; Anderson, K. A.; Chhoy, P., et al. Lysine Glutarylation Is a Protein Posttranslational Modification Regulated by SIRT5, *Cell Metab.* **2014**, *19*, pp. 605–617.

(46) Dai, L.; Peng, C.; Montellier, E.; Lu, Z., et al. Lysine 2-hydroxyisobutyrylation is a widely distributed active histone mark, *Nat. Chem. Biol.* **2014**, *10*, pp. 365–370.

(47) Xie, Z.; Di Zhang; Chung, D.; Tang, Z., et al. Metabolic Regulation of Gene Expression by Histone Lysine β-Hydroxybutyrylation, *Mol. Cell.* **2016**, *62*, pp. 194–206.

(48) Wagner, G. R.; Bhatt, D. P.; O'Connell, T. M.; Thompson, J. W., et al. A Class of Reactive Acyl-CoA Species Reveals the Non-enzymatic Origins of Protein Acylation, *Cell Metab.* **2017**, *25*, pp. 823–837.e8.

(49) Huang, H.; Di Zhang; Wang, Y.; Perez-Neut, M., et al. Lysine benzoylation is a histone mark regulated by SIRT2, *Nat. Commun.* **2018**, *9*, p. 90.

(50) James, P. Protein identification in the post-genome era: the rapid rise of proteomics, *Quart. Rev. Biophys.* **1997**, *30*, pp. 279–331.

(51) Simic, Z.; Weiwad, M.; Schierhorn, A.; Steegborn, C.; Schutkowski, M. The ε-Amino Group of Protein Lysine Residues Is Highly Susceptible to Nonenzymatic Acylation by Several Physiological Acyl-CoA Thioesters, *ChemBioChem.* **2015**, *16*, pp. 2337–2347.

(52) Corkey, B. E.; Hale, D. E.; Glennon, M. C.; Kelley, R. I., et al. Relationship between unusual hepatic acyl coenzyme A profiles and the pathogenesis of Reye syndrome, *J. Clin. Invest.* **1988**, *82*, pp. 782–788.

(53) Croes, K.; Van Veldhoven, Paul P; Mannaerts, G. P.; Casteels, M. Production of formyl-CoA during peroxisomal α-oxidation of 3-methyl-branched fatty acids, *FEBS Lett.* **1997**, *407*, pp. 197–200.

(54) Jansen, G. A.; Wanders, R. J. Alpha-Oxidation, *Biochim. Biophys. Acta.* **2006**, *1763*, pp. 1403–1412.

(55) Pietrocola, F.; Galluzzi, L.; Bravo-San Pedro, José Manuel; Madeo, F.; Kroemer, G. Acetyl Coenzyme A: A Central Metabolite and Second Messenger, *Cell Metab.* **2015**, *21*, pp. 805–821.

(56) Wongkittichote, P.; Ah Mew, N.; Chapman, K. A. Propionyl-CoA carboxylase – A review, *Mol. Genet. Metab.* **2017**, *122*, pp. 145–152.

(57) Adeva-Andany, M. M.; López-Maside, L.; Donapetry-García, C.; Fernández-Fernández, C.; Sixto-Leal, C. Enzymes involved in branched-chain amino acid metabolism in humans, *Amino Acids.* **2017**, *49*, pp. 1005–1028.

(58) Mosbach, E. H. Hepatic Synthesis of Bile Acids, *Arch. Intern. Med.* **1972**, *130*, pp. 478–487.

(59) Gibson, K. M.; Burlingame, T. G.; Hogema, B.; Jakobs, C., et al. 2-Methylbutyryl-Coenzyme A Dehydrogenase Deficiency: A New Inborn Error of L-Isoleucine Metabolism, *Pediat. Res.* **2000**, *47*, pp. 830–833.

(60) Lynch, C. J.; Halle, B.; Fujii, H.; Vary, T. C., et al. Potential role of leucine metabolism in the leucine-signaling pathway involving mTOR, *Am. J. Physiol.* **2003**, *285*, pp. E854–E863.

(61) Rao, K. S.; Albro, M.; Dwyer, T. M.; Frerman, F. E. Kinetic Mechanism of Glutaryl-CoA Dehydrogenase, *Biochemistry.* **2006**, *45*, pp. 15853–15861.

(62) Grabacka, M.; Pierzchalska, M.; Dean, M.; Reiss, K. Regulation of Ketone Body Metabolism and the Role of PPARα, *Int. J. Mol. Sci.* **2016**, *17*, pp. 2093–2116.

(63) Thompson, S. L.; Krisans, S. K. Rat liver peroxisomes catalyze the initial step in cholesterol synthesis. The condensation of acetyl-CoA units into acetoacetyl-CoA, *J. Biol. Chem.* **1990**, *265*, pp. 5731–5735.

(64) Buhaescu, I.; Izzedine, H. Mevalonate pathway: A review of clinical and therapeutical implications, *Clin. Biochem.* **2007**, *40*, pp. 575–584.

(65) Laffel, L. Ketone bodies: a review of physiology, pathophysiology and application of monitoring to diabetes, *Diabetes Metab. Res. Rev.* **1999**, *15*, pp. 412–426.

(66) Hirschey, M. D.; Zhao, Y. Metabolic Regulation by Lysine Malonylation, Succinylation, and Glutarylation, *Mol. Cell. Proteom.* **2015**, *14*, pp. 2308–2315.

(67) Matsubara, Y.; Kraus, J. P.; Yang-Feng, T. L.; Francke, U., et al. Molecular cloning of cDNAs encoding rat and human medium-chain acyl-CoA dehydrogenase and assignment of the gene to human chromosome 1, *Proc. Natl. Acad. Sci.* **1986**, *83*, pp. 6543–6547.

(68) Ikeda, Y.; Okamura-Ikeda, K.; Tanaka, K. Purification and characterization of short-chain, medium-chain, and long-chain acyl-CoA dehydrogenases from rat liver mitochondria. Isolation of the holo- and apoenzymes and conversion of the apoenzyme to the holoenzyme, *J. Biol. Chem.* **1985**, *260*, pp. 1311–1325.

(69) Choudhary, C.; Weinert, B. T.; Nishida, Y.; Verdin, E.; Mann, M. The growing landscape of lysine acetylation links metabolism and cell signalling, *Nat. Rev. Mol. Cell Biol.* **2014**, *15*, pp. 536–550.

(70) Zhang, Z.; Tan, M.; Xie, Z.; Dai, L., et al. Identification of lysine succinylation as a new post-translational modification, *Nat. Chem. Biol.* **2011**, *7*, pp. 58–63.

(71) Kaczmarska, Z.; Ortega, E.; Goudarzi, A.; Huang, H., et al. Structure of p300 in complex with acyl-CoA variants, *Nat. Chem. Biol.* **2017**, *13*, pp. 21–29.

(72) Ringel, A. E.; Wolberger, C. Structural basis for acyl-group discrimination by human Gcn5L2, *Acta Crystallogr. D Struct. Biol.* **2016**, *72*, pp. 841–848.

(73) Leemhuis, H.; Packman, L. C.; Nightingale, K. P.; Hollfelder, F. The Human Histone Acetyltransferase P/CAF is a Promiscuous Histone Propionyltransferase, *ChemBioChem.* **2008**, *9*, pp. 499–503.

(74) Berndsen, C. E.; Albaugh, B. N.; Tan, S.; Denu, J. M. Catalytic Mechanism of a MYST Family Histone Acetyltransferase, *Biochemistry.* **2007**, *46*, pp. 623–629.

(75) Han, Z.; Wu, H.; Kim, S.; Yang, X., et al. Revealing the protein propionylation activity of the histone acetyltransferase MOF (males absent on the first), *J. Biol. Chem.* **2018**, *293*, pp. 3410–3420.

(76) Anderson, K. A.; Green, M. F.; Huynh, F. K.; Wagner, G. R.; Hirschey, M. D. SnapShot: Mammalian Sirtuins, *Cell.* **2014**, *159*, pp. 956–956.e1.

(77) Michishita, E.; Park, J. Y.; Burneskis, J. M.; Barrett, J. C.; Horikawa, I. Evolutionarily Conserved and Nonconserved Cellular Localizations and Functions of Human SIRT Proteins, *Mol. Biol. Cell.* **2005**, *16*, pp. 4623–4635.

(78) Buler, M.; Andersson, U.; Hakkola, J. Who watches the watchmen? Regulation of the expression and activity of sirtuins, *FASEB J.* **2016**, *30*, pp. 3942–3960.

(79) Frye, R. A. Characterization of Five Human cDNAs with Homology to the Yeast SIR2 Gene: Sir2-like Proteins (Sirtuins) Metabolize NAD and May Have Protein ADP-Ribosyltransferase Activity, *Biochem. Biophys. Res. Commun.* **1999**, *260*, pp. 273–279.

(80) Carrico, C.; Meyer, J. G.; He, W.; Gibson, B. W.; Verdin, E. The Mitochondrial Acylome Emerges: Proteomics, Regulation by Sirtuins, and Metabolic and Disease Implications, *Cell Metab.* **2018**, *27*, pp. 497–512.

(81) Anderson, K. A.; Huynh, F. K.; Fisher-Wellman, K.; Stuart, J. D., et al. SIRT4 Is a Lysine Deacylase that Controls Leucine Metabolism and Insulin Secretion, *Cell Metab.* **2017**, *25*, pp. 838–855.e15.

(82) Mathias, R. A.; Greco, T. M.; Oberstein, A.; Budayeva, H. G., et al. Sirtuin 4 Is a Lipoamidase Regulating Pyruvate Dehydrogenase Complex Activity, *Cell.* **2014**, *159*, pp. 1615–1625.

(83) Jiang, H.; Khan, S.; Wang, Y.; Charron, G., et al. SIRT6 regulates TNF-α secretion through hydrolysis of long-chain fatty acyl lysine, *Nature.* **2013**, *496*, pp. 110–113.

(84) Liszt, G.; Ford, E.; Kurtev, M.; Guarente, L. Mouse Sir2 Homolog SIRT6 Is a Nuclear ADP-ribosyltransferase, *J. Biol. Chem.* **2005**, *280*, pp. 21313–21320.

(85) Blank, M. F.; Grummt, I. The seven faces of SIRT7, *Transcription.* **2017**, *8*, pp. 67–74.

(86) Canto, C.; Auwerx, J. Targeting Sirtuin 1 to Improve Metabolism: All You Need Is NAD+?, *Pharmacol. Rev.* **2011**, *64*, pp. 166–187.

(87) Finkel, T.; Deng, C.-X.; Mostoslavsky, R. Recent progress in the biology and physiology of sirtuins, *Nature.* **2009**, *460*, pp. 587–591.

(88) Gertler, A. A.; Cohen, H. Y. SIRT6, a protein with many faces, *Biogerontology.* **2013**, *14*, pp. 629–639.

(89) Barber, M. F.; Michishita-Kioi, E.; Xi, Y.; Tasselli, L., et al. SIRT7 links H3K18 deacetylation to maintenance of oncogenic transformation, *Nature.* **2012**, *487*, pp. 114–118.

(90) Sauve, A. A. Sirtuin chemical mechanisms, *Biochim. Biophys. Acta.* **2010**, *1804*, pp. 1591–1603.

(91) Hirsch, B. M.; Zheng, W. Sirtuin mechanism and inhibition: explored with Nε-acetyl-lysine analogs, *Mol. BioSyst.* **2011**, *7*, pp. 16–28.

(92) Kebede, A. F.; Nieborak, A.; Shahidian, L. Z.; Le Gras, S., et al. Histone propionylation is a mark of active chromatin, *Nat. Struct. Mol. Biol.* **2017**, *24*, pp. 1048–1056.

(93) Sabari, B. R.; Tang, Z.; Huang, H.; Yong-Gonzalez, V., et al. Intracellular Crotonyl-CoA Stimulates Transcription through p300-Catalyzed Histone Crotonylation, *Mol. Cell.* **2015**, *58*, pp. 203–215.

(94) Flynn, E. M.; Huang, O. W.; Poy, F.; Oppikofer, M., et al. A Subset of Human Bromodomains Recognizes Butyryllysine and Crotonyllysine Histone Peptide Modifications, *Structure.* **2015**, *23*, pp. 1801–1814.

(95) Li, Y.; Sabari, B. R.; Panchenko, T.; Wen, H., et al. Molecular Coupling of Histone Crotonylation and Active Transcription by AF9 YEATS Domain, *Mol. Cell.* **2016**, *62*, pp. 181–193.

(96) Xiong, X.; Panchenko, T.; Yang, S.; Zhao, S., et al. Selective recognition of histone crotonylation by double PHD fingers of MOZ and DPF2, *Nat. Chem. Biol.* **2016**, *12*, pp. 1111–1118.

(97) Stram, A. R.; Payne, R. M. Post-translational modifications in mitochondria: protein signaling in the powerhouse, *Cell. Mol. Life Sci.* **2016**, *73*, pp. 4063–4073.

(98) Park, J.; Chen, Y.; Tishkoff, D. X.; Peng, C., et al. SIRT5-Mediated Lysine Desuccinylation Impacts Diverse Metabolic Pathways, *Mol. Cell.* **2013**, *50*, pp. 919–930.

(99) Nishida, Y.; Rardin, M. J.; Carrico, C.; He, W., et al. SIRT5 Regulates both Cytosolic and Mitochondrial Protein Malonylation with Glycolysis as a Major Target, *Mol. Cell.* **2015**, *59*, pp. 321–332.

(100) Hong, S. Y.; Ng, L. T.; Ng, L. F.; Inoue, T., et al. The Role of Mitochondrial Non-Enzymatic Protein Acylation in Ageing, *PLoS ONE.* **2016**, *11*, pp. e0168752.

(101) Ledl, F.; Schleicher, E. New Aspects of the Maillard Reaction in Foods and in the Human Body, *Angew. Chem. Int. Ed. Engl.* **1990**, *29*, pp. 565–594.

(102) Hellwig, M.; Henle, T. Baking, ageing, diabetes: a short history of the Maillard reaction, *Angew. Chem. Int. Ed.* **2014**, *53*, pp. 10316–10329.

(103) Heyns, K.; Noack, H. Die Umsetzung von D-Fructose mit L-Lysin und L-Arginin und deren Beziehung zu nichtenzymatischen Bräunungsreaktionen, *Chem. Ber.* **1962**, *95*, pp. 720–727.

(104) Voigt, M.; Glomb, M. A. Reactivity of 1-Deoxy-d-erythro-hexo-2,3-diulose: A Key Intermediate in the Maillard Chemistry of Hexoses, *J. Agric. Food Chem.* **2009**, *57*, pp. 4765–4770.

(105) Smuda, M.; Voigt, M.; Glomb, M. A. Degradation of 1-Deoxy-d-erythro-hexo-2,3-diulose in the Presence of Lysine Leads to Formation of Carboxylic Acid Amides, *J. Agric. Food Chem.* **2010**, *58*, pp. 6458–6464.

(106) Smuda, M.; Glomb, M. A. Maillard Degradation Pathways of Vitamin C, *Angew. Chem. Int. Ed.* **2013**, *52*, pp. 4887–4891.

(107) Davidek, T.; Robert, F.; Devaud, S.; Vera, F. A.; Blank, I. Sugar fragmentation in the Maillard reaction cascade: Formation of short-chain carboxylic acids by a new oxidative α-dicarbonyl cleavage pathway, *J. Agric. Food Chem.* **2006**, *54*, pp. 6677–6684.

(108) Rabbani, N.; Thornalley, P. J. Dicarbonyl stress in cell and tissue dysfunction contributing to ageing and disease, *Biochem. Biophys. Res. Commun.* **2015**, *458*, pp. 221–226.

(109) Onyango, A. N. Small reactive carbonyl compounds as tissue lipid oxidation products; and the mechanisms of their formation thereby, *Chem. Phys. Lipids.* **2012**, *165*, pp. 777–786.

(110) Anderson, M. M.; Hazen, S. L.; Hsu, F. F.; Heinecke, J. W. Human neutrophils employ the myeloperoxidase-hydrogen peroxide-chloride system to convert hydroxy-amino acids into glycolaldehyde, 2-hydroxypropanal, and acrolein. A mechanism for the generation of highly reactive alpha-hydroxy and alpha,beta-unsaturated aldehydes by phagocytes at sites of inflammation, *J. Clin. Invest.* **1997**, *99*, pp. 424–432.

(111) Henning, C.; Liehr, K.; Girndt, M.; Ulrich, C.; Glomb, M. A. Analysis and Chemistry of Novel Protein Oxidation Markers in Vivo, *J. Agric. Food Chem.* **2018**, *66*, pp. 4692–4701.

(112) Thornalley, P. J.; Langborg, A.; Minhas, H. S. Formation of glyoxal, methylglyoxal and 3-deoxyglucosone in the glycation of proteins by glucose, *Biochem. J.* **1999**, *344*, pp. 109–116.

(113) Smuda, M.; Glomb, M. A. Novel Insights into the Maillard Catalyzed Degradation of Maltose, *J. Agric. Food Chem.* **2011**, *59*, pp. 13254–13264.

(114) Manini, P.; La Pietra, P.; Panzella, L.; Napolitano, A.; d'Ischia, M. Glyoxal formation by Fenton-induced degradation of carbohydrates and related compounds, *Carbohydr. Res.* **2006**, *341*, pp. 1828–1833.

(115) Awada, M.; Dedon, P. C. Formation of the 1,N2-glyoxal adduct of deoxyguanosine by phosphoglycolaldehyde, a product of 3'-deoxyribose oxidation in DNA, *Chem. Res. Toxicol.* **2001**, *14*, pp. 1247–1253.

(116) Degen, J.; Hellwig, M.; Henle, T. 1,2-Dicarbonyl Compounds in Commonly Consumed Foods, *J. Agric. Food Chem.* **2012**, *60*, pp. 7071–7079.

(117) Phillips, S. A.; Thornalley, P. J. The formation of methylglyoxal from triose phosphates. Investigation using a specific assay for methylglyoxal, *Eur. J. Biochem.* **1993**, *212*, pp. 101–105.

(118) Beisswenger, B. G. K.; Delucia, E. M.; Lapoint, N.; Sanford, R. J.; Beisswenger, P. J. Ketosis Leads to Increased Methylglyoxal Production on the Atkins Diet, *Ann. N. Y. Acad. Sci.* **2005**, *1043*, pp. 201–210.

(119) Dhar, A.; Desai, K.; Kazachmov, M.; Yu, P.; Wu, L. Methylglyoxal production in vascular smooth muscle cells from different metabolic precursors, *Metabolism.* **2008**, *57*, pp. 1211–1220.

(120) Glomb, M. A.; Monnier, V. M. Mechanism of Protein Modification by Glyoxal and Glycolaldehyde, Reactive Intermediates of the Maillard Reaction, *J. Biol. Chem.* **1995**, *270*, pp. 10017–10026.

(121) Jost, T.; Zipprich, A.; Glomb, M. A. Analysis of Advanced Glycation Endproducts in Rat Tail Collagen and Correlation to Tendon Stiffening, *J. Agric. Food Chem.* **2018**, *66*, pp. 3957–3965.

(122) Baldensperger, T.; Jost, T.; Zipprich, A.; Glomb, M. A. Novel α-Oxoamide Advanced-Glycation Endproducts within the N6-Carboxymethyl Lysine and N6-Carboxyethyl Lysine Reaction Cascades, *J. Agric. Food Chem.* **2018**, *66*, pp. 1898–1906.

(123) Glomb, M. A.; Pfahler, C. Amides Are Novel Protein Modifications Formed by Physiological Sugars, *J. Biol. Chem.* **2001**, *276*, pp. 41638–41647.

(124) Szwergold, B. S.; Howell, S.; Beisswenger, P. J. Human Fructosamine-3-Kinase: Purification, Sequencing, Substrate Specificity, and Evidence of Activity In Vivo, *Diabetes.* **2001**, *50*, pp. 2139–2147.

(125) Rabbani, N.; Xue, M.; Thornalley, P. J. Dicarbonyls and glyoxalase in disease mechanisms and clinical therapeutics, *Glycoconj. J.* **2016**, *33*, pp. 513–525.

(126) Himo, F.; Siegbahn, Per E. M. Catalytic Mechanism of Glyoxalase I: A Theoretical Study, *J. Am. Chem. Soc.* **2001**, *123*, pp. 10280–10289.

(127) Rabbani, N.; Thornalley, P. J. Dicarbonyls (glyoxal, methylglyoxal, and 3-deoxyglucosone), *Uremic Toxins.* **2012,** pp. 177–192.

(128) Baba, S. P.; Barski, O. A.; Ahmed, Y.; O'Toole, T. E., et al. Reductive Metabolism of AGE Precursors: A Metabolic Route for Preventing AGE Accumulation in Cardiovascular Tissue, *Diabetes.* **2009**, *58*, pp. 2486–2497.

(129) Feather, M. S.; Flynn, T. G.; Munro, K. A.; Kubiseski, T. J.; Walton, D. J. Catalysis of reduction of carbohydrate 2-oxoaldehydes (osones) by mammalian aldose reductase and aldehyde reductase, *Biochim. Biophys. Acta.* **1995**, *1244*, pp. 10–16.

(130) Vander Jagt, D. L.; Hunsaker, L. A. Methylglyoxal metabolism and diabetic complications: roles of aldose reductase, glyoxalase-I, betaine aldehyde dehydrogenase and 2-oxoaldehyde dehydrogenase, *Chem.-Biol. Interact.* **2003**, *143-144*, pp. 341–351.

(131) Izaguirre, G.; Kikonyogo, A.; Pietruszko, R. Methylglyoxal as substrate and inhibitor of human aldehyde dehydrogenase: comparison of kinetic properties among the three isozymes, *Comp. Biochem. Physiol. B.* **1998**, *119*, pp. 747–754.

(132) Collard, F.; Vertommen, D.; Fortpied, J.; Duester, G.; van Schaftingen, E. Identification of 3-deoxyglucosone dehydrogenase as aldehyde dehydrogenase 1A1 (retinaldehyde dehydrogenase 1), *Biochimie.* **2007**, *89*, pp. 369–373.

(133) Lee, J.; Song, J.; Kwon, K.; Jang, S., et al. Human DJ-1 and its homologs are novel glyoxalases, *Hum. Mol. Genet.* **2012**, *21*, pp. 3215–3225.

(134) Choi, D.; Kim, J.; Ha, S.; Kwon, K., et al. Stereospecific mechanism of DJ-1 glyoxalases inferred from their hemithioacetal-containing crystal structures, *FEBS J.* **2014**, *281*, pp. 5447–5462.

(135) Advedissian, T.; Deshayes, F.; Poirier, F.; Viguier, M.; Richarme, G. The Parkinsonism-associated protein DJ-1/Park7 prevents glycation damage in human keratinocyte, *Biochem. Biophys. Res. Commun.* **2016**, *473*, pp. 87–91.

(136) Richarme, G.; Dairou, J. Parkinsonism-associated protein DJ-1 is a bona fide deglycase, *Biochem. Biophys. Res. Commun.* **2017**, *483*, pp. 387–391.

(137) Richarme, G.; Mihoub, M.; Dairou, J.; Bui, L. C., et al. Parkinsonism-associated Protein DJ-1/Park7 Is a Major Protein Deglycase That Repairs Methylglyoxal- and Glyoxal-glycated Cysteine, Arginine, and Lysine Residues, *J. Biol. Chem.* **2015**, *290*, pp. 1885–1897.

(138) Zheng, Q.; Omans, N. D.; Leicher, R.; Osunsade, A., et al. Reversible histone glycation is associated with disease-related changes in chromatin architecture, *Nat. Commun.* **2019**, *10*, pp. 1289–1300.

(139) Rabbani, N.; Xue, M.; Thornalley, P. J. Activity, regulation, copy number and function in the glyoxalase system, *Biochem. Soc. Trans.* **2014**, *42*, pp. 419–424.

(140) Pfaff, D. H.; Fleming, T.; Nawroth, P.; Teleman, A. A. Evidence Against a Role for the Parkinsonism-associated Protein DJ-1 in Methylglyoxal Detoxification, *J. Biol. Chem.* **2017**, *292*, pp. 685–690.

(141) Pergola, P. E.; Raskin, P.; Toto, R. D.; Meyer, C. J., et al. Bardoxolone methyl and kidney function in CKD with type 2 diabetes, *N. Engl. J. Med.* **2011**, *365*, pp. 327–336.

(142) Zeeuw, D. de; Akizawa, T.; Audhya, P.; Bakris, G. L., et al. Bardoxolone Methyl in Type 2 Diabetes and Stage 4 Chronic Kidney Disease, *N. Engl. J. Med.* **2013**, *369*, pp. 2492–2503.

(143) Xue, M.; Weickert, M. O.; Qureshi, S.; Kandala, N.-B., et al. Improved Glycemic Control and Vascular Function in Overweight and Obese Subjects by Glyoxalase 1 Inducer Formulation, *Diabetes.* **2016**, *65*, pp. 2282–2294.

(144) Babaei-Jadidi, R.; Karachalias, N.; Ahmed, N.; Battah, S.; Thornalley, P. J. Prevention of incipient diabetic nephropathy by high-dose thiamine and benfotiamine, *Diabetes.* **2003**, *52*, pp. 2110–2120.

(145) Klaus, A.; Baldensperger, T.; Fiedler, R.; Girndt, M.; Glomb, M. A. Influence of Transketolase-Catalyzed Reactions on the Formation of Glycolaldehyde and Glyoxal

Specific Posttranslational Modifications under Physiological Conditions, *J. Agric. Food Chem.* **2018**, *66*, pp. 1498–1508.

(146) Thornalley, P. J.; Yurek-George, A.; Argirov, O. K. Kinetics and mechanism of the reaction of aminoguanidine with the α-oxoaldehydes glyoxal, methylglyoxal, and 3-deoxyglucosone under physiological conditions, *Biochem. Pharmacol.* **2000**, *60*, pp. 55–65.

(147) Thornalley, P. J. Use of aminoguanidine (Pimagedine) to prevent the formation of advanced glycation endproducts, *Arch. Biochem. Biophys.* **2003**, *419*, pp. 31–40.

(148) Vidal, N.; Cavaille, J. P.; Graziani, F.; Robin, M., et al. High throughput assay for evaluation of reactive carbonyl scavenging capacity, *Redox Biol.* **2014**, *2*, pp. 590–598.

(149) Mehta, R.; Wong, L.; O'Brien, P. J. Cytoprotective mechanisms of carbonyl scavenging drugs in isolated rat hepatocytes, *Chem.-Biol. Interact.* **2009**, *178*, pp. 317–323.

(150) Wondrak, G. T.; Cervantes-Laurean, D.; Roberts, M. J.; Qasem, J. G., et al. Identification of α-dicarbonyl scavengers for cellular protection against carbonyl stress, *Biochem. Pharmacol.* **2002**, *63*, pp. 361–373.

(151) Sell, D. R.; Monnier, V. M. Molecular basis of arterial stiffening: role of glycation–a mini-review, *Gerontology.* **2012**, *58*, pp. 227–237.

(152) Li, S.; Liu, S.; Ho, C.-T. Safety issues of methylglyoxal and potential scavengers, *Front. Agr. Sci. Eng.* **2018**, *5*, pp. 312–320.

(153) Wu, C.; Yen, G. Inhibitory Effect of Naturally Occurring Flavonoids on the Formation of Advanced Glycation Endproducts, *J. Agric. Food Chem.* **2005**, *53*, pp. 3167–3173.

(154) Sang, S.; Shao, X.; Bai, N.; Lo, C.-Y., et al. Tea Polyphenol (−)-Epigallocatechin-3-Gallate: A New Trapping Agent of Reactive Dicarbonyl Species, *Chem. Res. Toxicol.* **2007**, *20*, pp. 1862–1870.

(155) Lv, L.; Shao, X.; Chen, H.; Ho, C.-T.; Sang, S. Genistein Inhibits Advanced Glycation End Product Formation by Trapping Methylglyoxal, *Chem. Res. Toxicol.* **2011**, *24*, pp. 579–586.

(156) Wang, P.; Chen, H.; Sang, S. Trapping Methylglyoxal by Genistein and Its Metabolites in Mice, *Chem. Res. Toxicol.* **2016**, *29*, pp. 406–414.

(157) Simm, A.; Wagner, J.; Gursinsky, T.; Nass, N., et al. Advanced glycation endproducts: A biomarker for age as an outcome predictor after cardiac surgery?, *Exp. Gerontol.* **2007**, *42*, pp. 668–675.

(158) Cerami, A. Hypothesis: glucose as a mediator of aging, *J. Am. Geriatr. Soc.* **1985**, *33*, pp. 626–634.

(159) Smuda, M.; Henning, C.; Raghavan, C. T.; Johar, K., et al. Comprehensive Analysis of Maillard Protein Modifications in Human Lenses: Effect of Age and Cataract, *Biochemistry.* **2015**, *54*, pp. 2500–2507.

(160) Verzijl, N.; DeGroot, J.; Zaken, C. B.; Braun-Benjamin, O., et al. Crosslinking by advanced glycation end products increases the stiffness of the collagen network in human articular cartilage: a possible mechanism through which age is a risk factor for osteoarthritis, *Arthritis Rheumatol.* **2002**, *46*, pp. 114–123.

(161) Monnier, V. M.; Cerami, A. Nonenzymatic browning in vivo: possible process for aging of long-lived proteins, *Science.* **1981**, *211*, pp. 491–493.

(162) Nagaraj, R. H.; Sell, D. R.; Prabhakaram, M.; Ortwerth, B. J.; Monnier, V. M. High correlation between pentosidine protein crosslinks and pigmentation implicates ascorbate oxidation in human lens senescence and cataractogenesis, *Proc. Natl. Acad. Sci.* **1991**, *88*, pp. 10257–10261.

(163) López-Otín, C.; Blasco, M. A.; Partridge, L.; Serrano, M.; Kroemer, G. The Hallmarks of Aging, *Cell.* **2013**, *153*, pp. 1194–1217.

(164) Bento, C. F.; Marques, F.; Fernandes, R.; Pereira, P.; Cotterill, S. Methylglyoxal Alters the Function and Stability of Critical Components of the Protein Quality Control, *PLoS ONE.* **2010**, *5*, pp. e13007.

(165) Sun, F.; Suttapitugsakul, S.; Xiao, H.; Wu, R. Comprehensive Analysis of Protein Glycation Reveals Its Potential Impacts on Protein Degradation and Gene Expression in Human Cells, *J. Am. Soc. Mass Spectrom.* **2019**.

(166) Iannuzzi, C.; Irace, G.; Sirangelo, I. Differential effects of glycation on protein aggregation and amyloid formation, *Front. Mol. Biosci.* **2014**, *1*, pp. 623–630.

(167) Tsakiri, E. N.; Iliaki, K. K.; Höhn, A.; Grimm, S., et al. Diet-derived advanced glycation end products or lipofuscin disrupts proteostasis and reduces life span in Drosophila melanogaster, *Free Radic. Biol. Med.* **2013**, *65*, pp. 1155–1163.

(168) Gugliucci, A. Advanced glycation of rat liver histone octamers: an in vitro study, *Biochem. Biophys. Res. Commun.* **1994**, *203*, pp. 588–593.

(169) Ashraf, J. M.; Rabbani, G.; Ahmad, S.; Hasan, Q., et al. Glycation of H1 Histone by 3-Deoxyglucosone: Effects on Protein Structure and Generation of Different Advanced Glycation End Products, *PLoS ONE.* **2015**, *10,* pp. e0130630.

(170) Zhang, L.; Yu, C.; Vasquez, F. E.; Galeva, N., et al. Hyperglycemia Alters the Schwann Cell Mitochondrial Proteome and Decreases Coupled Respiration in the Absence of Superoxide Production, *J. Proteome Res.* **2010**, *9,* pp. 458–471.

(171) Wang, H.; Liu, J.; Wu, L. Methylglyoxal-induced mitochondrial dysfunction in vascular smooth muscle cells, *Biochem. Pharmacol.* **2009**, *77,* pp. 1709–1716.

(172) Hamelin, M.; Mary, J.; Vostry, M.; Friguet, B.; Bakala, H. Glycation damage targets glutamate dehydrogenase in the rat liver mitochondrial matrix during aging, *FEBS J.* **2007**, *274,* pp. 5949–5961.

(173) Rosca, M. G.; Mustata, T. G.; Kinter, M. T.; Ozdemir, A. M., et al. Glycation of mitochondrial proteins from diabetic rat kidney is associated with excess superoxide formation, *Am. J. Physiol.* **2005**, *289,* pp. F420.

(174) McCord, J. M.; Roy, R. S. The pathophysiology of superoxide: roles in inflammation and ischemia, *Can. J. Physiol. Pharmacol.* **1982**, *60,* pp. 1346–1352.

(175) Kislinger, T.; Fu, C.; Huber, B.; Qu, W., et al. Nε-(carboxymethyl) lysine adducts of proteins are ligands for receptor for advanced glycation end products that activate cell signaling pathways and modulate gene expression, *J. Biol. Chem.* **1999**, *274,* pp. 31740–31749.

(176) Vlassara, H.; Brownlee, M.; Cerami, A. High-affinity-receptor-mediated uptake and degradation of glucose-modified proteins: a potential mechanism for the removal of senescent macromolecules, *Proc. Natl. Acad. Sci.* **1985**, *82,* pp. 5588–5592.

(177) Schmidt, A. M.; Vianna, M.; Gerlach, M.; Brett, J., et al. Isolation and characterization of two binding proteins for advanced glycosylation end products from bovine lung which are present on the endothelial cell surface, *J. Biol. Chem.* **1992**, *267,* pp. 14987–14997.

(178) Bierhaus, A.; Humpert, P. M.; Morcos, M.; Wendt, T., et al. Understanding RAGE, the receptor for advanced glycation end products, *J. Mol. Med.* **2005**, *83,* pp. 876–886.

(179) Kalea, A. Z.; Schmidt, A. M.; Hudson, B. I. RAGE: a novel biological and genetic marker for vascular disease, *Clin. Sci.* **2009**, *116,* pp. 621–637.

(180) Koenig, R. J.; Peterson, C. M.; Jones, R. L.; Saudek, C., et al. Correlation of Glucose Regulation and Hemoglobin A Ic in Diabetes Mellitus, *N. Engl. J. Med.* **1976**, *295*, pp. 417–420.

(181) Scheijen, J. L.; Schalkwijk, C. G. Quantification of glyoxal, methylglyoxal and 3-deoxyglucosone in blood and plasma by ultra performance liquid chromatography tandem mass spectrometry: evaluation of blood specimen, *Clin. Chem. Lab. Med.* **2014**, *52*, pp. 85–91.

(182) Ahmed, N.; Thornalley, P. J. Advanced glycation endproducts: what is their relevance to diabetic complications?, *Diabetes Obes. Metab.* **2007**, *9*, pp. 233–245.

(183) Lopes-Virella, M. F.; Klein, R. L.; Lyons, T. J.; Stevenson, H. C.; Witztum, J. L. Glycosylation of low-density lipoprotein enhances cholesteryl ester synthesis in human monocyte-derived macrophages, *Diabetes.* **1988**, *37*, pp. 550–557.

(184) Duell, P. B.; Oram, J. F.; Bierman, E. L. Nonenzymatic Glycosylation of HDL and Impaired HDL-Receptor–Mediated Cholesterol Efflux, *Diabetes.* **1991**, *40*, pp. 377–384.

(185) Kesava Reddy, G. AGE-related cross-linking of collagen is associated with aortic wall matrix stiffness in the pathogenesis of drug-induced diabetes in rats, *Microvasc. Res.* **2004**, *68*, pp. 132–142.

(186) Wendt, T.; Harja, E.; Bucciarelli, L.; Qu, W., et al. RAGE modulates vascular inflammation and atherosclerosis in a murine model of type 2 diabetes, *Atherosclerosis.* **2006**, *185*, pp. 70–77.

(187) Vlassara, H.; Brownlee, M.; Cerami, A. Recognition and uptake of human diabetic peripheral nerve myelin by macrophages, *Diabetes.* **1985**, *34*, pp. 553–557.

(188) Brownlee, M.; Vlassara, H.; Cerami, A. Trapped immunoglobulins on peripheral nerve myelin from patients with diabetes mellitus, *Diabetes.* **1986**, *35*, pp. 999–1003.

(189) Sugiyama, S.; Miyata, T.; Horie, K.; Iida, Y., et al. Advanced glycation end-products in diabetic nephropathy, *Nephrol. Dial. Transplant.* **1996**, *11*, pp. 91–94.

(190) Monnier, V. M.; Sell, D. R.; Nagaraj, R. H.; Miyata, S., et al. Maillard Reaction-Mediated Molecular Damage to Extracellular Matrix and Other Tissue Proteins in Diabetes, Aging, and Uremia, *Diabetes.* **1992**, *41*, pp. 36–41.

(191) Rabbani, N.; Thornalley, P. J. Advanced glycation end products in the pathogenesis of chronic kidney disease, *Kidney Int.* **2018**, *93*, pp. 803–813.

(192) Stopper, H.; Schinzel, R.; Sebekova, K.; Heidland, A. Genotoxicity of advanced glycation end products in mammalian cells, *Cancer Lett.* **2003**, *190*, pp. 151–156.

(193) Schröter, D.; Höhn, A. Role of Advanced Glycation End Products in Carcinogenesis and their Therapeutic Implications, *Curr. Pharm. Des.* **2019**, *24*, pp. 5245–5251.

(194) Sharaf, H.; Matou-Nasri, S.; Wang, Q.; Rabhan, Z., et al. Advanced glycation endproducts increase proliferation, migration and invasion of the breast cancer cell line MDA-MB-231, *Biochim. Biophys. Acta.* **2015**, *1852*, pp. 429–441.

(195) Rodriguez-Teja, M.; Gronau, J. H.; Breit, C.; Zhang, Y. Z., et al. AGE-modified basement membrane cooperates with Endo180 to promote epithelial cell invasiveness and decrease prostate cancer survival, *J. Pathol.* **2015**, *235*, pp. 581–592.

(196) Vicente Miranda, H.; El-Agnaf, Omar M. A.; Outeiro, T. F. Glycation in Parkinson's disease and Alzheimer's disease, *Mov. Disord.* **2016**, *31*, pp. 782–790.

(197) Carvalho, C.; Cardoso, S.; Correia, S. C.; Santos, R. X., et al. Metabolic Alterations Induced by Sucrose Intake and Alzheimer's Disease Promote Similar Brain Mitochondrial Abnormalities, *Diabetes.* **2012**, *61*, pp. 1234–1242.

(198) Craft, S. Intranasal Insulin Therapy for Alzheimer Disease and Amnestic Mild Cognitive Impairment, *Arch. Neurol.* **2012**, *69*, p. 29.

(199) Ko, S.-Y.; Lin, Y.-P.; Lin, Y.-S.; Chang, S.-S. Advanced glycation end products enhance amyloid precursor protein expression by inducing reactive oxygen species, *Free Radic. Biol. Med.* **2010**, *49*, pp. 474–480.

(200) Vitek, M. P.; Bhattacharya, K.; Glendening, J. M.; Stopa, E., et al. Advanced glycation end products contribute to amyloidosis in Alzheimer disease, *Proc. Natl. Acad. Sci.* **1994**, *91*, pp. 4766–4770.

(201) Li, X.-H.; Du, L.-L.; Cheng, X.-S.; Jiang, X., et al. Glycation exacerbates the neuronal toxicity of β-amyloid, *Cell Death Dis.* **2013**, *4*, pp. e673.

(202) Henning, C.; Liehr, K.; Girndt, M.; Ulrich, C.; Glomb, M. A. Extending the Spectrum of α-Dicarbonyl Compounds in Vivo, *J. Biol. Chem.* **2014**, *289*, pp. 28676–28688.

(203) Borch-Johnsen, K.; Neil, A.; Balkau, B.; Larsen, S., et al. Glucose tolerance and cardiovascular mortality-Comparison of fasting and 2-hour diagnostic criteria, *Arch. Intern. Med.* **2001**, *161*, pp. 397–405.

(204) Thorpe, S. R.; Baynes, J. W. CML: a brief history, *Int. Congr. Ser.* **2002**, *1245*, pp. 91–99.

(205) Ahmed, M. U.; Frye, E. B.; Degenhardt, T. P.; Thorpe, S. R.; Baynes, J. W. Nε -(Carboxyethyl)lysine, a product of the chemical modification of proteins by methylglyoxal, increases with age in human lens proteins, *Biochem. J.* **1997**, *324*, pp. 565–570.

(206) Henning, C.; Smuda, M.; Girndt, M.; Ulrich, C.; Glomb, M. A. Molecular Basis of Maillard Amide-Advanced Glycation End Product (AGE) Formation in Vivo, *J. Biol. Chem.* **2011**, *286*, pp. 44350–44356.

(207) Hofmann, T.; Münch, P.; Schieberle, P. Quantitative Model Studies on the Formation of Aroma-Active Aldehydes and Acids by Strecker-Type Reactions, *J. Agric. Food Chem.* **2000**, *48*, pp. 434–440.

(208) Thornalley, P. J. Advanced Glycation End Products in Renal Failure, *J. Ren. Nutr.* **2006**, *16*, pp. 178–184.

(209) Svistounov, D.; Oteiza, A.; Zykova, S. N.; Sørensen, K. K., et al. Hepatic disposal of advanced glycation end products during maturation and aging, *Exp. Gerontol.* **2013**, *48*, pp. 549–556.

(210) Anderson, N. L.; Anderson, N. G. The Human Plasma Proteome, *Mol. Cell. Proteom.* **2002**, *1*, pp. 845–867.

(211) Smedsrod, B.; Melkko, J.; Araki, N.; Sano, H.; Horiuchi, S. Advanced glycation end products are eliminated by scavenger-receptor-mediated endocytosis in hepatic sinusoidal Kupffer and endothelial cells, *Biochem. J.* **1997**, *322*, pp. 567–573.

(212) Thornalley, P. J.; Battah, S.; Ahmed, N.; Karachalias, N., et al. Quantitative screening of advanced glycation endproducts in cellular and extracellular proteins by tandem mass spectrometry, *Biochem. J.* **2003**, *375*, pp. 581–592.

(213) Bakala, H.; Delaval, E.; Hamelin, M.; Bismuth, J., et al. Changes in rat liver mitochondria with aging, *Eur. J. Biochem.* **2003**, *270*, pp. 2295–2302.

(214) Schleicher, E. D.; Wagner, E.; Nerlich, A. G. Increased accumulation of the glycoxidation product N(epsilon)-(carboxymethyl)lysine in human tissues in diabetes and aging, *J. Clin. Invest.* **1997**, *99*, pp. 457–468.

(215) Zhou, W.-C. Pathogenesis of liver cirrhosis, *World J. Gastroenterol.* **2014**, *20*, pp. 7312–7324.

(216) Meng, X.; Nikolic-Paterson, D. J.; Lan, H. Y. TGF-β: the master regulator of fibrosis, *Nat. Rev. Nephrol.* **2016**, *12*, pp. 325–338.

(217) Fehrenbach, H. Up-regulated expression of the receptor for advanced glycation end products in cultured rat hepatic stellate cells during transdifferentiation to myofibroblasts, *Hepatology.* **2001**, *34*, pp. 943–952.

(218) Hyogo, H.; Yamagishi, S.-i. Advanced Glycation End Products (AGEs) and their Involvement in Liver Disease, *Curr. Pharm. Des.* **2008**, *14*, pp. 969–972.

(219) Šebeková, K.; Kupčová, V.; Schinzel, R.; Heidland, A. Markedly elevated levels of plasma advanced glycation end products in patients with liver cirrhosis – amelioration by liver transplantation, *J. Hepatol.* **2002**, *36*, pp. 66–71.

(220) Yagmur, E.; Tacke, F.; Weiss, C.; Lahme, B., et al. Elevation of Nε-(carboxymethyl)lysine-modified advanced glycation end products in chronic liver disease is an indicator of liver cirrhosis, *Clin. Biochem.* **2006**, *39*, pp. 39–45.

(221) Zipprich, A.; Loureiro-Silva, M. R.; Jain, D.; D'Silva, I.; Groszmann, R. J. Nitric oxide and vascular remodeling modulate hepatic arterial vascular resistance in the isolated perfused cirrhotic rat liver, *J. Hepatol.* **2008**, *49*, pp. 739–745.

(222) Moeller, M.; Thonig, A.; Pohl, S.; Ripoll, C., et al. Hepatic Arterial Vasodilation Is Independent of Portal Hypertension in Early Stages of Cirrhosis, *PLoS ONE.* **2015**, *10*, pp. e0121229.

(223) Dooley, S.; Dijke, P. ten TGF-β in progression of liver disease, *Cell Tissue Res.* **2012**, *347*, pp. 245–256.

(224) Carpino, G.; Morini, S.; Ginannicorradini, S.; Franchitto, A., et al. Alpha-SMA expression in hepatic stellate cells and quantitative analysis of hepatic fibrosis in cirrhosis and in recurrent chronic hepatitis after liver transplantation, *Dig. Liver Dis.* **2005**, *37*, pp. 349–356.

(225) Ahmed, N.; Thornalley, P. J.; Lüthen, R.; Häussinger, D., et al. Processing of protein glycation, oxidation and nitrosation adducts in the liver and the effect of cirrhosis, *J. Hepatol.* **2004**, *41*, pp. 913–919.

(226) Gracia-Sancho, J.; Laviña, B.; Rodríguez-Vilarrupla, A.; García-Calderó, H., et al. Increased oxidative stress in cirrhotic rat livers: A potential mechanism contributing to reduced nitric oxide bioavailability, *Hepatology.* **2008**, *47*, pp. 1248–1256.

(227) Kleff, S.; Andrulis, E. D.; Anderson, C. W.; Sternglanz, R. Identification of a gene encoding a yeast histone H4 acetyltransferase, *J. Biol. Chem.* **1995**, *270*, pp. 24674–24677.

(228) Paik, W. K.; Pearson, D.; Lee, H. W.; Kim, S. Nonenzymatic acetylation of histones with acetyl-CoA, *Biochim. Biophys. Acta.* **1970**, *213*, pp. 513–522.

(229) Zhao, Y.; Jensen, O. N. Modification-specific proteomics: Strategies for characterization of post-translational modifications using enrichment techniques, *Proteomics.* **2009**, *9*, pp. 4632–4641.

(230) Wiśniewski, J. R.; Zougman, A.; Mann, M. Nε-Formylation of lysine is a widespread post-translational modification of nuclear proteins occurring at residues involved in regulation of chromatin function, *Nucleic Acids Res.* **2008**, *36*, pp. 570–577.

(231) Baldensperger, T.; Di Sanzo, S.; Ori, A.; Glomb, M. A. Quantitation of Reactive Acyl-CoA Species Mediated Protein Acylation by HPLC–MS/MS, *Anal. Chem.* **2019**, *91*, pp. 12336–12343.

(232) Fountoulakis, M.; Lahm, H.-W. Hydrolysis and amino acid composition analysis of proteins, *J. Chromatogr. A.* **1998**, *826*, pp. 109–134.

(233) Narahashi, Y. Pronase, *Methods Enzymol.* **1970**, *19*, pp. 651–664.

(234) Delatour, T.; Fenaille, F.; Parisod, V.; Richoz, J., et al. A comparative study of proteolysis methods for the measurement of 3-nitrotyrosine residues: Enzymatic digestion versus hydrochloric acid-mediated hydrolysis, *J. Chromatogr. B.* **2007**, *851*, pp. 268–276.

(235) Tapias, A.; Wang, Z.-Q. Lysine Acetylation and Deacetylation in Brain Development and Neuropathies, *Genomics Proteomics Bioinformatics.* **2017**, *15*, pp. 19–36.

(236) Tyihák, E.; Trézl, L.; Kolonits, P. The isolation of Nϵ-formyl-l-lysine from the reaction between formaldehyde and l-lysine and its identification by OPLC and NMR spectroscopy, *J. Pharm. Biomed. Anal.* **1985**, *3*, pp. 343–349.

(237) Edrissi, B.; Taghizadeh, K.; Dedon, P. C.; Swenberg, J. Quantitative Analysis of Histone Modifications: Formaldehyde Is a Source of Pathological N6-Formyllysine That Is Refractory to Histone Deacetylases, *PLoS Genet.* **2013**, *9*, pp. e1003328.

(238) Edrissi, B.; Taghizadeh, K.; Moeller, B. C.; Kracko, D., et al. Dosimetry of N6 -Formyllysine Adducts Following [$^{13}C^{2}H2$]-Formaldehyde Exposures in Rats, *Chem. Res. Toxicol.* **2013**, *26*, pp. 1421–1423.

(239) Reingruber, H.; Pontel, L. B. Formaldehyde metabolism and its impact on human health, *Curr. Opin. Toxicol.* **2018**, *9*, pp. 28–34.

(240) Xiao, R.; He, R. Metabolism of Formaldehyde In Vivo. In *Formaldehyde and Cognition*, pp. 21–46.

(241) Edrissi, B.; Taghizadeh, K.; Moeller, B. C.; Yu, R., et al. N6 -Formyllysine as a Biomarker of Formaldehyde Exposure: Formation and Loss of N6 -Formyllysine in Nasal Epithelium in Long-Term, Low-Dose Inhalation Studies in Rats, *Chem. Res. Toxicol.* **2017**, *30*, pp. 1572–1576.

(242) Seidel, J.; Klockenbusch, C.; Schwarzer, D. Investigating Deformylase and Deacylase Activity of Mammalian and Bacterial Sirtuins, *ChemBioChem.* **2016**, *17*, pp. 398–402.

(243) Cheng, Z.; Tang, Y.; Chen, Y.; Kim, S., et al. Molecular Characterization of Propionyllysines in Non-histone Proteins, *Mol. Cell. Proteom.* **2009**, *8*, pp. 45–52.

(244) Smith, B. C.; Denu, J. M. Acetyl-lysine Analog Peptides as Mechanistic Probes of Protein Deacetylases, *J. Biol. Chem.* **2007**, *282*, pp. 37256–37265.

(245) Garrity, J.; Gardner, J. G.; Hawse, W.; Wolberger, C.; Escalante-Semerena, J. C. N -Lysine Propionylation Controls the Activity of Propionyl-CoA Synthetase, *J. Biol. Chem.* **2007**, *282*, pp. 30239–30245.

(246) Xu, G.; Wang, J.; Wu, Z.; Qian, L., et al. SAHA Regulates Histone Acetylation, Butyrylation, and Protein Expression in Neuroblastoma, *J. Proteome Res.* **2014**, *13*, pp. 4211–4219.

(247) Pougovkina, O.; te Brinke, H.; Wanders, Ronald J. A.; Houten, S. M.; de Boer, Vincent C. J. Aberrant protein acylation is a common observation in inborn errors of acyl-CoA metabolism, *J. Inherit. Metab. Dis.* **2014**, *37*, pp. 709–714.

(248) Wan, J.; Liu, H.; Chu, J.; Zhang, H. Functions and mechanisms of lysine crotonylation, *J. Cell. Mol. Med.* **2019**, *16*, pp. 258–264.

(249) Wan, J.; Liu, H.; Ming, L. Lysine crotonylation is involved in hepatocellular carcinoma progression, *Biomed. Pharmacother.* **2019**, *111*, pp. 976–982.

(250) Liu, S.; Yu, H.; Liu, Y.; Liu, X., et al. Chromodomain protein CDYL acts as a crotonyl-CoA hydratase to regulate histone crotonylation and spermatogenesis, *Mol. Cell.* **2017**, *67*, pp. 853–866.

(251) Fu, H.; Tian, C.-l.; Ye, X.; Sheng, X., et al. Dynamics of Telomere Rejuvenation during Chemical Induction to Pluripotent Stem Cells, *Stem Cell Rep.* **2018**, *11*, pp. 70–87.

(252) Smestad, J.; Erber, L.; Chen, Y.; Maher, L. J. Chromatin Succinylation Correlates with Active Gene Expression and Is Perturbed by Defective TCA Cycle Metabolism, *iScience.* **2018**, *2*, pp. 63–75.

(253) Weinert, B. T.; Schölz, C.; Wagner, S. A.; Iesmantavicius, V., et al. Lysine Succinylation Is a Frequently Occurring Modification in Prokaryotes and Eukaryotes and Extensively Overlaps with Acetylation, *Cell Rep.* **2013**, *4*, pp. 842–851.

(254) Ali, H. R.; Assiri, M. A.; Harris, P. S.; Michel, C. R., et al. Quantifying Competition among Mitochondrial Protein Acylation Events Induced by Ethanol Metabolism, *J. Proteome Res.* **2019**, *18*, pp. 1513–1531.

(255) Liu, C.; Liu, Y.; Chen, L.; Zhang, M., et al. Quantitative proteome and lysine succinylome analyses provide insights into metabolic regulation in breast cancer, *Breast Cancer.* **2019**, *26*, pp. 93–105.

(256) Wang, C.; Zhang, C.; Li, X.; Shen, J., et al. CPT1A-mediated succinylation of S100A10 increases human gastric cancer invasion, *J. Cell. Mol. Med.* **2019**, *23*, pp. 293–305.

(257) Nandi, S. K.; Rakete, S.; Nahomi, R. B.; Michel, C., et al. Succinylation Is a Gain-of-Function Modification in Human Lens αB-Crystallin, *Biochemistry.* **2019**, *58*, pp. 1260–1274.

(258) Galván-Peña, S.; Carroll, R. G.; Newman, C.; Hinchy, E. C., et al. Malonylation of GAPDH is an inflammatory signal in macrophages, *Nature Commun.* **2019**, *10*, pp. 338–348.

(259) Bowman, C. E.; Rodriguez, S.; Selen Alpergin, Ebru S.; Acoba, M. G., et al. The Mammalian Malonyl-CoA Synthetase ACSF3 Is Required for Mitochondrial Protein Malonylation and Metabolic Efficiency, *Cell Chem. Biol.* **2017**, *24*, pp. 673–684.e4.

(260) Liu, K.; Li, F.; Sun, Q.; Lin, N., et al. p53 β-hydroxybutyrylation attenuates p53 activity, *Cell Death Dis.* **2019**, *10*, p. 243.

(261) Zhang, X.; Cao, R.; Niu, J.; Yang, S., et al. Molecular basis for hierarchical histone de-β-hydroxybutyrylation by SIRT3, *Cell Discov.* **2019**, *5*, p. 15.

(262) Ruan, H.-B.; Crawford, P. A. Ketone bodies as epigenetic modifiers, *Curr. Opin. Clin. Nutr. Metab. Care.* **2018**, *21*, pp. 260–266.

(263) Roe, C. R.; Cederbaum, S. D.; Roe, D. S.; Mardach, R., et al. Isolated isobutyryl-CoA dehydrogenase deficiency: an unrecognized defect in human valine metabolism, *Mol. Genet. Metab.* **1998**, *65*, pp. 264–271.

(264) Abrankó, L.; Williamson, G.; Gardner, S.; Kerimi, A. Comprehensive quantitative analysis of fatty-acyl-Coenzyme A species in biological samples by ultra-high performance liquid chromatography–tandem mass spectrometry harmonizing hydrophilic interaction and reversed phase chromatography, *J. Chromatogr. A.* **2018**, *1534*, pp. 111–122.

(265) King, M.; Reiss, P. D. Separation and measurement of short-chain coenzyme-A compounds in rat liver by reversed-phase high-performance liquid chromatography, *Anal. Biochem.* **1985**, *146*, pp. 173–179.

(266) Hosokawa, Y.; Shimomura, Y.; Harris, R. A.; Ozawa, T. Determination of short-chain acyl-coenzyme A esters by high-performance liquid chromatography, *Anal. Biochem.* **1986**, *153*, pp. 45–49.

(267) Gauthier, N.; Wu, J. W.; Wang, S. P.; Allard, P., et al. A liver-specific defect of Acyl-CoA degradation produces hyperammonemia, hypoglycemia and a distinct hepatic Acyl-CoA pattern, *PLoS ONE.* **2013**, *8*, pp. e60581.

(268) Shibata, K.; Nakai, T.; Fukuwatari, T. Simultaneous high-performance liquid chromatography determination of coenzyme A, dephospho-coenzyme A, and acetyl-coenzyme A in normal and pantothenic acid-deficient rats, *Anal. Biochem.* **2012**, *430*, pp. 151–155.

(269) Demoz, A.; Garras, A.; Asiedu, D. K.; Netteland, B.; Berge, R. K. Rapid method for the separation and detection of tissue short-chain coenzyme A esters by reversed-phase high-performance liquid chromatography, *J. Chromatogr. B.* **1995**, *667*, pp. 148–152.

(270) Gao, L.; Chiou, W.; Tang, H.; Cheng, X., et al. Simultaneous quantification of malonyl-CoA and several other short-chain acyl-CoAs in animal tissues by ion-pairing reversed-phase HPLC/MS, *J. Chromatogr. B.* **2007**, *853*, pp. 303–313.

(271) Deutsch, J.; Rapoport, S. I.; Rosenberger, T. A. Coenzyme A and short-chain acyl-CoA species in control and ischemic rat brain, *Neurochem. Res.* **2002**, *27*, pp. 1577–1582.

(272) Tamvakopoulos, C. S.; Anderson, V. E. Detection of acyl-coenzyme a thioester intermediates of fatty acid β-oxidation as the N-acylglycines by negative-ion chemical ionization gas chromatography—Mass spectrometry, *Anal. Biochem.* **1992**, *200*, pp. 381–387.

(273) Nie, L.; Shuai, L.; Zhu, M.; Liu, P., et al. The Landscape of Histone Modifications in a High-Fat Diet-Induced Obese (DIO) Mouse Model, *Mol. Cell. Proteom.* **2017**, *16*, pp. 1324–1334.

(274) Pogo, A. O.; Allfrey, V. G.; Mirsky, A. E. Evidence for increased DNA template activity in regenerating liver nuclei, *Proc. Natl. Acad. Sci.* **1966**, *56*, pp. 550–557.

(275) Frezza, C.; Cipolat, S.; Scorrano, L. Organelle isolation: functional mitochondria from mouse liver, muscle and cultured filroblasts, *Nat. Protoc.* **2007**, *2*, pp. 287–295.

(276) Baldensperger, T.; Eggen, M.; Kappen, J.; Winterhalter, P. R.; Pfirrmann, T.; Glomb, M. A. Comprehensive analysis of posttranslational protein modifications in aging of subcellular compartments, *Sci. Rep.* **2020**, *10*, p. 7596.

(277) Piha, R. S.; Cuénod, M.; Waelsch, H. Metabolism of histones of brain and liver, *J. Biol. Chem.* **1966**, *241*, pp. 2397–2404.

(278) Kaschnitz, R. M.; Hatefi, Y.; Morris, H. P. Oxidative phosphorylation properties of mitochondria isolated from transplanted hepatoma, *Biochim. Biophys. Acta.* **1976**, *449*, pp. 224–235.

(279) Schneider, W. C.; Hogeboom, G. H. Intracellular distribution of enzymes, *J. Biol. Chem.* **1950**, *183*, p. 9.

(280) Dimauro, I.; Pearson, T.; Caporossi, D.; Jackson, M. J. A simple protocol for the subcellular fractionation of skeletal muscle cells and tissue, *BMC Res. Notes.* **2012**, *5*, pp. 513–517.

(281) Baeza, J.; Smallegan, M. J.; Denu, J. M. Mechanisms and Dynamics of Protein Acetylation in Mitochondria, *Trends Biochem. Sci.* **2016**, *41*, pp. 231–244.

(282) Weinert, B. T.; Moustafa, T.; Iesmantavicius, V.; Zechner, R.; Choudhary, C. Analysis of acetylation stoichiometry suggests that SIRT 3 repairs nonenzymatic acetylation lesions, *EMBO J.* **2015**, *34*, pp. 2620–2632.

(283) Zheng, Y.; Thomas, P. M.; Kelleher, N. L. Measurement of acetylation turnover at distinct lysines in human histones identifies long-lived acetylation sites, *Nat. Commun.* **2013**, *4*, pp. 436–443.

(284) Peleg, S.; Feller, C.; Ladurner, A. G.; Imhof, A. The Metabolic Impact on Histone Acetylation and Transcription in Ageing, *Trends Biochem. Sci.* **2016**, *41*, pp. 700–711.

(285) Cefalu, W. T.; Bell-Farrow, A.; Wang, Z. Q.; Ralapati, S. Determination of furosine in biomedical samples employing an improved hydrolysis and high-performance liquid chromatographic technique, *Carbohydr. Res.* **1991**, *215*, pp. 117–125.

(286) Lambert, A. J.; Portero-Otin, M.; Pamplona, R.; Merry, B. J. Effect of ageing and caloric restriction on specific markers of protein oxidative damage and membrane peroxidizability in rat liver mitochondria, *Mech. Ageing Dev.* **2004**, *125*, pp. 529–538.

(287) Leeuwenburgh, C.; Hansen, P. A.; Holloszy, J. O.; Heinecke, J. W. Oxidized amino acids in the urine of aging rats: potential markers for assessing oxidative stress in vivo, *Am. J. Physiol. Regul. Integr. Comp. Physiol.* **1999**, *276*, pp. R128–R135.

(288) Ahmed, N.; Thornalley, P. J. Quantitative screening of protein biomarkers of early glycation, advanced glycation, oxidation and nitrosation in cellular and extracellular proteins by tandem mass spectrometry multiple reaction monitoring, *Biochem. Soc. Trans.* **2003**, *31*, pp. 1417–1422.

(289) Vogt, W. Oxidation of methionyl residues in proteins: Tools, targets, and reversal, *Free Radic. Biol. Med.* **1995**, *18*, pp. 93–105.

(290) Moskovitz, J. Methionine sulfoxide reductases: ubiquitous enzymes involved in antioxidant defense, protein regulation, and prevention of aging-associated diseases, *Biochim. Biophys. Acta.* **2005**, *1703*, pp. 213–219.

(291) Curis, E.; Nicolis, I.; Moinard, C.; Osowska, S., et al. Almost all about citrulline in mammals, *Amino Acids.* **2005**, *29*, pp. 177–205.

(292) Song, S.; Yu, Y. Progression on Citrullination of Proteins in Gastrointestinal Cancers, *Front. Oncol.* **2019**, *9*, p. 113.

(293) Anantharaju, A.; Feller, A.; Chedid, A. Aging Liver, *Gerontology.* **2002**, *48*, pp. 343–353.

(294) Commerford, S. L.; Carsten, A. L.; Cronkite, E. P. Histone turnover within nonproliferating cells, *Proc. Natl. Acad. Sci.* **1982**, *79*, pp. 1163–1165.

(295) Hopgood, M. F.; Ballard, F. J. The relative stability of liver cytosol enzymes incubated in vitro, *Biochem. J.* **1974**, *144*, pp. 371–376.

(296) Bota, D. A.; Davies, K. J. Protein degradation in mitochondria: implications for oxidative stress, aging and disease, *Mitochondrion.* **2001**, *1*, pp. 33–49.

(297) Pfeifer, U. Inhibition by insulin of the formation of autophagic vacuoles in rat liver. A morphometric approach to the kinetics of intracellular degradation by autophagy, *J. Cell Biol.* **1978**, *78*, pp. 152–167.

(298) Gong, H.; Pang, J.; Han, Y.; Dai, Y., et al. Age-dependent tissue expression patterns of Sirt1 in senescence-accelerated mice, *Mol. Med. Rep.* **2014**, *10*, pp. 3296–3302.

(299) Zhou, C.-C.; Yang, X.; Hua, X.; Liu, J., et al. Hepatic NAD + deficiency as a therapeutic target for non-alcoholic fatty liver disease in ageing, *Br. J. Pharmacol.* **2016**, *173*, pp. 2352–2368.

(300) Murphy, M. P. How mitochondria produce reactive oxygen species, *Biochem. J.* **2009**, *417*, pp. 1–13.

(301) Merksamer, P. I.; Liu, Y.; He, W.; Hirschey, M. D., et al. The sirtuins, oxidative stress and aging: an emerging link, *Aging.* **2013**, *5*, pp. 144–150.

(302) Thornalley, P. J. Glyoxalase I – structure, function and a critical role in the enzymatic defence against glycation, *Biochem. Soc. Trans.* **2003**, *31*, pp. 1343–1348.

(303) Kawase, M.; Kondoh, C.; Matsumoto, S.; Teshigawara, M., et al. Contents of D-lactate and its related metabolites as well as enzyme activities in the liver, muscle and blood plasma of aging rats, *Mech. Ageing Dev.* **1995**, *84*, pp. 55–63.

(304) Höhn, A.; König, J.; Grune, T. Protein oxidation in aging and the removal of oxidized proteins, *J. Proteom.* **2013**, *92*, pp. 132–159.

(305) Abordo, E. A.; Minhas, H. S.; Thornalley, P. J. Accumulation of α-oxoaldehydes during oxidative stress: a role in cytotoxicity, *Biochem. Pharmacol.* **1999**, *58*, pp. 641–648.

(306) Yan, H.; Harding, J. J. Glycation-induced inactivation and loss of antigenicity of catalase and superoxide dismutase, *Biochem. J.* **1997**, *328*, pp. 599–605.

(307) Cai, W.; Ramdas, M.; Zhu, L.; Chen, X., et al. Oral advanced glycation endproducts (AGEs) promote insulin resistance and diabetes by depleting the antioxidant defenses AGE receptor-1 and sirtuin 1, *Proc. Natl. Acad. Sci.* **2012**, *109*, pp. 15888–15893.

(308) Ozden, O.; Park, S.-H.; Kim, H.-S.; Jiang, H., et al. Acetylation of MnSOD directs enzymatic activity responding to cellular nutrient status or oxidative stress, *Aging.* **2011**, *3*, pp. 102–107.

(309) James, A. M.; Hoogewijs, K.; Logan, A.; Hall, A. R., et al. Non-enzymatic N -acetylation of Lysine Residues by AcetylCoA Often Occurs via a Proximal S -acetylated Thiol Intermediate Sensitive to Glyoxalase II, *Cell Rep.* **2017**, *18*, pp. 2105–2112.

9 List of figures

Figure 1: Proposed reaction mechanisms for GNAT and MYST acetyltransferases 3

Figure 2: Proposed reaction mechanisms for p300/CBP acetyltransferases 3

Figure 3: Proposed reaction mechanism for Zn^{2+} dependent lysine deacetylases 4

Figure 4: Mechanism of non-enzymatic acylation 9

Figure 5: Mechanism of non-enzymatic acylation by succinyl-CoA 9

Figure 6: Proposed reaction mechanism for NAD^{+} dependent sirtuins 12

Figure 7: Initial phase of amine induced glucose degradation 14

Figure 8: Amine induced β-dicarbonyl cleavage of 1-deoxyglucosone 15

Figure 9: Amine induced oxidative α-dicarbonyl cleavage of 2,3-diketogulonic acid. 16

Figure 10: Isomerization cascades. 17

Figure 11: Mechanism of fructosamine-3-kinase 18

Figure 12: Detoxification of MGO by the glyoxalase system 18

Figure 13: Detoxification of MGO by aldo-keto reductases 19

Figure 14: Detoxification of MGO by aldehyde dehydrogenases 19

Figure 15: Scavenging of α-dicarbonyls by aminoguanidine 20

Figure 16: Scavenging of MGO by EGCG. 21

Figure 17: Equilibrium of GO (A) and MGO (B) hydration in aqueous solution 25

Figure 18: Mechanism of α-oxoamide AGE (A) and Strecker acid (B) formation 29

Figure 19: Stabilization of α-oxoamide AGEs by $NaBD_4$ reduction. 29

Figure 20: Lysine acylations by RACS quantitated in the present study 33

Figure 21: Connection between oxidative stress, dicarbonyl stress, and RACS stress. 46

10 List of tables

Table 1: Putative lysine acetyltransferases 2

Table 2: Zn^{2+} dependent lysine deacetylases. 4

Table 3: Bromodomain containing proteins 5

Table 4: Novel N^6-acyl lysine modifications. 7

Table 5: Reactive acyl-CoA species and their metabolic pathways. 8

Table 6: Potential acyltransferases 10

Table 7: NAD^+ dependent sirtuins 11

Table 8: Pathways of short-chain α-dicarbonyl formation 16

Table 9: Formation of AGEs in N^2-Boc-lysine incubations 26

Table 10: Effect of aeration and deaeration on formation of AGEs 27

Table 11: Effect of pH on formation of AGEs 28

Table 12: AGEs in cytosolic proteins from rat liver 30

Table 13: Markers of cirrhosis in rat liver 31

Table 14: Acylated lysine modifications in mouse organ lysates 34

Table 15: Additional acylated lysine modifications in enriched organ lysates 37

Table 16: Concentrations of acylation precursors reported in literature. 39

Table 17: Yield of protein extraction from liver. 40

Table 18: Protein acylation in subcellular compartments of mice liver 40

Table 19: Protein glycation in subcellular compartments of mice liver 42

Table 20: Protein oxidation in subcellular compartments of mice liver 43

Table 21: PTMs in aging of subcellular mouse liver compartments 45

11 Appendix

Supporting information

Quantitation of Reactive Acyl-CoA Species Mediated Protein Acylation by HPLC-MS/MS

Tim Baldensperger,[1] Simone Di Sanzo,[2] Alessandro Ori[2] and Marcus A. Glomb[1,] *

[1] Institute of Chemistry, Food Chemistry, Martin-Luther-University Halle-Wittenberg, Kurt-Mothes-Str. 2, 06120 Halle/Saale, Germany

[2] Leibniz Institute on Aging – Fritz Lipmann Institute (FLI), Beutenbergstraße 11, 07745 Jena, Germany

* To whom correspondence should be addressed (e-mail marcus.glomb@chemie.uni-halle.de, Fax ++049-345-5527341)

Contents:

1. Work-flow of analytical process
2. Structures of authentic reference standards
3. Synthesis routes of authentic reference standards

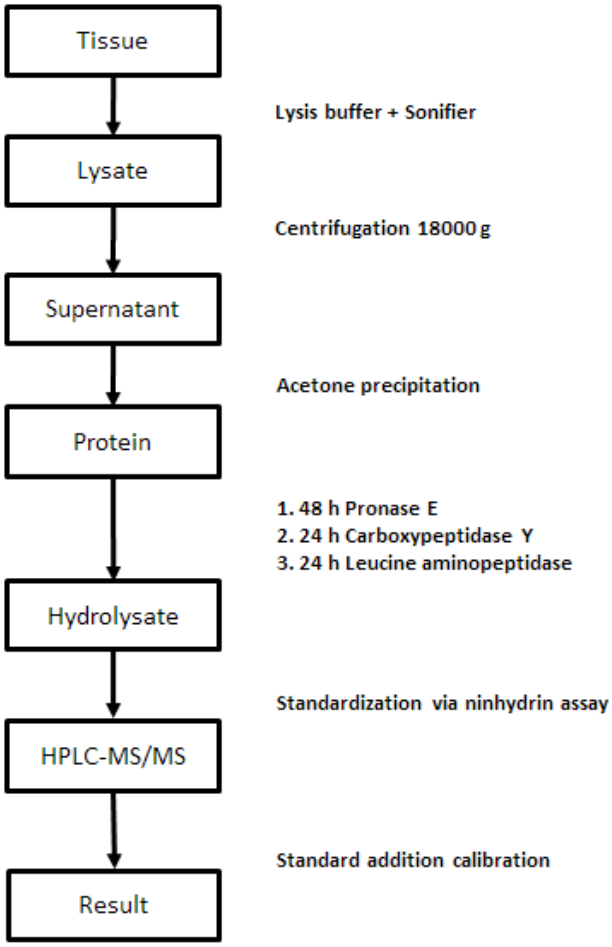

Figure S1. Work-flow of analytical process**.**

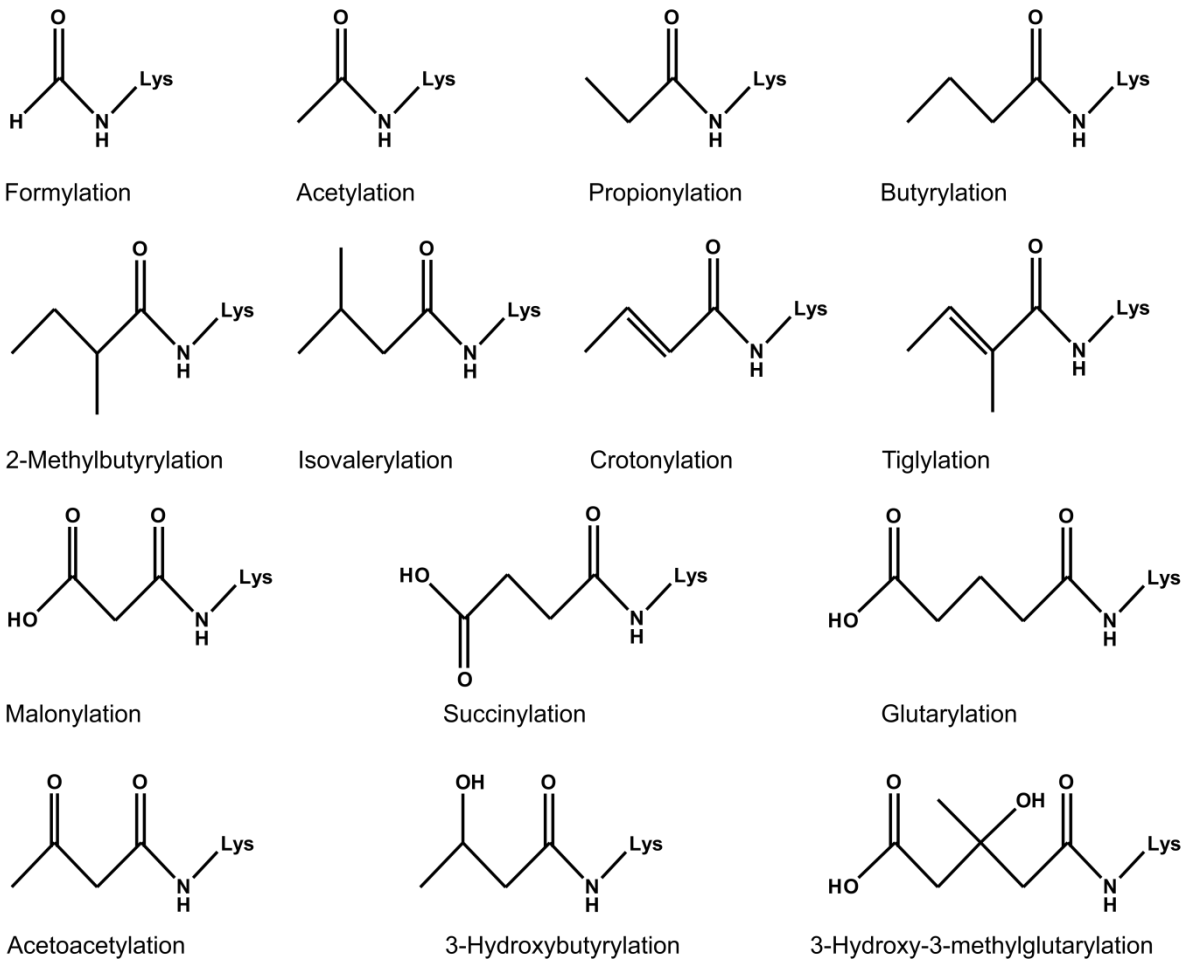

Figure S2. Structures of authentic reference standards**.**

Synthesis routes of authentic reference standards

***N*^{2}-Boc-*N*^{6}-propionyl lysine *t*-butyl ester.** Propionic acid (392 mg, 5.3 mmol) and hydroxybenzotriazole (HOBt) (590 mg, 4.37 mmol) were dissolved in 10 mL dry tetrahydrofuran (THF) under argon atmosphere at 0 °C. After 10 minutes 1-ethyl-3-(3-dimethylaminopropyl)carbodiimide **(**EDC) (904 mg, 5.8 mmol) was added. A solution of *N*^{2}-*t*-Boc-lysine *t*-butyl ester (1.319 g, 5.3 mmol) in 5 mL dry THF was added dropwise after 20 minutes. The reaction mixture was allowed to warm up to room temperature and was stirred for 16 h. The solvent was evaporated by rotary evaporation, the residue dissolved in 10 mL ethyl acetate (EtOAc) and washed with 10 mL each of saturated $NaHCO_3$ solution and 1 M HCl. The organic layer was evaporated with a rotary evaporator and the crude product was purified by column chromatography on silica gel 60 (hexane/acetone = 3/1, v/v). Fractions with positive ninhydrin detection (TLC: R_f 0.35 in hexane/acetone 3/1) were collected, evaporated and dried under high vacuum. Yield: 680 mg (36 %); ^{1}H NMR (400 MHz, $CDCl_3$): δ 6.28 (br s, 1H, CONH), 5.06 (br s, 1H, NH-Boc), 4.11 (m, 1H, CH), 3.24 (m, 2H, CH_2), 2.24 (q, *J* = 7.6 Hz, 2H, CH_2), 1.74 (m, 2H, CH_2), 1.57 (m, 2H, CH_2), 1.43 (s, 9H, 3xCH_3), 1.41 (s, 9H, 3xCH_3) 1.35 (m, 2H, CH_2), 1.14 (t, *J* = 7.6 Hz, 3H, CH_3); ^{13}C NMR (100 MHz, $CDCl_3$): δ 174.6 (CONH), 171.8 (COOtBu), 155.5, 81.8, 79.6, 53.6, 39.4, 32.6, 29.3, 28.8, 28.3, 27.9, 22.5, 10.3; HRMS (ESI+) *m*/*z*: $[M + H]^+$ calcd for $C_{18}H_{35}O_5N_2$ 359.2540, found 359.2531.

***N*^{6}-propionyl lysine.** *N*^{2}-Boc-*N*^{6}-propionyl lysine *t*-butyl ester (189 mg, 0.5 mmol) was dissolved in 10 mL each of acetone and 6 M HCl. After stirring for 30 minutes the mixture was diluted by 50 mL water and concentrated to a volume of approximately 2 mL by rotary evaporation. The crude product was purified by column chromatography on Lichroprep RP C18 (water/methanol = 9/1, v/v). Fractions with positive ninhydrin detection (RP C18 TLC: R_f 0.94 in water/methanol (9/1)) were collected, evaporated and lyophilized. Yield: 101 mg (95 %); ^{1}H NMR (400 MHz, D_2O): δ 3.96 (t, *J* = 6.4 Hz, 1H, CH), 3.07 (t, *J* = 6.8 Hz, 2H, CH_2), 2.11 (q, *J* = 7.6 Hz, 2H, CH_2), 1.84 (m, 2H, CH_2), 1.44 (m, 2H, CH_2), 1.33 (m, 2H, CH_2), 0.97 (t, *J* = 7.6 Hz, 3H, CH_3); ^{13}C NMR (100 MHz, D_2O): δ 177.9 (CONH), 171.9 (COOH), 52.6, 38.6, 29.2, 29.1, 27.7, 21.4, 9.6; HRMS (ESI+) *m*/*z*: $[M + H]^+$ calcd for $C_9H_{19}O_3N_2$ 203.1396, found 203.1385.

***N*^{2}-Boc-*N*^{6}-butyryl lysine *t*-butyl ester.** Butyric acid (88 mg, 1.0 mmol) was coupled with *N*^{2}-*t*-Boc-lysine *t*-butyl ester (302 mg, 1.0 mmol) by HOBt (135 mg, 1.0 mmol) and EDC (186 mg, 1.2 mmol). Reaction parameters and processing was as above. Column chromatography on silica gel 60 (hexane/acetone = 3/1, v/v). TLC: R_f 0.10 in hexane/acetone

3/1 with ninhydrin detection. Yield: 122 mg (33 %); ^{1}H NMR (400 MHz, $CDCl_3$): δ 5.72 (br s, 1H, CONH), 5.07 (br s, 1H, NH-Boc), 4.12 (m, 1H, CH), 3.23 (m, 2H, CH_2), 2.14 (q, *J* = 7.8 Hz, 2H, CH_2), 1.76 (m, 2H, CH_2), 1.63 (m, 2H, CH_2), 1.51 (m, 2H, CH_2), 1.44 (s, 9H, 3xCH_3), 1.43 (s, 9H, 3xCH_3), 1.37 (m, 2H, CH_2), 0.92 (t, *J* = 7.4 Hz, 3H, CH_3); ^{13}C NMR (100 MHz, $CDCl_3$): δ 173.1 (CONH), 171.8 (COOtBu), 155.5, 81.8, 79.6, 53.7, 39.1, 38.6, 32.7, 30.9, 28.3, 28.0, 22.5, 19.2, 13.8; HRMS (ESI+) *m*/*z*: $[M + H]^+$ calcd for $C_{19}H_{37}O_5N_2$ 373.2702, found 373.2693.

***N*^{6}-butyryl lysine.** *N*^{2}-Boc-*N*^{6}-butyryl lysine *t*-butyl ester (100 mg, 0.27 mmol) was processed as above. Column chromatography on Lichroprep RP C18 (water/methanol = 9/1, v/v). TLC: R_f 0.23 in butanol/acetic acid/water 8/1/1 with ninhydrin detection. Yield: 34 mg (58 %); ^{1}H NMR (400 MHz, D_2O): δ 3.70 (t, *J* = 6.2 Hz, 1H, CH), 3.09 (t, *J* = 6.9 Hz, 2H, CH_2), 2.09 (t, *J* = 7.4 Hz, 2H, CH_2), 1.78 (m, 2H, CH_2), 1.49 (m, 2H, CH_2), 1.45 (m, 2H, CH_2), 1.32 (m, 2H, CH_2), 0.78 (t, *J* = 7.4 Hz, 3H, CH_3); ^{13}C NMR (100 MHz, D_2O): δ 177.0 (CONH), 174.0 (COOH), 54.2, 38.8, 37.7, 29.9, 28.0, 21.7, 19.0, 12.7; HRMS (ESI+) *m*/*z*: $[M + H]^+$ calcd for $C_{10}H_{21}O_3N_2$ 217.1552, found 217.1543.

***N*^{2}-Boc-*N*^{6}-(2-methylbutyryl) lysine *t*-butyl ester.** 2-Methylbutyric acid (102 mg, 1.0 mmol) was coupled with *N*^{2}-*t*-Boc-lysine *t*-butyl ester (302 mg, 1.0 mmol) by HOBt (135 mg, 1.0 mmol) and EDC (186 mg, 1.2 mmol). Reaction parameters and processing was as above. Column chromatography on silica gel 60 (hexane/acetone = 4/1, v/v). TLC: R_f 0.26 in hexane/acetone 4/1 with ninhydrin detection. Yield: 69 mg (18 %); ^{1}H NMR (400 MHz, $CDCl_3$): δ 5.79 (br s, 1H, CONH), 5.09 (br s, 1H, NH-Boc), 4.07 (m, 1H, CH), 3.21 (m, 2H, CH_2), 2.06 (m, 1H, CH), 1.78 (m, 2H, CH_2), 1.61 (m, 2H, CH_2), 1.51 (m, 2H, CH_2), 1.42 (s, 9H, 3xCH_3), 1.40 (s, 9H, 3xCH_3), 1.33 (m, 2H, CH_2), 1.08 (d, *J* = 6.9 Hz, 3H, CH_3), 0.85 (t, *J* = 7.4 Hz, 3H, CH_3); ^{13}C NMR (100 MHz, $CDCl_3$): δ 176.6 (CONH), 171.9 (COOtBu), 155.5, 81.7, 79.5, 53.7, 43.1, 38.9, 32.5, 29.1, 28.3, 28.0, 27.2, 22.5, 17.5, 11.9; HRMS (ESI+) *m*/*z*: $[M + H]^+$ calcd for $C_{20}H_{39}O_5N_2$ 387.2859, found 387.2840.

***N*^{6}-(2-methylbutyryl) lysine.** *N*^{2}-Boc-*N*^{6}-(2-methylbutyryl) lysine *t*-butyl ester (69 mg, 0.18 mmol) was processed as above. Column chromatography on Lichroprep RP C18 (water/methanol = 9/1, v/v). Fractions with positive ninhydrin detection were collected, evaporated and lyophilized. Yield: 24 mg (56 %); ^{1}H NMR (400 MHz, D_2O): δ 3.96 (t, *J* = 6.4 Hz, 1H, CH), 3.09 (m, 2H, CH_2), 2.14 (m, 1H, CH), 1.85 (m, 2H, CH_2), 1.45 (m, 2H, CH_2), 1.35 (m, 2H, CH_2), 0.95 (d, *J* = 6.9 Hz, 3H, CH_3), 0.72 (t, *J* = 7.4 Hz, 3H, CH_3); ^{13}C NMR (100 MHz, D_2O): δ 180.3 (CONH), 172.0 (COOH), 52.7, 42.6, 38.5, 29.3, 27.9, 26.7,

21.5, 16.8, 11.1; HRMS (ESI+) *m/z*: $[M + H]^+$ calcd for $C_{11}H_{23}O_3N_2$ 231.1709, found 231.1693.

***N*^{2}-Boc-*N*^{6}-isovaleryl lysine *t*-butyl ester.** Isovaleric acid (102 mg, 1.0 mmol) was coupled with *N*^{2}-*t*-Boc-lysine *t*-butyl ester (302 mg, 1.0 mmol) by HOBt (135 mg, 1.0 mmol) and EDC (186 mg, 1.2 mmol). Reaction parameters and processing was as above. Column chromatography on silica gel 60 (hexane/acetone = 4/1, v/v). TLC: R_f 0.15 in hexane/acetone 4/1 with ninhydrin detection. Yield:162 mg (42 %); ^{1}H NMR (400 MHz, $CDCl_3$): δ 5.80 (br s, 1H, CONH), 5.07 (br s, 1H, NH-Boc), 4.12 (m, 1H, CH), 3.24 (m, 2H, CH_2), 2.03 (d, *J* = 7.4 Hz, 2H, CH_2), 1.75 (m, 1H, CH), 1.61 (m, 2H, CH_2), 1.53 (m, 2H, CH_2), 1.45 (s, 9H, 3xCH_3), 1.43 (s, 9H, 3xCH_3), 1.37 (m, 2H, CH_2), 0.93 (d, *J* = 6.6 Hz, 6H, 2xCH_3); ^{13}C NMR (100 MHz, $CDCl_3$): δ 172.7 (CONH), 171.8 (COOtBu), 155.5, 81.9, 79.6, 53.6, 46.0, 39.2, 32.7, 29.0, 28.3, 28.0, 26.1, 22.5, 22.4; HRMS (ESI+) *m/z*: $[M + H]^+$ calcd for $C_{20}H_{39}O_5N_2$ 387.2859, found 387.2840.

***N*^{6}-isovaleryl lysine.** *N*^{2}-Boc-*N*^{6}-isovaleryl lysine *t*-butyl ester (100 mg, 0.26 mmol) was processed as above. Column chromatography on Lichroprep RP C18 (water/methanol = 9/1, v/v). Fractions with positive ninhydrin detection were collected, evaporated and lyophilized. Yield: 33 mg (55 %); ^{1}H NMR (400 MHz, D_2O): δ 3.66 (t, *J* = 6.4 Hz, 1H, CH), 3.08 (t, *J* = 7.0 Hz, 2H, CH_2), 1.98 (d, *J* = 7.4 Hz, 2H, CH_2), 1.86 (m, 1H, CH), 1.76 (m, 2H, CH_2), 1.45 (m, 2H, CH_2), 0.80 (d, *J* = 6.6 Hz, 6H, 2xCH_3); ^{13}C NMR (100 MHz, D_2O): δ 176.3 (CONH), 174.2 (COOH), 54.4, 45.0, 38.8, 30.0, 28.0, 26.1, 21.8, 21.5; HRMS (ESI+) *m/z*: $[M + H]^+$ calcd for $C_{11}H_{23}O_3N_2$ 231.1709, found 231.1694.

***N*^{2}-Boc-*N*^{6}-crotonyl lysine *t*-butyl ester.** Crotonic acid (86 mg, 1.0 mmol) was coupled with *N*^{2}-*t*-Boc-lysine *t*-butyl ester (302 mg, 1.0 mmol) by HOBt (135 mg, 1.0 mmol) and EDC (186 mg, 1.2 mmol). Reaction parameters and processing was as above. Column chromatography on silica gel 60 (hexane/acetone = 3/1, v/v). TLC: R_f 0.12 in hexane/acetone 3/1 with ninhydrin detection. Yield: 48 mg (13 %); ^{1}H NMR (400 MHz, $CDCl_3$): δ 6.80 (m, 1H, HC=C), 5.86 (br s, 1H, CONH), 5.79 (d, *J* = 15.2 Hz, 1H, HC=C), 5.09 (br s, 1H, NH-Boc), 4.11 (m, 1H, CH), 3.28 (m, 2H, CH_2), 1.81 (d, *J* = 6.9 Hz, 3H, CH_3), 1.73 (m, 2H, CH_2), 1.56 (m, 2H, CH_2), 1.43 (s, 9H, 3xCH_3), 1.42 (s, 9H, 3xCH_3), 1.36 (m, 2H, CH_2); ^{13}C NMR (100 MHz, $CDCl_3$): δ 171.8 (COOtBu), 166.1 (CONH), 139.5 (C=C), 125.1 (C=C), 155.5, 81.8, 79.6, 53.6, 39.1, 32.7, 28.9, 28.3, 28.0, 22.5, 17.6; HRMS (ESI+) *m/z*: $[M + H]^+$ calcd for $C_{19}H_{35}O_5N_2$ 371.2546, found 371.2540.

***N*^{6}-crotonyl lysine.** *N*^{2}-Boc-*N*^{6}-crotonyl lysine *t*-butyl ester (48 mg, 0.13 mmol) was processed as above. Column chromatography on Lichroprep RP C18 (water/methanol = 9/1,

v/v). TLC: R_f 0.22 in butanol/acetic acid/water 8/1/1 with ninhydrin detection. Yield: 21 mg (75 %); ^{1}H NMR (400 MHz, D_2O): δ 6.66 (m, 1H, HC=C), 5.85 (d, J = 15.3 Hz, 1H, HC=C), 3.64 (t, J = 6.1 Hz, 1H, CH), 3.14 (t, J = 6.9 Hz, 2H, CH_2), 1.78 (m, 2H, CH_2), 1.74 (d, J = 6.8 Hz, 3H, CH_3), 1.47 (m, 2H, CH_2), 1.31 (m, 2H, CH_2); ^{13}C NMR (100 MHz, D_2O): δ 174.5 (COOH), 168.9 (CONH), 141.5 (C=C), 123.8 (C=C), 54.6, 38.8, 30.0, 28.0, 21.7, 17.1; HRMS (ESI+) *m/z*: $[M+H]^+$ calcd for $C_{10}H_{19}O_3N_2$ 215.1396, found 215.1386.

***N*^{2}-Boc-*N*^{6}-tiglyl lysine *t*-butyl ester.** Tiglic acid (100 mg, 1.0 mmol) was coupled with N^2-*t*-Boc-lysine *t*-butyl ester (302 mg, 1.0 mmol) by HOBt (135 mg, 1.0 mmol) and EDC (186 mg, 1.2 mmol). Reaction parameters and processing was as above. Column chromatography on silica gel 60 (hexane/acetone = 3/1, v/v). TLC: R_f 0.33 in hexane/acetone 3/1 with ninhydrin detection. Yield: 77 mg (20 %); ^{1}H NMR (400 MHz, $CDCl_3$): δ 6.36 (q, J = 7.0 Hz ,1H, HC=C), 5.90 (br s, 1H, CONH), 5.09 (br s, 1H, NH-Boc), 4.09 (m, 1H, CH), 3.25 (m, 2H, CH_2), 1.78 (s, 3H, CH_3), 1.69 (d, J = 7.0 Hz, 3H, CH_3), 1.58 (m, 2H, CH_2), 1.52 (m, 2H, CH_2), 1.41 (s, 9H, 3xCH_3), 1.39 (s, 9H, 3xCH_3), 1.33 (m, 2H, CH_2); ^{13}C NMR (100 MHz, $CDCl_3$): δ 171.9 (COOtBu), 169.6 (CONH), 131.8 (C=C), 130.3 (C=C), 155.5, 81.7, 79.5, 53.7, 39.3, 32.5, 29.1, 28.3, 27.9, 22.5, 13.8, 12.3; HRMS (ESI+) *m/z*: $[M + H]^+$ calcd for $C_{20}H_{37}O_5N_2$ 385.2702, found 385.2683.

***N*^{6}-tiglyl lysine.** N^2-Boc-N^6-tiglyl lysine *t*-butyl ester (77 mg, 0.2 mmol) was processed as above. Column chromatography on Lichroprep RP C18 (water/methanol = 9/1, v/v). Fractions with positive ninhydrin detection were collected, evaporated and lyophilized. Yield: 13 mg (29 %); ^{1}H NMR (400 MHz, D_2O): δ 6.27 (q, J = 7.0, 1H, HC=C), 3.74 (t, J = 6.1 Hz, 1H, CH), 3.15 (t, J = 6.8 Hz, 2H, CH_2), 1.80 (m, 2H, CH_2), 1.69 (s, 3H, CH_3), 1.64 (d, J = 7.0 Hz, 3H, CH_3), 1.49 (m, 2H, CH_2), 1.32 (m, 2H, CH_2); ^{13}C NMR (100 MHz, D_2O): δ 173.8 (COOH), 173.0 (CONH), 132.6 (C=C), 130.8 (C=C), 54.0, 39.0, 29.8, 28.0, 21.7, 13.2, 11.6; HRMS (ESI+) *m/z*: $[M+H]^+$ calcd for $C_{11}H_{21}O_3N_2$ 229.1552, found 229.1537.

***N*^{2}-Boc-*N*^{6}-(mono-*t*-butyl malonyl) lysine *t*-butyl ester.** Mono-*t*-butyl malonate (570 mg, 3.6 mmol) was coupled with N^2-*t*-Boc-lysine *t*-butyl ester (1087 mg, 3.6 mmol) by HOBt (486 mg, 3.6 mmol) and EDC (775 mg, 5.0 mmol). Reaction parameters and processing was as above. Column chromatography on silica gel 60 (hexane/acetone = 3/1, v/v). TLC: R_f 0.18 in hexane/acetone 3/1 with ninhydrin detection. Yield: 987 mg (62 %); ^{1}H NMR (400 MHz, $CDCl_3$): δ 7.33 (br s, 1H, CONH), 5.05 (br s, 1H, NH-Boc), 4.15 (m, 1H, CH), 3.28 (m, 2H, CH_2), 3.23 (s, 2H, CH_2), 1.75 (m, 2H, CH_2), 1.59 (m, 2H, CH_2), 1.47 (s, 9H, 3xCH_3), 1.46 (s, 9H, 3xCH_3), 1.44 (s, 9H, 3xCH_3), 1.27 (m, 2H, CH_2); ^{13}C NMR (100 MHz, $CDCl_3$): δ 171.8 (COOtBu), 169.0 (COOtBu), 165.7 (CONH), 155.4, 82.5, 81.8, 79.6, 53.8, 41.8, 39.3, 32.6,

29.0, 28.3, 28.0, 27.9, 22.6; HRMS (ESI+) *m/z*: $[M + H]^+$ calcd for $C_{22}H_{41}O_7N_2$ 445.2908, found 445.2896.

***N*^{6}-malonyl lysine. *N*^{2}-Boc-*N*^{6}-(mono-*t*-butyl malonyl) lysine *t*-butyl ester** (201 mg, 0.45 mmol) was processed as above. Column chromatography on Lichroprep RP C18 (water/methanol = 9/1, v/v). TLC: R_f 0.05 in butanol/acetic acid/water 8/1/1 with ninhydrin detection. Yield: 80 mg (76 %); ^{1}H NMR (400 MHz, D_2O): δ 3.97 (t, *J* = 6.3 Hz, 1H, CH), 3.27 (s, 2H, CH_2), 3.12 (t, *J* = 6.8 Hz, 2H, CH_2), 1.84 (m, 2H, CH_2), 1.46 (m, 2H, CH_2), 1.34 (m, 2H, CH_2); ^{13}C NMR (100 MHz, D_2O): δ 171.9 (COOH), 171.7 (COOH), 168.6 (CONH), 52.7, 42.0, 39.0, 29.2, 27.6, 21.4; HRMS (ESI+) *m/z*: $[M+H]^+$ calcd for $C_9H_{17}O_5N_2$ 233.1132, found 233.1125.

***N*^{2}-Boc-*N*^{6}-(mono-*t*-butyl succinyl) lysine *t*-butyl ester.** Mono-*t*-butyl succinate (348 mg, 2.0 mmol) was coupled with *N*^{2}-*t*-Boc-lysine *t*-butyl ester (604 mg, 2.0 mmol) by HOBt (270 mg, 2.0 mmol) and EDC (372 mg, 2.4 mmol). Reaction parameters and processing was as above. Column chromatography on silica gel 60 (hexane/acetone = 3/1, v/v). TLC: R_f 0.25 in hexane/acetone 3/1 with ninhydrin detection. Yield: 197 mg (36 %); ^{1}H NMR (400 MHz, MeOH-d_4): δ 3.93 (m, 1H, CH), 3.16 (t, *J* = 6.8 Hz, 2H, CH_2), 2.50 (t, *J* = 6.8 Hz, 2H, CH_2), 2.40 (t, *J* = 6.8 Hz, 2H, CH_2), 1.74 (m, 2H, CH_2), 1.51 (m, 2H, CH_2), 1.46 (s, 9H, 3xCH_3), 1.44 (s, 9H, 3xCH_3), 1.43 (s, 9H, 3xCH_3), 1.35 (m, 2H, CH_2); ^{13}C NMR (100 MHz, MeOH-d_4): δ 172.9 (COOtBu), 172.4 (COOtBu), 172.2 (CONH), 156.7, 81.0, 80.3, 79.0, 54.4, 38.6, 30.9, 30.4, 30.3, 28.5, 27.3, 27.0, 26.9, 22.8; HRMS (ESI+) *m/z*: $[M + H]^+$ calcd for $C_{23}H_{43}O_7N_2$ 459.3070, found 459.3058.

***N*^{6}-succinyl lysine. *N*^{2}-Boc-*N*^{6}-(mono-*t*-butyl succinyl) lysine *t*-butyl ester** (197 mg, 0.43 mmol) was processed as above. Column chromatography on Lichroprep RP C18 (water/methanol = 9/1, v/v). TLC: R_f 0.15 in butanol/acetic acid/water 8/1/1 with ninhydrin detection. Yield: 60 mg (57 %); ^{1}H NMR (400 MHz, D_2O): δ 3.98 (t, *J* = 6.2 Hz, 1H, CH), 3.10 (t, *J* = 6.5 Hz, 2H, CH_2), 2.86 (t, *J* = 6.3 Hz, 2H, CH_2), 2.53 (t, *J* = 6.3 Hz, 2H, CH_2), 1.97 (m, 2H, CH_2), 1.58 (m, 2H, CH_2), 1.47 (m, 2H, CH_2); ^{13}C NMR (100 MHz, D_2O): δ 176.9 (COOH), 174.6 (COOH), 172.0 (CONH), 52.7, 38.7, 30.3, 29.3, 27.8, 21.4; HRMS (ESI+) *m/z*: $[M+H]^+$ calcd for $C_{10}H_{19}O_5N_2$ 247.1293, found 247.1283.

***N*^{2}-Boc-*N*^{6}-(mono-*t*-butyl glutaryl) lysine *t*-butyl ester.** Mono-*t*-butyl glutarate (376 mg, 2.0 mmol) was coupled with *N*^{2}-*t*-Boc-lysine *t*-butyl ester (604 mg, 2.0 mmol) by HOBt (270 mg, 2.0 mmol) and EDC (372 mg, 2.4 mmol). Reaction parameters and processing was as above. Column chromatography on silica gel 60 (hexane/acetone = 3/1, v/v). TLC: R_f 0.15 in hexane/acetone 3/1 with ninhydrin detection. Yield: 563 mg (60 %); ^{1}H NMR (400 MHz,

MeOH-d_4): δ 3.93 (m, 1H, CH), 3.17 (t, J = 6.8 Hz, 2H, CH_2), 2.25 (t, J = 7.5 Hz, 2H, CH_2), 2.18 (t, J = 7.5 Hz, 2H, CH_2), 1.85 (m, 2H, CH_2), 1.62 (m, 2H, CH_2), 1.51 (m, 2H, CH_2), 1.46 (s, 9H, 3xCH_3), 1.45 (s, 9H, 3xCH_3), 1.44 (s, 9H, 3xCH_3), 1.35 (m, 2H, CH_2); ^{13}C NMR (100 MHz, MeOH-d_4): δ 173.8 (COOtBu), 172.8 (COOtBu), 172.3 (CONH), 156.7, 81.1, 80.1, 79.0, 54.4, 38.6, 34.6, 34.2, 28.6, 27.3, 27.2, 27.0, 26.9, 22.8, 21.0; HRMS (ESI+) *m/z*: $[M + H]^+$ calcd for $C_{24}H_{45}O_7N_2$ 473.3226, found 473.3226.

***N*^{6}-glutaryl lysine. *N*^{2}-Boc-*N*^{6}-(mono-*t*-butyl glutaryl) lysine *t*-butyl ester** (210 mg, 0.44 mmol) was processed as above. Column chromatography on Lichroprep RP C18 (water/methanol = 9/1, v/v). TLC: R_f 0.14 in butanol/acetic acid/water 8/1/1 with ninhydrin detection. Yield: 86 mg (72 %); ^{1}H NMR (400 MHz, D_2O): δ 3.98 (t, J = 6.2 Hz, 1H, CH), 3.10 (t, J = 6.5 Hz, 2H, CH_2), 2.30 (t, J = 7.3 Hz, 2H, CH_2), 2.19 (t, J = 7.3 Hz, 2H, CH_2), 1.88 (m, 2H, CH_2), 1.78 (m, 2H, CH_2), 1.46 (m, 2H, CH_2), 1.35 (m, 2H, CH_2); ^{13}C NMR (100 MHz, D_2O): δ 177.8 (COOH), 175.8 (COOH), 172.1 (CONH), 52.8, 38.7, 34.8, 32.8, 29.3, 27.8, 21.5, 20.7; HRMS (ESI+) *m/z*: $[M+H]^+$ calcd for $C_{11}H_{21}O_5N_2$ 261.1450, found 261.1447.

***N*^{6}-(3-hydroxy-3-methyl) glutaryl lysine.** 4-Hydroxy-4-methyl-dihydro-pyran-2,6-dione (144 mg, 1.0 mmol) and diisopropylethylamin (129 mg, 1.0 mmol) were dissolved in 5 mL dry THF and a solution of *N*^{2}-*t*-Boc-lysine *t*-butyl ester (302 mg, 1.0 mmol) in 5 mL dry THF was added at 0 °C. The reaction mixture was allowed to warm up to room temperature and stirred for 16 h. The solvent was evaporated by rotary evaporation, the residue dissolved in 10 mL EtOAc and washed with 10 mL each of saturated $NaHCO_3$ solution and 1 M HCl. The organic layer was evaporated with a rotary evaporator. The residue was dissolved in 10 mL each of acetone and 6 M HCl. After stirring for 30 minutes the mixture was diluted by 50 mL water and concentrated to a volume of approximately 2 mL by rotary evaporation. The crude product was purified by column chromatography on Lichroprep RP C18 (water/methanol = 9:1, v/v). Fractions with positive ninhydrin detection were collected, evaporated and lyophilized. Yield: 11 mg (4 %); ^{1}H NMR (400 MHz, D_2O): δ 3.95 (t, J = 6.3 Hz, 1H, CH), 3.11 (t, J = 6.8 Hz, 2H, CH_2), 2.54 (s, 2H, CH_2), 2.45 (s, 2H, CH_2), 1.85 (m, 2H, CH_2), 1.47 (m, 2H, CH_2), 1.35 (m, 2H, CH_2), 1.26 (s, 3H, CH_3); ^{13}C NMR (100 MHz, D_2O): δ 174.9 (COOH), 172.9 (CONH), 172.1 (COOH), 70.2, 52.8, 46.7, 45.4, 38.7, 29.3, 27.8, 26.3, 21.6; HRMS (ESI+) *m/z*: $[M+H]^+$ calcd for $C_{12}H_{23}O_6N_2$ 291.1556, found 291.1540.

2-(2-methyl-1,3-dioxolan-2-yl) acetic acid. Ethyl (2-methyl-1,3-dioxolan-2-yl) acetate (500 mg, 2.87 mmol) was dissolved in 5 mL acetone and 5 mL 1 M NaOH. The solution was stirred at room temperature for 1 h. The acetone was removed under reduced pressure, aqueous phase was washed with 5 mL EtOAc and pH adjusted to 2. After extraction with

3x10 mL EtOAc the organic layers were combined, evaporated and dried under high vacuum. Yield: 271 mg (41 %); ^{1}H NMR (400 MHz, $CDCl_3$): δ 10.70 (br s, 1H, COOH), 3.99 (s, 2H, 2xCH_2), 2.71 (s, 2H, CH_2), 1.50 (s, 3H, CH_3); ^{13}C NMR (100 MHz, $CDCl_3$): δ 174.9 (COOH), 107.4, 64.8, 44.0; HRMS (ESI-) *m*/*z*: $[M-H]^-$ calcd for $C_6H_9O_4$ 145.0501, found 145.0504.

***N*^{6}-acetoacetyl lysine.** 2-(2-methyl-1,3-dioxolan-2-yl) acetic acid (146 mg, 1.0 mmol) was coupled with *N*^{2}-*t*-Boc-lysine *t*-butyl ester (302 mg, 1.0 mmol) by HOBt (135 mg, 1.0 mmol) and EDC (186 mg, 1.2 mmol). Reaction parameters and processing was as above. Column chromatography on silica gel 60 (hexane/acetone = 2/1, v/v). TLC: R_f 0.27 in hexane/acetone 2/1 with ninhydrin detection. The intermediate was dissolved in 10 mL each of acetone and 6 M HCl. After stirring for 30 minutes the mixture was diluted by 50 mL water and concentrated to a volume of approximately 2 mL by rotary evaporation. The crude product was purified by column chromatography on Lichroprep RP C18 (water/methanol = 9:1, v/v). Fractions with positive ninhydrin detection were collected, evaporated and lyophilized. Yield: 19 mg (8 %); ^{1}H NMR (400 MHz, D_2O): δ 3.96 (t, *J* = 6.2 Hz, 1H, CH), 3.54 (s, 2H, CH_2), 3.12 (t, *J* = 6.6 Hz, 2H, CH_2), 2.15 (s, 3H, CH_3), 1.85 (m, 2H, CH_2), 1.46 (m, 2H, CH_2), 1.32 (m, 2H, CH_2); ^{13}C NMR (100 MHz, D_2O): δ 207.9 (C=O), 172.1 (COOH), 169.0 (CONH), 132.6 (C=C), 62.5, 52.8, 38.8, 29.7, 29.3, 27.6, 21.4; HRMS (ESI+) *m*/*z*: $[M+H]^+$ calcd for $C_{10}H_{19}O_4N_2$ 231.1345, found 231.1331.

3-acetoxybutyric acid. Acetic anhydride (3 mL) was cooled to 15 °C and 67 % $HClO_4$ (400 mg, 4 mmol) was added. 3-Hydroxybutyric acid (260 mg, 2.5 mmol) was slowly added to the mixture and the temperature was maintained below 40 °C. The mixture was allowed to warm up to room temperature until a homogenous solution was obtained. The reaction was quenched by addition of ice and extracted with chloroform (2x10 mL). Water (5 mL) and trimethylamine (400 µL) were added to the organic phase and stirred at room temperature for 16 h. The organic phase was washed with 1 M HCl (10 mL), evaporated and dried under high vacuum. Yield: 200 mg (54 %); ^{1}H NMR (400 MHz, $CDCl_3$): δ 8.70 (br s, 1H, COOH), 5.25 (m, 1H, CH), 2.61 (m, 2H, CH_2), 2.02 (s, 3H, CH_3), 1.31 (d, *J* = 6.3 Hz, 3H, CH_3); ^{13}C NMR (100 MHz, $CDCl_3$): δ 176.0 (COOH), 170.4 (C=O), 67.0, 40.4, 21.1, 19.8; HRMS (ESI-) *m*/*z*: $[M-H]^-$ calcd for $C_6H_9O_4$ 145.0501, found 145.0504.

***N*^{2}-Boc-*N*^{6}-(3-acetoxy) butyryl lysine *t*-butyl ester.** 3-Acetoxybutyric acid (36 mg, 0.25 mmol) was coupled with *N*^{2}-*t*-Boc-lysine *t*-butyl ester (76 mg, 0.25 mmol) by HOBt (34 mg, 0.25 mmol) and EDC (47 mg, 0.3 mmol). Reaction parameters and processing was as above. Column chromatography on silica gel 60 (hexane/acetone = 1/1, v/v). TLC: R_f 0.16 in

hexane/acetone 1/1 with ninhydrin detection. Yield: 38 mg (36 %); ^{1}H NMR (400 MHz, $CDCl_3$): δ 5.86 (br s, 1H, CONH), 5.20 (m, 1H, CH), 5.07 (br s, 1H, NH-Boc), 4.11 (m, 1H, CH), 3.23 (m, 2H, CH_2), 2.40 (m, 2H, CH_2), 2.01 (s, 3H, CH_3), 1.60 (m, 2H, CH_2), 1.50 (m, 2H, CH_2), 1.44 (s, 9H, 3xCH_3), 1.42 (s, 9H, 3xCH_3) 1.35 (m, 2H, CH_2), 1.29 (t, *J* = 6.3 Hz, 3H, CH_3); ^{13}C NMR (100 MHz, $CDCl_3$): δ 171.8 (COOtBu), 170.3, 169.4 (CONH), 155.5, 81.8, 79.6, 68.3, 53.7, 43.2, 39.2, 32.7, 29.0, 28.3, 28.0, 22.5, 21.2, 19.9, 13.8; HRMS (ESI+) *m*/*z*: $[M + H]^+$ calcd for $C_{21}H_{39}O_7N_2$ 431.2752, 431.2764.

***N*^{6}-(3-hydroxy) butyryl lysine.** *N*^{2}-Boc-*N*^{6}-(3-acetoxy) butyryl lysine *t*-butyl ester (38 mg, 0.09 mmol) was processed as above. Column chromatography on Lichroprep RP C18 (water/methanol = 9/1, v/v). Fractions with positive ninhydrin detection were collected, evaporated and lyophilized. Yield: 8.5 mg (42 %); ^{1}H NMR (400 MHz, D_2O): δ 4.06 (m, 1H, CH), 3.95 (t, *J* = 6.2 Hz, 1H, CH), 3.11 (t, *J* = 6.8 Hz, 2H, CH_2), 2.28 (t, *J* = 7.4 Hz, 2H, CH_2), 1.83 (m, 2H, CH_2), 1.47 (m, 2H, CH_2), 1.35 (m, 2H, CH_2), 1.10 (d, *J* = 6.2 Hz, 3H, CH_3; ^{13}C NMR (100 MHz, D_2O): δ 173.8 (CONH), 172.2 (COOH), 65.0, 52.8, 44.9, 38.7, 29.3, 27.8, 21.9, 21.5; HRMS (ESI+) *m*/*z*: $[M + H]^+$ calcd for $C_{10}H_{21}O_4N_2$ 233.1457, found 233.1488.

Supporting information for

Comprehensive analysis of posttranslational protein modifications in aging of subcellular compartments

Tim Baldensperger,[1] Michael Eggen,[1] Jonas Kappen,[1] Patrick R. Winterhalter,[2] Thorsten Pfirrmann[3] and Marcus A. Glomb[1, *]

[1] Institute of Chemistry, Food Chemistry, Martin-Luther-University Halle-Wittenberg, Kurt-Mothes-Str. 2, 06120 Halle/Saale, Germany

[2] Clinic for Heart Surgery, Martin-Luther-University Halle-Wittenberg, Ernst-Grube Str. 40, 06120 Halle/Saale, Germany

[3] Institute of Physiological Chemistry, Martin-Luther-University Halle-Wittenberg, Hollystr. 1, 06114 Halle/Saale, Germany

* To whom correspondence should be addressed (e-mail marcus.glomb@chemie.uni-halle.de, Tel. +49 345 552-5784, Fax. +49 345 552-7341)

Figure S1. Full-length blotting images of fractionation control. S-2

Figure S2. Structural formulas of analytes. S-3

Figure S3. Chromatographic separation of analytes by HPLC-MS/MS. S-4

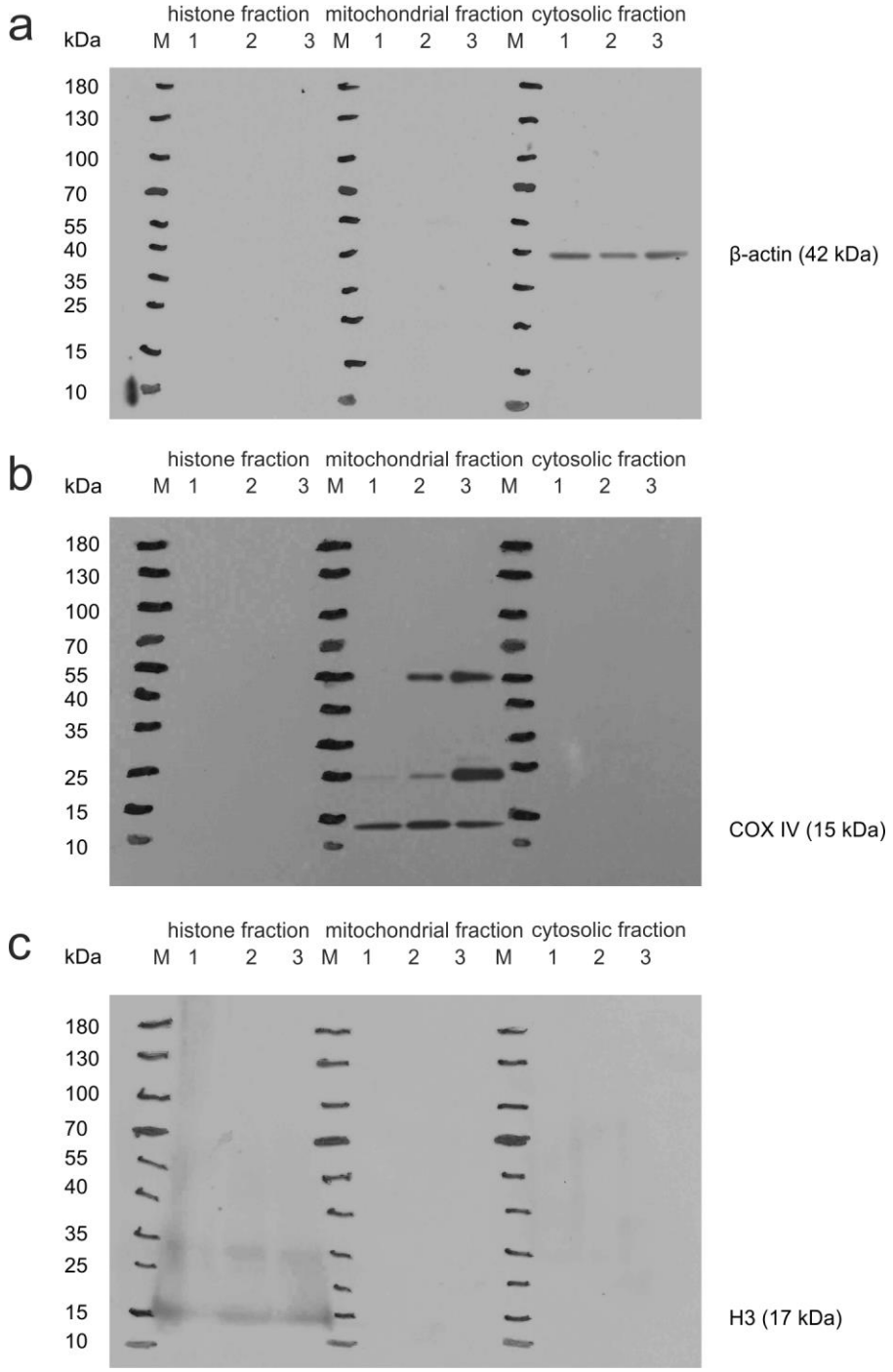

Figure S1. Full-length blotting images of fractionation control. Antibodies against cytosolic β-actin (**a**), mitochondrial COX IV (**b**), and histone H3 (**c**) were used.

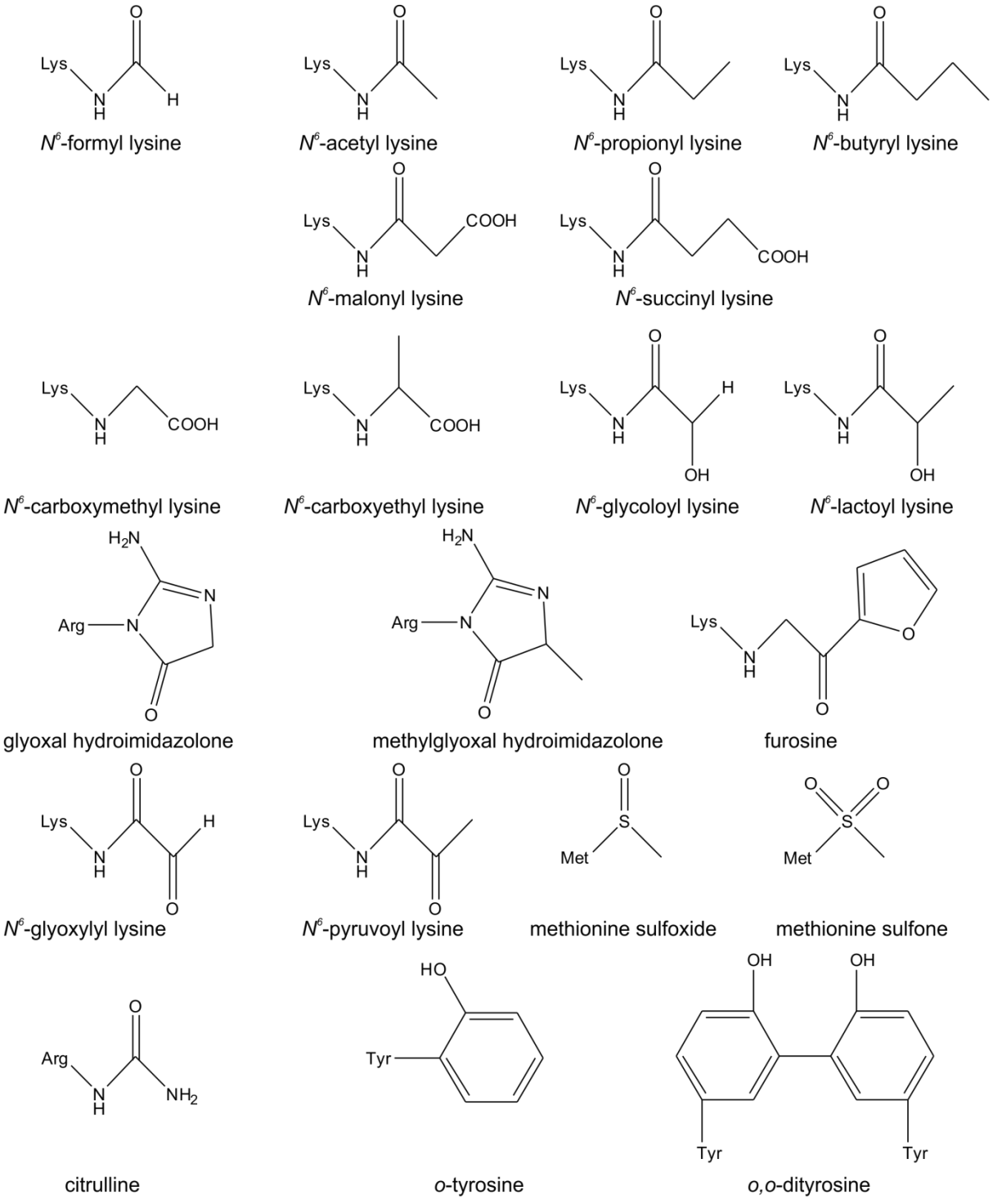

Figure S2. Structural formulas of analytes.

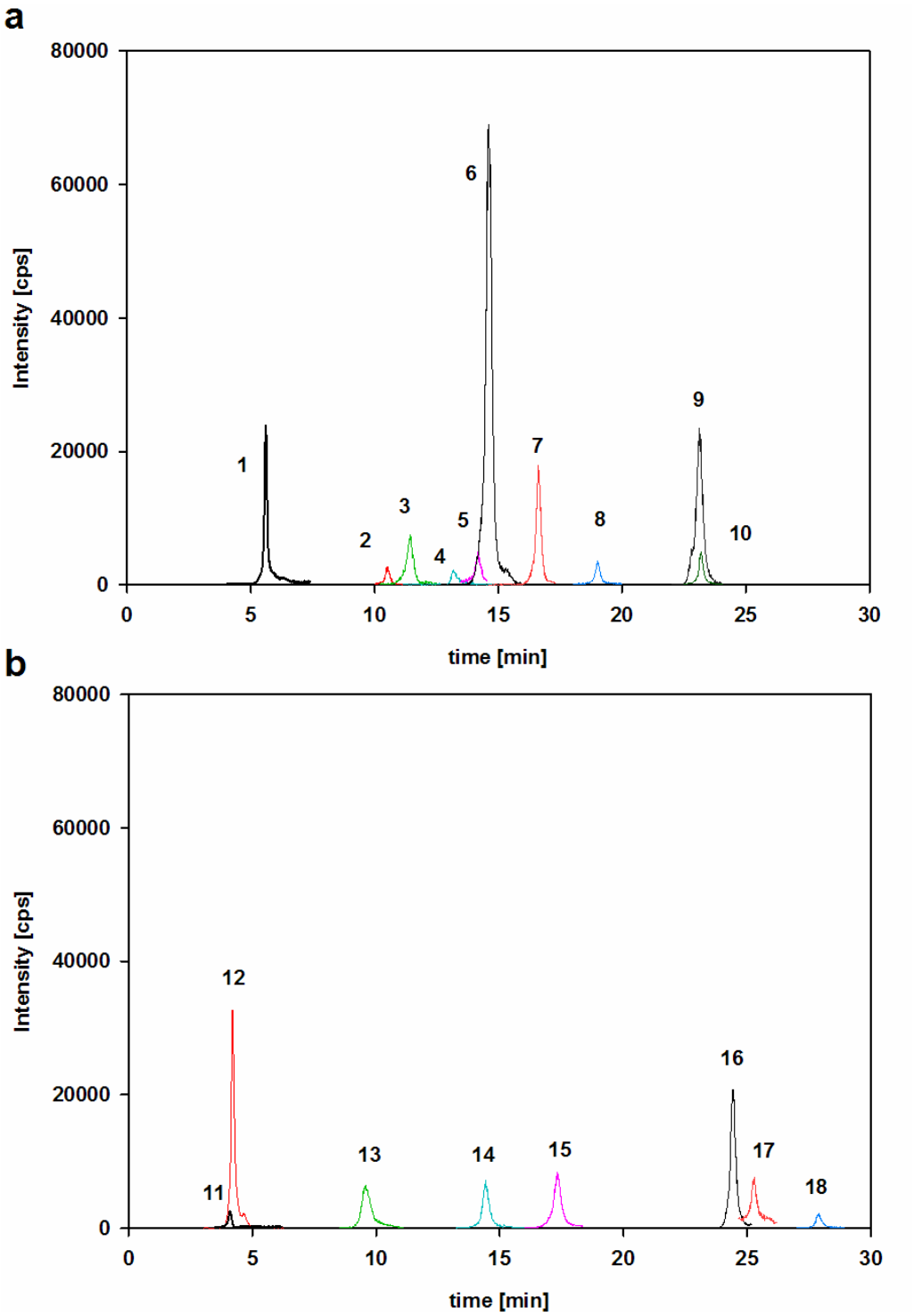

Figure S3. Chromatographic separation of analytes by HPLC-MS/MS in enzymatic (**a**) and acid (**b**) hydrolysates (**1** citrulline; **2** N^6-glycoloyl/glyoxylyl lysine; **3** N^6-formyl lysine; **4** N^6-malonyl lysine; **5** N^6-lactoyl/pyruvoyl lysine; **6** N^6-acetyl lysine; **7** N^6-succinyl lysine; **8** N^6-propionyl lysine; **9** methylglyoxal hydroimidazolone; **10** N^6-butyryl lysine; **11** methionine sulfone; **12** methionine sulfoxide; **13** N^6-carboxymethyl lysine, **14** N^6-carboxyethyl lysine, **15** glyoxal hydroimidazolone; **16** furosine; **17** *o*-tyrosine; **18** *o,o*-dityrosine).

Lebenslauf

Persönliche Angaben

Name	Tim Baldensperger
Geburtsdatum	16. März 1992 in Magdeburg
Nationalität	deutsch
Familienstand	ledig, keine Kinder

Berufstätigkeit

07/2016-12/2019	Institut für Chemie – Lebensmittelchemie, Martin-Luther-Universität Halle-Wittenberg, wiss. Mitarbeiter im Arbeitskreis von Prof. Glomb
05/2016-06/2016 und 11/2015	Institut für Chemie – Lebensmittelchemie, Martin-Luther-Universität Halle-Wittenberg, Hilfswissenschaftler im Arbeitskreis von Prof. Glomb
10/2010-07/2011	Grundwehrdienst

Ausbildung

10/2011-05/2016	Studium der Lebensmittelchemie an der Martin-Luther-Universität Halle-Wittenberg, Abschluss als Diplom Lebensmittelchemiker
06/2010	Abitur am Bördegymnasium Wanzleben

Eigenständigkeitserklärung

Hiermit erkläre ich, Tim Baldensperger, an Eides statt, dass ich die vorliegende Arbeit selbständig und ohne fremde Hilfe verfasst habe, keine anderen als die von mir angegebenen Quellen und Hilfsmittel benutzt und die den benutzten Werken wörtlich oder inhaltlich entnommenen Stellen als solche kenntlich gemacht habe.

Tim Baldensperger Halle (Saale), 05.05.2020